Universität
Rostock

Traditio et Innovatio

# Aktivierung kleiner stickstoffhaltiger Moleküle durch Lewis-Säuren

## Kumulative Dissertation

zur
Erlangung des akademischen Grades
*doctor rerum naturalium (Dr. rer. nat.)*
der Mathematisch-Naturwissenschaftlichen Fakultät
der Universität Rostock

vorgelegt von Fabian Reiß, geb. am 17.06.1983 in Goslar

Rostock, 17.06.2014

Die vorliegende Arbeit wurde am Lehrstuhl für Anorganische und Elementorganische Chemie der Universität Rostock von Oktober 2011 bis Juni 2014 unter der Betreuung von Professor Dr. Axel Schulz angefertigt.

1. Gutachter: Prof. Dr. Axel Schulz
2. Gutachter: Prof. Dr. Uwe Rosenthal

Tag des öffentlichen Promotionskolloqium 28.10.2014

## Erklärung

Hiermit versichere ich an Eides statt, dass ich die vorliegende Arbeit selbständig angefertigt und ohne fremde Hilfe verfasst habe. Dazu habe ich keine außer den von mir angegebenen Hilfsmitteln und Quellen verwendet. Die aus den benutzten Werken inhaltlich und wörtlich entnommenen Stellen sind als solche kenntlich gemacht.

Rostock, den 17.06.2014

……………………….
Fabian Reiß

# Zusammenfassung

In der vorliegenden Dissertation werden die Ergebnisse über die Aktivierung von stickstoffhaltigen kleinen Molekülen durch Lewis-Säuren präsentiert. Eine Serie neuartiger anorganischer Lewis-Säure-Base-Addukte des $(Me_3Si)_2NNC$ sowie einfacher Diazene konnte hierbei auf klassischem Wege synthetisiert werden. Dabei wurde erstmals eine Super-Lewis-Säure katalysierte Diazomethan/Aminoisonitril-Isomerisierung sowie die anschließende CC-Knüpfung und [3+2]-Cycloaddition aufgeklärt, die zu einem neuartigen Pyrazol-Derivat, dem formalen Trimer des $(Me_3Si)_2NNC$ führte. Die Aktivierung silylierter Diazene durch $B(C_6F_5)_3$ führte über eine *trans*/*cis*/*iso*-Isomerisierung zu dem ersten isolierbaren *iso*-Diazen. Die silylierten $B(C_6F_5)_3$-Diazen-Addukte zeigten Aminonitren-Reaktivität die zur Insertion der NN-Einheit in eine BC-Bindung führte. Es wurde gezeigt, dass sich die persilylierten Basen $Me_3SiNNSiMe_3$ und $(Me_3Si)_3N$ nicht direkt silylieren lassen. Diese Experimente führten sowohl zur Entwicklung einer neuartigen Zwei-Elektronen-Oxidation von Hydrazin-Derivaten, die erstmals die Synthese eines homoleptischen Diazenium-Salzes erlaubte, als auch zur Aufklärung einer Super-Lewis-Säure katalysierten Alkyl/Wasserstoff-Austauschreaktion an Silanen. Diese Arbeit zeigt neben dem Einblick in das enorme Synthesepotential moderner siliciumbasierter Super-Lewis-Säuren einen direkten Vergleich zu den Reaktionen klassischer oder sterisch anspruchsvoller Lewis-Säuren.

# Summary

This thesis reports on results about the activation of small nitrogen containing molecules by Lewis acids. A series of new inorganic Lewis acid base adducts of $(Me_3Si)_2NNC$ as well as simple diazenes could be synthesized by classical methods. Thereby, a super Lewis acid catalyzed diazomethane/aminoisonitrile isomerization followed by CC coupling and [3+2] cycloaddition was discovered for the first time which resulted in a novel pyrazole derivative, the formal trimer of $(Me_3Si)_2NNC$. The activation of silylated diazenes by $B(C_6F_5)_3$ led by *trans*/*cis*/*iso*-isomerization to the first isolable *iso*-diazene. The silylated $B(C_6F_5)_3$ diazene adducts showed aminonitrene reactivity which led to an insertion of the NN unit into the BC bond. It was shown that the persilylated bases $Me_3SiNNSiMe_3$ and $(Me_3Si)_3N$ could not be direct silylated. These experiments led both to the development of a novel two electron oxidation of hydrazine derivatives, to the first synthesis of a homoleptic diazonium salt, and to the elucidation of a super Lewis acid catalyzed alkyl/hydrogen exchange at silanes. This work gives an insight into the vast syntheticpotential of modern silicon based super Lewis acids as well as a direct comparision to the classical or sterically encumbered Lewis acids.

# Danksagungen

Mein ganz besonderer Dank gebührt Prof. Dr. Axel Schulz für die inspirierenden Lehrveranstaltungen, der Grundstein meiner Studien im Bereich der Anorganischen Chemie, die ich bei ihm besuchen durfte. Des Weiteren bin ich ihm zu großem Dank verpflichtet für das Bereitstellen eines interessanten Themas, das in mich gesetzte Vertrauen, die Bereitstellung eines Laborarbeitsplatzes sowie für das stete Interesse an den erzielten Ergebnissen und nicht zuletzt für die freundliche Aufnahme in den Arbeitskreis.

Weiterer besonderer Dank gebührt Dr. Alexander Villinger für die großartige Ausbildung und Betreuung im Bereich spezieller präparativer Arbeitstechniken, die ungezählten lehrreichen wissenschaftlichen Diskussionen sowie der akribischen Lösung von etlichen Strukturdaten.

Bei M. Sc. René Labbow bedanke ich mich für die gute zusammen Arbeit in dem Silylium-Projekt sowie für die zerstreuenden Kaffepausen.

Für die außerordentlich freundliche und produktive Arbeitsatmosphäre bedanke ich mich bei Dr. Ronald Wustrack, Dipl.-Chem. Christian Hering, M. Sc. Jonas Bresin, M. Sc. Alexander Hinz, B. Sc. Max Thomas, B. Sc. Kati Rosenstengel, B. Sc. Julia Rothe.

Mein Dank geht auch an alle weiteren Mitarbeiter des Arbeitskreises Schulz für die gute Zusammenarbeit und die freundliche Aufnahme.

Außerdem danke ich der analytischen Abteilung des IfCh und des LIKAT's für die gute und problemlose Zusammenarbeit sowie der Abteilung der Physikalischen Chemie für die Bereitstellung des Raman-Geräts. Besonderer Dank gilt hier Dr. Dirk Michalik für die Einarbeitung in die NMR-Spektroskopie sowie Frau Brigitte Goronzi für das Vermessen unzähliger NMR-Spektren.

Für die stete Unterstützung und das in mich gesetzte Vertrauen danke ich ganz besonders meiner Familie, ohne die dies Studium nicht möglich gewesen wäre.

Mein herzlichster Dank geht an Melanie und Moritz für die großartige Unterstützung während der Promotion und für die vielen schönen Stunden als Familie fernab der Chemie.

**Herzlichen Dank !**

*meinem Sohn*

# Inhaltsverzeichnis

**Abkürzungsverzeichnis .... iii**

**Vom SI-System abweichende Einheiten .... iv**

**1 Zielsetzung .... 1**

**2 Bisheriger Kenntnisstand .... 2**

2.1 Lewis-saure Medien .... 2

2.2 Lewis-Säure-Base-Addukte .... 5

2.3 Lewis-Säure katalysierte Reaktionen .... 9

**3 Diskussion der Ergebnisse .... 11**

3.1 Synthese von Lewis-Säure-Base-Addukten .... 11

3.1.1 Synthese von Pseudochalkogen-Addukten. .... 12

3.1.2 Synthese eines homoleptischen Diazenium-Kations .... 13

3.1.3 Synthese von Diazen-Addukten. .... 14

3.1.4 Synthese eines persilylierten Ammonium-Kations .... 16

3.2 Strukturanalyse der Lewis-Säure-Base-Addukte .... 16

3.2.1 Strukturanalysen der Lewis-Basen .... 18

3.2.2 Strukturanalyse der Aminoisonitril-Addukte .... 19

3.2.3 Strukturanalyse der Diazen-Addukte .... 20

3.2.4 Struktur des persilylierten Ammonium-Kations .... 22

3.3 Allgemeine Eigenschaften der Addukte .... 23

3.4 Folgereaktionen aktivierter Lewis-Basen .... 26

3.4.1 Trimerisation von Bis(silyl)diazomethan und Bis(silyl)aminoisonitril .... 26

3.4.2 Nitren-Reaktivität von silylierten Diazen $B(C_6F_5)_3$-Addukten .... 28

3.4.3 Katalysierte Alkyl-Austauschreaktionen an Silanen .... 30

**4 Literaturverzeichniss .... 33**

**5 Publikationen .... 38**

5.1 Catalytic Trimerization of Bis-silylated Diazomethane .... 39

5.2 Isolation of a Labile Homoleptic Diazenium Cation. .... 53

5.3 Synthesis, Structure and Reactivity of Diazene Adducts – Isolation of the First *iso*-Diazene stabilized as Borane Adduct .... 59

5.4 Synthesis of the First Persilylated Ammonium Ion $[(Me_3Si)_3NSi(H)Me_2]^+$ By Silylium Catalysed Alkyl/Hydrogen Redistribution .... 71

**6 Anhang ..... 77**
6.1 Abbildungsverzeichnis ..... 77
6.2 Tabellenverzeichnis ..... 78
6.3 Schemataverzeichnis ..... 78

# Abkürzungsverzeichnis

| | | | |
|---|---|---|---|
| **AO** | Atomorbital | **Mes** | 2,4,6-Trimethylphenyl |
| **Alk** | Alkylgruppe | **Mes*** | 2,4,6-Tri-*tert*-butylphenyl = Supermesityl |
| **Ar** | Arylgruppe | **MO** | Molekülorbital |
| **ATR** | *Attenuated Total Reflection* (abgeschwächte Totalreflexion) | **MS** | Massenspektrometrie |
| ***cf.*** | vergleiche (lat. *confer*) | **NBO** | *Natural Bond Analysis* |
| $\delta$ | Chemische Verschiebung (NMR) | **NMR** | *Nuclear Magnetic Resonance* (Kernspinresonanzspektroskopie) |
| **DFT** | Dichtefunktionaltheorie | **o** | *ortho* (Substitution) |
| **DSC** | *Differential Scanning Calometry* (Dynamische Differenzkalorimetrie) | **ORTEP** | *Oak Ridge Thermal Ellipsoid Plot* |
| ***et al.*** | und andere (lat. *et alii/aliae*) | **p** | *para* (Substitution) |
| **HOMO** | *Highest Occupied Molecular Orbital* | **Pemp** | 2,3,4,5,6-Pentamethylphenyl |
| **Hyp** | Tris(trimethylsilyl)silan = Hypersilyl | **Pn** | Pniktogen |
| **INEPT** | *Insensitive Nuclei Enhanced by Polarizaition Transfer* | **ppm** | *parts per million* |
| ***in situ*** | am Ort (lat.) | **RT** | Raumtemperatur |
| **IR** | Infrarotspektroskopie | **s** | *strong* (IR), Singulett (NMR) |
| $J$ | Kopplungskonstante | **Ter** | 2,6-Dimesitylphenyl = Terphenyl |
| **kov** | Kovalenz | **theor** | theoretisch |
| **LS** | Lewis-Säure | **Tipp** | 2,4,6-Triisopropylphenyl |
| **LB** | Lewis-Base | **Trityl** | Triphenylmethyl |
| **LUMO** | *Lowest Unoccupied Molecular Orbital* | **TMSA** | Trimethylsilyl Affinitäten |
| **LP** | *lone pair*<br>Nichtbindendes Elektronenpaar | $\tilde{\nu}$ | Wellenzahl in $cm^{-1}$ |
| **m** | *medium* (IR), *meta* (Substitution), Multiplett (NMR) | **vdW** | *van der Waals* |
| $Q_{CT}$ | *total charge transfer*<br>Gesammtladungstransfer | **WCA** | *Weakly coordinating anion*<br>schwach koordinierendes Anion |
| | | **Xylol** | 2,6-Dimethylphenyl |

# Vom SI-System abweichende Einheiten

In dieser Arbeit werden die im Internationalen Einheitensystem (SI) gültigen Maßeinheiten verwendet. Alle davon abweichenden Einheiten und deren Umrechnung in SI-Einheiten sind im Folgenden aufgeführt.

| **Größe** | **Symbol** | **Bezeichnung** | **Umrechnung in SI-Einheit** |
|---|---|---|---|
| Frequenz | MHz<br>Hz | Megahertz<br>Hertz | 1 MHz = $10^6$ $s^{-1}$<br>1 Hz = 1 $s^{-1}$ |
| Länge | Å | Ångström | 1 Å = $10^{-10}$ m |
| Leistung | mW | Milliwatt | 1 mW = $10^{-3}$ kg·$m^2$·$s^{-3}$ |
| Temperatur | °C | Grad Celsius | x°C = (x + 273.15) K |
| Volumen | mL | Milliliter | 1 mL = 1 $cm^3$ = $10^{-6}$ $m^3$ |
| Wärmemenge | kJ<br>kcal | Kilojoule<br>Kilokalorien | 1 kJ = $10^3$ $m^2$· kg· $s^{-2}$<br>1 kcal = 4.1858 kJ |
| Wellenzahl | $cm^{-1}$ | reziproke Zentimeter | 1 $cm^{-1}$ = 100 $m^{-1}$ |
| Zeit | h | Stunde | 1 h = 3600 s |
|  | min | Minute | 1 min = 60 s |

# 1 Zielsetzung

Im Rahmen dieser Arbeit sollte eine Reihe potentieller Lewis-basischer kleiner Moleküle durch den Einsatz von ausgewählten Lewis-Säuren in ihre Lewis-Säure-Base-Addukte überführt werden. Die erhaltenen Adduktspezies sollten hinsichtlich ihrer strukturellen, chemischen und physikalischen Eigenschaften untersucht werden. Im besonderen Interesse lag die Aktivierung der Lewis-Basen, die zu neuartigen und ungewöhnlichen Verbindungen führen sollte. Als zu untersuchende Lewis-basische Systeme wurden stickstoffhaltige Verbindungen des Typs $R_3N$, $R_2N_2$ und $R_2N_2C$ gewählt, wobei das Hauptaugenmerk auf den Substituenten $R = Me_3Si$ gelegt werden sollte. Zur Aktivierung der Lewis-Basen sollte in erster Linie das hochreaktive, formale Trimethylsilylium-Kation "$[Me_3Si]^+$" seinen Einsatz finden, da es in Kombination mit den gewählten Lewis-Basen einen Zugang zu faszinierenden homoleptisch koordinierten Kationen bieten könnte. Des Weiteren sollte die klassische Lewis-Säure $GaCl_3$ sowie das sterisch anspruchsvolle $B(C_6F_5)_3$ zum Einsatz kommen, um einen Vergleich der erhaltenen Produkte in Abhängigkeit der Lewis-Säure zu ermöglichen.

Die Untersuchung der Struktur sowie des chemischen und physikalischen Verhaltens der Verbindungen sollte durch schwingungsspektroskopische Methoden (UV/VIS-, IR-, Raman-Spektroskopie) und multinukleare Kernresonanzspektroskopie ($^{11}$B-, $^{13}$C-, $^{19}$F-, $^{1}$H-, $^{15}$N- und $^{29}$Si-NMR) in Lösung zum einen, zum anderen mit Hilfe der Röntgendiffraktometrie an geeigneten Einkristallen erfolgen. In Kombination mit quantenmechanischen *ab-initio-* und DFT-Rechnungen sollten die Bindungsverhältnisse der synthetisierten Verbindungen aufgeklärt und charakterisiert werden. Dadurch sollte sowohl der Zusammenhang zwischen Struktur und chemischer Bindung als auch die Ladungsverteilung und Reaktivität erklärt werden.

# 2 Bisheriger Kenntnisstand

## 2.1 Lewis-saure Medien

Im Jahre 1923 wurden drei grundlegenden Arbeiten zum Verständnis chemischer Reaktionen verfasst. In der Arbeit „Valence and Structure of Atoms and Molecules“ von Lewis[1] wird nicht nur das heutzutage allgemein etablierte Konzept der nach ihm benannten Symbolschreibweise für chemische Verbindungen „Lewis-Formeln“ beschrieben, sondern auch eine zu dieser Zeit neuartige Säure-Base Definition. Nach Lewis werden Elektronenpaardonoren als Lewis-Basen (LB) und Elektronenpaarakzeptoren als Lewis-Säuren (LS) klassifiziert, der Oktettregel folgend bilden sich durch deren Interaktion stabile Addukte aus (Abbildung 1).

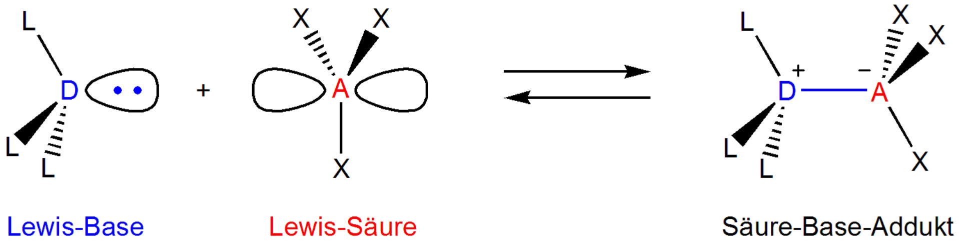

***Abbildung 1.*** Allgemeines Konzept der Säure-Base-Theorie nach Lewis.

Zur gleichen Zeit publizierten Brønsted und Lowry unabhängig voneinander ihre redundanten auf Protonen-Donor-Akzeptor beruhenden Säure-Base-Theorien.[2,3] Das Konzept von Lewis kann auch auf Brønsted-Lowry-Systeme angewandt werden und ist somit umfassender. Es wurde von Pearson 1963 um die Theorie der harten und weichen Lewis-Säuren und Basen (HSAB) erweitert.[4,5] Demnach sind harte Systeme kleine schlecht polarisierbare und weiche gut polarisierbare Atome/Moleküle, deren Addukt-Bindungen in den Paaren hart-hart und weich-weich besondere Stabilität aufweisen. Nach heutigem Verständnis sind Lewis-Säuren Atome oder Moleküle, deren niedrigstes unbesetztes Molekül Orbital (LUMO, LS-MO) in der Lage ist, mit einem besetzten Molekülorbital ähnlicher Energie einer Lewis-Base (HOMO, LB-MO), zu kombinieren (Abbildung 2). Als Donor-Orbitale können zum Beispiel nichtbindenden Elektronenpaare (LP) oder aromatische Molekülorbitale (π-MO) fungieren. Bei der Kombination wird ein neuer Satz an Molekülorbitalen gebildet ($\Psi,\Psi^*$) die die Addukt-Bindung beschreiben.

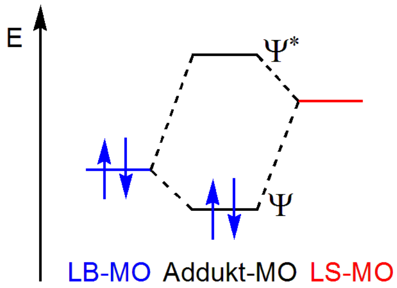

***Abbildung 2.*** Vereinfachtes Energiediagramm einer Addukt-Bindung.

Als klassische Lewis-Säuren können neutrale halogenierte Elektronenmangel-Verbindungen der 3. Hauptgruppe des Typs $AX_3$ angesehen werden (A = B, Al, Ga; X = F, Cl; Abbildung 1). Dem HSAB-Konzept folgend sollte das Bortrifluorid $BF_3$ die „härteste“ Lewis-Säure dieser Vertreter darstellen, jedoch konnte sowohl experimentell als auch auf der Grundlage quantenchemischer Rechnungen gezeigt werden, dass die Säurestärke der Borate bzw. die Bindungsdissoziationsenergien ihrer Addukte keinem monokausalem Trend folgen, vielmehr stellte sie sich als Überlagerung mehrerer Effekte heraus.[6,7] Erst 2010 identifizierten Yáñez *et al*. anhand einer quantenchemischen Analyse der einfachen Adduktspezies $X\text{-}BH_{3-n}F_n$ und $X\text{-}BH_{3-n}Cl_n$ mit den Lewis-Basen X = $N_2$, HCN, LiCN, $H_2CNH$, $NF_3$, $NH_3$ und $n$ = 0–3 die drei wesentlichen Einflussgrößen auf die Bindungsenergien der BN-Addukte: i) Das Herabsetzen der Elektronen-Akzeptanz des Bors durch intramolekulare π-Donation der Halogene. ii) Ein Anstieg der Elektronen-Akzeptanz des Bors durch Deformation. iii) Einen großen Anstieg der Deformationsenergie mit zunehmender Halogenierung.[8] Die Arbeit von Yáñez zeigt deutlich die Unabdingbarkeit moderner *ab-initio* und DFT-Methoden für ein tiefgreifendes Verständnis selbst einfacher Addukt-Systeme. Sogar Alkyl substituierte Derivate der klassischen Lewis-Säuren besitzen noch stark sauren Charakter und stabilisieren sich wie die $AX_3$ Systeme, durch intermolekulare Donor-Acceptor-Bindungen, über verbrückende Halogenatome wie in (Abbildung 3) an den Beispielen $[MeGaCl_2]_2$ (links) und $MeGaCl_2GaCl_3$ (rechts) dargestellt ist.[9]

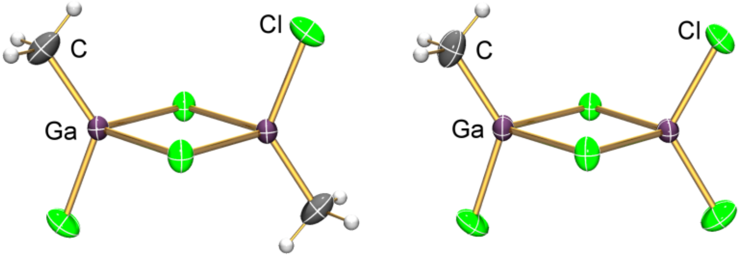

***Abbildung 3.*** Stabilisierung klassischer Lewis-Säuren über Halogenbrücken.

Neben den lang bekannten konventionellen Lewis-Säuren haben sich in jüngster Zeit die auf trivalenten Silicium-Kationen (Silylium-Ionen) basierenden Systeme als Super-Lewis-saure Medien etabliert. In Analogie zu den Super-Brønsted-Lowry-Säuren wie $HFSO_3/SbF_5$ oder $H[CHB_{11}F_{11}]$[10,11] sind Lewis-Supersäuren um ein Vielfaches stärker als die stärkste konventionelle Lewis-Säure $SbF_5$.[12] Bereits 1963 modifizierten Corey und West[13] die aus der Organischen Chemie bekannte Lewis-Säure assistierte Bartlett-Schneider-Condon[14] Wasserstoff/Halogen Austauschreaktion und nutzen sie erstmals in der Silicium Chemie (Schema 1). Diese Reaktion zeigte die höhere Lewis-Acidität der formal entstehenden Silylium-Kation „$[Ph_3Si]^+$“ im Vergleich zum $BBr_3$ auf, da diese vom eingesetzten Anion $[BBr_4]^-$ ein Bromid abstrahierten und sich unmittelbar das $Ph_3SiBr$ bildete.

$$[Ph_3C][BBr_4] + Ph_3SiH \longrightarrow Ph_3CH + BBr_3 + Ph_3SiBr$$

***Schema 1.*** Modifizierte Wasserstoff/Halogen Austauschreaktion nach Corey und West.

Erst dreißig Jahre später setzten Lambert *et al.*[15] in der von Corey beschriebenen Methode das schwachkoordinierenden Anion $[B(C_6F_5)_4]^-$ ein, dies führte zur allgemein gültigen Hydrid-Transferreaktion von Silanen auf Tritylium-Kationen (Schema 2). Bereits Lambert *et al.* zeigten, dass diese modifizierte Bartlett-Schneider-Condon Reaktion einen breiten Zugang zu einer Reihe neuartiger siliciumbasierter Super-Lewis-saurer Systeme bietet.

$$[Ph_3C][B(C_6F_5)_4] + R_3SiH \longrightarrow [R_3Si\cdot X][B(C_6F_5)_4] + Ph_3CH$$

***Schema 2.*** Allgemeine Synthese von Silylium-Supersäuren nach Lambert *et al.* (R = Me,Et, i-Pr, $Me_3Si$; X = Solvens = $R_3SiH$ oder Benzol).

Die extreme Acidität der Silylium-Ionen $[R_3Si]^+$ ist ihrem Elektronen-Sextett und einem leeren 3p Valenzorbital am Silicium geschuldet. Dies führt unweigerlich zur Adduktbildung sogar mit sehr schwachen Lewis-Basen (z.B. Toluol,[15–17] $Me_3Si–H$)[18,19] oder zu kurzen Kation-Anionen-Kontakten selbst mit den schwach koordinierenden Carborat-Anionen (z.B. $[CHB_{11}H_5Br_6]^-$,[20] $[CHB_{11}F_{11}]^-$).[21] Erst 2002 gelang es Reed und Lambert das erste „nackte“ Silylium-Kation im Salz $[(Mes)_3Si][CHB_{11}Me_5Br_6] \cdot C_6H_6$ zu isolieren und vollständig zu charakterisieren.[22] 2011 veröffentlichten Müller *et al.* eine neuartige, auf einem Austauschprozess basierende Syntheseroute, die einen leichten Zugang zu einer Reihe sterisch überfrachteter solvatfreier Silylium-Salze $[Ar_3Si][B(C_6F_5)_4]$ (Ar = Mes; Xylyl, Tipp, Pemp) bietet (Schema 3).[23] Aufbauend auf den Arbeiten von Manners *et al.*[24] gelang es 2009 Oestreich *et al.*[25] das erste solvensfreie Ferrocen-stabilisierte Silylium-Ion zu isolieren.

$$3\ \mathrm{Ar_2(Me)SiH} + 2\ [\mathrm{Ph_3C}][\mathrm{B(C_6F_5)_4}] \longrightarrow 2\ [\mathrm{Ar_3Si}][\mathrm{B(C_6F_5)_4}] + \mathrm{Me_3SiH} + 2\ \mathrm{Ph_3CH}$$

***Schema 3.*** Neuartige Synthese von sterisch überfrachteten Silylium-Salzen nach Müller *et al.*[23]

Als sterisch gehinderte Lewis-Säuren können Systeme des Typs $RB(C_6F_5)_2$ (R = H, Aryl, $C_6F_5$) aufgefasst werden, deren Kombination mit sterisch gehinderten Lewis-Basen wie Phosphinen oder Aminen zum Ausbilden neuartiger „frustrierter Lewis-Paare“ (FLPs) führt. Das Konzept der FLPs wurde in den Arbeitsgruppen Stephan und Erker entwickelt und führte zu einer Reihe ungewöhnlicher Reaktionen.[26–29] Diese Arbeiten zeigen die besondere Rolle des $B(C_6F_5)_3$ in der Aktivierung kleiner Moleküle.

## 2.2 Lewis-Säure-Base-Addukte

In der Arbeitsgruppe Schulz konnte über neuartige [3+2]-Cycloadditionen eine Reihe Lewis-Säure stabilisierter binärer, fünfgliedriger Pniktogen-Ringsysteme isoliert und charakterisiert werden. So konnten erstmals Tetrazaphosphole des Typs $RN_4P \cdot GaCl_3$ (R = Mes*,[30] Ter)[31] und Triazadiphosphole $RN_3P_2 \cdot GaCl_3$ (R = $N(SiMe_3)_2$,[32] Mes*)[33] sowie das homologe Tetrazarsol $Mes^*AsN_4 \cdot GaCl_3$[34,35] hergestellt werden. Dabei konnte ein Konzept entwickelt werden, bei dem versteckte Dipolarophile in Form silylierter Aminodichlorpniktane des Typs $RN(SiMe_3)ECl_2$ (E = P, As; R = Mes*, Ter, $N(SiMe_3)_2$) über eine $GaCl_3$-assistierte $Me_3SiCl$ Eliminierung *in situ* in hoch labile $[R\text{-}N{\equiv}E]^+$ Spezies überführt werden. Diese reagieren in Gegenwart von 1,3-Dipolen wie $Me_3SiN_3$ zu den Galliumtrichlorid-Addukten der Tetrazazapniktole (Schema 4 oben). Dabei zeigte sich, dass das silylierte Hydrazinodichlorphosphan $(Me_3Si)_2NN(SiMe_3)PCl_2$ sowohl als verstecktes Dipolarophil als auch als versteckter 1,3-Dipol reagieren kann, wobei die Reaktion zu dem Triazadiphosphol $(Me_3Si)_2NN_3P_2 \cdot GaCl_3$ führte (Schema 4 unten).[36]

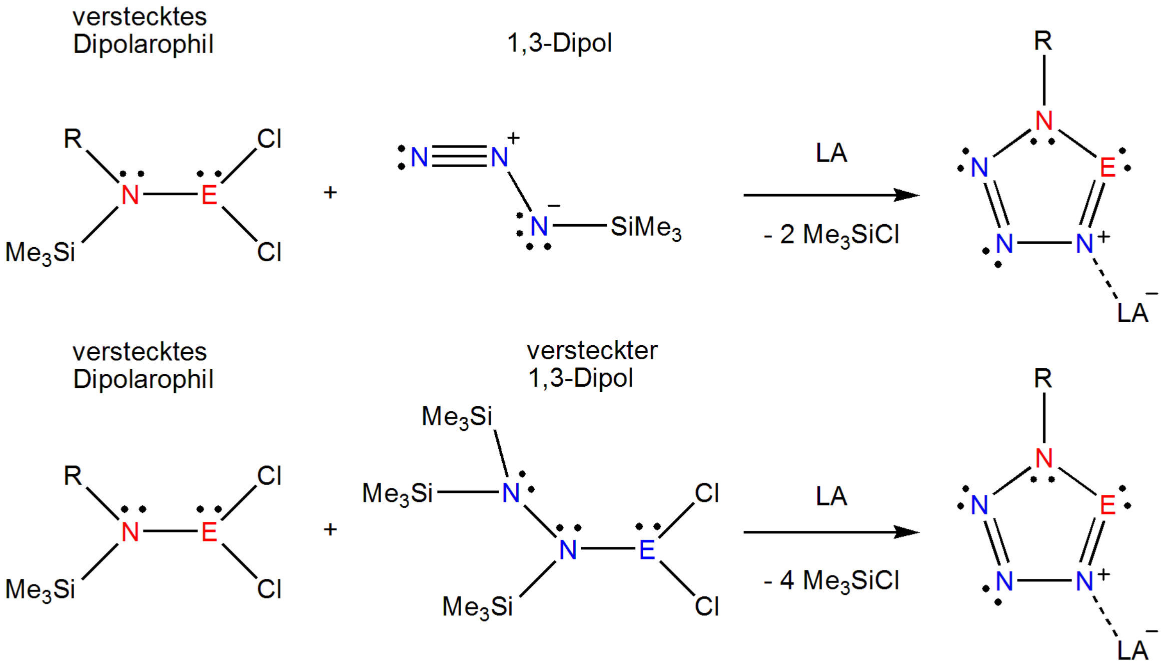
verstecktes Dipolarophil
1,3-Dipol
versteckter 1,3-Dipol
R
Cl
Me3Si
N
E
+
SiMe3
LA
- 2 Me3SiCl
- 4 Me3SiCl

***Schema 4.*** Lewis-Säure-assistierte [3+2]-Cycloadditionen unter Verwendung versteckter Dipolarophile und 1,3-Dipole bilden Addukt stabilisierte Azapniktole. (LS = $GaCl_3$; E =P, As; R = Mes*, Ter, $N(SiMe_3)_2$).

Die Substitution von $GaCl_3$ durch $B(C_6F_5)_3$ führte in derselben Reaktion zu dem unerwarteten Pentafluorophenyl substituierten cyclo-Diphosphadiazan-Derivat $[C_6F_5P(\mu\text{-}N(SiMe_3)NB(C_6F_5)_2)]_2$ (Schema 5).[37] Vergleichbare $C_6F_5$-Gruppenwanderungen waren bis zu diesem Zeitpunkt nur aus der Übergangsmetallchemie bekannt.[38] Wie Rosenthal *et al.*[39] zeigen konnten führen diese Reaktionen zur „Vergiftung“ der in der Olefin-Polymerisation eingesetzten Katalysatoren. Die von Schulz *et al.* beschriebene Reaktion kann als erste übergangsmetallfreie Bor-Kohlenstoff-Aktivierung und formale Insertion eines NNP-Fragmentes in die BC-Bindung angesehen werden.

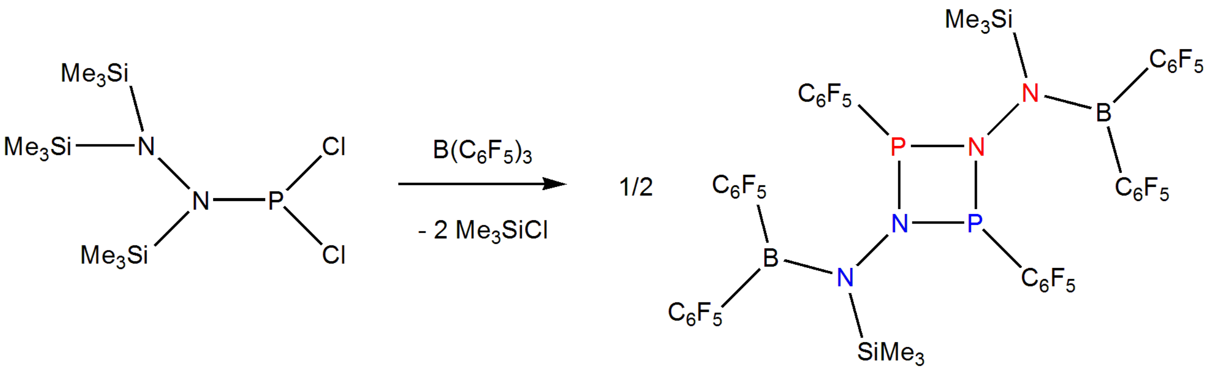
Me3Si
N
P
Cl
B(C6F5)3
- 2 Me3SiCl
1/2
C6F5
B
SiMe3

***Schema 5.*** Synthese eines *cyclo*-Diphosphadiazans über die formale Insertion eines NNP-Fragmentes in die BC-Bindung des $B(C_6F_5)_3$.

In weiteren Arbeiten der Schulz-Gruppe an hypersilylyliertem Aminodichlorophosphan (Hyp)N($SiMe_3$)$PCl_2$[40] sowie silylierten Aminodichlorarsanen des Typs $RAsCl_2$ (R = $(Me_3Si)_2NN(SiMe_3)$,[41] $(Me_3Si)_2N$, TerN($SiMe_3$)[36]) wurden Galliumtrichlorid-assistierte Chlor/Methyl-Austausch-Reaktionen beobachtet. Über einen ähnlichen Cl/Me-Austauschprozess, gefolgt von einer Kondensationsreaktion ließ sich ausgehend vom Bis(trimethylsilyl)schwefeldiimid Galliumtrichlorid Addukt $Me_3SiNSNSiMe_3 \cdot GaCl_3$ ein ungewöhnlicher sechsgliedriger Oxadisilathiadiazin-Ring isolieren(Schema 6).[42]

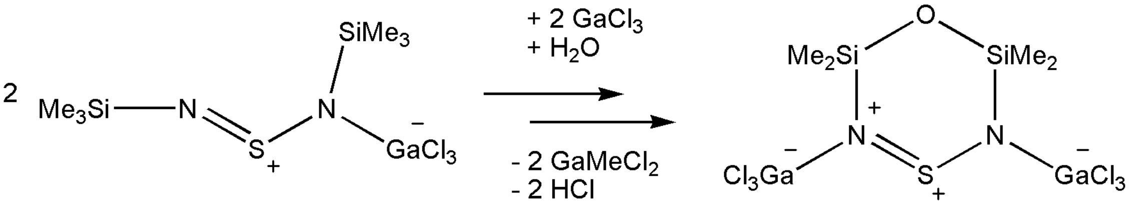

***Schema 6.*** Chlor/Methyl Austausch am $Me_3SiNSNSiMe_3 \cdot GaCl_3$ gefolgt von Bildung des isolierten Oxadisilathiadiazin-Ring nach Schulz *et. al.*[42]

Bereits 1964 beschrieben Massey und Parks erstmals die Synthese von $B(C_6F_5)_3$, die ersten LB · $B(C_6F_5)_3$-Addukte (LB = $H_3N$, $(CH_3)_3N$, $H_5C_5N$, $Ph_3P$) sowie die ersten $[X][B(C_6F_5)_4]$ (X = $Li^+$, $K^+$, $Et_4N^+$) Salze.[43] Seither wurde eine Vielzahl organischer stickstoffhaltiger Addukte mit Aminen, Iminen, Nitrilen aber auch mit heterocyclischen Triazinen, Pyrazolen und Imidazolen isoliert.[44,45] Über ein von Bochmann *et al.* begründetes, auf RCN · $B(C_6F_5)_3$ Addukt-Bindungen beruhendes Konzept, wurde Zugang zu einer Reihe neuartiger schwach koordinierender Anionen des Typs $[Z\{B(C_6F_5)_3\}_n]^{x-}$ (Z = CN, $Ni(CN)_4$,[46] $NH_2$;[47] $N(CN)_2$, $C(CN)_3$, $B(CN)_4$;[48] $n = 2, 3, 4$; $x = 1, 2$) erhalten. Weder in den Addukt-Anionen noch in den von Erker *et al.* isolierten Isonitril- und Nitril-Boran-Addukten[49] ist ein einfacher Trend in den Änderungen der CN-Bindungslängen durch die Addukt-Bindung zu erkennen. Jedoch zeigen sich die Schwingungsbanden der CN-Dreifachbindungen generell um bis zu $\Delta\tilde{\nu}_{CN} = 170\ cm^{-1}$ zu höheren Wellenzahlen verschoben.

Im Vergleich zu den Addukten der neutralen Lewis-Säuren $GaCl_3$ und $B(C_6F_5)_3$ bilden die Super-Lewis-sauren Silylium-Kationen mit Lewis Basen Salze aus. Die entstehenden Salze können nur durch den Einsatz schwach koordinierender Anionen[50] stabilisiert werden, wobei sich das Tetrakis(pentafluorphenyl)borat, $[B(C_6F_5)_4]^-$, und die halogenierten Carborate $[CHB_{11}H_nX_{11-n}]^-$ (X = F, Cl, Br; $n = 0, 5$)[20,51] etabliert haben. Im Gegensatz zu den überfrachteten Arylsilylium-Kationen können die Alkylsilylium-Ionen nur als Addukt-Spezies isoliert werden (z.B. $[Alk_3Si \cdot Toluol]^+$,[15–17] $[Me_3Si–H–SiMe_3]^+$)[18,19] die als potentielle Silylierungsreagenzien dienen. Das kleinste Alkylsilylium-Kation das

Trimethylsilylium-Ion $[Me_3Si]^+$ ähnelt in seiner Chemie dem $H^+$ und wird daher auch als großes Proton bezeichnet.[52] In Analogie zu den Protonen-Affinitäten[53] wurde im Arbeitskreis Schulz das Konzept der Trimethylsilyl Affinitäten (TMSA) entwickelt, die als Enthalpie-Änderung der Dissoziation eines Lewis-Säure-Base-Adduktes definiert wird (Schema 7).[52]

$$[LB{-}SiMe_3]^+{}_{(g)} \longrightarrow LB_{(g)} + [Me_3Si]^+{}_{(g)} \qquad \Delta H_{298}$$

***Schema 7.*** Definition der Trimethylsilyl-Affinität.

Im Einklang mit diesem Konzept ließen sich Lewis-Basen mit einem größeren TMSA-Wert als $Me_3SiH$ oder Benzol in ihre Trimethylsilylium-Addukte überführen. Von besonderem akademischen Interesse sind hierbei homoleptische Onium-Ionen von denen bisher die Bis-silylierten Halonium- und Pseudohalonium-Kationen $[Me_3Si–X–SiMe_3]^+$ (X = F, Cl, Br, I;[52] CN, OCN, SCN, NNN),[54] isoliert und vollständig charakterisiert werden konnten. Von Olah *et al.*[55,56] wurden die persilylierten Chalkogonium-Ionen $[(Me_3Si)_3O]^+$ und $[(Me_3Si)_3S]^+$ *in situ* generiert und über NMR-Spektroskopie nachgewiesen. Als erste persilylierte Pniktogonium-Kationen wurden das Phosphonium $[(Me_3Si)_4P]^+$ und Arsonium $[(Me_3Si)_4As]^+$ von Driess *et al.*[57] isoliert und vollständig charakterisiert. Die beschriebenen Onium-Ionen konnten als $[B(C_6F_5)_4]^-$-Salze durch Kombination der Super-Lewis-Säuren $[Me_3Si \cdot Solvens][B(C_6F_5)_4]$ mit den Persilylierten Gruppe 15-17 Verbindungen in geeigneten Lösungsmitteln erhalten werden (Schema 8).

$$[Me_3Si \cdot X][B(C_6F_5)_4] + (Me_3Si)_nE \longrightarrow [(Me_3Si)_{n+1}E][B(C_6F_5)_4] + X$$

***Schema 8.*** Allgemeine Synthese von homoleptischen Onium-Kationen ($n$ = 1: E = F, Cl, Br, I, CN, OCN, SCN, NNN, wobei X = $Me_3SiH$; $n$ = 2: E = O, S, mit X = $Me_3SiH$; $n$ = 3: E = P, As mit X = Benzol).

In einer umfassenden Studie über Addukte des Trimethylsilylium-Kations mit einer Reihe aromatischer Lösungsmittel $[Me_3Si \cdot Aromat][B(C_6F_5)_4]$ (Aromat = Benzol, Ethylbenzol, *n*-Propylbenzol, *iso*-Propylbenzol, *o*-Xylol, *m*-Xylol, *p*-Xylol, 1,2,3-Trimethylbenzol, 1,2,4-Trimethylbenzol, 1,3,5-Trimethylbenzol)[17] wurde die *para*-Position, in Bezug auf den Substituenten am Aromaten, als bevorzugte Position für die in allen Addukten beobachtete Wheland-Komplex artige $\eta^1$ Koordination identifiziert. Es wurde gezeigt, dass diese Addukte in Lösung sehr labil sind, was zu einer durch Fluoridabstraktion initiierten Zersetzung der Salze in hochreaktives „$C_6F_4$“ führt. Dies konnte anhand einer Abfangreaktion mit $CS_2$

aufgeklärt werden, bei der ein neuartiges S-heterocyclisches Carben-Boran-Addukt isoliert wurde (Schema 9).[17]

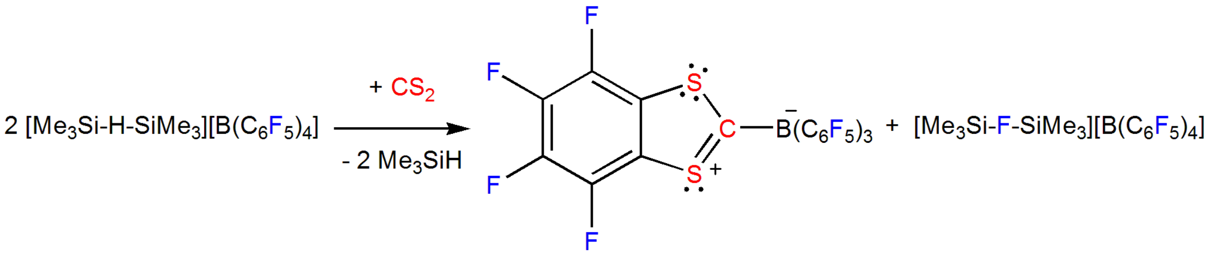

***Schema 9.*** Aufklärung des Zerfalls von labilen Trimethylsilylium-Verbindungen über die Abfangreaktion mit $CS_2$ nach Schulz *et al.*[17]

Diese Arbeiten zeigen eindrucksvoll, dass Lewis-Säuren kleine Moleküle in ungewöhnlichen Reaktionen aktivieren und dabei instabile Systeme gleichermaßen stabilisieren können.

## 2.3 Lewis-Säure katalysierte Reaktionen

Die Entdeckung der Lewis-Säure katalysierten Alkylierung und Acylierung von Friedel und Craft[58] im Jahre 1877 führte zu einer sprunghaften Entwicklung in der organischen Synthese. So konnten bis heute vielfältige Synthesemethoden zur CC- und CX-Knüpfung unter Verwendung klassischer Lewis-saurer Systeme entwickelt werden. Dabei sind im Besonderen Acylierungen, Glycosidierungen, SS-Spaltungen, Cyclotrimerisierungen von Ketonen, Allylierungen von Aldehyden, Mukaiyama Aldol Reaktionen, Diels-Alder Cycloadditionen sowie die Baeyer-Villiger-Oxidation zu nennen.[59–61] Durch die Kombination von chiralen Verbindungen mit klassischen Lewis-Säuren konnten katalysierte, asymmetrische Reaktionen entwickelt werden.[62]

Auf den ersten Blick scheint es verwunderlich, dass trotz dieser vielfältigen Syntheserouten der klassischen Lewis-Säuren die Super-Lewis-Säuren bisher noch keinen breiten Einzug in dieses Gebiet gehalten haben. Aufgrund ihrer extremen Säurestärke sind außergewöhnliche und neuartige Synthesen zu erwarten. Jedoch führt in vielen Fällen eine größere Lewis-Acidität zu einer erhöhten Hydrolyseempfindlichkeit, so dass die Lewis-Säuren durch sterisch anspruchsvolle Substituenten oder schwachkoordinierende Anionen kinetisch stabilisiert werden müssen.[63] Dennoch gelang es 2005 Ozerov *et al.*[64] die erste Silylium-Kationen katalysierte Hydrodefluorierung von Aliphatischen CF-Bindungen mit Hilfe des $[Et_3Si–H–SiEt_3][B(C_6F_5)_4]$-Salzes zu entwickeln, die von Müller *et al.*[65] auf Naphthyl verbrückte $[(C_{10}H_6)Si_2(H)Me_4][B(C_6F_5)_4]$-Salze als Katalysatoren übertragen wurde (Schema 10, rechts).

Die Hydrodefluorierung konnte von Douvris und Ozerov durch den Einsatz der stabileren Carboratsalze $[Et_3Si–H–SiEt_3][CHB_{11}H_nX_{11-n}]$ (X = Cl, Br; $n = 0, 5$) optimiert werden.[66] Diese Reaktionen werden durch die CF-Spaltung, die die hohe SiF-Bindungsenergie als Triebkraft nutzt, eingeleitet, wobei die Silylium-Kationen als Katalysator dienen und die Silane $R_3SiH$ als stöchiometrische Reduktionsäquivalente verbraucht werden (Schema 10, links). Des weitern konnten bereits $C_{aryl}$–$C_{aryl}$- und $C_{alkyl}$–$C_{aryl}$-Kupplungsreaktionen beobachtet werden (Schema 10, rechts).[67,68]

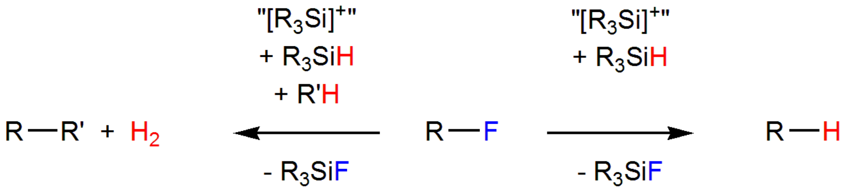

$$R{-}R' + H_2 \xleftarrow[- R_3SiF]{"[R_3Si]^+" + R_3SiH + R'H} R{-}F \xrightarrow[- R_3SiF]{"[R_3Si]^+" + R_3SiH} R{-}H$$

***Schema 10.*** Silylium katalysierte CC-Kupplung (links) und Hydrodefluorierung (rechts).

Ebenfalls zu den Silylium katalysierten CC-Kupplungreaktionen können die von Sawamura *et al.*[69] durchgeführten Diels-Alder- und Mukaiyama-Aldol-Reaktionen gezählt werden. Die von Oestreich *et al.*[25] in analogen Diels-Alder Reaktionen eingesetzten Ferrocen-substituierten [*t*-BuFcMeSi]$[B(C_6F_5)_4]$-Salze katalysierten die Reaktion sogar bei –78 °C und weisen damit wesentlich höhere Aktivitäten als das „Lambert's Salz" $[Et_3Si \cdot \text{Toluol}][B(C_6F_5)_4]$ auf. Es wurden mit beiden Katalysator-Systemen selektiv die *endo*-Diastereoisomere in sehr guten Ausbeuten erhalten. Zusätzlich zeigt das chirale Ferrocen-stabilisierte Silylium-Kation eine hohe Regioselektivität und kann sogar halogenierte Butadiene aktivieren (Schema 11).[70]

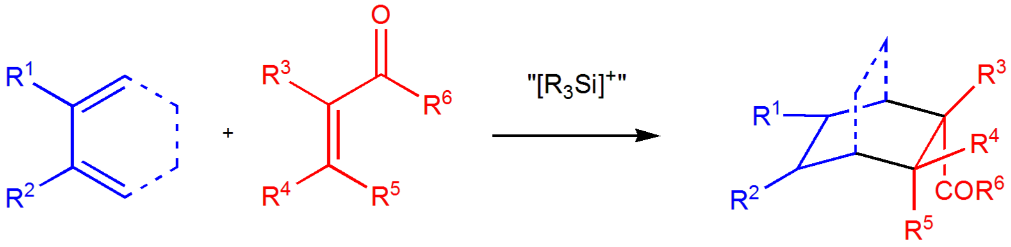

***Schema 11.*** Silylium katalysierte Diels-Alder Cyclisierung.

Die Entwicklung des FLP-Konzeptes rücken selbst die von Massey beschriebenen $B(C_6F_5)_3$-Addukte in ein neues Licht und verleiht ihnen in der übergangsmetallfreien Katalyse zunehmendes Interesse. So konnte gezeigt werden, dass die Kombination von $R_3P$ (R = *t*-Bu, $C_6H_2Me_3$) und $B(C_6F_5)_3$ aufgrund ihrer sterischen Überfrachtung nicht zu den erwarteten Addukten führt. Diese Mischungen sind in der Lage, Wasserstoff bei Raumtemperatur heterolytisch zu spalten und bilden Salze des Typs $[R_3PH][HB(C_6F_5)_3]$ aus. Diese können als katalytisch aktive Spezies Imine, Amine, Enamine und Silylenolether unter stöchiometrischem Bedarf an Wasserstoff hydrieren.[26,29,71]

# 3 Diskussion der Ergebnisse

## 3.1 Synthese von Lewis-Säure-Base-Addukten

Das Kapitel 3.1 Synthese ist in dieser Arbeit in vier Themenbereiche gegliedert. Es behandelt ausgewählte Besonderheiten und Beobachtungen der Synthese die thematisch mit den untersuchten Lewis-Basen verknüpft sind. Die im Rahmen dieser Arbeit untersuchten Lewis-Basen $(Me_3Si)_2CNN$ (**1**),[72] $(Me_3Si)_2NNC$ (**2**),[73] $Me_3SiNCNSiMe_3$ (**3**), $Me_3SiNNSiMe_3$ (**4**),[74] $Me_3SiNNPh$ (**5**),[75] PhNNPh (**6**) sowie $(Me_3Si)_3N$ (**7**)[76] konnten durch modifizierte, literaturbekannte Synthesemethoden hergestellt werden oder sind im Falle von **6** und **3** kommerziell erhältlich. Die für diese Studie eingesetzten Lewis-Säuren $[Me_3Si{-}H{-}SiMe_3][B(C_6F_5)_4]$ (**8**),[16,19,52] $[Me_3Si][CHB_{11}H_5Br_6]$ (**9**),[77] $[Me_3Si][CHB_{11}H_5Cl_6]$ (**10**)[78] sowie $[Ph_3C][B(C_6F_5)_4]$ (**11**),[52] $B(C_6F_5)_3$ (**12**)[52] und $GaCl_3$ (**13**) sind ebenfalls über literaturbekannte Methoden zugänglich bzw. im Fall von $GaCl_3$ käuflich zu erwerben. Als allgemeine Synthesemethodik kann die Kombination der gewünschten Lewis-Base mit einer Lewis-Säure in einem geeigneten Lösungsmittel angesehen werden. Hierbei ist darauf zu achten, dass die Lösungsmittel im Idealfall sowohl die Lewis-Säure als auch die Lewis-Base bei der gegebenen Temperatur gut lösen und nicht mit diesen reagieren. Die Säuren $[Ph_3C][B(C_6F_5)_4]$, $B(C_6F_5)_3$ sowie $GaCl_3$ zeigen in Dichlormethan bei üblichen Synthesetemperaturen von –80 °C bis maximal +70 °C gute Lösungseigenschaften und weisen nur langsame Zersetzung auf. Im drastischen Gegensatz hierzu zersetzen sich die Super-Lewis-sauren Silylium-Kationen unmittelbar in Dichlormethan-Lösungen und können nur in sehr schwach Lewis-basischen Lösungsmitteln wie Benzol, Toluol und 1,2-Dichlorbenzol gehandhabt werden. Jedoch sind die entstehenden Addukt-Salze mit dem $[B(C_6F_5)_4]^-$-Anion auch in diesen Lösungsmitteln nur bedingt stabil.[17] Im Gegensatz hierzu weisen die erheblich stabileren Carborat-Salze $[Me_3Si][CHB_{11}H_nX_{11-n}]$ (X = Cl, Br; n = 0, 5) nur geringe Löslichkeit in Benzol und Toluol auf, was zu einer niedrigeren Reaktivität dieser Verbindungen führt.

### 3.1.1 Synthese von Pseudochalkogen-Addukten.

Im ersten Themenbereich sollten Addukte von Bis(trimethylsilyl)diazomethan $(Me_3Si)_2CNN$ (**1**), Bis(trimethylsilyl)aminoisonitril $(Me_3Si)_2NNC$ (**2**) und Bis(trimethylsilyl)carbodiimid $Me_3SiNCNSiMe_3$ (**3**) synthetisiert und charakterisiert werden. Zunächst wurden die flüssigen Lewis-Basen **1**, **2** und **3** als Lösungsmittel und Reaktand mit $[Me_3Si–H–SiMe_3][B(C_6F_5)_4]$ bei Raumtemperatur zur Reaktion gebracht. Dabei fiel auf, dass sich sowohl bei dem Diazomethan als auch beim Aminoisonitril die zuvor schwachgelblichen Lösungen tiefrot färbten und zu einem zähen Öl abreagierten. Im Gegensatz hierzu bildete sich mit Carbodiimid lediglich eine farblose Suspension, aus der nach Entfernen des Überstandes und Umkristallisation aus Toluol das farblose $[(Me_3Si)_2NCNSiMe_3][B(C_6F_5)_4]$ (**14**) erhalten werden konnte (Abbildung 7, rechts). Zur besseren Handhabung wurden weitere Reaktionen von **1** und **2** mit den Silylium-Salzen in *n*-Pentan Lösung bei –78 °C durchgeführt. Jedoch schien auch bei tiefer Temperatur eine komplexe Reaktion abzulaufen, nach zwölf Stunden Reaktionszeit war in der dunkelroten Reaktionslösung ein heller Bodensatz zu erkennen. Nach Filtration und Umkristallisation konnten diese Bodensätze in beiden Fällen als $[(Me_3Si)_2NNCSiMe_3][B(C_6F_5)_4]$ (**15[Boran]**) identifiziert werden (Schema 12, Abbildung 7, links).

$$[Me_3Si\text{-}H\text{-}SiMe_3][WCA] + (Me_3Si)_2NNC \xrightarrow[\text{RT}]{\text{Toluol}} [(Me_3Si)_2NNCSiMe_3][WCA] + Me_3Si\text{-}H$$

***Schema 12.*** Synthese von $[(Me_3Si)_2NNCSiMe_3][WCA]$ Salzen in stöchiometrisch geführten Reaktionen ($[WCA]^- = [B(C_6F_5)_4]^-$, $[CHB_{11}H_5Br_6]^-$).

Aus dem dunkelroten Überstand konnte ein unerwartetes silyliertes 4-Diazenyl-3-hydrazinylpyrazol (**16**) isoliert werden, welches als Trimer des Diazomethans bzw. Aminoisonitrils aufgefasst werden kann. In einer ausführlichen Studie konnte diese Reaktion näher untersucht und spezifiziert werden (siehe Kapitel 3.4.1; Seite 26). Des Weiteren ist es gelungen, in analoger Weise das $[(Me_3Si)_2NNCSiMe_3][CHB_{11}H_5Br_6]$ (**15[CB]**) Salz zu isolieren. Das neutrale $(Me_3Si)_2NNCB(C_6F_5)_3$ (**17**) Boran Addukt, sowie das $[(Me_3Si)_2NNCCPh_3][B(C_6F_5)_4]$ (**18**) Salz konnten bei stöchiometrisch geführten Reaktionen aus Dichlormethan erhalten werden.

### 3.1.2 Synthese eines homoleptischen Diazenium-Kations

Im zweiten Themengebiet sollte eine Synthese für das homoleptische $[(Me_3Si)_2NNSiMe_3]^+$-Diazenium-Kation entwickelt werden. Als geeignete Persilylierte Spezies wurde das $Me_3SiNNSiMe_3$ (**4**) mit seinem berechneten TMSA-Wert von 57.1 kcal/mol (*cf.* 30.4 Toluol; 71.7 kcal/mol $Me_3SiNCNSiMe_3$) identifiziert und nach der von Wiberg *et al.*[74] ausgearbeiteten Synthese hergestellt. Da sich die Diazen-Spezies **4** oberhalb von –30 °C zersetzt, mussten die Reaktionen unterhalb dieser Temperatur geführt werden. In einer Serie von Experimenten wurde mithilfe verschiedener Silylierungsreagenzien und Syntheserouten die direkte Silylierung zum Diazenium-Salz untersucht (Schema 13). Dabei stellte sich sowohl der Einsatz von klassischen Lewis-Säuren (Schema 13; Route A) als auch von Silbersalzen schwach koordinierender Anionen (Schema 13; Route B) in Kombination mit Trimethylsilylhalogeniden als erfolglos heraus. Es konnten lediglich Zersetzungsprodukte isoliert und identifiziert werden. In weiteren Experimenten wurden Super-Lewis-saure Systeme als formale $[Me_3Si]^+$-Überträger eingesetzt. Diese zeigten sogar bei sehr tiefen Temperaturen von –78 °C enorme Reaktivitäten, die jedoch in allen Fällen zu farblosen Zersetzungsprodukten führten (Schema 13; Route C).

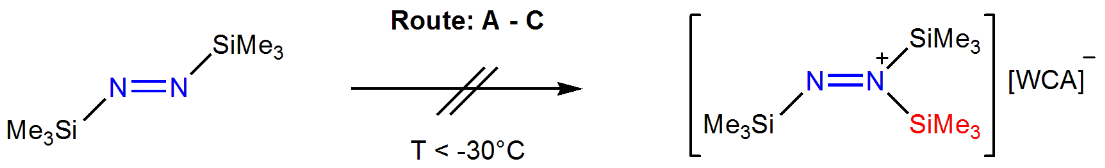

**A:**

+ $Me_3Si$-Cl
+ LS

LS = $GaCl_3$, $SbCl_5$

**B:**

+ Ag[WCA]
+ $Me_3Si$-Z

Z = Cl, I
Solvens: Toluol, $CH_2Cl_2$

**C:**

+ $[Me_3Si \bullet X][WCA]$

1) X = Toluol
Solvens: $CH_2Cl_2$, Toluol

2) X = $Me_3Si$-H
Solvens: $CH_2Cl_2$, Toluol,
*n*-Pentan, $Me_3Si$-F, $Me_3Si$-Cl

3) X = $Me_3Si$-Y
Solvens: $Me_3Si$-Y
Y = F, Cl

***Schema 13.*** Fehlgeschlagene direkte Silylierungen des Bis(trimethylsilyl)diazens (A: [WCA] = $[GaCl_4]$, $[SbF_6]$; B: [WCA] = $[GaCl_4]$, $[SbF_6]$, $[B(C_6F_5)_4]$, $[AsF_6]$; C: $[B(C_6F_5)_4]$, $[CHB_{11}H_5X_6]$, X = Br, Cl).

Da eine direkte Silylierung des Diazenes nicht möglich schien, wurde im Rahmen dieser Arbeit eine neuartige Syntheseroute entwickelt, die zu dem sehr labilen homoleptischen

$[(Me_3Si)_2NNSiMe_3]^+$-Tris(trimethylsilyl)diazenium Kation führen sollte. Hierbei wurden als Edukte die Hydrazinoverbindungen $Hg[(N(SiMe_3)N(SiMe_3)_2]_2$ und $[Bi\{(N(SiMe_3)N(SiMe_3)_2\}_2][GaCl_4]$ gewählt, da sie bereits das gewünschte Hydrazinyl-Strukturmotiv aufweisen. Ausgehend von einer tiefblauen Lösung des Dihydrazinobismutsalzes $[Bi\{(N(SiMe_3)N(SiMe_3)_2\}_2][GaCl_4]$ in Dichlormethan ließ sich tatsächlich mit Hilfe von $GaCl_3$ und den Oxidationsmitteln $Cl_2$ oder $SOCl_2$ das gewünschte Diazenium-Salz in schlechten Ausbeuten isolieren (Schema 14, oben). Die geringen Ausbeuten sind den hohen Reaktivitäten und der damit verbundenen erschwerten Handhabung der Oxidationsmittel geschuldet. Wird jedoch eine auf –80 °C gekühlte farblose Dichlormethan-Lösung des Quecksilber(II)-dihydrazids $Hg[(N(SiMe_3)N(SiMe_3)_2]_2$ mit zwei äquivalenten $Ag[GaCl_4]$ versetzt und auf –40 °C erwärmt, so scheidet sich ein schwarzes Amalgam ab und das tiefblaue $[(Me_3Si)_2NNSiMe_3][GaCl_4]$ (**19**) Salz, welches bei –80 °C auskristallisiert, bildet sich in nahezu quantitativen Ausbeuten. Diese neuartige Reaktion kann als eine Zwei-Elektronen-Oxidation des $[(Me_3Si)_2NNSiMe_3]^-$ zum Diazenium-Kation $[(Me_3Si)_2NNSiMe_3]^+$ aufgefasst werden (Schema 14, unten; Abbildung 8, links).

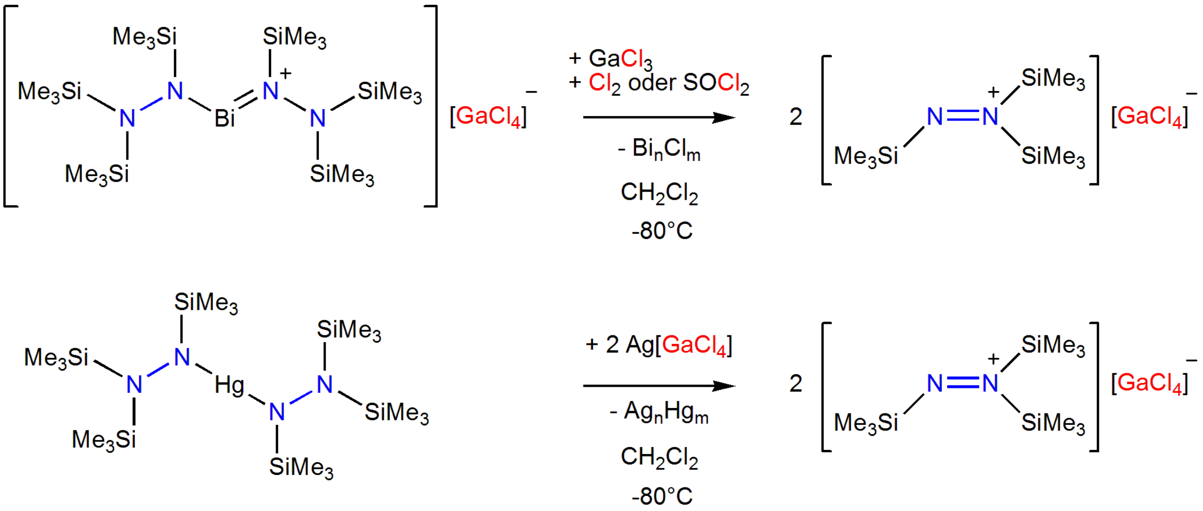
Me3Si
SiMe3
Me3Si
N
N
Bi
N
N
SiMe3
Me3Si
SiMe3
[GaCl4]−
+ GaCl3
+ Cl2 oder SOCl2
- BinClm
CH2Cl2
-80°C
2
N=N
SiMe3
Me3Si
SiMe3
[GaCl4]−
SiMe3
Me3Si
N
N
Hg
SiMe3
N
N
SiMe3
Me3Si
SiMe3
+ 2 Ag[GaCl4]
- AgnHgm
CH2Cl2
-80°C
2
N=N
SiMe3
Me3Si
SiMe3
[GaCl4]−

***Schema 14.*** Synthesen des homoleptischen Diazenium-Salzes über Oxidation von Hydrazinoverbindungen.

### 3.1.3 Synthese von Diazen-Addukten.

Im dritten Themengebiet wurde eine systematische Studie über das Reaktionsverhalten der Diazen-Spezies $Me_3SiNNSiMe_3$ (**4**), $Me_3SiNNPh$ (**5**) sowie PhNNPh (**6**) gegenüber den Lewis-Säuren $[Me_3Si–H–SiMe_3][B(C_6F_5)_4]$, $GaCl_3$ und $B(C_6F_5)_3$ durchgeführt. Dabei bildeten auch die Verbindungen **5** und **6** mit den Silylierungsreagenzien $[Me_3Si–H–SiMe_3][B(C_6F_5)_4]$

und [$Me_3Si \cdot$ Toluol][$B(C_6F_5)_4$] keine definierten Produkte. Im Gegensatz hierzu führten die Reaktionen der neutralen Lewis-Säuren **12** und **13** in Dichlormethan-Lösungen mit den gewählten Diazenen zu definierten Verbindungen. Dabei wurden die Diazene in einer auf –80 °C gekühlten $CH_2Cl_2$ Lösung vorgelegt und die gelösten Lewis-Säuren hinzugetropft. Die Addukt-Bildung konnte unmittelbar durch eine signifikante Farbveränderung beobachtet werden. Die erhaltenen Lösungen wurden nachgerührt, auf Temperaturen oberhalb von –50 °C erwärmt und auf ein minimales Lösungsmittelvolumen eingeengt. Nach erneutem Abkühlen der gesättigten Lösungen konnten die Addukt-Spezies in kristalliner Form in moderaten Ausbeuten isoliert werden (Tabelle 1).

***Tabelle 1.*** Zusammenfassung der isolierten Diazen-Addukte.

| **Lewis-Base** | **Lewis-Säure** | **Addukt** | **Ausbeute** |
|---|---|---|---|
| *trans*-$Me_3SiNNSiMe_3$ | $GaCl_3$ | *trans*-$Me_3SiNNSiMe_3 \cdot GaCl_3$ (**20**) | 80 % |
| *trans*-$Me_3SiNNPh$ | $GaCl_3$ | *trans*-$PhNNSiMe_3 \cdot GaCl_3$ (**21**) | 40 % |
| *trans*-PhNNPh | $GaCl_3$ | *trans*-$PhNNPh \cdot GaCl_3$ (**22**) | 52 % |
| *trans*-$Me_3SiNNSiMe_3$ | $B(C_6F_5)_3$ | *cis*-$Me_3SiNNSiMe_3 \cdot B(C_6F_5)_3$ (**23**) | 32 % |
| *trans*-$Me_3SiNNPh$ | $B(C_6F_5)_3$ | *iso*-$Me_3Si(Ph)NN \cdot B(C_6F_5)_3$ (**24**) | 30 % |
| *trans*-PhNNPh | $B(C_6F_5)_3$ | *cis*-$PhNNPh \cdot B(C_6F_5)_3$ (**25**) | 23 % |

Lediglich das Diphenyldiazen reagierte unter diesen Bedingungen nicht mit dem sterisch anspruchsvollen $B(C_6F_5)_3$. Erst bei Raumtemperatur und in Gegenward von Tageslicht ließ sich eine sehr langsame Reaktion anhand von $^{19}F\{^1H\}$-NMR Spektren beobachten. Jedoch konnte durch den Einsatz von energiereicher ultravioletter Strahlung eine selektive *trans*/*cis*-Isomerie ausgelöst werden. Dies führte innerhalb von drei Stunden zu dem Boran Addukt *cis*-$PhNNPh \cdot B(C_6F_5)_3$ (**25**), dass isoliert und vollständig charakterisiert werden konnte (Abbildung 4).

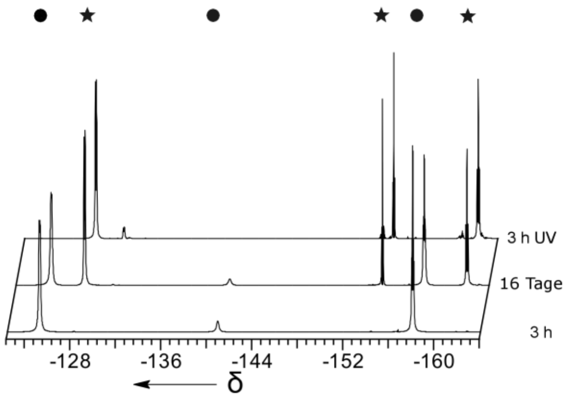

***Abbildung 4.*** Synthese von **25**; $^{19}F\{^1H\}$-NMR Spektren nach 3 h Reaktionszeit (unten), 16 Tagen (mitte) und 3 h Photoaktivierung (oben) mit einer UV-Lampe (366 nm/ 245 nm). Mit Punkt markierte Spezies ist das Edukt ($B(C_6F_5)_3$), der Stern markiert das Produkt **25**.

### 3.1.4 Synthese eines persilylierten Ammonium-Kations

Als letzter Themenabschnitt sollte das Lewis-basische $(Me_3Si)_3N$ (**7**) in das homoleptische $[(Me_3Si)_4N]^+$-Kation überführt werden. Jedoch führten auch hier eine Reihe von Experimenten mit formalen „$[Me_3Si]^+$"-Überträgern $[Me_3Si \cdot \text{Toluol}][B(C_6F_5)_4]$, $[Me_3Si][CHB_{11}H_5Br_6]$ sowie $[Me_3Si][CHB_{11}H_5Cl_6]$ nicht zu dem gewünschten Produkt. Diese Erkenntnis ist im Einklang mit den Beobachtungen von Driess,[57] der analoge Experimente bereits durchgeführt hatte. Da sich das Salz $[Me_3Si \cdot \text{Toluol}][B(C_6F_5)_4]$ während des Trocknens bereits teilweise zersetzt, wurde nach einer Synthesemethode gesucht, mit der sich diese entstehenden Verunreinigungen vermeiden lassen. Zu diesem Zweck wurde $[Me_3Si\text{–}H\text{–}SiMe_3][B(C_6F_5)_4]$-Salz in Toluol dispergiert, wobei die dabei auftretende Gasentwicklung dem Entweichen des bei Raumtemperatur gasförmigen Trimethylsilans zugeschrieben werden kann. Ein vollständiges Entfernen des Silans sollte über ein mehrfaches Entgasen erreicht werden. Das so *in situ* präparierte farblose $[Me_3Si \cdot \text{Toluol}][B(C_6F_5)_4]$ wurde mit dem $(Me_3Si)_3N$ vereint und bis zum Ausbilden eines Zweiphasen-Gemisches auf 70 °C erwärmt. Das langsame Abkühlen auf −40 °C führte überraschenderweise zur Kristallisation des persilylierten Ammonium-Salzes $[(Me_3Si)_3NSi(H)Me_2][B(C_6F_5)_4]$ (**26**). Dieses Produkt kann als Lewis-Säure-Addukt eines Dimethylsilylium-Kations mit dem Tris(trimethylsilyl)amin aufgefasst werden (Abbildung 9). Im Rahmen einer grundlegenden Untersuchung der Edukte und ihrer Synthese konnte ein bisher versteckt ablaufender durch Silylium-Kationen katalysierter Umverteilungsprozess an Alkylsilanen als Ursache für den Verlust der Methylgruppe aufgedeckt werden (siehe Abschnitt 3.4.3).

## 3.2 Strukturanalyse der Lewis-Säure-Base-Addukte

Alle im vorherigen Abschnitt beschriebenen Addukt-Spezies konnten anhand von geeigneten Einkristallen einer Strukturanalyse unter zogen werden. Auf deren Grundlage lassen sich weitreichende Struktur-Eigenschafts-Beziehungen erkennen und ein allgemeines Verständnis über inter- und intramolekulare Wechselwirkungen im Festkörper erlangen. Für einen direkten Vergleich der Bindungssituationen werden in der Regel literaturbekannte Referenzverbindungen oder berechnete, allgemeinere Summen der Kovalenz bzw. Van-der-Waals-Radien herangezogen. In dieser Arbeit wurden die Kovalenzradien (Tabelle 2) für einen Vergleich der Grundlegenden Arbeit von Pekka Pyykkö entnommen.[79] Zusätzlich wurden alle in dieser Arbeit diskutierten Verbindungen einer quantenmechanischen Analyse unterzogen um ein näheres Verständnis der Bindungssituationen und Ladungsverteilungen zu erlangen. Die Berechnungen wurden, wie in den Publikationen angegeben, in *Gaussian 03/09* mit den DFT-Methoden b3lyp und pbe1pbe in Kombination mit den Basissätzen 6-31G(d,p), aug-cc-pVDZ und aug-cc-pwVDZ durchgeführt.[80–87]

***Tabelle 2.*** Summe der NX-Kovalenzradien nach P. Pyykkö.[79]

| X | **$\sum r_{kov}$(N–X)** | **$\sum r_{kov}$(N=X)** | **$\sum r_{kov}$(N≡X)** |
|---|---|---|---|
| N | 1.42 | 1.20 | 1.08 |
| C | 1.46 | 1.27 | 1.14 |
| B | 1.56 | 1.38 | 1.27 |
| Si | 1.87 | 1.67 | 1.56 |
| Ga | 1.95 | 1.77 | 1.75 |

Der Einfluss der Adduktbildung auf die Struktur der Lewis-Base sowie wesentliche Unterschiede ausgewählter Spezies soll im Folgenden zusammenfassend diskutiert werden. In Abbildung 5 sind die Verknüpfungen der in dieser Arbeit diskutierten Verbindungen veranschaulicht.

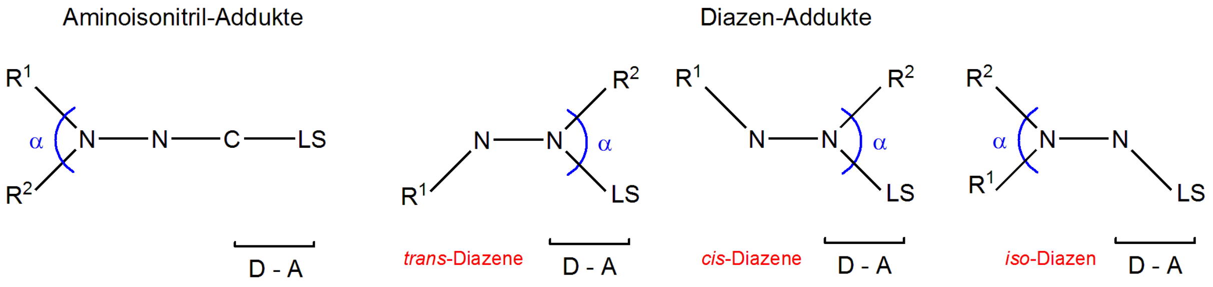

***Abbildung 5.*** Verknüpfungsschemata der Aminoisonitril- und Diazen-Addukte (R$^1$, R$^2$ = $Me_3Si$ in Aminoisonitrilen, **4**, **20**, **23** **19**; R$^1$ = $Me_3Si$, R$^2$ = Ph in **5**, **21**, **24**; R$^1$, R$^2$ = Ph in **6**, **22**, **25**).

Die wesentlichen Strukturparameter der eingesetzten Lewis-Basen und deren isolierten Addukt-Spezies sind in Tabelle 3 zusammengetragen. Es zeigt sich deutlich, dass sich alle dreifachkoordinierten Stickstoff-Atome in einer planaren Koordinations-Umgebung (Σ<N> = 360-358°) befinden, was auf eine Hyperkonjugation des nichtbindenden Elektronen-Paares des zweifachkoordinierten Stickstoffes in die parallelen NSi und SiC σ*-Orbitale, beziehungsweise im Falle der Phenyl-Diazene auf eine Konjugation mit dem π-Elektronensystem der Phenyl-Substituenten, zurückzuführen ist (Tabelle 3).

***Tabelle 3.*** Ausgewählte Strukturparameter der Lewis-Basen und ihrer isolierten Addukt-Spezies. Bindungslängen in Å, Bindungswinkel in °.

| Verbindung | N–N | D–A | R$^1$–N | R$^2$–N | α[a] | ∑<N> |
|---|---|---|---|---|---|---|
| $(Me_3Si)_2CNN$[b,c] (**1**) | 1.135(2) | - | 1.855(2) | 1.852(2) | 130.5(2) | 359.9 |
| $(Me_3Si)_2NNC$ (**2**) | 1.366(2) | - | 1.777(2) | 1.774(2) | 131.5(2) | 359.6 |
| $Me_3SiNCNSiMe_3$[d] (**3**) | - | - | 1.777(2) | 1.777(2) | - | - |
| *trans*-$Me_3SiNNSiMe_3$[e] (**4**) | 1.227(2) | - | 1.807(3) | 1.807(3) | - | - |
| *trans*-$Me_3SiNNPh$[f] (**5**) | 1.238(2) | - | 1.804(1) | 1.447(2) | - | - |
| *trans*-PhNNPh[g] (**6**) | 1.249(4) | - | 1.431(4) | 1.431(4) | - | - |
| $(Me_3Si)_3N$[h] (**7**) | - | - | 1.755(3) | 1.755(3) | 120 | 360 |
| $[(Me_3Si)_2NCNSiMe_3][B(C_6F_5)_4]$ (**14**) | - | 1.795(2) | 1.835(2) | 1.838(2) | 128.9(2) | 360.0 |
| $[(Me_3Si)_2NNCSiMe_3][B(C_6F_5)_4]$ (**15[Boran]**) | 1.309(2) | 1.897(2) | 1.818(2) | 1.816(2) | 131.3(2) | 360.0 |
| $[(Me_3Si)_2NNCSiMe_3][CHB_{11}H_5Br_6]$ (**15[CB]**) | 1.309(3) | 1.901(3) | 1.816(3) | 1.809(3) | 129.4(2) | 360.0 |
| $[(Me_3Si)_2NNCCPh_3][B(C_6F_5)_4]$ (**18**) | 1.334(4) | 1.480(4) | 1.823(3) | 1.818(3) | 132.6(2) | 357.8 |
| $(Me_3Si)_2NNCB(C_6F_5)_3$ (**17**) | 1.331(2) | 1.617(2) | 1.805(1) | 1.805(1) | 133.4(2) | 359.8 |
| *trans*-$Me_3SiNNSiMe_3 \cdot GaCl_3$ (**20**) | 1.243(2) | 2.036(2) | 1.884(2) | 1.826(2) | 121.5(2) | 360.0 |
| *trans*-$PhNNSiMe_3 \cdot GaCl_3$ (**21**) | 1.249(2) | 2.042(2) | 1.885(2) | 1.413(3) | 122.8(2) | 358.2 |
| *trans*-$PhNNPh \cdot GaCl_3$ (**22**) | 1.254(4) | 2.064(3) | 1.460(4) | 1.414(4) | 115.8(2) | 358.6 |
| *cis*-$Me_3SiNNSiMe_3 \cdot B(C_6F_5)_3$ (**23**) | 1.242(2) | 1.643(2) | 1.885(2) | 1.801(2) | 125.6(2) | 359.1 |
| *iso*-$Me_3Si(Ph)NN \cdot B(C_6F_5)_3$ (**24**) | 1.243(2) | 1.591(2) | 1.888(2) | 1.461(2) | 121.0(2) | 360.0 |
| *cis*-$PhNNPh \cdot B(C_6F_5)_3$ (**25**) | 1.263(4) | 1.657(5) | 1.465(5) | 1.414(4) | 119.5(3) | 359.7 |
| $[(Me_3Si)_2NNSiMe_3][GaCl_4]$ (**19**) | 1.254(2) | 1.894(2) | 1.899(2) | 1.829(2) | 124.1(2) | 359.9 |
| $[(Me_3Si)_3NSi(H)Me_2][B(C_6F_5)_4]$[i] (**26**) | - | 1.870(2) | 1.889(2) | 1.899(2) | - | 330.5 |

[a] Bei Pseudochalkogenen und deren Addukten gilt R = $Me_3Si$, Y = $SiMe_3$; Bei Diazen-Addukten Y = LS, R = $Me_3Si$ oder Ph, [b] R$^1$-C, R$^2$-C und Si-C-Si angegeben, [c] Strukturdaten des ersten Moleküls in der asymmetrischen Einheit, [d] Entnommen aus Referenz [78], [e] Nur Strukturdaten des Teiles A mit größter Besetzung des fehlgeordneten Moleküls sind aufgeführt, [f] wie in [e] wobei gilt R$^1$ = $SiMe_3$, R$^2$ = Ph, [g] Entnommen aus Referenz [79], [h] Gas-Phasen-Struktur entnommen aus Referenz [80], [i] Hier ist Dimethylsilylium als Lewis-Säure angegeben.

### 3.2.1 Strukturanalysen der Lewis-Basen

Es finden sich im $(Me_3Si)_2CNN$ ein sehr kurzer NN-Abstand mit 1.135(2) Å und eine wesentlich längere CN-Bindung mit 1.312(2) Å. Eine gegenteilige Bindungssituation findet sich im $(Me_3Si)_2NNC$ wieder, bei dem der NN Abstand mit 1.366(2) Å im Bereich einer polarisierten Einfachbindung liegt und der sehr kurze CN-Abstand von 1.152(2) Å auf einen deutlichen Dreifach-Bindungscharakter hinweist. Anhand der Strukturlösungen der Silyl-Diazen-Spezies konnte nachgewiesen werden, dass auch die Derivate $Me_3SiNNSiMe_3$ und $Me_3SiNNPh$ einer Positionsfehlordnung entlang der R–N=N–R‘ Bindung unterliegen (Abbildung 6). Diese wurde erstmals 1997 von Ogawa *et al.*[88] an dem Diphenyldiazen berücksichtigt, diese Fehlordnung wurde in der 1974 von Bärnighausen und Veith publizierten Struktur des $Me_3SiNNSiMe_3$ nicht bedacht, welches zu einem jahrzehntelang kontrovers diskutierten kurzen NN-Abstand von 1.171(7) Å führte.[89]

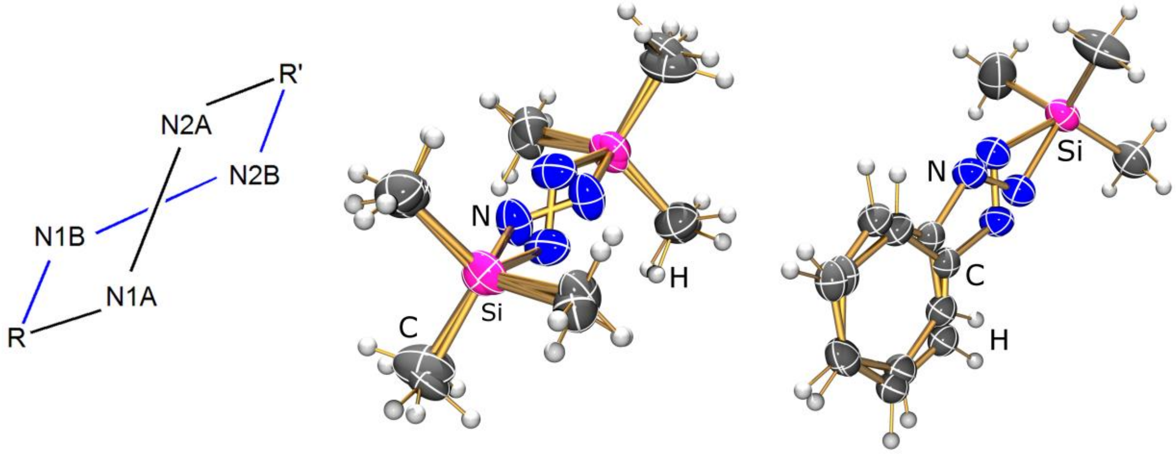

***Abbildung 6.*** Darstellung der Positionsfehlordnung in den Silyl-substituierten-Diazenen.

Die drei Diazen-Spezies zeichnen sich mit NN-Bindungslängen zwischen 1.249(4) in PhNNPh und 1.227(2) Å in $Me_3SiNNSiMe_3$ durch einen deutlichen Doppelbindungscharakter aus und liegen in ihrem Grundzustand als *trans*-Diazen-Spezies vor. Es ist auffällig, dass sich mit zunehmender Silylierung der NN-Abstand verkürzt, dies ist im Einklang mit einer NBO-Analyse die einen deutlichen Ladungszuwachs in der NN-Einheit aufzeigt (*cf*. PhNNPh*:* $q(N1) + q(N2) = -0.394$, $Me_3SiNNPh$: −0.757, $Me_3SiNNSiMe_3$: −1.106 e).

### 3.2.2 Strukturanalyse der Aminoisonitril-Addukte

In allen Bis(trimethysilyl)aminoisonitril-Addukten bleibt die Zentrale NNC-Einheit mit Winkeln zwischen 179.3(1)° in $[(Me_3Si)_2NNCSiMe_3][B(C_6F_5)_4]$ und 177.7(1)° in $(Me_3Si)_2NNCB(C_6F_5)_3$ nahezu linear und unverändert durch die Adduktbildung (*cf.* 177.7(2)° in $(Me_3Si)_2NNC$). Es lässt sich deutlich erkennen, dass die Bindungen zu den $Me_3Si$-Substituenten in den Addukten im Vergleich zur freien Lewis-Base aufgeweitet werden (*cf.* maximal 0.046 Å in $[(Me_3Si)_2NNCCPh_3][B(C_6F_5)_4]$ und minimal 0.031 Å in $(Me_3Si)_2NNCB(C_6F_5)_3$) dies lässt sich mit dem Ladungstransfer aus der Zentralen NNC-Gruppe auf die Lewis-Säure erklären. Die NN-Bindungen sind mit 1.309(2) Å in $[(Me_3Si)_2NNCSiMe_3][B(C_6F_5)_4]$ und 1.334(4) Å in $[(Me_3Si)_2NNCCPh_3][B(C_6F_5)_4]$ im Vergleich zur freien Lewis-Base mit 1.366(2) Å in $(Me_3Si)_2NNC$ leicht verkürzt, und liegen zwischen einer NN-Einfach- und Doppelbindung, was auf einen partiellen Doppelbindungscharakter und eine Polarisation der Bindung hinweist.

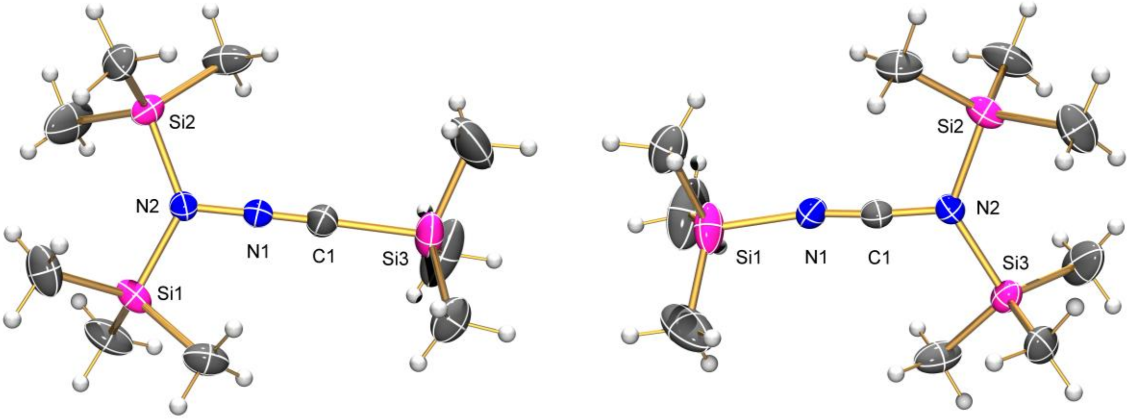

***Abbildung 7.*** ORTEP Darstellung der Pseudochalkogonium-Kationenstrukturen von **15** (links) und **14** (rechts). Die thermischen Ellipsoide entsprechen 50% Aufenthaltswahrscheinlichkeit bei 173 K.

Die sehr kurzen CN-Bindungslängen mit 1.143(2) Å in **15[Boran]**, 1.147(4) Å in **15[CB]**, 1.145(2) Å in **17** und 1.145(4) in **18** sprechen unmissverständlich für eine Dreifachbindung, die durch die Adduktbildung im Vergleich zum Aminoisonitril nur minimal verkürzt wird. (*cf*. 1.152(2) in $(Me_3Si)_2NNC$). Diese Beobachtungen weisen auf einen nahezu nichtbindenden Charakter des freien Elektronenpaares am Kohlenstoffzentrum hin, welches in die Addukt-Bindung involviert ist. Auf dieser Grundlage lassen sich die beschriebenen Addukte am besten durch die Lewis-Formel $[(Me_3Si)_2N{-}N^{+}{\equiv}C{-}LS^{-}]$ beschreiben. Beim Vergleich der beiden Kationen-Strukturen der Salze **15[Boran]** und **15[CB]** ist auffällig, dass diese im Rahmen der dreifachen Standardabweichung identisch sind. Dies bestätigt die schwach koordinierenden Eigenschaften der $[B(C_6F_5)_4]^{-}$- und $[CHB_{11}H_5Br_6]^{-}$-Anionen, die keine strukturbestimmenden Wechselwirkungen mit dem Kation eingehen.

### 3.2.3 Strukturanalyse der Diazen-Addukte

Die Strukturanalysen der Diazene zeigen deutlich, dass die Diazen-Einheit im Falle der Galliumtrichlorid-Addukte in ihrer *trans*-Konfiguration erhalten bleibt. Im deutlichen Gegensatz hierzu konnten die Addukte des sterisch anspruchsvollen Tris(pentafluorphenyl)borans nur als *cis*-$Me_3SiNNSiMe_3 \cdot B(C_6F_5)_3$, *cis*-$PhNNPh \cdot B(C_6F_5)_3$ sowie *iso*-$Me_3Si(Ph)NN \cdot B(C_6F_5)_3$ (Abbildung 8, rechts) isoliert werden. Diese ungewöhnliche Isomerisierung und ihre daraus folgende Reaktivität der Silyl-Diazen-Addukte wurde auf der Grundlage quantenchemischer Berechnungen und experimenteller Arbeiten näher untersucht. (Siehe Abschnitt 3.4.2, Seite 28).

Wie den Strukturdaten unmissverständlich zu entnehmen ist, enthalten alle Diazen-Addukt-Spezies ein nahezu planares $N_2R^1R^2E$-Gerüst ($R^{1,2}$ = Ph, $Me_3Si$; E = Ga, B, Si) mit der größten Abweichung von 22.5° im *trans*-PhNNPh · $GaCl_3$ und der kleinsten Abweichung von 4.67° im $[(Me_3Si)_2NNSiMe_3]^+$. Des Weiteren ist auffällig, dass die $R^1$-N-Bindungen am dreifachkoordinierten Stickstoff im Vergleich zu den freien Lewis-Basen aufgeweitet wird (*cf.* maximal 0.09 Å in $[(Me_3Si)_2NNSiMe_3][GaCl_4]$ und minimal 0.03 Å in *trans*-PhNNPh · $GaCl_3$). Dies lässt sich sowohl mit dem Ladungstransfer der zentralen NN-Gruppe auf die Lewis-Säure sowie dem sterischen Anspruch des zusätzlichen Substituenten erklären. Im Gegensatz hierzu verkürzt sich die $R^2$-N-Bindung am zweifachkoordinierten Stickstoff der Phenyl-substituierten Diazen-Addukte um bis zu 0.03 Å im *trans*-$PhNNSiMe_3$ · $GaCl_3$. Als Ursache kann die nach NBO-Analysen um 5 kcal/mol begünstigte Delokalisation von π-Elektronen des Phenyl-Substituenten in das konjugierte $\pi^*_{NN}$-Orbital der NN-Einheit der Addukte angesehen werden. (Tabelle 3).

Als charakteristisches Merkmal bleibt die Stickstoff-Stickstoff-Bindung, die sowohl in allen neutralen Diazen-Addukten (z.B. 1.242(2) Å für *cis*-$Me_3SiNNSiMe_3$ · $B(C_6F_5)_3$) sowie im Diazenium-Kation mit 1.254(2) Å am besten als Doppelbindung beschrieben werden kann (Tabelle 3). Die NN-Bindung der Addukte wird im Vergleich zu ihren *trans*-Diazenen nur geringfügig aufgeweitet (*cf.* 0.016 Å in *trans*-$Me_3SiNNSiMe_3$ · $GaCl_3$ und 0.005 Å in *iso*-$Me_3Si(Ph)NN$ · $B(C_6F_5)_3$). Dies weist, im Einklang mit NBO-Analysen, auf einen nahezu nichtbindenden Charakter des freien Elektronenpaares am Stickstoffzentrum hin, welches in die Addukt-Bindung involviert ist. Die Stickstoff-Gallium-Donor-Acceptor-Bindungen liegen mit 2.036(2) in **20**, 2.042(2) in **21** und 2.064(3) Å in **22** in dem erwarteten Bereich für ein Gallium-Stickstoff-Addukt[90] und sind im Einklang mit vergleichbaren Verbindungen (*cf.* 1.965(2) Å in $Me_3SiNSNSiMe_3$ · $GaCl_3$).[42] In dieser Reihe lässt sich erkennen, dass sich mit zunehmender Silylierung am Diazen sowohl die NN- als auch die NGa-Bindung verkürzt. Betrachtet man die Donor-Acceptor-Bindungen der Boran-Addukte, fällt deutlich auf, dass das *iso*-Diazen-Addukt mit 1.591(2) Å verglichen mit 1.657(5) Å in *cis*-PhNNPh · $B(C_6F_5)_3$ und 1.643(2) Å in *cis*-$Me_3SiNNSiMe_3$ · $B(C_6F_5)_3$ eine wesentlich kürzere Bindung aufweist (*cf.* 1.616(3) Å in MeCN · $B(C_6F_5)_3$,[49]). Dies kann der geringeren sterischen Hinderung am *iso*-Diazen zugeschrieben werden und führt zu einem größeren Ladungstransfer vom Diazen auf die Lewis-Säure ($Q_{CT}$ : 0.354 in *cis*-PhNNPh · $B(C_6F_5)_3$, 0.353 in *cis*-$Me_3SiNNSiMe_3$ · $B(C_6F_5)_3$ und 0.426 *e* in *iso*-$Me_3Si(Ph)NN$ · $B(C_6F_5)_3$).

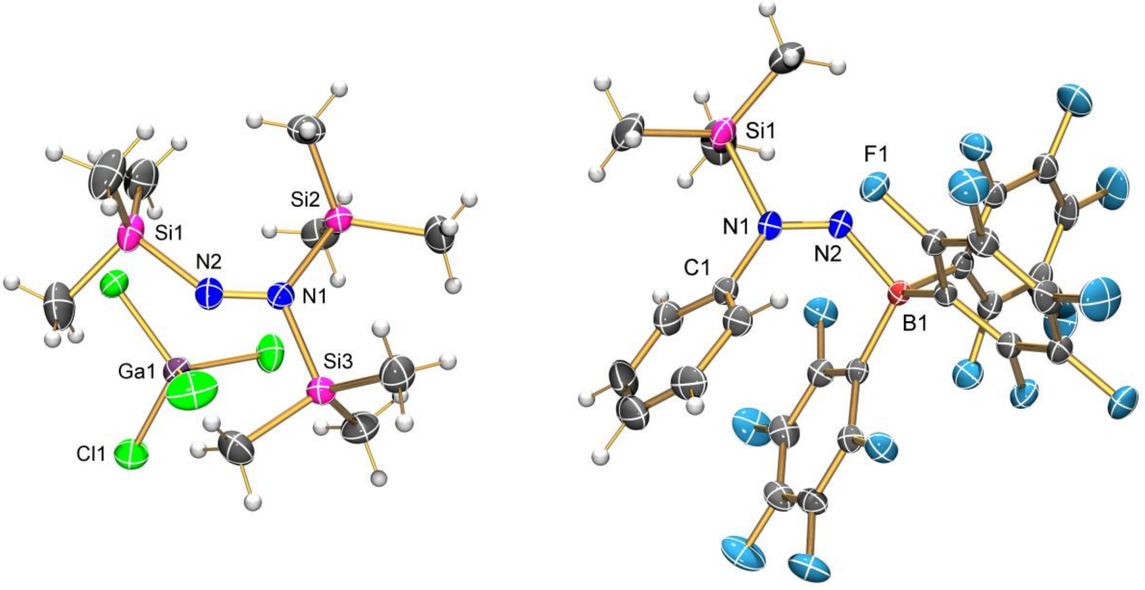

***Abbildung 8.*** ORTEP-Darstellung von **19** (links) und **24** (rechts). Die thermischen Ellipsoide entsprechen 50% Aufenthaltswahrscheinlichkeit bei 173 K.

Betrachtet man die Bindungssituation im Diazenium-Salz $[(Me_3Si)_2NNSiMe_3][GaCl_4]$ (Abbildung 8, links), so kann dieses formal als das *trans*-Bis(trimethylsilyl)diazen-Addukt des Trimetylsilylium-Kations aufgefasst werden. Es liegen weder besonders kurze Anionen-Kationen-Abstände noch bemerkenswerte Anionen-Anionen-Kontakte vor. Trotz seiner Sonderstellung bezüglich der Synthese und seiner positiven Ladung reiht es sich in die Diazen-Addukte ein und zeigt keine wesentlichen strukturellen Ausreißer.

### 3.2.4 Struktur des persilylierten Ammonium-Kations

Das Salz des persilylierten Ammonium-Kations $[(Me_3Si)_3NSi(H)Me_2][B(C_6F_5)_4]$ zeigt ebenfalls weder bemerkenswerte Anionen-Kationen- noch Anionen-Anionen-Kontakte. Die beobachtete Struktur des Kations enthält, wie erwartet, ein nahezu tetraedrischkoordiniertes Stickstoffatom mit SiNSi-Winkeln zwischen 106.32(2)° und 112.27(2)° (Abbildung 9). Im Vergleich zu den von Driess publizierten Stukturen des Phosphoniums und Arsoniums fällt auf, dass die Abweichungen vom idealen Tetraederwinkel 109.4° in der Reihe $N > P > As$ abnehmen (*cf.* SiPSi 107.30(7)° - 111.06(7)° in $[(Me_3Si)_4P]^+$, SiAsSi 108.8(1)° - 110.0(1)° in $[(Me_3Si)_4As]^+$). Dies kann den in gleicher Weise wachsenden kovalenten Pniktogen-Silicium-Bindungen zugeschrieben werden, was zu einer geringeren sterischen Spannung dieser Systeme und dem annähern an die ideale Tetraederkoordination führt. Die NSi-Bindungen von **26** (NSi1 1.889(2), NSi2 1.899(2), NSi3 1.891(2), NSi4 1.870(2) Å) sind in guter Übereinstimmung mit denen im persilylierten Diazenium-Kation $[(Me_3Si)_2NN(SiMe_3)]^+$ (*cf.* 1.829(1), 1.894(1), 1.899(1) Å). Im Vergleich mit der literaturbekannten Gasphasen-Struktur des $(Me_3Si)_3N$,[91] in dem der Stickstoff in einer planaren Umgebung mit drei gleich langen NSi-Abständen von 1.755(3) Å zu finden ist, weiten sich die NSi-Bindungen um bis zu 0.144 Å durch die Adduktbildung auf. Bemerkenswert ist, dass die NSi4 Bindung der Dimethylsilygruppe als Folge des geringeren Raumanspruches signifikant kürzer ist als die der Trimethylsilyl-Gruppen.

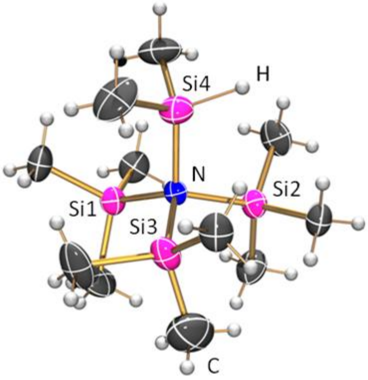

***Abbildung 9.*** ORTEP-Darstellung der Kationenstruktur von **26**. Die thermischen Ellipsoide entsprechen 50% Aufenthaltswahrscheinlichkeit bei 173 K.

## 3.3 Allgemeine Eigenschaften der Addukte

Alle Verbindungen können in größeren Mengen dargestellt werden und lassen sich für einen längeren Zeitraum lagern, vorausgesetzt sie werden unter einer Argon-Schutzgas-Atmosphäre, gekühlt und unter Lichtausschluss aufbewahrt. Alle Verbindungen weisen gute bis mäßige Löslichkeit und Stabilität in Toluol auf. Im Gegensatz hierzu, zersetzen sich die persilylierten Verbindungen $[(Me_3Si)_2NNSiMe_3][GaCl_4]$ und $[(Me_3Si)_3NSi(H)Me_2][B(C_6F_5)_4]$ augenblicklich in Dichlormethan Lösungen bei Raumtemperatur, selbst die neutralen Addukte wie z.B. *trans*-PhNNPh · $GaCl_3$ zeigen sich nicht über einen längeren Zeitraum tolerant gegenüber diesen Bedingungen. In kristalliner Substanz zeigen sich die isolierten Donor-Acceptor-Verbindungen, mit Ausnahme der Verbindungen **19**, **20** und **21,** mit ihren Zersetzungspunkten oberhalb von 100 °C erstaunlich thermisch stabil (Tabelle 4). Bemerkenswert hierbei ist, dass der Austausch des $[B(C_6F_5)_4]^-$-Anions gegen das $[CHB_{11}H_5Br_6]^-$-Anion in den Pseudochalkogonium Salzen $[(Me_3Si)_2NNCSiMe_3]^+$ einen um

97 °C höheren Zersetzungspunkt induziert. Daraus lässt sich schließen, dass in den vorliegenden Salzen die thermische Stabilität des Anions einen maßgeblichen Einfluss auf deren Zersetzungstemperaturen besitzt. Beim Vergleich der $GaCl_3$-Addukte mit ihren verwandten $B(C_6F_5)_3$-Addukten fällt auf, dass die sterisch anspruchsvolle Lewis-Säure $B(C_6F_5)_3$ die Addukt-Spezies kinetisch stabilisiert was zu höheren Zersetzungstemperaturen führt. Die Verbindungen *trans*-$Me_3SiNNSiMe_3 \cdot GaCl_3$, *trans*-$PhNNSiMe_3 \cdot GaCl_3$ und $[(Me_3Si)_2NNSiMe_3][GaCl_4]$ sind sehr labil und zersetzen sich bereits bei Temperaturen unterhalb von −20 °C und konnten aus diesem Grund nur auf Basis aufwendiger Tieftemperatur-Einkristalldiffraktometrie sowie NMR- und Raman-Spektroskopie charakterisiert werden. Es liegt der Schluss nahe, dass die direkte Nachbarschaft einer GaCl Bindung zu einer NSi Bindung das Abspalten von $N_2$ und $Me_3SiCl$ aus diesen Verbindungen begünstigt. Hinzu kommt wie bereits 1970 von N. Wiberg beschrieben, dass die Trimethylsilyl-Substituenten zu einer Erhöhung der $n_N$ (HOMO) und Erniedrigung der $\pi^*_{NN}$ (LUMO) Energien führen, was sowohl die bathochrome Verschiebung der Diazen-Absorptions-Banden als auch eine höhere Reaktivität nach sich zieht.[92] Es lässt sich eindrucksvoll erkennen, dass durch die Adduktbildung der Diazene die Energiedifferenz zwischen dem HOMO und LUMO wieder aufgeweitet wird, was zu einer hypsochromen Farbänderung führt (*cf.* $Me_3SiNNSiMe_3$ hellblau → $[(Me_3Si)_2NNSiMe_3][GaCl_4]$ dunkelblau; $Me_3SiNNPh$ dunkelblau → *trans*-$PhNNSiMe_3 \cdot GaCl_3$ orange; Tabelle 4).

***Tabelle 4.*** Zusammenfassung ausgewählter Eigenschaften der isolierten Addukte.

| **Verbindung** | **$T_{Zers}$/ °C** | **Farbe** | **$^{11}$B-NMR/ ppm** | **IR/Raman ($\tilde{\nu}_{NN}$)/ cm$^{-1}$** |
|---|---|---|---|---|
| $[(Me_3Si)_2NCNSiMe_3][B(C_6F_5)_4]$ (**14**) | 106 | farblos | −16.6 | - |
| $[(Me_3Si)_2NNCSiMe_3][B(C_6F_5)_4]$ (**15[Boran]**) | 109 | farblos | −16.6 | 1081 |
| $[(Me_3Si)_2NNCSiMe_3][CHB_{11}H_5Br_6]$ (**15[CB]**) | 206 | farblos | −20.2 (d, 5 BH)<br>−9.8 (s, 5 BBr)<br>−1.7 (s, 1 BBr) | 1113/1053 |
| $[(Me_3Si)_2NNCCPh_3][B(C_6F_5)_4]$ (**18**) | 136 | gelb | −16.6 | 1084/1033 |
| $(Me_3Si)_2NNCB(C_6F_5)_3$ (**17**) | 124 | farblos | −20.3 | 1095/1029 |
| *trans*-$Me_3SiNNSiMe_3{\cdot}GaCl_3$ (**20**) | −20 | blau | - | 1568 |
| *trans*-$PhNNSiMe_3{\cdot}GaCl_3$ (**21**) | −20 | orange | - | 1479 |
| *trans*-$PhNNPh{\cdot}GaCl_3$ (**22**) | 108 | orange | - | 1463 |
| *cis*-$Me_3SiNNSiMe_3{\cdot}B(C_6F_5)_3$ (**23**) | 127 | blau | 0.8 | 1593 |
| *iso*-$Me_3Si(Ph)NN{\cdot}B(C_6F_5)_3$ (**24**) | 104 | orange | −4.4 | 1556 |
| *cis*-$PhNNPh{\cdot}B(C_6F_5)_3$ (**25**) | 168 | orange | −0.2 | 1516 |
| $[(Me_3Si)_2NNSiMe_3][GaCl_4]$ (**19**) | −30 | blau | - | 1570 |
| $[(Me_3Si)_3NSi(H)Me_2][B(C_6F_5)_4]$ (**26**) | 152 | farblos | −17.0 | - |

Im Vergleich zu den für ihre Farbigkeit berühmten Diazenen (Azoverbindungen) zeichnen sich die isolierten Aminoisonitril-Addukte nicht durch eine besondere Farbgebung aus. Dies ist im Einklang mit den beobachteten langen NN-Bindungen sowie den Infrarot-Schwingungs-Banden die im Bereich von 1029 und 1113 $cm^{-1}$ zu finden sind und für eine NN-Einfachbindung sprechen (*cf.* $\tilde{\nu}_{NN} = 1031,\ 1120\ cm^{-1}$ in $(Me_3Si)_2NNC$). Im Gegensatz hierzu zeigen alle Raman-Spektren der Diazen-Spezies signifikante Banden im Bereich zwischen 1463 und 1593 $cm^{-1}$, die den Schwingungen einer NN-Doppelbindung zuzuordnen sind (*cf.* $\tilde{\nu}_{NN} = 1555\ cm^{-1}$ in $Me_3SiNNSiMe_3$ und $\tilde{\nu}_{NN} = 1491\ cm^{-1}$ in PhNNPh). Gestützt durch eine quantenchemische Analyse der Schwingungsdaten konnte gezeigt werden, dass die Adduktbildung keinen einheitlichen Einfluss auf die NN-Schwingungen hat, was darauf zurückzuführen ist, dass das in die Addukt-Bindung involvierte Elektronenpaar einen hohen nichtbindenden Charakter besitzt. Im Rahmen dieser Analyse wurde zudem deutlich, dass die Konfiguration der Substituenten an den Diazenen einen größeren Einfluss auf die Lage der NN-Banden besitzt als das Ausbilden der Donor-Acceptor-Bindung (*cf.* 1667 in *cis*-$Me_3SiNNSiMe_3$, 1592 in *trans*-$Me_3SiNNSiMe_3$, 1464 $cm^{-1}$ in *iso*-$(Me_3Si)_2NN$).

Die $^{11}B$-NMR Spektroskopie ist eine geeignete Methode um zwischen dreifach- und vierfachkoordinierten Bor-Atomen zu unterscheiden.[48] So findet sich in den Salzen des $[B(C_6F_5)_4]^-$ eine Resonanz bei $\delta[^{11}B] = -16.8 \pm 2$ ppm die charakteristisch für das Tetrakis(pentafluorophenyl)borat Anion ist, auch das $[CHB_{11}H_5Br_6]^-$ lässt sich anhand der drei charakteristischen Signale ($\delta[^{11}B] = -20.2$, $-9.8$ und $-1.7$) eindeutig identifizieren. Als nützliches Hilfsmittel während der Synthese dient die $^{11}B$-NMR Spektroskopie, da während der Adduktbildung die Resonanz der freien Lewis-Säure $B(C_6F_5)_3$ (*cf.* $\delta[^{11}B] = 59.1$ ppm in $CD_2Cl_2$) stark hochfeld verschoben wird und sich so der Reaktionsverlauf gut beobachten lässt (Tabelle 4). Dieser Shift der $\delta[^{11}B]$ Verschiebungen der neutralen $B(C_6F_5)_3$-Addukte zeigt eine direkte Proportionalität zu dem Ladungstransfer der Lewis-Base, so findet sich das $(Me_3Si)_2NNCB(C_6F_5)_3$ mit dem größten $Q_{CT}$ von 0.576 am stärksten hochfeld verschoben bei $\delta[^{11}B] = -20.3$ ppm wieder.

## 3.4 Folgereaktionen aktivierter Lewis-Basen

Da die Aktivierung der Lewis-Basen durch Adduktbildung ein wesentlicher Bestandteil dieser Arbeit war, soll im folgenden Abschnitt auf die näher untersuchten Folgereaktionen eingegangen werden.

### 3.4.1 Trimerisation von Bis(silyl)diazomethan und Bis(silyl)aminoisonitril

Wie bereits im Abschnitt 3.1.1 beschrieben wurde, konnte kein direktes Silylium-Addukt des Bis(trimethylsily)diazomethans $[(Me_3Si)_2CNNSiMe_3]^+$ isoliert werden, statt dessen wird ausschließlich das isomere Bis(trimethylsily)aminoisonitril Addukt $[(Me_3Si)_2NNCSiMe_3]^+$ nach Umkristallisation isoliert. In einer grundlegenden Arbeit von Seyfert wurde gezeigt, dass sich reines $(Me_3Si)_2CNN$ in Gegenwart von katalytischen Mengen $Cu^{2+}$ zu dem isomeren $Me_3SiNCNSiMe_3$ Umlagert, jedoch wurde keine Isomerisierung zum Aminoisonitril unter diesen Bedingungen beobachtet.[72] Das aktivierte $[(Me_3Si)_2NNCSiMe_3]^+$ katalysiert in Gegenwart eines Überschusses an **1** oder **2** eine bemerkenswerte Trimerisation zum Pyrazolderivat **16** (Schema 15).

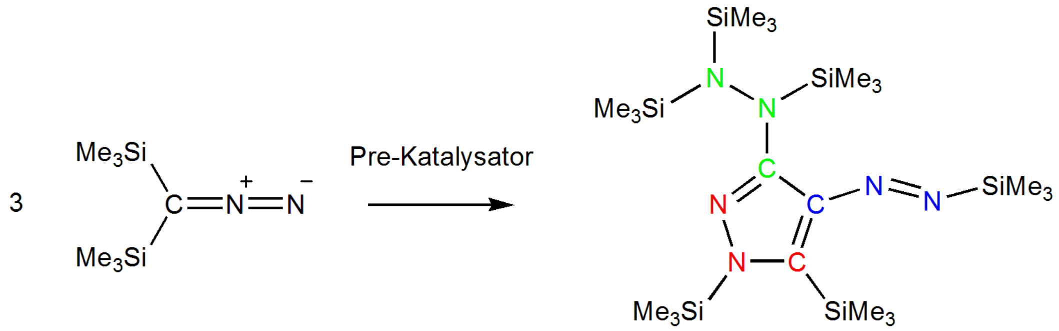

***Schema 15.*** Trimerization von **1** zum Pytrazolderivat (**16**).

Bei einer tiefgreifenden Studie konnte gezeigt werden, dass die Trimerisation von **2** durch eine Reihe von Super-Lewis-Säuren als Pre-Katalysatoren in guten bis mäßigen Umsätzen katalysiert wird. Bemerkenswert ist hierbei, dass sowohl die klassische Lewis-Säure $GaCl_3$ als auch das Silbersalz $Ag[CHB_{11}H_5Br_6]$ diesen Prozess nicht begünstigen (Tabelle 5).

***Tabelle 5.*** Als Pre-Katalysatoren der Trimerisation identifizierte Lewis-Säuren.

| Pre-Katalysator | mol% cat. | Umsatz | Zeit / min | TON[a] |
|---|---|---|---|---|
| $[Me_3Si{-}H{-}SiMe_3][B(C_6F_5)_4]$ | 1.0 | 0.92 | 1080 | 92 |
| $[Me_3Si][CHB_{11}H_5Br_5]$ | 2.0 | 0.90 | 180 | 45 |
| $[(Et_2O)_2H][B(C_6F_5)_4]$ | 1.2 | 0.84 | 30 | 72 |
| $[Me_3SiOEt_2][B(C_6F_5)]$ | 1.3 | 0.74 | 30 | 59 |
| $B(C_6F_5)_3$ | 1.9 | 0.84 | 14400 | 45 |
| $[Ph_3C][B(C_6F_5)_4]$ | 0.9 | 0.89 | 240 | 100 |
| $GaCl_3$[b] | 4.9 | 0.00 | 780 | 0 |
| $Ag[CHB_{11}H_5Br_5]$[b] | 1.3 | 0.00 | 780 | 0 |
| $[(Me_3Si)_2NCNSiMe_3][B(C_6F_5)_4]$ | 1.0 | 0.70 | 30 | 71 |

[a] TON = n(NNC) x Umsatz/n(Pre-Katalysator). [b] = Nur Zersetzung zu unidentifizierten Produkten beobachtet.

Um ein besseres Verständnis der zugrundeliegenden, sowohl thermodynamischen, als auch kinetischen Isomerisierungs- und Trimerizationsprozesse zu erlangen, wurde eine Reihe quantenchemischer Analysen durchgeführt. Im Einklang mit Experimenten von Seyfert, der **1** für mehrere Tage bei 151 °C unter Rückfluss kochte,[72] zeigen die Berechnungen, dass eine intrinsische Isomerisierung von **1** zu **2** mit einer Aktivierungsbarriere von 56 kcal/mol unwahrscheinlich bleibt. Zwar sinkt diese Aktivierungsbarriere unter Berücksichtigung eines cyclischen $[(Me_3Si)_2CNNSiMe_3]^+$-Intermediates auf 41 kcal/mol ab, jedoch scheint die Annahme eines bimolekularen Isomerisierungs-Prozesses mit Barrieren niedriger als 10 kcal/mol am wahrscheinlichsten (Schema 16).

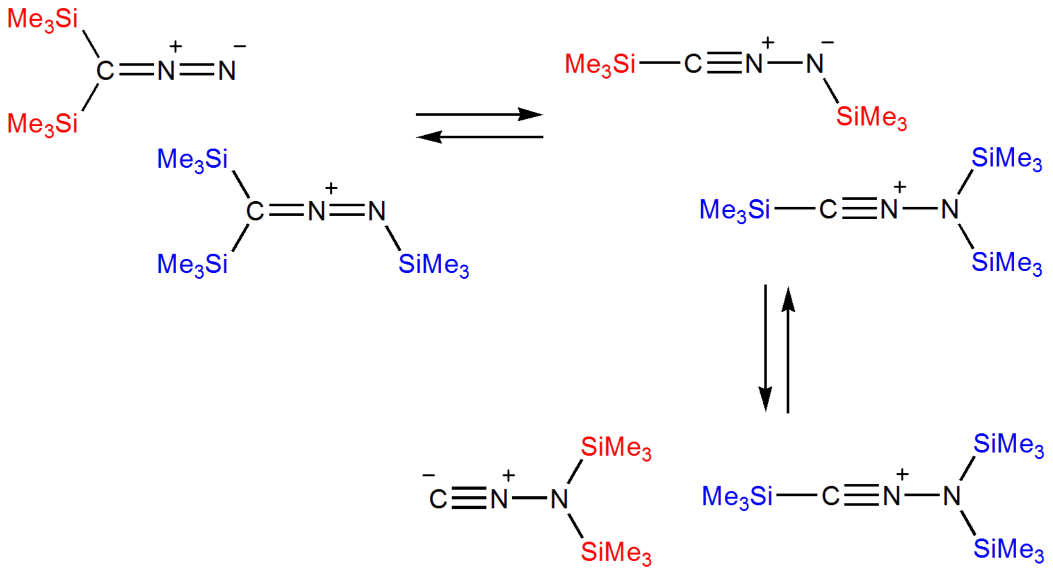

***Schema 16.*** Ein möglicher bimolekularer Isomerisierungsweg.

Diese formale 1,3-$Me_3Si$-Gruppenwanderung entlang der CNN-Einheit bestätigt die Analogie der Trimethylsilylium-Kationen zu den Protonen, die für ihre Austauschreaktionen bekannt sind.[93–95] Bereits 1967 konnten West *et al.*[96] zeigen, dass sich in Gegenwart von katalytischen Mengen $Li^+$, welches ebenfalls als Lewis-Säure angesehen werden kann, sowohl $[Me_3Si]^+$ als auch $H^+$ entlang der NN-Gruppe verschieden substituierter Hydrazine wandern. Nach retrosynthetischer Betrachtung (Abbildung 10) folgt dem Isomerisierungs-Prozess formal i) eine CC-Kupplung vor einer [3+2]-Cycloaddition; ii) eine CC-Kupplung vor einer [4+1]-Cycloaddition; oder iii) eine CN-Kupplung vor einer [4+1]-Cycloaddition.

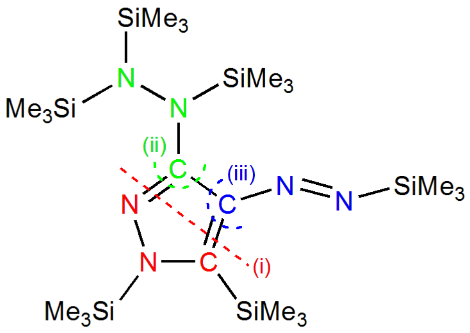

***Abbildung 10.*** Retrosynthetische Betrachtung der möglichen Cycloadditionen zur Bildung des Trimers.

Durch ein abschießendes Silylgruppen-Rearrangement wird schlussendlich das ungewöhnliche Pyrazol **16** in einer Eintopfsynthese erhalten. In der Summe zeigt sich die Reaktion von Bis(trimethylsilyl)diazomethan zu seinem Trimer in der Gasphase mit −67/−35 kcal/mol sowohl exotherm als auch exergonisch. Die entlang des Trimerisationsprozesses isolierten, katalytisch aktiven Salze $[(Me_3Si)_2NNCSiMe_3][B(C_6F_5)_4]$, $[(Me_3Si)_2NNCSiMe_3][CHB_{11}H_5Br_6]$ und $[(Me_3Si)_2NCNSiMe_3][B(C_6F_5)_4]$ können als erste Vertreter der homoleptischen Pseudochalkogonium-Kationen eingestuft werden. Des Weiteren ist die Gesamtsynthese zu **16** als erste gekoppelte Super-Lewis-Säure katalysierte Heteroatom-Kupplung und Cycloadditions-Reaktion anzusehen.

### 3.4.2 Nitren-Reaktivität von silylierten Diazen $B(C_6F_5)_3$-Addukten

Bei der Analytik der silylierten Diazen-Addukte des $B(C_6F_5)_3$ viel auf, dass diese Vertreter eine Sonderrolle unter den Diazen-Adduktspezies einnehmen. Es ist bemerkenswert, dass sich ausgehend von den *trans*-Diazenen ohne Einsatz von harter UV-Stahlung, wie sie bei *cis*-$PhNNPh \cdot B(C_6F_5)_3$ benötigt wird, die isomeren *cis*-$Me_3SiNNSiMe_3 \cdot B(C_6F_5)_3$ und *iso*-$Me_3Si(Ph)NN \cdot B(C_6F_5)_3$ isolieren lassen (Abbildung 11; A und B).

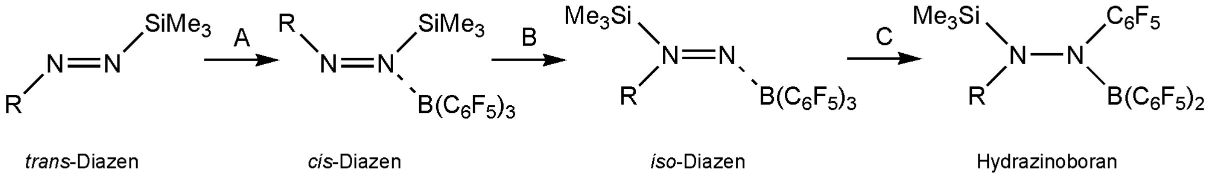

***Abbildung 11.*** Isomerisierung an silylierten Diazen $B(C_6F_5)_3$-Addukten (R = $SiMe_3$ oder Ph).

Da diese Isomerisierung nur im Falle der sterisch anspruchvollen Lewis-Säure $B(C_6F_5)_3$ auftritt, kann dies formal auf den „Frust“ des in Lösung vorliegenden Lewis-Säure-Base-Paares zurückgeführt werden, der durch Isomerisierung der Diazene abgebaut werden kann. Die quantenchemischen Rechnungen zeigten deutlich, dass lediglich in den Boran-Addukten die *trans*/*cis*/*iso*-Isomerisierung mit einem Energiegewinn von −8 kcal/mol für *cis*-$PhNNPh \cdot B(C_6F_5)_3$, −3 kcal/mol für *iso*-$Me_3Si(Ph)NN \cdot B(C_6F_5)_3$ bzw. geringem Energieverlust von 3 kcal/mol für *cis*-$Me_3SiNNSiMe_3 \cdot B(C_6F_5)_3$ einhergeht. Die bei Raumtemperatur aufgenommenen $^1H$- und $^{11}B$-NMR-Spektren der silylsubstituierten Derivate weisen sehr breite Signale auf. Außerdem ließen sich im Fall von *iso*-$Me_3Si(Ph)NN \cdot B(C_6F_5)_3$ keine $^{29}Si$- und $^{13}C$-NMR Signale für die $Me_3Si$-Gruppen erkennen. Diese Beobachtungen ließen auf eine intramolekulare Folgereaktion dieser Addukte schließen. Dies veranlasste eine nähere Untersuchung der thermodynamischen Endprodukte. Dazu wurden **23** und **24** in $CH_2Cl_2$ gelöst und für 3 Stunden bei 75 °C gelagert. In den $^1H$-, $^{11}B$-, $^{29}Si$-, $^{13}C$- und $^{19}F$-NMR Spektren dieser Lösungen war eindeutig nur eine neue Hauptspezies zu erkennen. Diese konnten durch Röntgenstrukturanalyse zweifelsfrei als Hydrazinoboran-Spezies $(Me_3Si)_2NN(C_6F_5)B(C_6F_5)_2$ (**27**) und $Me_3Si(Ph)NN(C_6F_5)B(C_6F_5)_2$ (**28**) identifiziert werden (Abbildung 12).

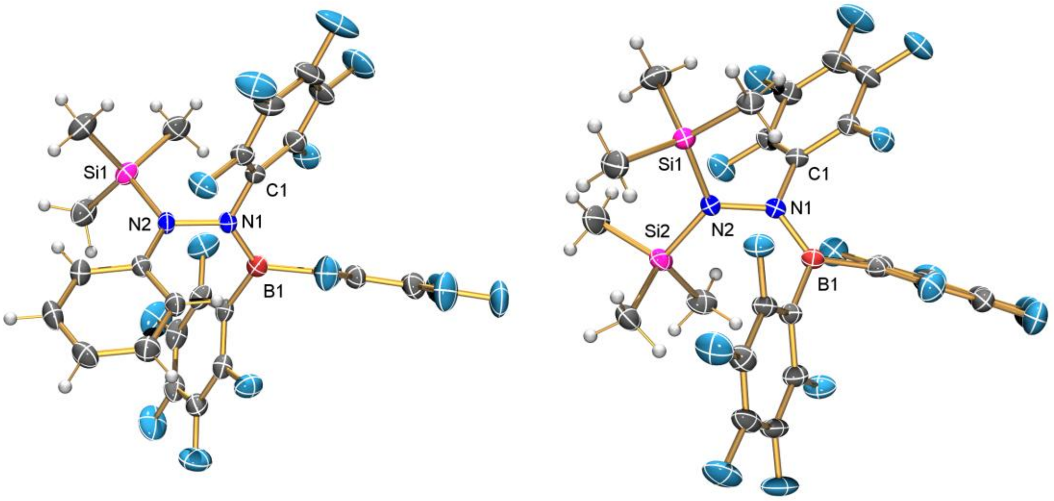

***Abbildung 12.*** ORTEP-Darstellung der Molekülstrukturen von **28** (links) und **27** (rechts) im Kristall. Die thermischen Ellipsoide entsprechen 50% Aufenthaltswahrscheinlichkeit bei 173 K.

Diese einheitliche Folgereaktion der Diazen-Addukte lässt den Schluss zu, dass sich das *cis*-$Me_3SiNNSiMe_3 \cdot B(C_6F_5)_3$ ebenfalls in das *iso*-$(Me_3Si)_2NN \cdot B(C_6F_5)_3$ als intermediäre Spezies umformt. Zwar beobachteten Wiberg *et al.* bereits bei Reaktionen von Bis(trimethylsilyl)diazen mit Metallocenen analoge 1,2-Trimethylsily-Gruppenwanderungen jedoch besitzen die isolierten Verbindungen $Cp_2MN_2(SiMe_3)_2$ (M = V, Ti) und $[Cp_2MN_2(SiMe_3)_2]_2$ (M = Cr, Mn) MN-Doppel- und NN-Einfachbindungen und weisen damit keinen *iso*-Diazen-Charakter mehr auf.[97–99] Als einzige bekannte Arbeiten zur Isolation von reaktiven *iso*-Diazenen sind die *in situ* UV/IR-Spektroskopischen Studien von Dervan *et al.* zu nennen, der die kinetisch stabilisierten *N*-(2,2,6,6-Tetramethylpiperidyl)nitrene bezüglich ihrer Dimerisation zu den Tetrazenen, $R_2N{-}N{=}N{-}NR_2$ untersucht hat.[100] Die *iso*-Diazen-Spezies besitzen zu einem geringen Anteil einen Aminonitren Charakter, der in dem Fall der beschriebenen Boran-Addukte nicht zu einer Dimerisierung führt aber für die beobachtete Insertion der NN-Einheit in die BC-Bindung verantwortlich ist. Vergleichbare Insertionsreaktionen wurden an einer $R{-}N^{-}{-}N^{+}{\equiv}P$-Einheit (Schema 5)[37] sowie von Erker *et al.*[101] als Arylborylierung an einer $R{-}C{\equiv}C$-Spezies beschrieben. Dieses Beispiel repräsentiert die erste detaillierte Studie der Lewis-Säure-Aktivierung von silylierten Diazenen die über eine *trans*/*cis*/*iso*-Isomerisierung zu einer intramolekularen Bildung von Hydrazinoboranen führt. Im Rahmen dieser Arbeit konnte das erste *iso*-Diazen als $B(C_6F_5)_3$-Addukt stabilisiert und vollständig charakterisiert werden.

### 3.4.3 Katalysierte Alkyl-Austauschreaktionen an Silanen

Die unerwartete Synthese des Ammonium-Salzes $[(Me_3Si)_3NSi(H)Me_2][B(C_6F_5)_4]$ führte zu einer grundlegenden Untersuchung der eingesetzten Edukte $(Me_3Si)_3N$, $[Me_3Si{-}H{-}SiMe_3][B(C_6F_5)_4]$ sowie $[Me_3Si \cdot \text{Toluol}][B(C_6F_5)_4]$. In diesem Zusammenhang wurde, das bei der Synthese von $[Me_3Si{-}H{-}SiMe_3][B(C_6F_5)_4]$ in reinem $Me_3SiH$ nach Lambert *et al.*[15] erhaltene, überschüssige Silan mittels NMR- und Raman-Spektroskopie analysiert. Den Spektren war eindeutig zu entnehmen, dass ein komplexes Gemisch verschiedener Silane während der Synthese von $[Me_3Si{-}H{-}SiMe_3][B(C_6F_5)_4]$ entstanden sein musste (Abbildung 13).

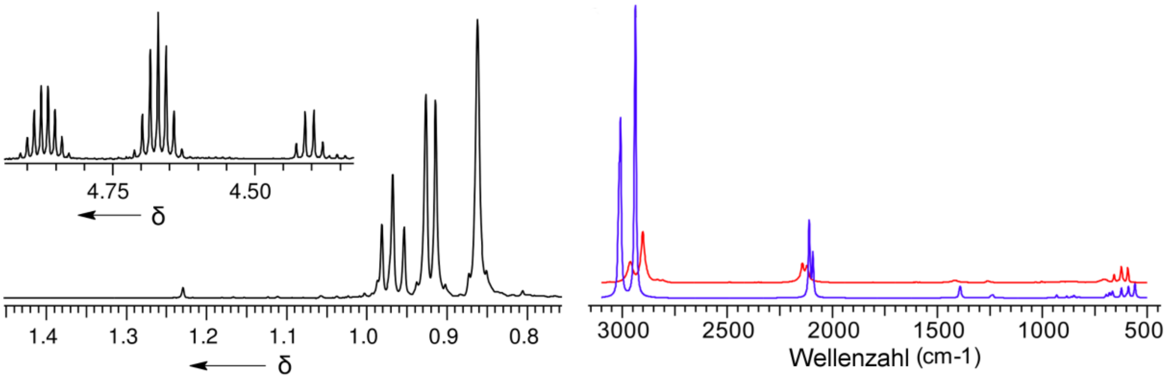

***Abbildung 13.*** $^1$H-NMR-Spektrum (links), Raman-Spektrum (rechts) der Silanmischung aus $Me_4Si$, $Me_3SiH$ und $Me_2SiH_2$ (rot gemessenes Spektrum, blau berechnetes Spektrum).

Dieses Silangemisch ließ sich sowohl anhand von Referenzspektren, die bereits 1964 von Schmidbaur aufgenommen wurden,[102] als auch über quantenmechanisch simulierte Raman-Schwingungsspektren eindeutig als ein Gemisch aus $Me_4Si$, $Me_3SiH$, $Me_2SiH_2$ und $MeSiH_3$ identifizieren. Diese zunächst überraschende Umverteilung der Substituenten des Silans ähnelt der von Müller *et al.*[23] publizierten Synthese sterisch überfrachteter Arylsilylium-Kationen (Schema 3). In jüngster Zeit beschrieben Oestreich *et al.*[103] einen analogen Substituenten-Austausch an Ferrocen-stabilisierten Silylium-Kationen, jedoch wurden in diesen Beispielen keine katalytischen Reaktionen in der Bulk-Phase beschrieben. Eine katalysierte Umverteilung von $Me_2EtSiH$ zu den Silanen $Et_2MeSiH$, $Me_2EtSiH$, $Me_3SiH$ und $Et_3SiH$ wurde unter Einwirkung des Übergansgmetall-Komplexes $Et_3Si(H)_2Ir(\mu\text{-}SiEt_2)_2Ir(H)_2SiEt_3$ von Brookhart *et al.*[104] beschrieben. In einer weiterführenden Studie konnte gezeigt werden, dass die beobachtete katalytische Umverteilung sich auch auf das $Et_3SiH$ übertragen lässt, was zu einer Mischung aus $Et_4Si$, $Et_3SiH$ und $Et_2SiH_2$ führt. Es lässt sich ableiten, dass ein allgemeingültiger Silylium-Kationen katalysierter Substituenten-Austausch-Prozess aufgedeckt wurde (Abbildung 14).

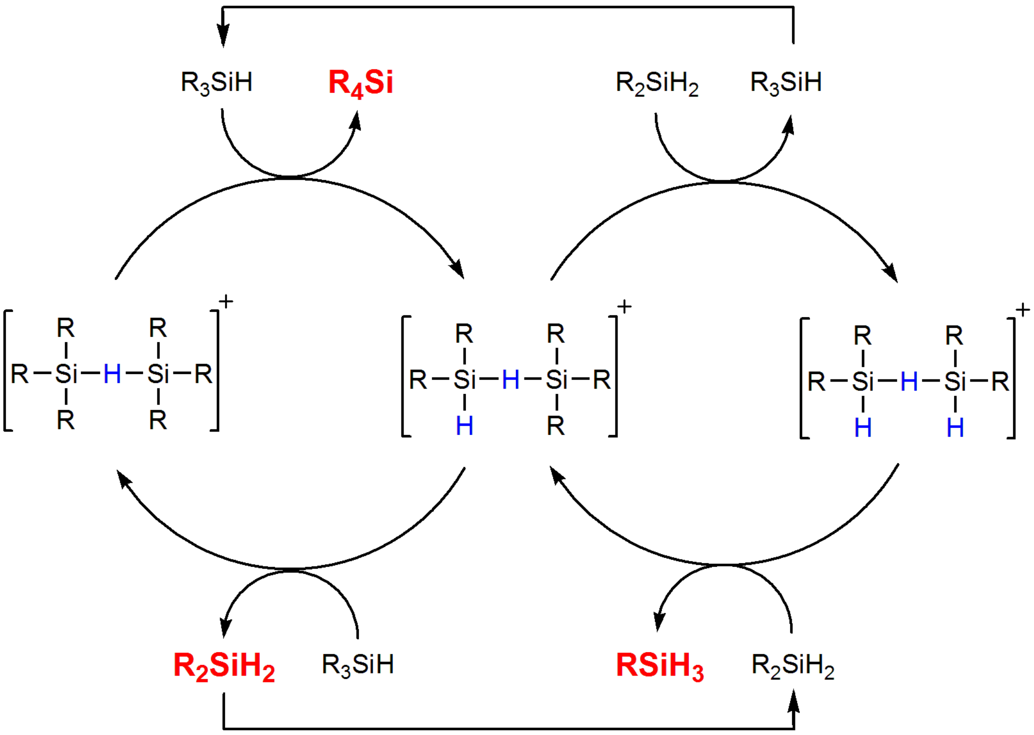

***Abbildung 14.*** Allgemeine Darstellung des katalytischen Alkylgruppenaustausches (R = Me,Et).

Dieser Prozess führt zur formalen Bildung von Dimethylsilylium-Kationen, die sowohl aus thermodynamischer als auch kinetischer Sicht bevorzugt ein Lewis-Säure-Base-Addukt mit dem $(Me_3Si)_3N$ ausbilden und klärt somit den Reaktionspfad zu dem ersten persilylierten Ammonium-Salz $[(Me_3Si)_3NSi(H)Me_2][B(C_6F_5)_4]$ auf. Dieses Beispiel zeigt deutlich das enorme Potential der Trialkysilylium-Kationen zur Aktivierung selbst sehr schwach Lewis-basischer Systeme wie den Silanen auf.

# 4 Literaturverzeichniss

[1] G. N. Lewis, *Valence and the Structure of Atoms and Molecules*, Chemical Catalog Company, New York, **1923**.

[2] J. N. Brönsted, *Recl. des Trav. Chim. des Pays-Bas* **1923**, *42*, 718–728.

[3] T. M. Lowry, *Chem. Ind.* **1923**, *42*, 43–47.

[4] R. G. Pearson, *J. Am. Chem. Soc.* **1963**, *85*, 3533–3539.

[5] R. G. Pearson, *Coord. Chem. Rev.* **1990**, *100*, 403–425.

[6] V. Jonas, G. Frenking, M. T. Reetz, *J. Am. Chem. Soc.* **1994**, *116*, 8741–8753.

[7] F. Bessac, G. Frenking, *Inorg. Chem.* **2003**, *42*, 7990–7994.

[8] I. Alkorta, J. Elguero, J. E. Del Bene, O. Mó, M. Yáñez, *Chem. Eur. J.* **2010**, *16*, 11897–11905.

[9] C. J. Carmalt, J. D. Mileham, A. J. White, D. J. Williams, J. W. Steed, *Inorg. Chem.* **2001**, *40*, 6035–6038.

[10] M. Juhasz, S. Hoffmann, E. Stoyanov, K.-C. Kim, C. A. Reed, *Angew. Chem.* **2004**, *116*, 5466–5469.

[11] M. Nava, I. V. Stoyanova, S. Cummings, E. S. Stoyanov, C. A. Reed, *Angew. Chem.* **2014**, *126*, 1149–1152.

[12] L. O. Müller, D. Himmel, J. Stauffer, G. Steinfeld, J. Slattery, G. Santiso-Quiñones, V. Brecht, I. Krossing, *Angew. Chem.* **2008**, *120*, 7772–7776.

[13] J. Y. Corey, R. West, *J. Am. Chem. Soc.* **1963**, *85*, 2430–2433.

[14] P. D. Bartlett, F. E. Condon, A. Schneider, *J. Am. Chem. Soc.* **1944**, *66*, 1531–1539.

[15] J. B. Lambert, S. Zhang, *J. Chem. Soc. Chem. Commun.* **1993**, 383.

[16] J. B. Lambert, S. Zhang, S. M. Ciro, *Organometallics* **1994**, *13*, 2430–2443.

[17] M. F. Ibad, P. Langer, A. Schulz, A. Villinger, *J. Am. Chem. Soc.* **2011**, *133*, 21016–21027.

[18] S. P. Hoffmann, T. Kato, F. S. Tham, C. A. Reed, *Chem. Commun.* **2006**, 767–769.

[19] M. Nava, C. A. Reed, *Organometallics* **2011**, *30*, 4798–4800.

[20] Z. Xie, R. Bau, A. Benesi, C. A. Reed, *Organometallics* **1995**, *14*, 3933–3941.

[21] T. Küppers, E. Bernhardt, R. Eujen, H. Willner, C. W. Lehmann, *Angew. Chem.* **2007**, *119*, 6462–6465.

[22] K.-C. Kim, C. A. Reed, D. W. Elliott, L. J. Mueller, F. Tham, L. Lin, J. B. Lambert, *Science* **2002**, *297*, 825–827.

[23] A. Schäfer, M. Reißmann, A. Schäfer, W. Saak, D. Haase, T. Müller, *Angew. Chem.* **2011**, *123*, 12845–12848.

[24] S. C. Bourke, M. J. Maclachlan, A. J. Lough, I. Manners, *Chem. Eur. J.* **2005**, *11*, 1989–2000.

[25] H. F. T. Klare, K. Bergander, M. Oestreich, *Angew. Chem.* **2009**, *121*, 9241–9243.

[26] D. W. Stephan, *Org. Biomol. Chem.* **2008**, *6*, 1535–1539.

[27] K. Takeuchi, D. W. Stephan, *Chem. Commun.* **2012**, *48*, 11304–11306.

[28] M. A. Dureen, D. W. Stephan, *J. Am. Chem. Soc.* **2009**, *131*, 8396–8397.

[29] D. W. Stephan, G. Erker, *Angew. Chem.* **2010**, *122*, 50–81.

[30] A. Villinger, P. Mayer, A. Schulz, *Chem. Commun.* **2006**, 1236–1238.

[31] D. Michalik, A. Schulz, A. Villinger, N. Weding, *Angew. Chem.* **2008**, *120*, 6565–6568.

[32] S. Herler, P. Mayer, J. Schmedt auf der Günne, A. Schulz, A. Villinger, J. J. Weigand, *Angew. Chem.* **2005**, *117*, 7968–7971.

[33] P. Mayer, A. Schulz, A. Villinger, *J. Organomet. Chem.* **2007**, *692*, 2839–2842.

[34] A. Schulz, A. Villinger, *Angew. Chem.* **2008**, *120*, 614–617.

[35] M. Kuprat, A. Schulz, A. Villinger, *Angew. Chem.* **2013**, *125*, 7266–7270.

[36] D. Michalik, A. Schulz, A. Villinger, *Inorg. Chem.* **2008**, *47*, 11798–11806.

[37] M. Kowalewski, B. Krumm, P. Mayer, A. Schulz, A. Villinger, *Eur. J. Inorg. Chem.* **2007**, *2007*, 5319–5322.

[38] T. Wondimagegn, Z. Xu, K. Vanka, T. Ziegler, *Organometallics* **2005**, *24*, 2076–2085.

[39] P. Arndt, U. Jäger-Fiedler, M. Klahn, W. Baumann, A. Spannenberg, V. V. Burlakov, U. Rosenthal, *Angew. Chem.* **2006**, *118*, 4301–4304.

[40] A. Villinger, A. Westenkirchner, R. Wustrack, A. Schulz, *Inorg. Chem.* **2008**, *47*, 9140–9142.

[41] A. Schulz, P. Mayer, A. Villinger, *Inorg. Chem.* **2007**, *46*, 8316–8322.

[42] C. Hubrich, A. Schulz, A. Villinger, *Z. anorg. allg. Chem.* **2007**, *633*, 2362–2366.

[43] A. G. Massey, A. J. Park, *J. Organomet. Chem.* **1964**, *2*, 245–250.

[44] F. Focante, P. Mercandelli, A. Sironi, L. Resconi, *Coord. Chem. Rev.* **2006**, *250*, 170–188.

[45] W. E. Pierrs, *Adv. Organomet. Chem* **2004**, *52*, 1–76.

[46] J. Zhou, S. J. Lancaster, D. A. Walker, S. Beck, M. Thornton-Pett, M. Bochmann, *J. Am. Chem. Soc.* **2001**, *123*, 223–237.

[47] S. J. Lancaster, A. Rodriguez, A. Lara-Sanchez, M. D. Hannant, D. A. Walker, D. H. Hughes, M. Bochmann, *Organometallics* **2002**, *21*, 451–453.

[48] A. Bernsdorf, H. Brand, R. Hellmann, M. Köckerling, A. Schulz, A. Villinger, K. Voss, *J. Am. Chem. Soc.* **2009**, *131*, 8958–8970.

[49] H. Jacobsen, H. Berke, S. Döring, G. Kehr, G. Erker, R. Fröhlich, O. Meyer, *Organometallics* **1999**, *18*, 1724–1735.

[50] I. Krossing, I. Raabe, *Angew. Chem.* **2004**, *116*, 2116–2142.

[51] T. Küppers, E. Bernhardt, R. Eujen, H. Willner, C. W. Lehmann, *Angew. Chem.* **2007**, *119*, 6462–6465.

[52] M. Lehmann, A. Schulz, A. Villinger, *Angew. Chem.* **2009**, *121*, 7580–7583.

[53] M. Swart, E. Rösler, F. M. Bickelhaupt, *J. Comput. Chem.* **2006**, *27*, 1486–1493.

[54] A. Schulz, A. Villinger, *Chem. Eur. J.* **2010**, *16*, 7276–7281.

[55] G. A. Olah, X.-Y. Li, Q. Wang, G. Rasul, G. K. S. Prakash, *J. Am. Chem. Soc.* **1995**, *117*, 8962–8966.

[56] G. Prakash, C. Bae, Q. Wang, G. Rasul, G. Olah, *J. Org. Chem.* **2000**, *65*, 7646–7649.

[57] M. Driess, R. Barmeyer, C. Monsé, K. Merz, *Angew. Chem.* **2001**, *113*, 2366–2369.

[58] C. Friedel, J. M. Crafts, *J. Prakt. Chem.* **1877**, *16*, 233–237.

[59] A. Corma, H. García, *Chem. Rev.* **2003**, *103*, 4307–4365.

[60] A. Corma, H. García, *Chem. Rev.* **2002**, *102*, 3837–3892.

[61] R. Qiu, Y. Chen, S.-F. Yin, X. Xu, C.-T. Au, *RSC Adv.* **2012**, *2*, 10774–10793.

[62] K. Narasaka, *Synthesis* **1991**, *1991*, 1–11.

[63] R. Qiu, G. Zhang, X. Xu, K. Zou, L. Shao, D. Fang, Y. Li, A. Orita, R. Saijo, H. Mineyama, et al., *J. Organomet. Chem.* **2009**, *694*, 1524–1528.

[64] V. J. Scott, R. Celenligil-Cetin, O. V Ozerov, *J. Am. Chem. Soc.* **2005**, *127*, 2852–2853.

[65] R. Panisch, M. Bolte, T. Müller, *J. Am. Chem. Soc.* **2006**, *128*, 9676–9682.

[66] C. Douvris, O. V Ozerov, *Science* **2008**, *321*, 1188–1190.

[67] S. Duttwyler, C. Douvris, N. L. P. Fackler, F. S. Tham, C. A. Reed, K. K. Baldridge, J. S. Siegel, *Angew. Chem.* **2010**, *122*, 7681–7684.

[68] O. Allemann, S. Duttwyler, P. Romanato, K. K. Baldridge, J. S. Siegel, *Science* **2011**, *332*, 574–577.

[69] K. Hara, R. Akiyama, M. Sawamura, *Org. Lett.* **2005**, *7*, 5621–5623.

[70] A. Schulz, A. Villinger, *Angew. Chem.* **2012**, *124*, 4602–4604.

[71] G. Erker, *Pure Appl. Chem.* **2012**, *84*, 2203–2217.

[72] D. Seyferth, T. C. Flood, *J. Organomet. Chem.* **1971**, *29*, C25–C28.

[73] N. Wiberg, G. Hübler, *Z. Naturforsch.* **1976**, 1317–1321.

[74] N. Wiberg, W.-C. Joo, W. Uhlenbrock, *Angew. Chem.* **1968**, *80*, 661–662.

[75] J. C. Bottaro, *J. Chem. Soc. Chem. Commun.* **1978**, 990.

[76] E. H. Amonoo-Neizer, R. A. Shaw, D. O. Skovlin, B. C. Smith, *Inorganic Syntheses*, John Wiley & Sons, Inc., Hoboken, NJ, USA, **1966**.

[77] F. Reiß, A. Schulz, A. Villinger, *Eur. J. Inorg. Chem.* **2012**, *2012*, 261–271.

[78] G. Alcaraz, R. Reed, A. Baceiredo, G. Bertrand, *J. Chem. Soc. Chem. Commun.* **1993**, *4*, 1354.

[79] P. Pyykkö, M. Atsumi, *Chem. Eur. J.* **2009**, *15*, 12770–12779.

[80] M. J. Frisch, G. W. Trucks, H. B. Schlegel, G. E. Scuseria, M. A. Robb, J. R. Cheeseman, G. Scalmani, V. Barone, B. Mennucci, G. A. Petersson, et al., *Gaussian 09, Revis. C.01* **2010**, Gaussian, Inc., Wallingford CT.

[81] T. H. J. Dunning, *J. Phys. Chem.* **1989**, *90*, 1007.

[82] D. E. Woon, T. H. J. Dunning, *J. Phys. Chem.* **1993**, *98*, 1358.

[83] T. H. J. Dunning, K. A. Peterson, *J. Phys. Chem.* **2002**, *117*, 10548.

[84] E. D. Glendering, A. E. Reed, J. E. Carpenter, F. Weinold, in *NBO Version 3.1*

[85] J. E. Carpenter, F. Weinold, *J. Mol. Struc.* **1988**, *169*, 41.

[86] J. E. Weinold, F. Carpenter, in *Struct. Small Mol. Ions*, Plenum Press, **1988**, p. 211.

[87] F. Weinold, C. Landis, in *Val. Bond. A Nat. Bond Orbital Donor Accept. Perspect.*, Cambridge University Press, **2005**, and references therein.

[88] J. Harada, K. Ogawa, S. Tomoda, *Acta Cryst.* **1997**, *B53*, 662–672.

[89] M. Veith, H. Bärnighausen, *Acta Cryst.* **1974**, *B30*, 1806–1813.

[90] E. I. Davydova, T. N. Sevastianova, A. V. Suvorov, A. Y. Timoshkin, *Coord. Chem. Rev.* **2010**, *254*, 2031–2077.

[91] D. G. Anderson, D. W. H. Rankin, H. E. Robertson, G. Gundersen, R. Seip, *J. Chem. Soc. Dalt. Trans.* **1990**, 161–164.

[92] H. Seidl, H. Bock, N. Wiberg, M. Veith, *Angew. Chem.* **1970**, *82*, 42–43.

[93] C. Charrier, H. Bonnard, G. De Lauzon, F. Mathey, *J. Am. Chem. Soc.* **1983**, *105*, 6871–6877.

[94] V. A. Soloshonok, V. P. Kukhar, *Tetrahedron* **1996**, *52*, 6953–6964.

[95] M. Yasumoto, H. Ueki, V. a. Soloshonok, *J. Fluor. Chem.* **2007**, *128*, 736–739.

[96] R. West, M. Ishikawa, R. E. Bailey, *J. Am. Chem. Soc.* **1967**, *107*, 4068–4072.

[97] N. Wiberg, H. W. Häring, O. Schieda, *Angew. Chem.* **1976**, *88*, 383–384.

[98] M. Veith, *Angew. Chem.* **1976**, *88*, 384–385.

[99] N. Wiberg, H.-W. Häring, G. Huttner, P. Friedrich, *Chem. Ber.* **1978**, *111*, 2708–2715.

[100] P. B. Dervan, M. E. Squillacote, P. M. Lahti, A. P. Sylwester, J. D. Roberts, *J. Am. Chem. Soc.* **1981**, *103*, 1120–1122.

[101] G. Dierker, J. Ugolotti, G. Kehr, R. Fröhlich, G. Erker, *Adv. Synth. Catal.* **2009**, *351*, 1080–1088.

[102] H. Schmidbaur, *Chem. Ber.* **1964**, *97*, 1639–1648.

[103] K. Müther, P. Hrobárik, V. Hrobáriková, M. Kaupp, M. Oestreich, *Chem. Eur. J.* **2013**, *19*, 16579–16594.

[104] S. Park, B. G. Kim, I. Göttker-Schnetmann, M. Brookhart, *ACS Catal.* **2012**, *2*, 307–316.

# 5 Publikationen

Dieses Kapitel beinhaltet die Original-Publikationen zu den im Kapitel 3 zusammengefassten Arbeiten. Der eigene Beitrag zu der betreffenden Publikation ist jeweils gesondert hervorgehoben.

## 5.1 Catalytic Trimerization of Bis-silylated Diazomethane

Muhammad Farooq Ibad, Peter Langer, Fabian Reiß, Axel Schulz und Alexander Villinger

*J. Am. Chem. Soc.* **2012**, *134*, 17757–17768.

In dieser Publikation wurde ein Teil der experimentellen Arbeiten von mir durchgeführt. Von mir wurden die Verbindungen $[(Me_3Si)_2NCNSiMe_3][B(C_6F_5)_4]$, $[(Me_3Si)_2NNCSiMe_3][CHB_{11}H_5Br_6]$, $[(Me_3Si)_2NNCCPh_3][B(C_6F_5)_4]$ sowie $(Me_3Si)_2NNCB(C_6F_5)_3$ synthetisiert und vollständig charakterisiert. Desweiteren wurde die Studie zur katalytischen Aktivität verschiedener Lewis-Säuren von mir durchgeführt. Ich habe beim verfassen des Manuskriptes mitgewirkt und das Supportingfile mit verfasst. Der eigene Beitrag liegt bei ca. 50 %.

Ein ausführliches Supportingfile steht online zur freien Verfügung:

DOI: 10.1021/ja308104k

JACS
JOURNAL OF THE AMERICAN CHEMICAL SOCIETY

Article

pubs.acs.org/JACS

# Catalytic Trimerization of Bis-silylated Diazomethane

Muhammad Farooq Ibad,[†,‡] Peter Langer,[‡,§] Fabian Reiß,[†] Axel Schulz,*[,†,§] and Alexander Villinger*[,†]

[†]Abteilung Anorganische Chemie and [‡]Abteilung Organische Chemie, Institut für Chemie, Universität Rostock,
Albert-Einstein-Straße 3a, D-18059 Rostock, Germany

[§]Leibniz-Institut für Katalyse e.V. an der Universität Rostock, Albert-Einstein-Straße 29a, D-18059 Rostock, Germany

*Supporting Information*

**ABSTRACT:** $(Me_3Si)_2CNN$ isomerizes upon addition of traces of $[Me_3Si]^+$ ions to give $(Me_3Si)_2NNC$, which then undergoes an unusual trimerization reaction to give exclusively 4-diazenyl-3-hydrazinylpyrazole. As catalyst the isonitrilium ion, $[(Me_3Si)_2NNC(SiMe_3)]^+$, was identified and fully characterized. Experiments and computations indicate a three-step reaction including isomerization of diazomethane, a C−C or N−C coupling, and a formal cycloaddition reaction. The kinetics and thermodynamics are discussed on the basis of DFT calculations.

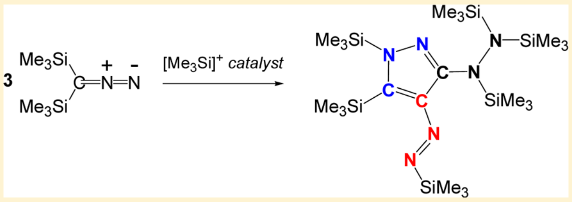

## 1. INTRODUCTION

More than a decade after the first isolation and characterization of silylium ions,[1] their chemistry has been an area of rapid growth,[2] since many applications have been found due to their useful properties such as enormous Lewis acidity and catalytic behavior.[3−6] For example, Ozerov et al.[4] and Müller et al.[3j] utilized silylium ions as reactive catalysts for the activation of C−F bonds. The Ozerov group introduced a class of carborane-supported, highly electrophilic silylium compounds that act as long-lived catalysts for hydro-defluorination of perfluoroalkyl groups by widely accessible silanes under mild conditions. The reactions are completely selective for aliphatic carbon−fluorine bonds in preference to aromatic carbon−fluorine bonds.[4] Recently, Oestreich et al.[3h] demonstrated that a tamed, ferrocene-based silylium ion catalyzes demanding Diels−Alder reactions in an unprecedented temperature range.

Tri-coordinate silylium (also silylenium or silicenium) ions,[2,7] with their electron sextet and a vacant p orbital, are electron-deficient species and therefore strong Lewis acids. Even relatively weak Lewis bases such as $\pi/\sigma$-donor solvents (toluene,[8] $CH_3CN$,[9] etc.) form tetrahedral complexes with silylium ions.[8,10] In addition, intramolecular $\pi$ coordination in silylium ions containing a 2,6-diarylphenyl scaffold was observed, which forms a Wheland-like complex.[11] The first well-documented examples of intramolecular $\pi$-stabilization in silyl cations were silanorbornyl cations.[12] The long search for a "naked" $[R_3Si]^+$ cation,[2,13] free of interactions with the environment, was finally brought to an end with the isolation and full characterization of $[(Mes)_3Si][CHB_{11}Me_5Br_6]\cdot C_6H_6$ (Mes = 2,4,6-trimethylphenyl) by the groups of Lambert and Reed in 2002.[14]

The silylium ion $[Me_3Si]^+$ might be regarded as a sterically demanding big proton,[15] and, similar to a proton, the bulky silylium ion is always solvated, forming the $[Me_3Si_{(solv)}]^+$ ion.[8b,15−18] For example, the full series of salts containing the bis-silylated halonium/pseudo-halonium cations $[Me_3Si{-}X{-}SiMe_3]^+$ (X = F, Cl, Br, I;[15] CN, $N_3$, OCN, SCN;[19] $CF_3SO_3$[20]) were generated and fully characterized using the super Lewis acidic silylating media $Me_3Si{-}X$ and $[Me_3Si_{(solv)}]^+$ salt.[15] In view of the success of the pseudo-halogen concept in super Lewis acidic silylating media,[15,19,20] we were intrigued by the idea of utilizing the enormous Lewis acidity of the $[Me_3Si]^+$ ion to activate small molecules such as bis-silylated diazomethane $(Me_3Si)_2CNN$, aminoisonitrile $(Me_3Si)_2NNC$, and carbodiimide $(Me_3Si)NCN(SiMe_3)$, which can be considered as 16-electron-containing pseudo-chalcogens.[21] In analogy to pseudo-halogens, pseudo-chalcogens are species that form a homologous series $H_2Y$, MYH, $M_2Y$, in which alkali, alkaline earth, and heavy metals are typical representatives for M, and Y = NCN, CNN, NNC, CCO, CC, etc. Furthermore, the pseudo-chalcogen group is completely integrated in the resulting mesomeric bond system, and localization of the ionic charge at the terminal atoms is observed. Pseudo-chalcogenide anions can also act as bidentate ligands and are distinguished by their ambident nature.[21] To the best of our knowledge, salts containing silylated $[(Me_3Si)_2CNN(SiMe_3)]^+$, $[(Me_3Si)_2NNC(SiMe_3)]^+$, and $[(Me_3Si)_2NCN(SiMe_3)]^+$ have not yet been reported.

In this study, special attention was given to the diazomethane compound, as it is an ambivalent reagent.[22,23] While electrophiles commonly attack at the nucleophilic C atom,[24] nucleophiles prefer the terminal N atom of diazomethane.[25] This ambivalent behavior was also observed in [3+2] cycloaddition reactions with dipolarophiles.[26] Herein, we report what is, to the best of our knowledge, the first trimerization of a bis-silylated diazomethane, which provides, based on the use of $[(Me_3Si)_2NNC(SiMe_3)]^+$ as a catalyst, an efficient and facile synthesis of 4-diazenyl-3-hydrazinyl-1*H*-pyrazoles. Pyrazoles represent one of the most important classes of heterocyclic

**Received:** August 15, 2012
**Published:** September 22, 2012

ACS Publications © 2012 American Chemical Society

compounds.[27] Although a great variety of substituted pyrazoles are known, only a few examples of diazenyl- or hydrazinylpyrazoles have been described in the literature so far.[28] Likewise, di(hydrazinylidene)pyrazoles have only been scarcely reported in the literature.[29] To the best of our knowledge, trimerization reactions of diazomethane compounds have not yet been described; however, dimerizations of ethyl diazoacetate[30a,b] and of a (diazomethylene)phosphorane[30c] were previously reported to yield 1,2,4,5-tetrazine derivatives. As early as 1947, Meerwein reported the catalytic decomposition of diazomethane, yielding polymethylene.[31]

## 2. RESULTS AND DISCUSSION

For the molecule (Me$_3$Si)$_2$CNN, three acyclic constitutional isomers with an NNC unit can be formulated (Scheme 1).[32]

**Scheme 1. Isomerization of Bis-silylated Diazomethane Catalyzed by [Me$_3$Si−S]$^+$ with S = Isomer 1, 2, or 3[32]**

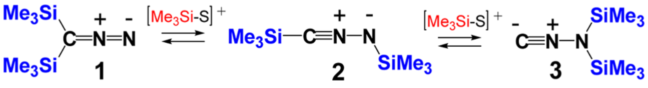

Bis(trimethylsilyl)diazomethane (**1**)[33] and bis(trimethylsilyl)-aminoisonitrile ((Me$_3$Si)$_2$NNC, **3**)[34] are experimentally known, but no structural data are available (Figure 1). Wiberg et al. have shown that nitrilimine isomer **2** cannot be isolated since it undergoes rapid isomerization to carbodiimide **4** (Scheme 2).[34] Ever since the discovery of the first *C*,*N*-nitrilimines by Huisgen,[35] the development of their chemistry has been hampered because of their potential instability and the lack of suitable preparative methods. Bertrand et al. established efficient routes for preparing stable nitrilimines.[36−38] Moreover, the importance of steric hindrance was shown in the stabilization of *C*,*N*-nitrilimines. For instance, the reaction of *n*-BuLi with R(H)CN$_2$ followed by addition of R−Cl yields the bis-silylated diazomethane R$_2$CNN for R = Me$_3$Si,[33] while the analogous reaction for the bulkier substituent R = $^i$Pr$_3$Si results in the formation of the thermally stable nitrilimine R−CNN−R, which only isomerizes to the carbodiimide R−NCN−R under photolytic conditions.[39]

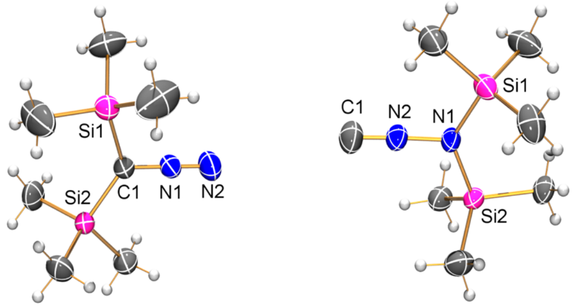

**Figure 1.** ORTEP drawing of the molecular structures of (Me$_3$Si)$_2$CNN (left) and (Me$_3$Si)$_2$NNC (right) in the crystal. Thermal ellipsoids with 50% probability at 173 K. Selected bond lengths (Å) and angles (°): for (Me$_3$Si)$_2$CNN, N1−N2 1.135(2), N1−C1 1.312(2), C1−N1−N2 179.6(2); for (Me$_3$Si)$_2$NNC, N1−N2 1.366(2), N2−C1 1.152(2), C1−N1−N2 177.7(2).

**Scheme 2. Isomerization of Bis-silylated Carbodiimide Catalyzed by [Me$_3$Si−S]$^+$ (S = Solvent)**

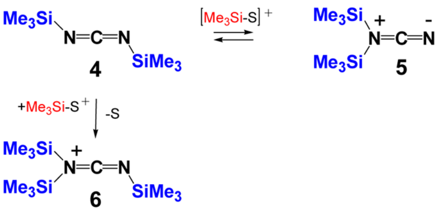

Besides **1** and **3**, bis-silylated carbodiimde species **4** (Scheme 2)[40] was studied for comparison. **4** can be regarded as a constitutional isomer of **1**−**3** regarding the NCN unit. Only the *N*,*N*′-substituted carbodiimide species **4** can be isolated and structurally characterized,[40] while *N*,*N*-bis-silylated carbodiimde species **5** is unstable regarding the isomerization to species **4**. For the reaction with silylium ions, compounds **1**, **2**, and **4** were utilized as starting materials. All three compounds are thermally stable liquids and do not isomerize or show any other reactivity in pure form at 298 K in the dark.

**Scheme 3. Catalytic Trimerization of Bis-silylated Diazomethane[32]**

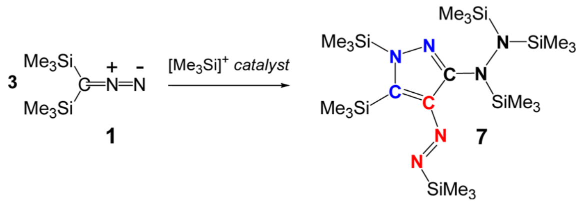

### 2.1. Reaction of (Me$_3$Si)$_2$CNN, (Me$_3$Si)$_2$NNC, and (Me$_3$Si)NCN(SiMe$_3$) with Silylium Ions and Other Strong Lewis Acids.

The reaction of bis(trimethylsilyl)diazomethane (Me$_3$Si)$_2$CNN with a [Me$_3$Si$_{(\mathrm{solv})}$]$^+$ source was studied in two series of experiments (Schemes 3 and 4). At first, the reaction was carried out in neat (Me$_3$Si)$_2$CNN, generating a super Lewis acidic silylating medium. However, upon addition of [Me$_3$Si$_{(\mathrm{solv})}$]$^+$ salt (solv = Me$_3$Si−H), an immediate complex reaction contrary to the analogous reaction with Me$_3$Si−X (X = halogen, pseudo-halogen) was observed, resulting in a deep red, highly viscous reaction mixture. Thus *n*-pentane was added, which makes the workup and isolation of the products much easier due to a considerable decrease in the viscosity of the reaction mixture. However, it should be noted that the reaction in neat bis(trimethylsilyl)diazomethane yielded the same product. In a typical reaction setup, to a stirred suspension of [Me$_3$Si$_{(\mathrm{solv})}$][B(C$_6$F$_5$)$_4$] in *n*-pentane was added a mixture of liquid (Me$_3$Si)$_2$CNN (large excess) and *n*-pentane at −78 °C. The resulting suspension was allowed to warm to ambient temperature and stirred for 36 h. The reaction was followed by $^1$H NMR experiments, and it was obvious that diazomethane (Me$_3$Si)$_2$CNN was involved in a more complex chemistry under these extreme Lewis acidic conditions, beyond the simple formation of [(Me$_3$Si)$_2$CNN(SiMe$_3$)]$^+$ (**8**) or [(Me$_3$Si)$_2$NNC-(SiMe$_3$)]$^+$ (**9**) (Scheme 5). Furthermore, these $^1$H NMR experiments showed the exclusive and quantitative formation of pyrazole species **7** and the complete consumption of the starting material bis(trimethylsilyl)diazomethane (Scheme 3). The end of the reaction is indicated by deposition of the catalyst, **9**[B(C$_6$F$_5$)$_4$], as a crystalline solid. Moreover, during the course of the reaction, the color of the supernatant changed gradually from yellow to dark red. Thus, both the precipitate and the reaction solution were further studied. The supernatant

**Scheme 4. Catalytic Trimerization of Bis-silylated Diazomethane Utilizing 9[$CHB_{11}H_5Br_6$] as Catalyst**[32]

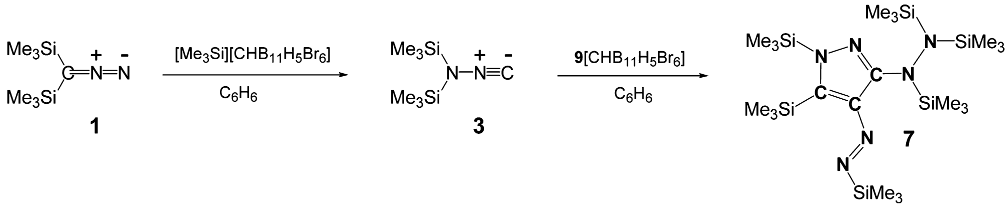

**Scheme 5. Calculated Relative Gibbs Free Energies of Isomers of Neutral ($(Me_3Si)_2CNN$ (1, 2, and 3) and Cationic $[(Me_3Si)_3CNN]^+$ Species (8 and 9)**[a]

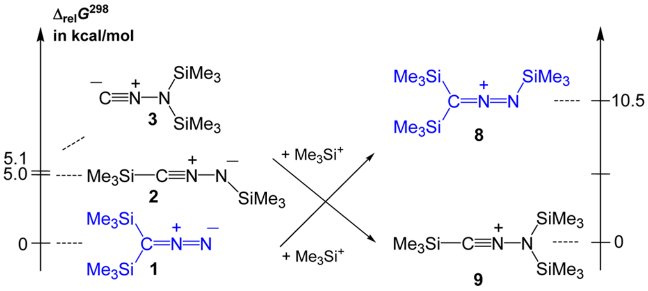

[a]Higher-lying cyclic isomers are omitted for clarity (see Supporting Information).[32]

was removed by filtration, and the brownish residue was washed with *n*-pentane. Recrystallization from a minimum of toluene at −25 °C resulted in the deposition of **9**[$B(C_6F_5)_4$] as colorless crystals (49% yield based on [$Me_3Si_{(solv)}$][$B(C_6F_5)_4$]; Figure 2). Notably, exclusively **9**[$B(C_6F_5)_4$] was isolated instead of the expected [$(Me_3Si)_2CNN(SiMe_3)$][$B(C_6F_5)_4$]. From the combined solutions of the filtration and washing processes, the silylated 4-diazenyl-3-hydrazinylpyrazole species (**7**) was isolated as dark green crystals (Scheme 3; see below, Figure 5 left). The overall isolated yield is about 51% (referring to $(Me_3Si)_2CNN$, which was used in a 22-fold excess both as reactant and as solvent instead of *n*-pentane) after 36 h at ambient temperatures. Referring to [$Me_3Si_{(solv)}$][$B(C_6F_5)_4$]), this trimerization corresponds to a catalytic process with a turnover number (TON) of about 10.8.

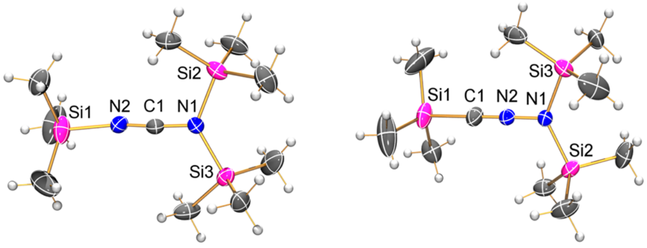

**Figure 2.** ORTEP drawing of the molecular structure of the $[(Me_3Si)_2NCN(SiMe_3)]^+$ ion in **6**[$B(C_6F_5)_4$] (left) and the $[(Me_3Si)_2NNC(SiMe_3)]^+$ ion in **9**[$B(C_6F_5)_4$] (right) in the crystal. Thermal ellipsoids with 50% probability at 173 K. Selected bond lengths (Å) and angles (°): for **6**, C1−N2 1.18(1), N1−C1 1.279 (2), N1−Si2 1.835(1), N1−Si3 1.838(1), C1−N2−Si1 159.4(9), C1−N1−Si2 115.01(8), C1−N1−Si3 116.04(8), Si2−N1−Si3 128.93(6), N1−C1−N2 173.3(5); for **9**, N1−N2 1.309(2), N2−C1 1.143(2), Si2−N1 1.818(1), Si3−N1 1.816(1), Si1−C1 1.897(2), C1−N2−N1 179.3(1), N2−N1−Si3 113.76(8), N2−N1−Si2 114.89(8), N2−C1−Si1 174.6(1), Si3−N1−Si2 131.34(6).

Since DFT calculations (see below) indicated the catalytic formation of bis(trimethylsilyl)aminoisonitrile **3** in the first reaction step (Schemes 2 and 3), in a second series of experiments isomeric **3** was reacted with $[Me_3Si_{(solv)}]^+$ under the same reaction conditions as discussed before for bis(trimethylsilyl)diazomethane (isomer **1**). Indeed, the reaction of isomer **3** with $[Me_3Si_{(solv)}]^+$ resulted also in the exclusive formation of pyrazole species **7** along with **9**[$B(C_6F_5)_4$], thus proving the computational results (see below). Since no isomerization step is needed prior to the C−C coupling and [3+2] cyclization, this reaction is faster (12 h for a complete conversion). The long-term activity and reuse of the catalyst was also studied (Table 1; see Supporting Information). Even after 14 days and several reuses, the catalyst was still active as well as when the catalyst concentration was decreased to less than 1 mol%. For instance, the reaction of aminoisonitrile **3** afforded in three runs isolated yields of pyrazole species **7** between 74 and 82% when 1 mol% catalyst was used, displaying a constant activity over all runs. A TON of 230 was estimated (36 h). After each cycle, the amount of catalyst remained almost unchanged. The catalyst can always be recovered in good yield as crystalline material at the end of the reaction.

**Table 1. Details of the Catalytic Trimerization of $(Me_3Si)_2NNC$**

| precatalyst[a] | mol% cat. | conversion | time/ min | TON[b] |
|---|---|---|---|---|
| [$Me_3Si{-}H{-}SiMe_3$][$B(C_6F_5)_4$] | 1.0 | 0.92 | 1080 | 92 |
| [$Me_3Si$][$CHB_{11}H_5Br_5$] | 2.0 | 0.90 | 180 | 45 |
| [$(Et_2O)_2H$][$B(C_6F_5)_4$] | 1.2 | 0.84 | 30 | 72 |
| [$Me_3SiOEt_2$][$B(C_6F_5)$] | 1.3 | 0.74 | 30 | 59 |
| $B(C_6F_5)_3$ | 1.9 | 0.84 | 14400 | 45 |
| [$Ph_3C$][$B(C_6F_5)_4$][d] | 0.9 | 0.89 | 240 | 100 |
| $GaCl_3$[c] | 4.9 | 0.00 | 780 | 0 |
| Ag[$CHB_{11}H_5Br_5$][c] | 1.3 | 0.00 | 780 | 0 |
| [$(Me_3Si)_2NCN(SiMe_3)$][$B(C_6F_5)_4$] | 1.0 | 0.70 | 30 | 71 |

[a]Precatalyst that forms the catalyst $[LA\text{-}CNN(SiMe_3)_2]^+$ (LA = Lewis acid). [b]TON = *n*(NNC)×conversion/*n*(precatalyst). [c]No conversion to 7, but slow decomposition to unidentified side products was observed. [d]Trityl ions do not catalyze the isomerization step.

For comparison, the reaction of carbodiimide **4** with 1 equiv of [$Me_3Si_{(solv)}$][$B(C_6F_5)_4$] (solv = $Me_3Si{-}H$, toluene) dissolved in toluene leads in a straightforward, almost quantitative reaction (isolated yield 77%) to the formation of the silylated species **6** with $[B(C_6F_5)_4]^-$ as counterion (Scheme 2, Figure 2). Interestingly, no isomerization to the *N*,*N*-bis-silylated carbodiimde species **5** (Scheme 2) nor any other reactivity was observed, even under reflux conditions.

*Variation of the Counteranion and the Lewis Acids.* To study the influence of the anion on the trimerization process, we prepared trimethylsilylium *closo*-7,8,9,10,11,12-hexabromocarboranate $[Me_3Si][CHB_{11}H_5Br_6]$ and reacted it with (i) stoichiometrically amounts of diazomethane **1** or aminoisonitrile **3** in benzene and (ii) a large excess of **1** and **3** ($[Me_3Si][CHB_{11}H_5Br_6]$ as catalyst). As shown in Scheme 4, pyrazole species **7** was generated with the same reactivity, and it was also possible to isolate the catalytic species $\mathbf{9}[CHB_{11}H_5Br_6]$ (Figure 3, Table 1).

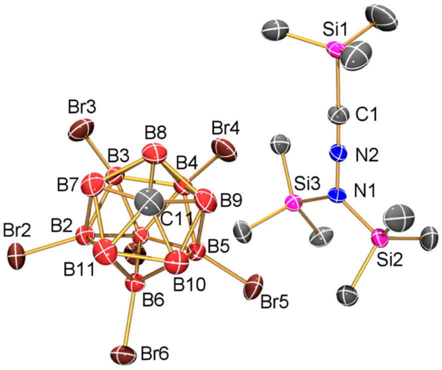

**Figure 3.** ORTEP drawing of the molecular structure of $\mathbf{9}[CHB_{11}H_5Br_6]$ in the crystal. Thermal ellipsoids with 50% probability at 173 K. Selected bond lengths (Å) and angles (°): N1−N2 1.309(3), N2−C1 1.147(4), Si2−N1 1.816(3), Si3−N1 1.809(3), Si1−C1 1.901(3), N2−N1−Si3 115.1(2), N2−N1−Si2 115.5(2), Si3−N1−Si2,129.4(1), C1−N2−N1 178.6(4).

As listed in Table 1, in a next series of experiments several neutral ($GaCl_3$, $B(C_6F_5)_3$) and cationic Lewis acids ($Ag^+$, $[(Me_3Si)_2NCN(SiMe_3)]^+$ (**6**), $[Ph_3C]^+$, $[Me_3SiOEt_2]^+$, and $[(Et_2O)_2H]^+$) were tested. Except for $Ag^+$ and $GaCl_3$, all other Lewis acids showed a significant reactivity and can be used for the generation of pyrazole species **7**. Interestingly, in contrast to $[Ph_3C]^+$, the neutral Lewis acid $B(C_6F_5)_3$ also catalyzes the isomerization and trimerization process; however, the rates of both processes are much slower. For both $[Ph_3C]^+$ and $B(C_6F_5)_3$, we were also able to isolate and fully characterize the catalysts $[(Me_3Si)_2NNC(CPh_3)]^+$ (**10**) and $[(Me_3Si)_2NNC(B(C_6F_5)_3)]^+$ (**11**), respectively (Figure 4).

## 2.2. Properties and Spectroscopic Characterization.

All experimentally studied compounds ($\mathbf{6}[B(C_6F_5)_4]$, $\mathbf{9}[B(C_6F_5)_4]$, $\mathbf{9}[CHB_{11}H_5Br_6]$, **10**, and **11** as well as pyrazole species **7** and **12**) are easily prepared in large scale and are stable when stored in a sealed tube and kept at ambient temperature. All these compounds have been fully characterized. All salts are extremely air- and moisture-sensitive but stable under argon atmosphere over a long period as a solid. Toluene is a good solvent for all species; however, the three salts $\mathbf{6}[B(C_6F_5)_4]$, $\mathbf{9}[B(C_6F_5)_4]$, and $\mathbf{9}[CHB_{11}H_5Br_6]$ are poorly soluble in non-aromatic organic solvents such as *n*-hexane or slowly decompose in, e.g., $CH_2Cl_2$, in contrast to neutral **10** and **11**. The $[B(C_6F_5)_4]^-$ salts of **6** and **9** melt at 104 and 108 °C, respectively, while for $\mathbf{9}[CHB_{11}H_5Br_6]$ (206 °C) and **10** (136 °C) only decomposition is observed. The highest melting point is found for the neutral compound **11**, at 122 °C (Table 2).

The IR and Raman data of all isonitrile species show a sharp band in the expected region[33,41] between 2209 and 2302 $cm^{-1}$, which can be approximately assigned to the stretching frequency $\nu_{CN}$ (cf. 2041 $cm^{-1}$ (IR) in $(Me_3Si)_2CNN$ and 2102 $cm^{-1}$ (Raman) in $(Me_3Si)_2NNC$)). It should be noted that the entire CNN moiety vibrates in an asymmetric mode; however, to a good approximation the small movement of the amino nitrogen can be neglected. As previously shown, the coordination of $B(C_6F_5)_3$ to a R−CN species causes a significant band shift to higher wave numbers; thus, for the $B(C_6F_5)_3$ adduct **11**, a shift of $\Delta\nu$ = 197 $cm^{-1}$ was observed.[42] A shift with a similar magnitude was also observed for all salts containing cation **9** (Table 2). Hence, both IR and Raman spectroscopy are particularly well suited to distinguish between the starting material **3** and the silylated cation **9**. The shift to higher wave numbers upon adduct formation correlates nicely with a smaller C−N distance (**3**, $d$(CN) = 1.152(2) Å vs $\mathbf{9}[B(C_6F_5)_4]$, 1.143(2); $\mathbf{9}[CHB_{11}H_5Br_6]$, 1.147(2); **10**, 1.145(2); and **11**, 1.145(4) Å; see X-ray structure elucidation, Table 3). Interestingly, the CN distance in neutral adduct **11** is almost the same as found in all cationic adducts **9** and **10**.

Pyrazole species **7** (Figure 5 left) is neither very air- nor moisture-sensitive, melts at 66 °C, and dissolves in almost all common organic solvents. Depending on the solvent, several solvates of **7** can be obtained, such as **7**·*n*-hexane and **7**·disiloxane (see below). Interestingly, one $Me_3Si$ group can be selectively hydrolyzed by addition of 1 equiv of $CF_3SO_3H$ or water/*n*-hexane to give pyrazole species **12** (Scheme 6, Figure 5 right).[43] It is interesting to note that crystals of **12** show dichroism under polarized light which results in a violet or orange appearance.

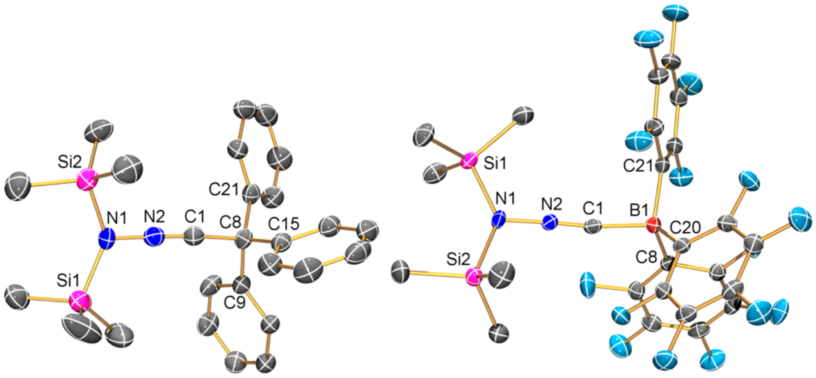

**Figure 4.** ORTEP drawing of the molecular structures of **10** (left) and **11** (right) in the crystal. Thermal ellipsoids with 50% probability at 173 K. Selected bond lengths (Å) and angles (°): for **10**, N2−C1 1.145(4), N2−N1 1.334(4), C1−C8 1.480(4), N1−Si2 1.818(3), N1−Si1 1.823(3), C1−N2−N1 179.1(3), N2−N1−Si2 111.9(2), N2−N1−Si1 113.3(2), Si2−N1−Si1 132.6(2); for **11**, N2−C1 1.145(2), N2−N1 1.331(2), N1−Si1 1.805(1), N1−Si2 1.805(1), C1−B1 1.617(2), C1−N2−N1 177.7(1), N2−N1−Si1 114.91(6), N2−N1−Si2 111.52(6), Si1−N1−Si2 133.35(4).

**Table 2. Spectroscopic Details**

| | $6[B(C_6F_5)_4]$ | $9[B(C_6F_5)_4]$ | $9[CHB_{11}H_5Br_6]$ | **10** | **11** |
|---|---|---|---|---|---|
| mp/°C | 104 | 108 | 206[a] | 136[a] | 122 |
| $^{11}$B NMR | −16.64[c] | −16.64[c] | −20.22 (d, 5B, *B*H), −9.84 (s, 5B, *B*Br), −1.74 (s, 1B, 12-*B*Br) | −16.64 | −21.27 |
| Ra: $\nu_{CN}$/cm$^{-1}$ | 2251(4) | 2209(9) | [b] | [b] | 2299(10), 2220(3), |
| IR: $\nu_{CN}$/cm$^{-1}$ | 2287(w), 2243(m) | 2215(m) | 2236(w), 2165(w) | 2285(w) | 2302(w) |

[a] Decomposition temperature. [b] Strong fluorescence. [c] Slow decomposition in $CD_2Cl_2$

**Table 3. Selected Bond Lengths (Å) and Angles (°) from X-ray Structure Analyses**

| compound[d] | X−Y | Y−Z | Z−R | XYZ |
|---|---|---|---|---|
| $NNC(SiMe_3)_2$ (**1**) | 1.135(2) | 1.312(2) | 1.885(1) | 179.6(2) |
| $(Me_3Si)_2NNC$ (**3**)[b] | 1.366(2) | 1.152(2) | – | 177.7(2) |
| $(Me_3Si)_2NNC$ (**3**)[b] | 1.361(2) | 1.153(2) | – | 178.4(2) |
| $(Me_3Si)NCN(SiMe_3)$ (**4**)[c] | 1.201(2) | 1.194(2) | 1.722(2) | 176.6(2) |
| $[(Me_3Si)_2NCN(SiMe_3)][B(C_6F_5)_4]$ | 1.279(2) | 1.18(1) | 1.795(11) | 173.3(5) |
| $[(Me_3Si)_2NNC(SiMe_3)][B(C_6F_5)_4]$ | 1.309(2) | 1.143(2) | 1.897(2) | 179.3(1) |
| $[(Me_3Si)_2NNC(SiMe_3)][CHB_{11}H_5Br_6]$ | 1.309(3) | 1.147(4) | 1.901(3) | 178.6(4) |
| $(Me_3Si)_2NNC(B(C_6F_5)_3)$ (**11**)[a] | 1.331(2) | 1.145(2) | 1.617(2) | 177.7(1) |
| $(Me_3Si)_2NNC(B(C_6F_5)_3)$ (**11**)[a] | 1.342(2) | 1.143(2) | 1.615(2) | 177.7(2) |
| $[(Me_3Si)_2NNC(CPh_3)][B(C_6F_5)_4]$ (**10**) | 1.334(4) | 1.145(4) | 1.480(4) | 179.1(3) |

[a] Two slightly different data sets were obtained from different experiments. [b] Two independent molecules in the unit cell. [c] See ref 44. [d] All compounds can formally be written as R′X−Y−Z−R; e.g., for **1** and **3**, X = N, Y = N, Z = C; for **4**, X = N, Y = C, Z = N, etc.

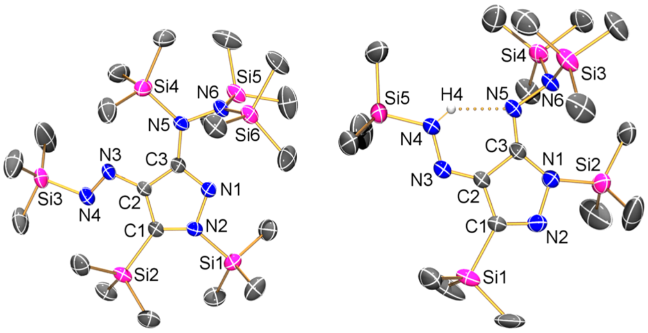

**Figure 5.** ORTEP drawing of the molecular structures of pyrazole species **7** (left) and **12** (right) in the crystal. Thermal ellipsoids with 50% probability at 173 K. Except from H4, all other hydrogen atoms are omitted for clarity. Selected bond lengths (Å): for **7**, N1−C3 1.324(3), N1−N2 1.400(2), N2−C1 1.355(2), N3−N4 1.272(2), N3−C2 1.389(3), N5−C3 1.387(2), N5−N6 1.455(2), C1−C2 1.398(3), C2−C3 1.425(3); for **12**, N1−C3 1.381(3), N1−N2 1.433(3), N2−C1 1.314(3), N3−C2 1.310(3), N3−N4 1.348(3), N5−C3 1.307(3), N5−N6 1.467(3), C1−C2 1.437(3), C2−C3 1.470(3).

**2.3. X-ray Structural Analysis.** As far as we know, there are no structural data available for the starting materials **1** and **3**, while the structures of bis-silylated carbodiimide **4** and its tetramer were reported in 1994 by Riedel et al.[44] The structures of silylium cation-containing species $\mathbf{6}[B(C_6F_5)_4]$, $\mathbf{9}[B(C_6F_5)_4]$, and $\mathbf{9}[CHB_{11}H_5Br_6]$, as well as **10** and **11**, besides pyrazoles **7** and **12**, were determined. Tables S1−S4 (see Supporting Information) present the X-ray crystallographic data. X-ray-quality crystals of all considered species were selected in Fomblin YR-1800 (Alfa Aesar) at ambient temperature. All samples were cooled to −100(2) °C during the measurement. The molecular structures are shown in Figures 1−5, along with selected bond lengths and angles. More details are found in the Supporting Information, including the data for the solvates **7**·*n*-hexane and **7**·disiloxane.

*Structure of the Room-Temperature Liquids $(Me_3Si)_2CNN$ (**1**), $(Me_3Si)_2NNC$ (**3**), and $(Me_3Si)NCN(SiMe_3)$ (**4**).* Crystals of **1** and **3** suitable for X-ray crystallographic analysis were obtained by slow cooling of neat **1** and **3**, respectively, to −80 °C over a period of 8 h. Both species crystallized (space group for **1**, $P\bar{1}$; for **3**, *Pbca*; cf. for **4**, $P2_1/c$[44]) with two independent molecules per unit cell. Only very weak van der Waals interaction can be assumed since large distances between molecules of **1**, **3**, and **4** are observed. There are only very small differences between the structural parameters of the independent molecules. Hence only one set of data is given for **1** and **3** in Figure 1 and Table 3. In general, in both isoelectronic species **1** and **3** the NNC moiety is almost linear, with short NN and CN bond lengths displaying partial double- and triple-bond character. For diazomethane species **1** a very short NN distance, indicating triple-bond character (N1−N2 1.135(2) Å, cf. $\sum r_{cov}(N{\equiv}N)$ = 1.08 Å),[45] is found, while the CN bond is much longer, at 1.312(2) Å. This situation is exactly the other way around in **3**, with a CN triple bond (1.152(2) Å, $\sum r_{cov}(C{\equiv}N)$ = 1.14 Å)

**Scheme 6. Selective Hydrolysis of 7**

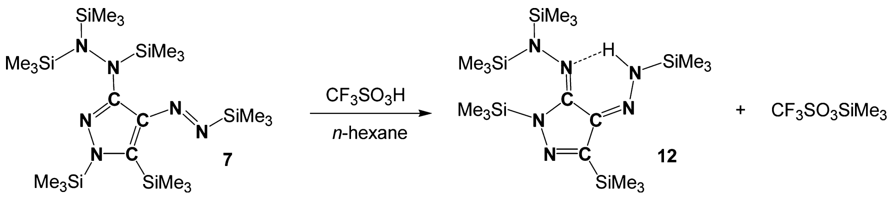

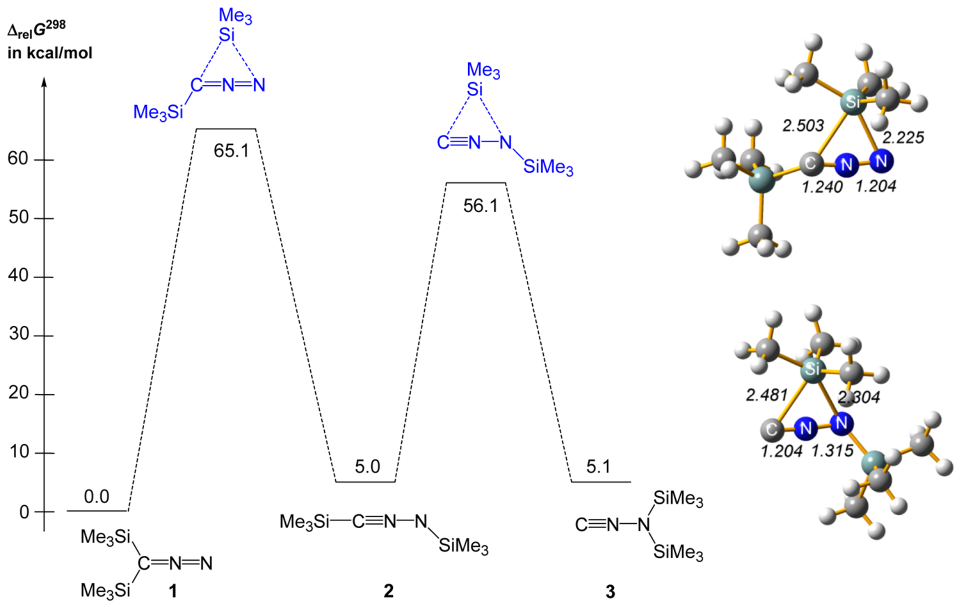

**Figure 6.** Left: Energies of the intrinsic isomerization process without a $[Me_3Si]^+$ ion as catalyst. Right: Calculated transition states for the intrinsic 1,3-$Me_3Si$ shift in **1** (distances in Å).

and a rather long NN bond, at 1.366(2) Å (cf. $\sum r_{cov}(N{=}N)$ = 1.20 Å and $\sum r_{cov}(N{-}N)$ = 1.42 Å).[45] For comparison, in the carbodiimide species **4** the CN bond lengths amount to 1.201(2) and 1.194(2) Å, and the NCN unit is also almost linear (176.6(2)°).[44]

*$[(Me_3Si)_2NCN(SiMe_3)][B(C_6F_5)_4]$ (**6**$[B(C_6F_5)_4]$).* The X-ray diffraction analyses (space group $P2_1/c$) revealed a disordered cation with a di-coordinated and tri-coordinated (planar) nitrogen center (sum of the angles around N1 = 360°, Figure 2 left). The strong interaction of carbodiimide with the formally added, electron-deficient $[Me_3Si]^+$ center is clearly apparent from the Si−N bond lengths (N1−Si2 1.835(1), N1−Si3 1.838(1), and N2−Si1 1.794(1) Å), which are slightly shorter than the sum of the covalent radii (1.87 Å).[45] Due to the di- and tri-coordination, respectively, two significantly different CN bond lengths (N1−C1 1.279(2), N2−C1 1.18(1) Å) are observed, in contrast to the neutral parent molecule **4** (1.201(2) and 1.194(2) Å).[44] The NCN unit is slightly bent, with 173.3(5)°, and all Si atoms are not part of the plane formed by these three atoms. Only weak interactions are found between the ions.

*$[(Me_3Si)_2NNC(SiMe_3)][B(C_6F_5)_4]$ (**9**$[B(C_6F_5)_4]$).* Compound **9** crystallizes in the monoclinic space group $P2_1/c$ with four units per cell. As depicted in Figure 2 (right), the cation adopts a $C_1$-symmetric structure with an almost linear CNN unit (C1−N2−N1 179.3(1)°, cf. 179.6(2) in $(Me_3Si)_2CNN$ and 177.7(2)° in $(Me_3Si)_2NNC$, Figure 1), and a slightly bent Si1−C1−N2 angle of 174.6(1)° is found. The C−N bond length amounts to 1.143(2) Å, which nicely agrees with the sum of the covalent radii for a CN triple bond ($\sum r_{cov}(C{\equiv}N)$ = 1.14 Å;[45] cf. 1.152(2) Å in $(Me_3Si)_2NNC$ or 1.157(2) Å in $[Me_3Si{-}C{\equiv}N{-}SiMe_3]^+$).[19] The N1−N2 bond is rather long, at 1.309(2) Å (cf. $\sum r_{cov}(N{=}N)$ = 1.20 Å and $\sum r_{cov}(N{-}N)$ = 1.42;[45] 1.135(2) Å in $(Me_3Si)_2CNN$ and 1.366(2) Å in $(Me_3Si)_2NNC$), indicating partial double-bond character. In accord with natural bond orbital analysis,[46] thus the best Lewis representation is that with a CN triple bond and an NN single bond: $[Me_3Si{-}C{\equiv}N^+{-}N(SiMe_3)_2]^+$. The tri-coordinated N1 atom sits in a trigonal planar environment ($\sum\angle N$ = 360.0°) with two small N2−N1−Si angles (113.76(8) and 114.89(8)°) and one large Si3−N1−Si2 angle (131.34(6)°).

*$[(Me_3Si)_2NNC(SiMe_3)][CHB_{11}H_5Br_6]$ (**9**$[CHB_{11}H_5Br_6]$).* As displayed in Table 3 and Figure 3, the structural parameters (bond lengths and angles) of the cation are identical (within the standard deviation) with those of **9**$[B(C_6F_5)_4]$, indicating that both borate anions are true weakly coordinating anions (shortest distances between $C1_{cation}\cdots Br_{anion}$ = 3.734 Å; cf. $C1_{cation}\cdots F_{anion}$ = 3.632 Å in **9**$[B(C_6F_5)_4]$).

*$[(Me_3Si)_2NNC(CPh_3)][B(C_6F_5)_4]$ (**10**) and $[(Me_3Si)_2NNC(B(C_6F_5)_3)]$ (**11**).* The formal change of the Lewis acid ($Me_3Si^+$ in **9**), as in **10** ($Ph_3C^+$) and **11** ($B(C_6F_5)_3$), leads to small differences in the NN distance, which are a little longer (**10**, 1.334(4), and **11**, 1.342(2) Å vs **9**$[CHB_{11}H_5Br_6]$, 1.309(3), and **9**$[B(C_6F_5)_4]$, 1.309(2) Å), while the CN bond lengths are identical to those in **9**$[CHB_{11}H_5Br_6]$ and **9**$[B(C_6F_5)_4]$) (Figure 4, Table 3). The donor−acceptor bond lengths are in the expected range, at 1.480(4) (C1−C8) and 1.615(2) (C1−B1), respectively ($\sum r_{cov}(C{-}C)$ = 1.50 Å and $\sum r_{cov}(C{-}B)$ = 1.60 Å).[45]

*Pyrazole Species **7** and **12**.* Both pyrazole species crystallize in the triclinic space group $P\bar{1}$ with two molecules per unit cell. As illustrated in Figure 5, the major difference in the molecular structure of both species arises from an intramolecular hydrogen bond in **12**, which forces a change of the configuration along the diazenyl substituent (cf. **7**, N4 trans to C3 vs **12**, N4 cis to C3), allowing the formation of a six-membered ring closed by the H-bridge. Furthermore, due to the hydrogen bond, the amino nitrogen atom of the $(Me_3Si)_2N$ moiety pyramidalizes ($\sum\angle N$ = 338.1°) since the nitrogen lone pair cannot be delocalized by hyperconjugation. Hyperconjugative effects are known to be responsible for the planarization of the amino nitrogen atom, as found in **7**.[47] Both N atoms of the hydrazine substituent in **12** have a distorted trigonal-planar geometry ($\sum\angle N$ = 359.4 and 359.7°), and both trigonal planes are almost perpendicular to each other (∠Si4−N5−N6−Si6 = 93.8°). Both (amino)silyl groups adopt a staggered configuration in contrast to **12**, for which an eclipsed configuration is observed. While the N5−N6 bond

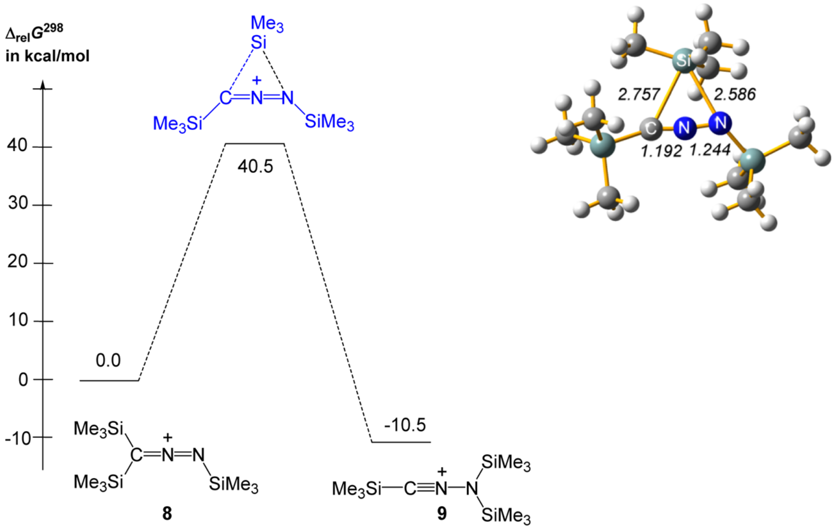

**Figure 7.** Left: Energies of the intrinsic isomerization process with a $[Me_3Si]^+$ ion as catalyst. Right: Calculated transition state for the intrinsic 1,3-$Me_3Si$ shift in **8** (distances in Å).

lengths are similar in **7** (1.455(2) Å) and **12** (1.467(3) Å), the N3–N4 bond length of the diazenyl unit increases upon hydrogen bond formation in **12** (cf. 1.272(2) vs 1.348(3) Å; $\sum r_{cov}(N{=}N) = 1.20$ Å, $\sum r_{cov}(N{-}N) = 1.42$ Å;[45] 1.247(3) Å in Ph–N=N–Ph).[48] The central five-membered pyrazole ring is planar (deviation from planarity less than 2°), with bond lengths and angles in the expected ranges.[49]

### 2.4. Theoretical Aspects of the Trimerization Process.

The astonishing isolation of $[(Me_3Si)_2NNC(SiMe_3)]^+$ instead of isomeric $[(Me_3Si)_2CNN(SiMe_3)]^+$ as well as the isolation of the trimerization product **7** prompted us to carry out quantum chemical calculations at the pbe1pbe/aug-cc-pwCVDZ level of theory to gain insight into the thermodynamics and kinetics of this complex reaction. In any case, the formation of pyrazole species **7**, starting from diazomethane, includes several successive reaction steps, including (i) a C–C or C–N coupling and (ii) a [3+2] or [4+1] cycloaddition reaction. Experimentally, it is known that pure $(Me_3Si)_2CNN$ is thermally stable for a long time. However, it is rearranged to bis(trimethylsilyl)carbodiimide, $(Me_3Si)NCN(SiMe_3)$, when it is heated in the presence of suitable catalysts such as $Cu^{2+}$.[33,41a] Thus, we studied the potential energy surface of neutral $(Me_3Si)_2CNN$ and cationic $[(Me_3Si)_3CNN]^+$ species, always retaining the CNN unit. As depicted in Scheme 5, the diazomethane isomer **1** is favored by 5.0 and 5.1 kcal/mol over nitrilimine **2** and aminoisonitrile **3**, respectively (cf. $(Me_3Si)NCN(SiMe_3)$ lies 42.1 kcal/mol below **1**). Upon $[Me_3Si]^+$ addition this situation switches. Now isomer **9** generated from **2** and **3** represents the lowest-lying isomer, separated by 10.5 kcal/mol from cation **8**, in accord with the experimental observation (cf. $[(Me_3Si)_2NCN(SiMe_3)]^+$ lies 49.7 kcal/mol below **9**).

Two questions were addressed with respect to our experimental findings: (i) Why does diazomethane **1** isomerize to isonitrile **3** (which then trimerizes) upon addition of traces of $[Me_3Si]^+$, and (ii) why is cation **9** exclusively formed from diazomethane species **1** upon adding stoichiometric amounts of $[Me_3Si]^+$? To answer these questions we have calculated the transition states for the instrinsic 1,3-shift of a $Me_3Si$ group in the neutral species **1** (Figure 6) and the cationic species **8** (Figure 7). In accord with our experimental data, the intrinsic isomerization process in neutral **1** at ambient temperatures is rather unlikely, since activation barriers larger than 56 kcal/mol need to be overcome. These barriers for a 1,3-shift considerably decrease once the $[Me_3Si]^+$ ion is added. However, they are still too large (ca. 40.5 kcal/mol, Figure 7) to allow such an intrinsic process at ambient or even low temperatures. Therefore, it can be assumed that bimolecular processes such as illustrated in Scheme 7 have to be considered. For the equilibrium of the isomerization process, which includes both the neutral and the cationic species as catalyst according to Scheme 7, the $\Delta G^{298}$ values are estimated to be −5.5 and 0.1 kcal/mol, respectively, displaying $[Me_3Si]^+$ exchange equilibria. The barriers for $[Me_3Si]^+$ exchange are dramatically decreased under solvation conditions, as can be seen by studying the bimolecular reaction paths (Scheme 7). Now, the exchange of a $[Me_3Si]^+$ ion between cations **8** or **9** and the neutral isomers **1**, **2**, and **3** occurs almost barrier-free (less than 10 kcal/mol, see Supporting Information) at ambient temperatures, resulting in monosolvate formation of the type $[Me_3Si]^+{\cdot}2S$ adduct (S = **1**, **2**, and **3**). In the cases of **1** and **3**, these solvate adducts feature a trigonal planar $[Me_3Si]^+$ ion that is almost symmetrically stabilized by two S donor molecules (Figure 8). From these computational data, which are in agreement with experimental data, it can be concluded that the initial reaction step for the trimerization is the catalytic isomerization of diazomethane **1** and the cation **8** in a bimolecular process, as

**Scheme 7. Isomerization Equilibria of Bis-silylated Diazomethane Catalyzed by Silylium Ions**

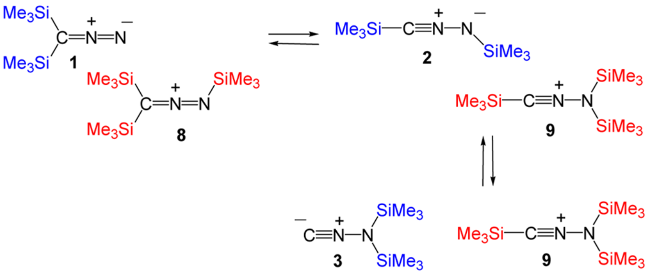

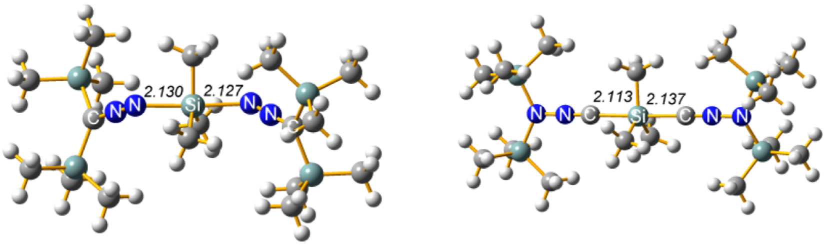

**Figure 8.** Calculated structures of stable $[Me_3Si]^+ \cdot 2S$ adducts: left, S = $(Me_3Si)_2CNN$ (**1**); right, S = $(Me_3Si)_2NNC$ (**3**). Distances in Å.

shown in Scheme 7, generating the reactive species **2** and **3**, respectively, besides cation **9**.

The trimethylsilylium affinity, which describes the enthalpy change associated with the dissociation of the conjugated acid,[50] is largest for isomer **2** (71.1 kcal/mol), followed by **3** (69.0 kcal/mol) and **1** (53.1 kcal/mol) (cf. $Me_3Si-H$, 31.3; $Me_3Si-CN$, 54.4; and $(Me_3Si)NCN(SiMe_3)$ 71.7 kcal/mol),[19] indicating that $[(Me_3Si)_2NNC(SiMe_3)]^+$ (**9**) is the most stable ion in the reaction mixture, in accord with experiment. Once the isomerization is triggered by the action of $[(Me_3Si)_2NNC(SiMe_3)]^+$, probably a dimerization via C−C or N−C coupling reaction of aminoisonitrile **3** occurs prior to a formal [3+2] or even [4+1] cycloaddition, as illustrated in Scheme 8. It is also possible that species **2** and **3** undergo dimerization. Since aminoisonitrile **3** is thermally stable in pure state and reacts only when the catalyst **9** is present, it can be concluded that also the dimerization reaction is catalyzed by strong Lewis acids (e.g., silylium ions $[(Me_3Si)_2NNC(SiMe_3)]^+$ + $(Me_3Si)_2NNC$). All three reactions steps are accompanied by formal $Me_3Si$ shifts, which can easily occur upon addition of $Me_3Si^+$ ions (vide supra). Interestingly, according to *in situ* NMR experiments (see above), there is no experimental proof for the generation of a dimer or any other species involved in the proposed formal [3+2] or [4+1] cycloaddition. The fact that only pyrazole species **7** is observed besides the starting material indicates either a fast reaction on the NMR time scale or a very low concentration of the intermediates. The overall trimerization process according to Scheme 3 is exothermic/exergonic, with −67.0/−35.1 kcal/mol in the gas phase.

**Scheme 8. Retrosynthetic Analysis of 7: (i) C−C Coupling Prior to [3+2] Cycloaddition, (ii) C−C Coupling Prior to [4+1] Cycloaddition, and (iii) C−N Coupling Prior to [4+1] Cycloaddition**

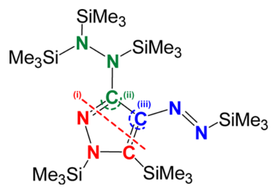

**2.5. Conclusions.** We present an efficient and facile trimerization reaction of bis-silylated diazomethane, triggered by the action of silylium ions to give exclusively 4-diazenyl-3-hydrazinylpyrazole. As catalyst the isonitrilium ion $[(Me_3Si)_2NNC(SiMe_3)]^+$, a formal pseudo-chalcogonium ion, was identified and fully characterized for the first time. The reaction is described by an isomerization process followed by a C−C or N−C coupling reaction and a formal cycloaddition to give finally the pyrazole derivative. From a mechanistic viewpoint, we report the first trimerization of diazomethane derivatives, which could also be extended to the aminoisonitrile isomer. This transformation can be regarded as a domino reaction.[51] From a practical viewpoint, the chemistry reported herein provides a facile approach to novel hydrazine-diazene-substituted pyrazoles that are of pharmacological relevance and not readily available by other methods.[52,53]

## 3. EXPERIMENTAL DETAILS

**3.1. General Information.** All manipulations were carried out under oxygen- and moisture-free conditions under argon using standard Schlenk or drybox techniques.

Toluene and diethyl ether were dried over Na/benzophenone. *n*-Hexane and *n*-pentane were dried over Na/benzophenone/tetraglyme. Carbon tetrachloride, dichloromethane, and hexamethyldisiloxane $(Me_3Si)_2O$ were dried over $P_4O_{10}$. Acetone was dried by distillation from $K_2CO_3$ followed by storage over 3 Å molecular sieves for 24 h. All solvents were freshly distilled prior to use. *n*-Heptane, chlorotrimethylsilane $Me_3SiCl$ (98%, Merck), and *N*,*N*-bis(trimethylsilyl)carbodiimide $(Me_3Si)NCN(SiMe_3)$ (97%, abcr) were freshly distilled prior to use. Lithium (99.9%, Merck), gallium trichloride $GaCl_3$ (abcr, 99.9%), chloromethyltrimethylsilane $Me_3SiCH_2Cl$ (97%, abcr), *n*-BuLi (2.5 M, Acros), and magnesium sulfate $MgSO_4$ (98%, VWR) were used as received. Alumina (aluminum oxide, basic, type T, Merck), was activated with triethylamine (98%, Merck) and dried in an oven at 120 °C for 36 h. *p*-Toluenesulfonylazide $MePhSO_2N_3$,[54] bis(trimethylsilyl)-hydronium tetrakis(pentafluorophenyl)borate $[Me_3Si-H-SiMe_3][B(C_6F_5)_4]$,[8b,15,55] tris(pentafluorophenyl)borane $B(C_6F_5)_3$,[55] tri(phenyl)methylium tetrakis(pentafluorophenyl)borate $[Ph_3C][B(C_6F_5)_4]$,[55] trimethylsilyl(diethyl)oxonium tetrakis(pentafluorophenyl)borate $[Me_3SiOEt_2][B(C_6F_5)]$,[20,56] silver *closo*-7,8,9,10,11,12-hexabromocarboranate $Ag[CHB_{11}H_5Br_6]$,[57] trimethylsilylium *closo*-7,8,9,10,11,12-hexabromocarboranate $[Me_3Si][CHB_{11}H_5Br_6]$,[57] and bis(diethyloxo)hydronium tetrakis(pentafluorophenyl)borate $[(Et_2O)_2H][B(C_6F_5)_4]$[58] were prepared as previously reported. Trimethylsilyldiazomethane $Me_3SiCHNN$, bis(trimethylsilyl)-diazomethane $(Me_3Si)_2CNN$, *N*,*N*-bis(trimethylsilyl)aminoisonitrile dichloride $(Me_3Si)_2NNCCl_2$, and *N*,*N*-bis(trimethylsilyl)-aminoisonitrile $(Me_3Si)_2NNC$ have been reported in the literature and were prepared by slightly modified procedures.[33,34,59]

*NMR.* $^{29}Si$ INEPT, $^{13}C\{^1H\}$, $^{13}C$ DEPT, and $^1H$ NMR spectra were obtained on a Bruker AVANCE 250 or 300 spectrometer and were referenced internally to the deuterated solvent ($^{13}C$: $CDCl_3$, $\delta_{reference}$ = 77 ppm, $CD_2Cl_2$, $\delta_{reference}$ = 54 ppm, $C_6D_6$, $\delta_{reference}$ = 128 ppm) or to protic impurities in the deuterated solvent ($^1H$: $CHCl_3$, $\delta_{reference}$ = 7.26 ppm, $CDHCl_2$, $\delta_{reference}$ = 5.31 ppm, $C_6D_5H$, $\delta_{reference}$ = 7.16 ppm). $CDCl_3$ and $CD_2Cl_2$ were dried over $P_4O_{10}$; $C_6D_6$ was dried over Na/benzophenone and freshly distilled prior to use.

*IR.* A Nicolet 6700 FT-IR spectrometer with a Smart Endurance ATR device was used.

*Raman.* A Bruker VERTEX 70 FT-IR spectrometer with a RAM II FT-Raman module, equipped with a Nd:YAG laser (1064 nm), was used.

*CHN Analyses.* A C/H/N/S-Mikronalysator TruSpec-932 instrument from Leco was used.

*DSC.* A DSC 823e instrument from Mettler-Toledo (heating rate, 5 °C/min) was used. Melting points (and decomposition points) were corrected. In addition, clearing points are given in brackets.

*MS.* A Finnigan MAT 95-XP spectrometer from Thermo Electron was used (CI$^+$, isobutene; EI$^+$, $T$ = 200 °C, 70.0 V).

*HRMS.* A 6210 time-of-flight LC/MS instrument from Agilent Technologies (MeOH/0.1% HCOOH in $H_2O$ 90:10) was used.

**3.2. Synthesis of 6[B($C_6F_5$)$_4$].** To a stirred suspension of [$Me_3Si$−H−$SiMe_3$][B($C_6F_5$)$_4$] (0.1 mmol, 0.083 g) in toluene (0.5 mL) was added neat ($Me_3Si$)NCN($SiMe_3$) (0.1 mmol, 0.019 g) at ambient temperature. The resulting colorless solution was concentrated *in vacuo*, resulting in a colorless oil. Storage at −25 °C for 24 h led to the deposition of colorless crystals. Removal of supernatant by decantation and drying *in vacuo* yields 0.072 g (0.077 mmol, 77%) of **6**[B($C_6F_5$)$_4$]. Mp: 104 °C (106 °C). Anal. Calcd (found): C, 43.51 (43.52); H, 2.90 (2.98); N, 2.98 (2.95). IR (ATR, 16 scans): 3467 (w), 3408 (w), 3381 (w), 3327 (w), 2962 (w), 2912 (w), 2359 (w), 2320 (m), 2287 (w), 2243 (m), 1643 (m), 1558 (w), 1512 (s), 1456 (s), 1412 (m), 1383 (m), 1374 (m), 1317 (m), 1263 (s), 974 (s), 907 (m), 853 (s), 823 (s), 768 (s), 755 (s), 726 (m), 700 (w), 683 (m), 661 (s), 634 (m), 610 (m), 603 (m), 573 (m). Raman (190 mW, 25 °C, 400 scans, cm$^{-1}$): 2982 (4), 2973 (4), 2913 (10), 2251 (4), 1648 (4), 1516 (1), 1468 (1), 1422 (1), 1380 (2), 1322 (2), 1277 (1), 1266 (1), 1127 (1), 1110 (1), 1098 (1), 1088 (1), 1056 (1), 980 (1), 824 (3), 774 (2), 760 (1), 710 (1), 687 (1), 664 (1), 645 (8), 587 (6), 531 (1), 494 (5), 479 (5), 452 (6), 425 (5), 398 (5), 381 (1), 361 (1), 350 (1), 290 (1), 248 (2), 210 (1), 190 (2), 161 (1), 124 (1), 76 (1). MS (CI$^+$, isobutane): 259 [($SiMe_3$)$_3CN_2$]$^+$, 187 [($SiMe_3$)$_2CN_2$ + H]$^+$, 115 [($SiMe_3$)$CN_2$ + 2H]$^+$. Crystals suitable for X-ray crystallographic analysis were obtained from slowly cooling a saturated toluene solution of **6**[B($C_6F_5$)$_4$] to 5 °C over a period of 12 h.

**3.3. Synthesis of 9[B($C_6F_5$)$_4$] and Catalytic Reaction to 7.** *Procedure 1: Reaction with ($Me_3Si$)$_2$CNN.* To a stirred suspension of [$Me_3Si$−H−$SiMe_3$][B($C_6F_5$)$_4$] (0.05 mmol, 0.040 g) in *n*-pentane (2 mL) was added a solution of ($Me_3Si$)$_2$CNN (1.06 mmol, 0.197 g) in *n*-pentane (2 mL) at −78 °C. The resulting suspension was allowed to warm to ambient temperature. Stirring for 36 h resulted in the deposition of crystals while the color of the supernatant changed gradually from yellow to dark red. The supernatant was removed by filtration (F4), and the brownish residue was washed three times with *n*-pentane (3 mL). Recrystallization from a minimum of toluene at −25 °C resulted in the deposition of colorless crystals. Removal of supernatant by decantation and drying *in vacuo* yielded 0.022 g (0.02 mmol, 49% yield based on 0.05 mmol of [$Me_3Si$−H−$SiMe_3$][B($C_6F_5$)$_4$]) of **9**[B($C_6F_5$)$_4$] as colorless crystals. The solutions from filtration and washing were combined, and the solvent was removed *in vacuo*, resulting in a dark red solution. Storage at −25 °C led to the deposition of greenish crystals. Removal of supernatant and drying *in vacuo* yielded 0.097 g (0.17 mmol, 51%) of **7** as dark green crystals.

*Procedure 2: Reaction with ($Me_3Si$)$_2$NNC.* To a stirred suspension of [$Me_3Si$−H−$SiMe_3$][B($C_6F_5$)$_4$] (0.05 mmol, 0.041 g) in *n*-hexane (4 mL) was added neat ($Me_3Si$)$_2$NNC (1.0 mmol, 0.186 g) at −78 °C. The resulting suspension was allowed to warm slowly to ambient temperature. Stirring for 12 h resulted in the deposition of yellowish crystals while the color of the supernatant changed gradually from yellow to dark red. The supernatant was removed by filtration (F4), and the yellowish residue was washed with *n*-hexane (3 mL). Recrystallization from a minimum of toluene at 5 °C resulted in the deposition of colorless crystals. Removal of supernatant by decantation and drying *in vacuo* yielded 0.027 g (0.03 mmol, 58% yield based on 0.05 mmol [$Me_3Si$−H−$SiMe_3$][B($C_6F_5$)$_4$]) of **9**[B($C_6F_5$)$_4$] as colorless crystals. The solutions from filtration and washing were combined and concentrated *in vacuo*, resulting in a dark red solution. Storage at −25 °C led to the deposition of greenish crystals. Removal of supernatant and drying *in vacuo* yielded 0.120 g (0.21 mmol, 68%) of **7** as dark green crystals.

*Data for **9**[B($C_6F_5$)$_4$].* Mp: 108 °C (109 °C). Anal. Calcd (found): C, 43.51 (43.75); H, 2.90 (2.85); N, 2.98 (2.86). IR (ATR, 16 scans): 3374 (w), 3224 (w), 2962 (w), 2912 (w), 2327 (w), 2215 (m), 1643 (m), 1600 (w), 1556 (w), 1512 (s), 1460 (s), 1413 (m), 1382 (m), 1374 (m), 1340 (w), 1261 (m), 1167 (m), 1081 (s), 976 (s), 923 (w), 907 (w), 855 (s), 822 (s), 773 (m), 768 (m), 756 (s), 726 (m), 700 (w), 683 (m), 660 (m), 643 (m) 626 (m), 611 (m), 602 (m), 573 (m). Raman (1500 mW, 25 °C, 800 scans, cm$^{-1}$): 2970 (4), 2910 (10), 2209 (9), 1643 (3), 1598 (1), 1576 (1), 1536 (1), 1513 (1), 1454 (1), 1417 (1), 1375 (2), 1314 (1), 1276 (1), 1263 (1), 1125 (1), 1106 (1), 976 (1), 960 (1), 945 (1), 862 (1), 845 (1), 820 (3), 771 (1), 757 (1), 733 (1), 700 (1), 685 (1), 661 (1), 643 (5), 628 (5), 584 (7), 509 (2), 491 (5), 476 (4), 448 (6), 422 (4), 394 (5), 371 (1), 359 (1), 348 (1), 320 (1), 287 (1), 265 (1), 244 (1), 206 (1), 186 (2), 157 (1), 119 (1). MS (CI$^+$, isobutane): 259 [($SiMe_3$)$_3CN_2$]$^+$, 187 [($SiMe_3$)$_2CN_2$ + H]$^+$. Crystals suitable for X-ray crystallographic analysis were obtained from toluene as depicted above.

*Data for **7**.* Mp: 66 °C (70 °C). Anal. Calcd (found): C, 45.10 (45.15); H, 9.73 (9.44); N, 15.03 (15.05). $^1$H NMR (25 °C, $CD_2Cl_2$, 300.13 MHz): 0.15 (s, 18H, Si($CH_3$)$_3$), 0.16 (s, 9H, Si($CH_3$)$_3$), 0.28 (s, 9H, Si($CH_3$)$_3$), 0.32 (s, 9H, Si($CH_3$)$_3$), 0.48 (s, 9H, Si($CH_3$)$_3$). $^1$H NMR (25 °C, $C_6D_6$, 300.13 MHz): 0.23 (s, 9H, Si($CH_3$)$_3$), 0.35 (s, 18H, Si($CH_3$)$_3$), 0.37 (s, 9H, Si($CH_3$)$_3$), 0.44(s, 9H, Si($CH_3$)$_3$), 0.48(s, 9H, Si($CH_3$)$_3$). $^{13}$C{$^1$H} NMR (25 °C, $CD_2Cl_2$, 62.89 MHz): −3.35 (s, Si($CH_3$)$_3$), −0.21 (s, Si($CH_3$)$_3$), 0.08 (s, (Si($CH_3$)$_3$)$_2$), 0.11 (s, Si($CH_3$)$_3$), 0.29 (s, Si($CH_3$)$_3$), 137.29 (*C*), 146.91(*C*), 158.15 (*C*). $^{13}$C{$^1$H} NMR (25 °C, $C_6D_6$, 62.89 MHz): −0.64 (s, Si($CH_3$)$_3$), 2.58 (s, Si($CH_3$)$_3$), 2.75 (s, Si($CH_3$)$_3$), 3.02 (s, 2 Si($CH_3$)$_3$), 140.26 (*C*), 149.72 (*C*), 161.15 (*C*). $^{29}$Si{$^1$H} NMR (25 °C, $CD_2Cl_2$, 49.69 MHz): −13.39 (m, 1Si, $J$($^1$H−$^{29}$Si) = 6.82 Hz), 6.22 (m, 1Si, $J$($^1$H−$^{29}$Si) = 6.79 Hz), 8.94 (m, 2Si, $J$($^1$H−$^{29}$Si) = 6.65 Hz), 11.31 (m, 1Si, $J$($^1$H−$^{29}$Si) = 6.59 Hz), 17.15 (m,1Si, $J$($^1$H−$^{29}$Si) = 6.71 Hz). $^{29}$Si{$^1$H} NMR (25 °C, $C_6D_6$, 49.69 MHz): −13.71 (m, 1Si, $J$($^1$H−$^{29}$Si) = 6.54 Hz), 6.00 (m, 1Si, $J$($^1$H−$^{29}$Si) = 6.54 Hz), 9.09 (m, 2Si, $J$($^1$H−$^{29}$Si) = 6.54 Hz), 11.40 (m, 1Si, $J$($^1$H−$^{29}$Si) = 6.54 Hz), 17.17 (m, 1Si, $J$($^1$H−$^{29}$Si) = 6.54 Hz). IR (ATR, 16 scans): 2956 (m), 2899 (m), 2864 (w), 1603 (w), 1574 (w), 1565 (w), 1521 (w), 1510 (w), 1490 (m), 1454 (m), 1388 (m), 1363 (m), 1298 (w), 1279 (m), 1245 (s), 1178 (m), 1142 (w), 1103 (w), 1074 (m), 1022 (w), 1004 (w), 981(w), 939 (m), 875 (m), 832 (s), 822 (s), 753 (s), 726 (m), 890 (m), 632 (m), 621 (m), 561 (w), 532 (m). Raman (1500 mW, 25 °C, 1209 scans, cm$^{-1}$): 2957 (3), 2903 (10), 1490 (2), 1453 (2), 1388 (7), 1364 (9), 1282 (5), 1245 (1), 1103 (1), 1080 (1), 1006 (1), 964 (2), 946 (1), 878 (1), 838 (1), 748 (1), 726 (1), 693 (3), 610 (3), 535 (1), 472 (1), 454 (1), 407 (1), 376 (1), 351 (1), 340 (1), 308 (1), 256 (1), 204 (1), 182 (1), 114 (1). MS (CI$^+$, isobutane): 558 [M]$^+$, 543 [M − $CH_3$]$^+$, 486 [M − $SiMe_3$]$^+$. UV−vis (25 °C, $CH_2Cl_2$, nm): 556, 393, 321, 255. Crystals suitable for X-ray crystallographic analysis were obtained by slowly cooling a saturated solution of **7** in either *n*-pentane, *n*-hexane, hexamethyldisiloxane, or acetone to −25 °C over a period of up to 12 h. Crystals obtained from *n*-hexane and hexamethyldisiloxane solutions could be characterized as *n*-hexane hemisolvate (**7**·*n*-hexane) or hexamethyldisiloxane hemisolvate (**7**·disiloxane), while crystals from *n*-pentane or acetone solutions did not contain solvent. However, the *n*-hexane was easily removed upon drying at ambient temperature for a few minutes.

**3.4. Synthesis of 9[$CHB_{11}H_5Br_6$].** To a stirred brownish suspension of [$Me_3Si$][$CHB_{11}H_5Br_6$] (0.1 mmol, 0.069 g) in toluene (3.0 mL) was added neat ($Me_3Si$)$_2$NNC (0.6 mmol, 0.120 g) at ambient temperature. The resulting colorless suspension was allowed to stir for an additional 1 h. Removal of supernatant by syringe and drying *in vacuo* yielded 0.068 g (0.0785 mmol, 79%) of **9**[$CHB_{11}H_5Br_6$] as pale brownish microcrystalline solid. Mp (dec): 206 °C. Anal. Calcd (found): C, 15.08 (14.88); H, 3.80 (4.06); N, 3.20 (3.50). $^1$H NMR (25 °C, $CD_2Cl_2$, 300.13 MHz): 0.47 (s, 18H, $J$($^1$H−$^{29}$Si) = 6.6 Hz, $J$($^1$H−$^{13}$C) = 121 Hz), 0.64 (s, 9H, $J$($^1$H−$^{29}$Si) = 7.18 Hz, $J$($^1$H−$^{13}$C) = 124 Hz), 1.12−3.57 (m, 5H, B*H*, $J$($^1$H−$^{11}$B) = 159 Hz), 2.59 (s, 1H, C*H-carboranate*). $^{11}$B NMR (25 °C, $CD_2Cl_2$, 96.29 MHz) −20.22 (d, 5B, *B*H), −9.84 (s, 5B, *B*Br), −1.74 (s, 1B, 12-BBr). $^{13}$C{$^1$H} NMR (25 °C, $CD_2Cl_2$, 75.48 MHz): −1.32 (s, Si($CH_3$)$_3$), −0.15 (s, 2Si($CH_3$)$_3$). $^{29}$Si{$^1$H} NMR (25 °C, $CD_2Cl_2$, 59.62 MHz): 4.78 (1*Si*), 29.01 (2*Si*). IR (ATR, 16 scans): 3051 (w), 2958 (w), 2902 (w), 2606 (m), 2236 (w), 2165 (w), 1682 (w), 1417 (w), 1309 (w), 1256 (s), 1113 (m), 1054 (m), 1002 (m), 991 (m), 953 (m), 933 (m), 855 (s), 819 (s), 746 (s), 702 (m), 633 (s). MS (CI−, isobutane): 616 *m/e* [$CHB_{11}H_5Br_6$]$^-$. Crystals suitable for X-ray crystallographic analysis of **9**[$CHB_{11}H_5Br_6$] were obtained from the saturated catalyst phase of the benzene reaction mixture after 12 h.

**3.5. Synthesis of [($Me_3Si)_2NNC(CPh_3)]B(C_6F_5)_4$] (10).** To a stirred orange solution of [$Ph_3C$][$B(C_6F_5)_4$] (0.5 mmol, 0.427 g) in dichloromethane (3 mL) was added neat ($Me_3Si)_2NNC$ (0.5 mmol, 0.093 g) at ambient temperature. The mixture was allowed to stir for 1 h while the color of the solution changed within 20 min from orange to yellow. Slow addition of *n*-hexane (5 mL) resulted in the deposition of a yellow greenish, microcrystalline solid. The yellow supernatant was removed by syringe, and the residue was re-dissolved in dichloromethane (2 mL) and again precipitated by addition of *n*-hexane (4 mL). This procedure was repeated a further two times. Removal of supernatant by decantation and drying *in vacuo* yielded 0.324 g (0.29 mmol, 58%) of [($Me_3Si)_2NNC(CPh_3)]B(C_6F_5)_4$] as microcrystalline solid. Mp (dec): 136 °C. Anal. Calcd (found): C, 54.16 (54.03); H, 3.00 (3.09); N, 2.53 (2.62). $^1$H NMR (25 °C, $CD_2Cl_2$, 300.13 MHz): 0.38 (s, 18H, $J(^1H-^{29}Si) = 6.8$ Hz, $J(^1H-^{13}C) = 121$ Hz), 7.08−7.53 (m, 15H, C*H*). $^{19}F\{^1H\}$ NMR (25 °C, $CD_2Cl_2$, 282.4 MHz): $\delta = -167.5$ (m, *m*-CF), −163.6 (m, *p*-CF), −133.0 (m, *o*-CF). $^{11}$B NMR (25 °C, $CD_2Cl_2$, 96.29 MHz) −16.64. $^{13}C\{^1H\}$ NMR (25 °C, $CD_2Cl_2$, 75.48 MHz): 0.10 (s, $Si(CH_3)_3$), 124.59 (br, *ipso*-C), 129.11 (s, CH), 130.43 (s, CH), 130.75 (s, *p*-CH), 136.91 (dm, *m*-CF, $^1J(^{13}C-^{19}F) = 247.59$ Hz), 138.90 (dm, *p*-CF, $^1J(^{13}C-^{19}F) = 232.18$ Hz), 148.76 (dm, *o*-CF, $^1J(^{13}C-^{19}F) = 240.44$ Hz). $^{29}Si\{^1H\}$ NMR (25 °C, $CD_2Cl_2$, 59.62 MHz): 30.87. IR (ATR, 16 scans): 2959 (w), 2913 (w), 2285 (w), 1643 (m), 1599 (w), 1584 (w), 1512 (s), 1493 (w), 1460 (s), 1456 (s), 1411 (m), 1383 (w), 1373 (w), 1359 (w), 1265 (m), 1186 (w), 1171 (w), 1160 (w), 1145 (w), 1084 (s), 1033 (w), 1001 (w), 974 (s), 942 (m), 902 (m), 854 (s), 823 (s), 773 (m), 756 (s), 748 (s), 726 (m), 698 (s), 683 (s), 660 (s), 635 (m), 610 (m), 603 (m), 573 (m). MS (CI+, isobutane): 431 (40) [M + H], 521 (10) [$B(C_6F_5)_3$], 357 (10) [$Me_3SiN(H)NCCPh_3$], 167 (78) [$C_6F_5$], 187 (10) [($SiMe_3)_2NNC$ + H], 270 (38) [$Ph_3CCN$ + H]. Crystals suitable for X-ray crystallographic analysis were obtained from slow diffusion of *n*-hexane onto the saturated dichloromethane solution of **10** at ambient temperature over a period of 36 h.

**3.6. Synthesis of ($Me_3Si)_2NNC(B(C_6F_5)_3$) (11).** *Procedure 1: Reaction with ($Me_3Si)_2NNC$.* To a stirred solution of $B(C_6F_5)_3$ (0.5 mmol, 0.256 g) in dichloromethane (2.5 mL) neat ($Me_3Si)_2NNC$ (0.5 mmol, 0.094 g) was added at 0 °C. The stirred reaction mixture was allowed to warm to ambient temperature within 1 h. The pale yellow solution was filtered (F4), concentrated approximately to 0.7 mL and stored in the refrigerator (5 °C) for 12 h. The resulting colorless Crystals were washed with dichloromethane (0.5 mL). Removal of supernatant by syringe and drying *in vacuo* yielded 0.250 g (0.358 mmol, 72%) of ($Me_3Si)_2NNC(B(C_6F_5)_3$) (**11**).

*Procedure 2: Reaction with ($Me_3Si)_2CNN$.* To a stirred solution of $B(C_6F_5)_3$ (0.5 mmol, 0.256 g) in dichloromethane (2.5 mL) was added neat ($Me_3Si)_2CNN$ (0.6 mmol, 0.120 g) at 0 °C. The stirred reaction mixture was allowed to warm to ambient temperature within 1 h. The pale yellow solution was filtered (F4), concentrated approximately to 0.7 mL, and stored in the refrigerator (5 °C) for 12 h. The resulting colorless crystals were washed with dichloromethane (0.5 mL). Removal of supernatant by syringe and drying *in vacuo* yielded 0.178 g (0.255 mmol, 51%) of ($Me_3Si)_2NNCB(C_6F_5)_3$ (**11**).

*Data for 11.* Mp: 122 °C (124 °C). Anal. Calcd (found): C, 42.99 (43.04); H, 2.60 (2.84); N, 4.01 (3.75). $^1$H NMR (25 °C, $CD_2Cl_2$, 300.13 MHz): 0.29 (s, 18H, $J(^1H-^{29}Si) = 6.8$ Hz, $J(^1H-^{13}C) = 121$ Hz). $^{19}F\{^1H\}$ NMR (25 °C, $CD_2Cl_2$, 282.4 MHz): $\delta = -164.5$ (m, *m*-CF), −157.9 (m, *p*-CF), −133.4 (m, *o*-CF). $^{11}$B NMR (25 °C, $CD_2Cl_2$, 96.29 MHz): −21.27. $^{13}C\{^1H\}$ NMR (25 °C, $CD_2Cl_2$, 75.48 MHz): −0.36 (s, $Si(CH_3)_3$), 116.02 (br, *ipso*-C), 137.63 (dm, *m*-CF, $^1J(^{13}C-^{19}F) = 229.43$ Hz), 140.77 (dm, *p*-CF, $^1J(^{13}C-^{19}F) = 214.03$ Hz), 148.58 (dm, *o*-CF, $^1J(^{13}C-^{19}F) = 240.99$ Hz). $^{29}Si\{^1H\}$ NMR (25 °C, $CD_2Cl_2$, 59.62 MHz): 25.46. IR (ATR, 16 scans): 2972 (w), 2911 (w), 2302 (w), 1645 (m), 1557 (w), 1514 (s), 1470 (s), 1466 (s), 1456 (s), 1418 (m), 1392 (m), 1382 (s), 1287 (m), 1282 (m), 1261 (s), 1134 (m), 1127 (m), 1095 (s), 1029 (w), 979 (s), 968 (s), 928 (w), 890 (m), 880 (m), 854 (s), 826 (s), 800 (s), 764 (m), 747 (m), 728 (m), 700 (m), 680 (m), 672 (m), 647 (m), 630 (m), 577 (w). Raman (460 mW, 25 °C, 200 scans, cm$^{-1}$): 2974 (5), 2913 (10), 2797 (4), 2539 (3), 2299 (10), 2220 (3), 1650 (4), 1474 (1), 1422 (1), 1394 (2), 1279 (2), 1138 (1), 1098 (1), 861 (1), 803 (2), 766 (1), 753 (1), 710 (1), 685 (1), 676 (1), 652 (6),635 (1), 622 (1), 585 (10), 510 (2), 496 (4), 471 (8), 450 (7), 419 (4), 398 (6), 357 (1), 344 (1), 288 (1), 271 (1), 244 (2), 188 (2), 159 (2), 91 (3). MS (EI, 70 eV): 698 (10) [M], 531 (14) [M − $C_6F_5$], 512 (100) [$B(C_6F_5)_3$], 364 (13) [M − $2C_6F_5$], 186 (11) [($SiMe_3)_2NNC$], 73 (83) [($SiMe_3$)]. Crystals suitable for X-ray crystallographic analysis were obtained by slowly cooling a saturated dichloromethane solution of **11** to 5 °C over a period of 12 h.

**3.7. Synthesis of 12.** *Procedure 1.* To a stirred solution of **7** (0.48 mmol, 0.271 g) in *n*-hexane (5 mL) was added neat $CF_3SO_3H$ (0.50 mmol, 0.075 g) dropwise at ambient temperature with stirring. The resulting suspension was stirred for 2 h while the color of the supernatant changed gradually from brown red to yellowish orange, and the yellowish precipitate was dissolved completely. Concentration to an approximate volume of 0.5 mL and storage at 5 °C resulted in the deposition of yellow crystals. Removal of supernatant, washing with a few drops of *n*-hexane, and drying *in vacuo* yielded 0.140 g (59%) of **12** as yellow crystals.

*Procedure 2.* **7** (0.179 mmol, 0.1 g) was dissolved in distilled (but not anhydrous) *n*-hexane (3 mL) at ambient temperature with stirring. The resulting orange solution was stirred for 15 min. Concentration to an approximate volume of 0.5 mL and storage at 5 °C resulted in the deposition of yellowish crystals. Removal of supernatant and drying *in vacuo* yielded 0.085 g (97%) of **12** as yellow crystals.

*Data for 12.* Mp: 94 °C (101 °C). Anal. Calcd (found): C, 44.39 (44.57); H, 9.523 (9.33); N, 17.26 (17.25). $^1$H NMR (25 °C, $C_6D_6$, 500.13 MHz): 10.15 (s, 1H, N*H*), 0.52 (s, 9H, $Si(CH_3)_3$, N-1), 0.41 (s, 9H, $Si(CH_3)_3$, C-1), 0.27 (s, 9H, $Si(CH_3)_3$, N-4), 0.15 (s, 18H, 2 $Si(CH_3)_3$, N-6). $^{13}C\{^1H\}$ NMR (25 °C, $C_6D_6$, 128.0 MHz): 161.9, 142.1 (*C*-2, *C*-3), 157.3 (*C*-1), 0.3 (s, 2 $Si(CH_3)_3$, N-6), −0.5 (s, $Si(CH_3)_3$, N-1), −0.6 (s, $Si(CH_3)_3$, N-4), −1.5 (s, $Si(CH_3)_3$, *C*-1). $^{29}Si\{^1H\}$ NMR (25 °C, $C_6D_6$, TMS = 0, 99.3 MHz): 10.1, 7.4 (*Si*Me$_3$(N-1), *Si*Me$_3$(N-4)), 6.6 (2, *Si*Me$_3$(N-6)), −8.6 (*Si*Me$_3$(C-1)). $^1$H NMR (25 °C, $CD_2Cl_2$, 300.13 MHz): 0.10 (s, 18H, $N(Si(CH_3)_3)_2$, $J(^1H-^{29}Si) = 6.6$ Hz), 0.24 (s, 9H, $Si(CH_3)_3$, $J(^1H-^{29}Si) = 6.9$ Hz, $J(^1H-^{13}C) = 121$ Hz), 0.29 (s, 9H, $Si(CH_3)_3$), 0.37 (s, 9H, $Si(CH_3)_3$, $J(^1H-^{29}Si) = 6.9$ Hz, $J(^1H-^{13}C) = 120$ Hz), 9.97 (s, 1H, N*H*). $^{13}C\{^1H\}$ NMR (25 °C, $CD_2Cl_2$, 62.89 MHz): −1.36 (s, $Si(CH_3)_3$), −0.32 (s, $Si(CH_3)_3$), −0.21 (s, $Si(CH_3)_3$), 0.56 (s, ($Si(CH_3)_3)_2$), 141.9 (*C*), 157.7 (*C*), 161.9 (*C*). $^{29}Si\{^1H\}$ NMR (25 °C, $CD_2Cl_2$, 99.3 MHz): −8.79, 6.91, 7.91, 9.91. IR (ATR, 16 scans): 2956 (m), 2899 (m), 2855 (w), 1573 (m), 1563 (m), 1520 (m), 1465 (m), 1405 (m), 1345 (w), 1325 (w), 1300 (m), 1245 (s), 1179 (s), 1076 (m), 1050 (m), 982 (m), 961 (m), 930 (m), 898 (m), 870 (m), 828 (s), 818 (s), 753 (s), 693 (m), 662 (m), 628 (s), 601 (m). Raman (1500 mW, 25 °C, 800 scans, cm$^{-1}$): 2960 (5), 2900 (10), 1562 (1), 1522 (1), 1466 (4), 1411 (1), 1345 (1), 1300 (1), 1250 (1), 1179 (1), 1076 (1), 983 (1), 963 (1), 941 (1), 898 (1), 843 (1), 763 (1), 694 (1), 663 (1), 634 (2), 601 (1), 531 (1), 462 (1), 435 (1), 357 (1), 318 (1), 303 (1), 235 (1), 177 (1), 117 (1). MS (CI$^+$, isobutane): 486 [M]$^+$, 471 [M − $CH_3$]$^+$, 413 [M − $SiMe_3$]$^+$. UV−vis (25 °C, $CH_2Cl_2$, nm): 412, 294.

## ■ ASSOCIATED CONTENT

### Ⓢ Supporting Information

Experimental and computational details, crystallographic information, and further experimental and theoretical data of all considered species. This material is available free of charge via the Internet at http://pubs.acs.org.

## ■ AUTHOR INFORMATION

### Corresponding Author

axel.schulz@uni-rostock.de

## Notes

The authors declare no competing financial interest.

## ■ ACKNOWLEDGMENTS

Martin Ruhmann (University Rostock) is acknowledged for the measurement of Raman spectra. Financial support by the DFG is gratefully acknowledged.

## ■ REFERENCES

(1) (a) Lambert, J. B.; Zhao, Y. *Angew. Chem., Int. Ed. Engl.* **1997**, *36*, 400−402. (b) Lambert, J. B.; Zhao, Y.; Wu, H.; Tse, W. C.; Kuhlmann, B. *J. Am. Chem. Soc.* **1999**, *121*, 5001−5008. (c) Lambert, J. B.; Lin, L. *J. Org. Chem.* **2001**, *66*, 8537−8539.

(2) Reviews: (a) Schulz, A.; Villinger, A. *Angew. Chem., Int. Ed.* **2012**, *51*, 4526−4528. (b) Lee, V. Y.; Sekiguchi, A. *Organometallic Compounds of Low-Coordinate Si, Ge, Sn and Pb*; Wiley: Chichester, 2010. (c) Klare, H. F. T.; Oestreich, M. *Dalton Trans.* **2010**, *39*, 9176−9184. (d) Lee, V. Y.; Sekiguchi, A. In *Reviews of Reactive Intermediate Chemistry*; Platz, M. S., Moss, R. A., Jones, M., Eds.; Wiley: New York, 2007; pp 47−120. (e) Lee, V. Y.; Sekiguchi, A. *Acc. Chem. Res.* **2007**, *40*, 410−419. (f) Müller, T. *Adv. Organomet. Chem.* **2005**, *53*, 155−215. (g) Kochina, T. A.; Vrazhnov, D. V.; Sinotova, E. N.; Voronkov, M. G. *Russ. Chem. Rev.* **2006**, *75*, 95−110. (h) Lambert, J. B.; Zhao, Y.; Zhang, S. M. *J. Phys. Org. Chem.* **2001**, *14*, 370−379. (i) Reed, C. A. *Acc. Chem. Res.* **1998**, *31*, 325−332. (j) Lickiss, P. D. In *The Chemistry of Organic Silicon Compounds*; Rappoport, Z., Apeloig, Y., Eds.; Wiley: Chichester, 1998; Vol. 2, pp 557−594. (k) Lambert, J. B.; Kania, L.; Zhang, S. *Chem. Rev.* **1995**, *95*, 1191−1201.

(3) For example: (a) Schäfer, A.; Reißmann, M.; Schäfer, A.; Saak, W.; Haase, D.; Müller, T. *Angew. Chem., Int. Ed.* **2011**, *50*, 12636−12638. (b) Allemann, O.; Duttwyler, S.; Romanato, P.; Baldrige, K. K.; Siegel, J. S. *Science* **2011**, *332*, 574−577. (c) Müther, K.; Fröhlich, R.; Mück-Lichtenfeld, C.; Grimme, S.; Oestreich, M. *J. Am. Chem. Soc.* **2011**, *133*, 12442−12444. (d) Müther, K.; Oestreich, M. *Chem. Commun.* **2011**, *47*, 334−336. (e) Leszczyńska, K.; Mix, A.; Berger, R. J. F.; Rummel, B.; Neumann, B.; Stammler, H.-G.; Jutzi, P. *Angew. Chem., Int. Ed.* **2011**, *50*, 6843−6846. (f) Duttwyler, S.; Douvris, C.; Nathanael, C. D.; Fackler, N. L.; Tham, F. S.; Reed, C. A.; Baldrige, K. K.; Siegel, J. S. *Angew. Chem., Int. Ed.* **2010**, *49*, 7519−7522. (g) Lühmann, N.; Panisch, R.; Müller, T. *Appl. Organomet. Chem.* **2010**, *24*, 533−537. (h) Klare, H. F. T.; Bergander, K.; Oestreich, M. *Angew. Chem., Int. Ed.* **2009**, *48*, 9077−9079. (i) Douvris, C.; Ozerov, O. *Science* **2008**, *321*, 1188−1190. (j) Panisch, R.; Boldte, M.; Müller, T. *J. Am. Chem. Soc.* **2006**, *128*, 9676−9682. (k) Hara, K.; Akiyama, R.; Sawamura, M. *Org. Lett.* **2005**, *7*, 5621−5623.

(4) Scott, V. J.; Çelenligil-Çetin, R.; Ozerov, O. V. *J. Am. Chem. Soc.* **2005**, *127*, 2852−2853.

(5) Meier, G.; Braun, T. *Angew. Chem., Int. Ed.* **2009**, *48*, 1546−1548.

(6) Zhang, Y.; Huynh, K.; Manners, I.; Reed, C. A. *Chem. Commun.* **2008**, 494−496.

(7) In contrast, siliconium ions are positively charged species in which silicon has higher than four coordination. Some authors prefer to restrict the term silylium ion to the fully tricoordinate form. See also: http://old.iupac.org/publications/books/rbook/Red_Book_2005.pdf.

(8) (a) Lambert, J. B.; Zhang, S.; Stern, C. L.; Huffman, J. C. *Science* **1993**, *260*, 1917−1918. (b) Lambert, J. B.; Zhang, S.; Ciro, S. M. *Organometallics* **1994**, *13*, 2430−2443.

(9) Xie, Z.; Liston, D. J.; Jelinek, T.; Mitro, V.; Bau, R.; Reed, C. A. *J. Chem. Soc., Chem. Commun.* **1993**, 384−386.

(10) Ibad, M. F.; Langer, P.; Schulz, A.; Villinger, A. *J. Am. Chem. Soc.* **2011**, *133*, 21016−21027.

(11) Duttwyler, S.; Do, Q.-Q.; Linden, A.; Baldridge, K. K.; Siegel, J. S. *Angew. Chem., Int. Ed.* **2008**, *47*, 1719−1722.

(12) Müller, T.; Bauch, C.; Ostermeier, M.; Bolte, M.; Auner, N. *J. Am. Chem. Soc.* **2003**, *125*, 2158−2168.

(13) Maerker, C.; Kapp, J.; Schleyer, P. von, R. In *Organosilicon Chemistry II*; Auner, N., Weis, J., Eds.; VCH: Weinheim, Germany, 1996; pp 329−358.

(14) Kim, K.-C.; Reed, C. A.; Elliott, D. W.; Mueller, L. J.; Tham, F.; Lin, L.; Lambert, J. B. *Science* **2002**, *297*, 825−827.

(15) Lehmann, M.; Schulz, A.; Villinger, A. *Angew. Chem., Int. Ed.* **2009**, *48*, 7444−7447.

(16) Lambert, J. B.; Zhang, S. *J. Chem. Soc., Chem. Commun.* **1993**, 383−384.

(17) Reed, C. A.; Xie, Z.; Bau, R.; Benesi, A. *Science* **1993**, *262*, 402−404.

(18) (a) Prakash, G. K. S.; Keyaniyan, S.; Aniszfeld, R.; Heiliger, L.; Olah, G. A.; Stevens, R. C.; Choi, H.-K.; Bau, R. *J. Am. Chem. Soc.* **1987**, *109*, 5123−5126. (b) Lambert, J. B.; Schulz, W. J., jr.; McConnell, J. A.; Schilf, W. *J. Am. Chem. Soc.* **1988**, *110*, 2201−2210.

(19) Schulz, A.; Villinger, A. *Chem.—Eur. J.* **2010**, *16*, 7276−7281.

(20) Schulz, A.; Thomas, J.; Villinger, A. *Chem. Commun.* **2010**, *46*, 3696−3698.

(21) Jäger, L.; Köhler, H. *Sulfur Rep.* **1992**, *12*, 159−212.

(22) Huisgen, R. In *1,3-Dipolar Cycloaddition Chemistry*; Padwa, A., Ed.; Wiley: New York, 1984; pp 1−31.

(23) (a) Regitz, M. *Diazoalkane: Eigenschaften und Synthesen*; Thieme Verlag: Stuttgart, 1977. (b) Zollinger, H. *Diazo Chemistry I*; VCH: Weinheim, 1994. (c) Zollinger, H. In *Diazo Chemistry II*; VCH: Weinheim, 1995. (d) Ye, T.; McKervey, M. A. *Chem. Rev.* **1994**, *94*, 1091−1160.

(24) (a) Fink, J.; Regitz, M. *Synthesis* **1985**, 569−585. (b) Bug, T.; Hartnagel, M.; Schlierf, C.; Mayr, H. *Chem.—Eur. J.* **2003**, *9*, 4068−4076.

(25) Huisgen, R. *Angew. Chem.* **1955**, *67*, 439−461.

(26) (a) Ledwith, A.; Shih-Lin, Y. *J. Chem. Soc. B* **1967**, 83−84. (b) Huisgen, R. *Angew. Chem., Int. Ed. Engl.* **1963**, *2*, 565−598. (c) Huisgen, R. *Angew. Chem., Int. Ed. Engl.* **1963**, *2*, 633−696.

(27) (a) Fustero, S.; Sánchez-Roselló, M.; Barrio, P.; Simón-Fuentes, A. *Chem. Rev.* **2011**, *111*, 6984−7034. (b) Elguero, J.; Silva, A. M. S.; Tome, A. C. In *Modern Heterocyclic Chemistry*, Vol. 2; Alvarez-Builla, J., Vaquero, J. J., Barluenga, J., Eds.; Wiley-VCH: Weinheim, 2011; pp 635−725.

(28) (a) Metwally, M. A.; Darwish, Y. M.; Amer, F. A. *Indian J. Chem., Sect. B* **1989**, *28*, 1069−1071. (b) Zauhar, L. *Can. J. Chem.* **1968**, *46*, 1079−1085. (c) Karci, F.; Sener, N.; Yamac, M.; Sener, I.; Demircali, A. *Dyes Pigm.* **2008**, *80*, 47−52. (d) Fahmy, S. H.; El-Hosami, M.; El-Gamal, S.; Elnagdi, M. H. *J. Chem. Technol. Biotechnol.* **1982**, *32*, 1042−1048.

(29) Mohareb, R. M.; Ho, J. Z.; Alfarouk, F. O. *J. Chin. Chem. Soc.* **2007**, *54*, 1053−1066.

(30) (a) Boger, D. L.; Coleman, R. S.; Panek, J. S.; Huber, F. X.; Sauer, J. *J. Org. Chem.* **1985**, *50*, 5377−5379. (b) Boger, D. L.; Panek, J. S.; Duff, S. R. *J. Am. Chem. Soc.* **1985**, *107*, 5745−5754. (c) Sotiropoulos, J. M.; Baceiredo, A.; Bertrand, G. *Bull. Soc. Chim. Fr.* **1992**, *129*, 367−375.

(31) (a) Meerwein, H. *Angew. Chem.* **1948**, *60*, 78. (b) Kantor, S. W.; Osthoff, R. C. *J. Am. Chem. Soc.* **1953**, *75*, 931−932.

(32) Only one major resonance Lewis formula is shown for clarity.

(33) Seyferth, D.; Flood, T. C. *J. Organomet. Chem.* **1971**, *29*, C25−C28.

(34) Wiberg, N.; Hübler, G. *Z. Naturforsch.* **1976**, *31b*, 1317−1321.

(35) (a) Huisgen, R.; Seidel, M.; Sauer, J.; McFarland, J. W.; Wallbillich, G. *J. Org. Chem.* **1959**, *24*, 892−893. (b) Huisgen, R.; Seidel, M.; Wallbillich, G.; Knupfer, H. *Tetrahedron* **1962**, *17*, 3−29.

(36) Bertrand, G.; Wentrup, C. *Angew. Chem., Int. Ed. Engl.* **1994**, *33*, 527−545.

(37) Granier, M.; Baceiredo, A.; Dartiguenave, Y.; Dartiguenave, M.; Menu, M. J.; Bertrand, G. *J. Am. Chem. Soc.* **1990**, *112*, 6277−6285.

(38) Emig, N.; Gabbaï, F. P.; Krautscheid, H.; Réau, R.; Bertrand, G. *Angew. Chem., Int. Ed.* **1998**, *37*, 989−992.

(39) Castan, F.; Baceiredo, A.; Bertrand, G. *Angew. Chem., Int. Ed.* **1989**, 1250−1251.

(40) (a) Pump, J.; Wannagat, U. *Liebigs Ann.* **1962**, *652*, 21−27. (b) Stenzel, J.; Sundermeyer, W. *Chem. Ber.* **1967**, *100*, 3368−3370. (c) Drake, J. E.; Glavincevski, B. M.; Henderson, H. E.; Wong, C. *Can. J. Chem.* **1979**, *57*, 1162−1166. (d) Kienzle, A.; Obermeyer, A.; Riedel, R.; Aldinger, F.; Simon, A. *Chem. Ber.* **1993**, *126*, 2569−2571.

(41) (a) Seyferth, D.; Menzel, H.; Dow, A. W.; Flood, T. C. *J. Organomet. Chem.* **1972**, *44*, 279−290. (b) Seyferth, D.; Dow, A. W.; Menzel, H.; Flood, T. C. *J. Am. Chem. Soc.* **1968**, *90*, 1080−1082.

(42) Jacobsen, H.; Berke, H.; Doering, S.; Kehr, G.; Erker, G.; Froehlich, R.; Meyer, O. *Organometallics* **1999**, *18*, 1724−1735.

(43) Addition of an excess of $CF_3SO_3H$ leads to a complete $Me_3Si/H$ substitution of all N-bound $Me_3Si$ groups. Only the C-bound $SiMe_3$ group remains intact.

(44) Obermeyer, A.; Kienzle, A.; Weidlein, J.; Riedel, R.; Simon, A. *Z. Anorg. Allg. Chem.* **1994**, *620*, 1357−1363.

(45) Pyykkö, P.; Atsumi, M. *Chem.—Eur. J.* **2009**, *15*, 12770−12779.

(46) (a) Glendening, E. D.; Reed, A. E.; Carpenter, J. E.; Weinhold, F. *NBO*, Version 3.1. (b) Carpenter, J. E.; Weinhold, F. *J. Mol. Struct. (Theochem)* **1988**, *169*, 41−62. (c) Weinhold, F.; Carpenter, J. E. *The Structure of Small Molecules and Ions*; Plenum Press: New York, 1988; p 227. (d) Weinhold, F.; Landis, C. *Valency and Bonding. A Natural Bond Orbital Donor-Acceptor Perspective*; Cambridge University Press: Cambridge, UK, 2005; and references therein.

(47) Fischer, G.; Herler, S.; Mayer, P.; Schulz, A.; Villinger, A.; Weigand, J. J. *Inorg. Chem.* **2005**, *44*, 1740−1751.

(48) Brown, C. J. *Acta Crystallogr.* **1966**, *21*, 146.

(49) Prasad, T. N. M.; Raghava, B.; Sridhar, M. A.; Rangappa, K. S.; Prasad, J. S. *X-ray Struct. Anal. Online* **2010**, *26*, 75.

(50) Swart, M.; Rösler, E.; Bickelhaupt, M. *J. Comput. Chem.* **2006**, 1485−1492.

(51) Reviews: (a) Tietze, L. F.; Beifuss, U. *Angew. Chem., Int. Ed. Engl.* **1993**, *32*, 131−163. (b) Tietze, L. F. *Chem. Rev.* **1996**, *96*, 115−136.

(52) (a) Musad, E. A.; Lokanatha, R. K. M.; Mohamed, R.; Saeed, A. B.; Vishwanath, B. S.; Rao, K. M. L. *Bioorg. Med. Chem. Lett.* **2011**, *21*, 3536−3540. (b) Kaymakcioglu, B. K.; Rollas, S. *Farmaco* **2002**, *57*, 595−600. (c) Coumar, M. S.; Leou, J.-S.; Shukla, P.; Wu, J.-S.; Dixit, A. K.; Lin, W.-H.; Chang, C.-Y.; Lien, T.-W.; Chen, C.-H.; Hsu, J. T.-A; Chao, Y.-S.; Wu, S.-Y.; Hsieh, H.-P.; Tan, U.-K., Jr. *J. Med. Chem.* **2009**, *52*, 1050−1062. (d) Ali, T. E.; Abdel-Aziz, S. A.; El-Shaaer, H. M.; Hanafy, F. I.; El-Fauomy, A. Z. *Phosphorus, Sulfur, Silicon Relat. Elem.* **2008**, *183*, 2139−2160. (e) Silveira, I. A. F. B.; Paulo, L. C.; de Miranda, A. L. P.; Rocha, S. O.; Freitas, A. C. C.; Barreiro, E. J. *J. Pharm. Pharmacol.* **1993**, *45*, 646−649.

(53) (a) El-Shafei, A.; Fadda, A. A.; Khalil, A. M.; Ameen, T. A. E.; Badria, F. A. *Bioorg. Med. Chem.* **2009**, *17*, 5096−5105. (b) El-Hawash, S. A.; Habib, N. S.; Fanaki, N. H. *Pharmazie* **1999**, *54*, 808−813. (c) Khalil, Z. H.; Yanni, A. S.; Gaber, A. M.; Abdel-Mohsen, S. A. *Phosphorus, Sulfur, Silicon Relat. Elem.* **2000**, *166*, 57−70. (d) Bekhit, A. A.; Ashour, H. M. A.; Guemei, A. A. *Arch. Pharm.* **2005**, *338*, 167−174. (e) Amir, M.; Khan, S. A.; Drabu, S. *J. Indian Chem. Soc.* **2002**, *79*, 280−281. (f) Krystof, V.; Cankar, P.; Frysova, I.; Slouka, J.; Kontopidis, G.; Dzubak, P.; Hajduch, M.; Srovnal, J.; de Azevedo, W. F.; Orsag, M.; Paprskarova, M.; Rolccik, J.; Latr, A.; Fischer, P. M.; Strnad, M. *J. Med. Chem.* **2006**, *49*, 6500−6509.

(54) Reiß, F.; Schulz, A.; Villinger, A.; Weding, N. *Dalton. Trans.* **2010**, *39*, 9962−9972.

(55) Nava, M.; Reed, C. A. *Organometallics* **2011**, *30*, 4798−4800.

(56) Driess, M.; Barmeyer, R.; Monsé, C.; Merz, K. *Angew. Chem., Int. Ed.* **2001**, *40*, 2308−2310.

(57) (a) Dunks, G. B.; Palmer-Ordonez, K. *Inorg. Chem.* **1978**, *17*, 1514−1516. (b) Dunks, G. B.; Barker, K.; Hedaya, E.; Hefner, C.; Palmer-Ordonez, K.; Remec, P. *Inorg. Chem.* **1981**, *20*, 1692−1697. (c) Franken, A.; King, B. T.; Rudolph, J.; Rao, P.; Noll, B. C.; Michl, J. *Collect. Czech. Chem. Commun.* **2001**, *66*, 1238−1249. (d) Xie, Z.; Jelinek, T.; Bau, R.; Reed, C. A. *J. Am. Chem. Soc.* **1994**, *116*, 1907−1913. (e) Xie, Z.; Bau, R.; Benesi, A.; Reed, C. *Organometallics* **1995**, *14*, 3933−3941.

(58) (a) Reiß, F.; Schulz, A.; Villinger, A. *Eur. J. Inorg. Chem.* **2012**, 261−271. (b) Jutzi, P.; Müller, C.; Stammler, A.; Stammler, H.-G. *Organometallics* **2000**, *19*, 1442−1444.

(59) Barton, T. J.; Hoekman, S. K. *Synth. React. Inorg. Met.-Org. Chem.* **1979**, *9*, 297−300.

## 5.2 Isolation of a Labile Homoleptic Diazenium Cation.

W. Baumann, D. Michalik, F. Reiß, A. Schulz, A. Villinger

*Angew. Chem.* **2014**, *126*, 3314-3318*; Angew. Chem. Int Ed.* **2014**, *53*, 3250-3253.

In dieser Publikation wurde ein groß Teil der experimentellen Arbeiten von mir durchgeführt. Die Direkt-Silylierungen wurden von mir verifiziert, alle Oxidations-Experimente wurden von mir durchgeführt. Ich habe das Manuskript mit verfasst und das Supportingfile verfasst. Der eigene Beitrag liegt bei ca. 75 %.

Ein ausführliches Supportingfile steht online zur freien Verfügung:

DOI: 10.1002/anie.201310186

Diazenium Ions

DOI: 10.1002/anie.201310186

# Isolation of a Labile Homoleptic Diazenium Cation[**]

*Wolfgang Baumann, Dirk Michalik, Fabian Reiß, Axel Schulz,[*] and Alexander Villinger[*]*

**Abstract:** *Following our interest in nitrogen chemistry, we now describe the synthesis, structure, and bonding of labile disilylated diazene, its $GaCl_3$ adduct, and the intriguing trisilylated diazenium ion $[(Me_3Si)_2N{=}N\text{-}SiMe_3]^+$, a dark blue and highly labile ($T_{decomp} > -30\,°C$) homoleptic cation of the type $[R_3N_2]^+$. Although direct silylation of $Me_3Si\text{-}N{=}N\text{-}SiMe_3$ failed, the $[(Me_3Si)_2N{=}N\text{-}SiMe_3]^+$ ion was generated in a straightforward two-electron oxidation reaction from mercury(II) dihydrazide and $Ag[GaCl_4]$. Moreover, previous structure data of $Me_3Si\text{-}N{=}N\text{-}SiMe_3$ were revised on the basis of new data.*

The rise of the synthetic dyestuffs industry during the 19th century began with the discovery of diazonium salts, for example, $[R\text{-}N{\equiv}N]^+Cl^-$, and diazotation reactions by Griess as early as 1858.[1,2] Azo dyes, compounds that usually contain two aromatic fragments connected by a N=N bond, still have a large impact and versatile scientific, medical, ecological, and technical importance.[3] Although aryl-substituted diazenes have been extensively investigated and represent a class of stable compounds, much less is known about alkyl- and silyl-substituted diazenes R-N=N-R (also known as diimines). It was not until 1968 that Wiberg et al. succeeded in the isolation of pale blue *N,N'*-bis(trimethylsilyl)diazene (**2**) from the reaction of *p*-tosylazide with lithium tris(trimethylsilyl)hydrazide (**1**) at low temperatures (Scheme 1).[4] In 1974 Veith and Bärnighausen published a single-crystal structure determination of **2**, which confirmed the postulated *trans* configuration but revealed an extraordinary short N–N distance of 1.171(7) Å.[5] This value, however, lies outside the reported range for known *trans* diazenes (1.219–1.254 Å; cf. $\Sigma r_{cov}(N{=}N) = 1.20$ Å),[6] and therefore provoked controversial remarks in the literature. Moreover, computational studies predicted longer N−N bonds, which were consistent with experimental and theoretical trends found for other diazenes.[5,7]

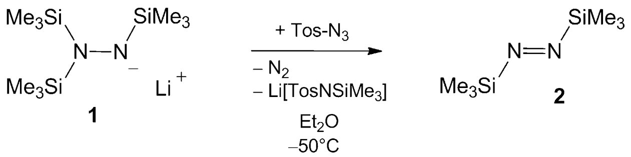

***Scheme 1.*** Synthesis of *N,N'*-bis(trimethylsilyl) diazene (**2**); Tos = *p*-$MeC_6H_4SO_2$.

Reports on the chemistry of diazenium cations $[R_2N{=}N\text{-}R]^+$ (R = alkyl, aryl) are restricted to only a few examples or are even unknown (R = $SiMe_3$) in the literature.[8–10] Herein, we focus on the synthesis of highly labile silylated diazenium species. Interestingly, the formation of mostly transient diazenium ions such as $[Ph_2N{=}N\text{-}H]^+$[11] was previously discussed in Diels–Alder, thermolysis, and solvolysis reactions, or electrochemically induced redox processes, often without any characterization.[12–15]

As shown by Wiberg, the reaction of tosylazide with **1** at low temperatures provides ready access to light blue, disilylated *trans* diazene **2** in approximately 65% yield (Scheme 1, Figure 1 left).[4] The major challenge when dealing with **2** arises from its very low decomposition point $T_{decomp} < -40\,°C$ (cf. *t*Bu-N=N-*t*Bu > 200 °C, Ph-N=N-Ph > 600 °C), which even lies below its melting point of about −3 °C.[16,17] Since diazene **2** decomposes at ambient temperatures with a half-time of 7.6 h (zero-order reaction, in a 5:1 mixture of *n*-pentane/toluene) it must be kept at temperatures below −50 °C in solution or in the solid state (see Figure S14 in the Supporting Information).[18] A suitable low-temperature synthesis had to be found to generate the tris(trimethylsilyl)diazenium ion $[(Me_3Si)_2N{=}N\text{-}SiMe_3]^+$ from diazene **2**.[19] We thought that the obvious route to the desired $[(Me_3Si)_2N{=}N\text{-}SiMe_3]^+$ cation was the direct silylation of diazene **2** with salts of the type $[Me_3Si{\cdot}LB]^+[B(C_6F_5)_4]^-$ or $[Me_3Si]^+[CB]^-$ at low temperatures (Scheme 2, route A; LB = weak Lewis base = toluene, $Me_3Si\text{-}H$, $Me_3Si\text{-}X$ with X = Cl, F; CB = $[CHB_{11}H_5X_6]$, X = Br, Cl). The calculated gas-phase reaction (1)[18g] with $\Delta H_{298} = -57.1$ kcal mol$^{-1}$ also supported the idea of direct silylation (cf. $-8.9\,N_2$, $-30.4$ toluene,

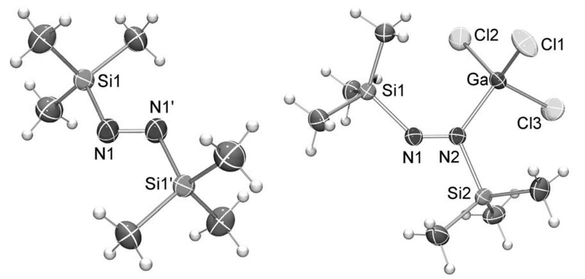

***Figure 1.*** ORTEP representation of the molecular structure of **2** (left) and **3** (right) in the crystal. Thermal ellipsoids correspond to 50% probability at 173 K.

---

[*] Dr. W. Baumann, Dr. D. Michalik, Prof. Dr. A. Schulz, Dr. A. Villinger
Universität Rostock, Institut für Chemie
Albert-Einstein-Strasse 3a, 18059 Rostock (Deutschland)
and
Leibniz-Institut für Katalyse e.V. an der Universität Rostock
Albert-Einstein-Strasse 29a, 18059 Rostock (Germany)
E-mail: axel.schulz@uni-rostock.de
alexander.villinger@uni-rostock.de
Homepage: http://www.chemie.uni-rostock.de/ac/schulz

[**] We are indebted to N. Wiberg, G. Fischer, and H. Brand (Ludwig-Maximilians-Universität München).

Supporting information for this article is available on the WWW under http://dx.doi.org/10.1002/anie.201310186.

© 2014 Wiley-VCH Verlag GmbH & Co. KGaA, Weinheim

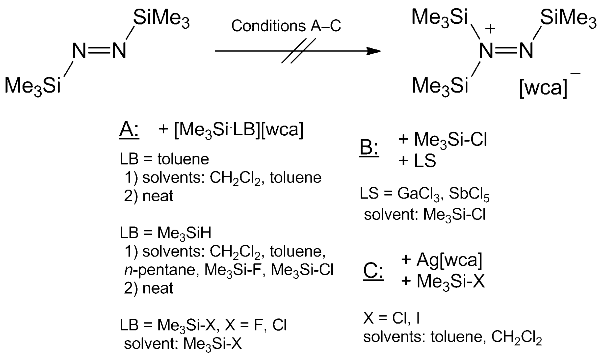

**Scheme 2.** Unsuccessful attempts for the synthesis of salts bearing the diazenium ion $4^+$ (A: [wca] = $[B(C_6F_5)_4]$, $[CHB_{11}H_6X_6]$, X = Br, Cl; B/C: [wca] = $[B(C_6F_5)_4]$, $[SbCl_6]$, $[AsF_6]$, $[GaCl_4]$).

−31.3 $Me_3Si$-H, −34.8 $Me_3Si$-F, −54.4 $Me_3Si$-CN, and −71.7 kcal mol$^{-1}$ for $Me_3Si$-N=C=N-$SiMe_3$).[19]

$$Me_3Si\text{-}N{=}N\text{-}SiMe_{3(g)} + [Me_3Si]^+_{(g)} \rightarrow [(Me_3Si)_2N{=}N\text{-}SiMe_3]^+_{(g)} \quad (1)$$

Reactions of all the utilized silylating agents (Scheme 2) with an excess of **2** in the absence of solvent led to violent decomposition even at very low temperatures (< −150 °C), but the reactions in all the applied solvents were also not successful due to decomposition of the reactants and the $[B(C_6F_5)_4]^-$ ion. In contrast, $[Me_3Si]^+[CHB_{11}H_5X_6]^-$ (X = Cl, Br) did not decompose under these reaction conditions; however, because of the limited solubility of $[Me_3Si]^+[CHB_{11}H_5X_6]^-$ no reaction with **2** below its decomposition temperature was observed. Since all these attempts failed, we then treated **2** with $Me_3Si$-X (X = Cl, I) in the presence of Ag[wca] (wca = weakly coordinating anion) or strong Lewis acids (LA) such as $GaCl_3$ and $SbCl_5$ (Scheme 2, routes B and C; [wca] = $[AsF_6]$, $[SbCl_6]$, $[B(C_6F_5)_4]$, $[GaCl_4]$). Again, only decomposition or undesired side reactions were observed. Although the initially precipitation of AgX (X = I, Cl) was observed, all the reactions led to the complete decomposition of **2** into $N_2$ and $Me_3Si$-X, along with the formation of $E^{(III)}X_3$ (E = As, Sb, Ga; X = F, Cl).[18] This is in accord with the observation by Wiberg that **2** reduces main group element chlorides such as $GeCl_4$ with release of $N_2$ and $Me_3Si$-Cl.[16c] However, the reaction of **2** with $GaCl_3$ as the Lewis acid or with $Ag[GaCl_4]/Me_3Si$-I in dichloromethane at low temperatures resulted in the formation of the diazene adduct $Me_3Si$-N=N-$SiMe_3\cdot GaCl_3$ (**3**, Figure 1, right) in the form of dark blue crystals (yield ca. 95 %), which were thermally stable up to −20 °C (Scheme 2, routes B and C).

Although gas-phase computations predict an almost barrier-free approach of the $[Me_3Si]^+$ ion to diazene **2** (see Figure S16 in the Supporting Information), all the synthetic routes used did not succeed in preparing the diazenium ion.[18] We therefore decided to attempt the preparation of the diazenium salt $[(Me_3Si)_2N{=}N\text{-}SiMe_3]^+[GaCl_4]^-$ (**4**[$GaCl_4$]) by redox reactions starting from heavy metal hydrazide derivatives already bearing a $[(Me_3Si)_2N\text{-}N\text{-}SiMe_3]^-$ unit. For example, the dihydrazinobismuth cation in $[Bi\{N(SiMe_3)N(SiMe_3)_2\}_2]^+[GaCl_4]^-$ (**5**[$GaCl_4$])[20] and the neutral mercury(II) dihydrazide $Hg[N(SiMe_3)N(SiMe_3)_2]_2$ (**6**)[21] seemed to be promising candidates, since the 100 % signal in the CI$^+$ mass spectra of **5**[$GaCl_4$] and **6** could be assigned to diazenium cation **4**$^+$, thus indicating their potential as diazenium sources. Indeed, the reaction of **5**[$GaCl_4$] with $GaCl_3$ and elemental chlorine or sulfuryl chloride as the oxidizer in dichloromethane at temperatures below −50 °C gave, after filtration to remove precipitates, concentration in vacuum, and storage at −80 °C, low yields of blue, highly temperature-sensitive crystals, which were identified as **4**[$GaCl_4$] by X-ray studies (Scheme 3, top).[18] However, the decomposition of the bismuth salt **5**[$GaCl_4$] to **4**[$GaCl_4$] and bismuth chlorides was difficult to carry out because of the high reactivity of $Cl_2$ and $SO_2Cl_2$ leading to many side reactions and low yields.

Finally, we found that treatment of mercury salt **6** with two equivalents of Ag[$GaCl_4$] at −80 °C led in a clean, almost quantitative reaction to pure, crystalline **4**[$GaCl_4$] as well as elemental mercury and silver. The latter form an amalgam which can be easily removed by low-temperature filtration (Scheme 3, bottom).[18h] It is interesting to note, that the analogous reaction of **6** with other silver salts such as $Ag(toluene)_3[B(C_6F_5)_4]$, $Ag[CF_3SO_3]$, $Ag[CHB_{11}H_5X_6]$, or $Ag[AsF_6]$ was not successful.[18] The overall process represents a remarkable two-electron oxidation of the $[(Me_3Si)_2N\text{-}N\text{-}SiMe_3]^-$ ion according to the following formal Equations (2) and (3).[18h]

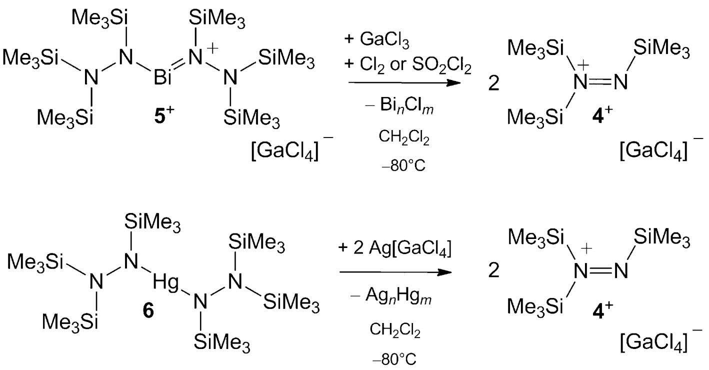

**Scheme 3.** Synthesis of **4**[$GaCl_4$].

$$2\,[(Me_3Si)_2N\text{-}N\text{-}SiMe_3]^- \rightarrow 2\,[(Me_3Si)_2N{=}N\text{-}SiMe_3]^+ + 4\,e^- \quad (2)$$

$$Hg^{2+} + 2\,Ag^+ + 4\,e^- \rightarrow HgAg_2 \quad (3)$$

Blue **4**[$GaCl_4$] is extremely air and moisture sensitive, and decomposes at temperatures above −30 °C. In solution it also decomposes rapidly at temperatures above −30 °C. Nonetheless, **4**[$GaCl_4$] could be fully characterized by low-temperature $^1$H, $^{13}$C, $^{14/15}$N, $^{29}$Si NMR, and Raman spectroscopy as well as by single-crystal X-ray diffraction (Table 1). $^{15}$N NMR spectroscopy (−60 °C, $CD_2Cl_2$) is particularly well suited to distinguish between two-coordinate and the three-coordinate nitrogen atoms found in diazene species (**2**: $\delta = 605$ (N1/N2) versus **4**$^+$: 612 (N1) and 214 ppm (N2)). Silylation at N2 results in the resonance for N2 being dramatically upfield shifted by more than $\Delta\delta = 404$ ppm, while the resonance for

**Table 1:** Spectroscopic data of diazene species **2**, **3**, **4**[GaCl$_4$] and for comparison mercury(II) dihydrazide **6**.

| Species[a] | **2** | **3** | **4**[GaCl$_4$] | **6** |
|---|---|---|---|---|
| Mp/$T_{decomp}$/°C | −3/−30[d] | 36/−20 | −/−30 | −/156 |
| NMR[a] | | | | |
| $^{15}$N, N1 | 605 | 596 | 612 | −269 |
| $^{15}$N, N2 | 605 | 248 | 214 | −309 |
| $^{29}$Si, N1 | 5.2 | 23.8 | 24.26 | 9.77 |
| $^{29}$Si, N2 | 5.2 | 45.6 | 44.99 | 5.18 |
| $^{13}$C, N1 | −4.0 | −1.6 | −0.9 | 3.09 |
| $^{13}$C, N2 | −4.0 | −1.8 | −0.4 | 2.63 |
| $^{1}$H, N1 | 0.17 | 0.64 | 0.70 | 0.277 |
| $^{1}$H, N2 | 0.17 | 0.46 | 0.55 | 0.284 |
| $\nu_{NN,Raman}$/cm$^{-1}$ | 1555[b] | 1568[b] | 1570[b] | 1062 |
| N1-N2/Å | 1.227(2)[e] | 1.243(2) | 1.254(2) | 1.462(4) |
| N1-Si1/Å | 1.807(3)[e] | 1.826(2) | 1.829(1) | 1.725(3) |
| N2-Si2/Å | 1.807(3)[e] | 1.884(2) | 1.894(1) | 1.735(3) |
| N2-Si3/Å | – | – | 1.899(1) | 1.737(3) |
| Si1-N1-N2/° | 117.3(2)[e] | 134.6(1) | 140.5(1) | 123.8(2) |
| Si1-N1-N2-Si2/° | 180 | 175.5(1) | 175.3(1) | −98.0(3)[g] |
| $q$(N1)/$e$ | −0.55 | −0.43 | −0.40 | −1.15 |
| $q$(N2)/$e$ | −0.55 | −0.59 | −0.59 | −1.21 |
| $Q_{CT}$/$e$[f] | – | 0.24 | 0.33 | 0.48 |

[a] $\delta$ [ppm], −75 °C, CD$_2$Cl$_2$. [b] The sample decomposes in the laser beam. [c] No signals were detected. [d] Slow decomposition starts earlier. [e] Only structural parameters of part A with the larger occupancy of the disordered molecule are listed. [f] $Q_{CT}$ = total charge transfer from the diazene to the Lewis acid. [g] The hydrazide group adopts an almost perpendicular arrangement as a result of Pauli repulsion between the lone pairs of electrons localized on the two N atoms (see Figure S1).

dicoordinated N1 is only shifted by about $\delta = 8$ ppm to a higher field (cf. $\delta = 357/-11$ ppm by the addition of GaCl$_3$ to **3**). These values display an extreme nuclear magnetic deshielding of both nitrogen atoms in **2** and N1 in **3** and **4**$^+$, a fact which was already observed and studied by Wrackmeyer and co-workers in a series of diazenes (cf. **2**: $\delta = 618$–630, Ph-N=N-SiMe$_3$: 251,[18j] Ph-N=N-Ph: 131, Et-N=N-Et: 151 ppm).[17a,22] Wrackmeyer and co-workers found that the remarkable downfield shift of $\delta$[$^{14}$N] upon substituting one or both alkyl or phenyl groups in R-N=N-R by Me$_3$Si can be attributed to a decrease in the energy gap for magnetic dipole allowed electronic transitions, in particular of the $n \rightarrow \pi^*$ type, and thus reflects the unique influence of silyl substituents on the electronic structures, and is also responsible for the blue color.[22,23] Thus, the $^{15}$N resonance of azo compounds of the type R-N=N-SiMe$_3$ was observed approximately in the middle of the $^{15}$N resonances of the symmetrically substituted compounds. A similar effect can be discussed when **2** is silylated to yield **4**$^+$. The $^{29}$Si NMR data illustrate that when silylation occurs both $^{29}$Si resonances are shifted downfield with respect to those of diazene **2** by $\Delta\delta = 19$ (N1) and 39 ppm (N2) (**2**: $\delta = 5.2$ (N1/N2) versus **4**$^+$: 24.3 (N1) and 45.0 ppm (N2)). The Raman data of all the considered diazene species (Table 1) show sharp bands in the expected region between 1560 and 1600 cm$^{-1}$, which can be assigned to the $\nu_{NN}$ stretching frequency (cf. 1589 cm$^{-1}$ in Ph-N=N-Ph). The coordination of [Me$_3$Si]$^+$ and GaCl$_3$ to diazene **2** causes no significant shift in the band to lower wave numbers, thus indicating an almost pure nonbonding character of the lone pair of electrons at the nitrogen donor center. It should be mentioned that **2**, **3**, and **4**[GaCl$_4$] quickly decompose in the laser beam to form molecular nitrogen and the hydrazine derivative (Me$_3$Si)$_4$N$_2$, which is in accord with observations by Wiberg et al.[4]

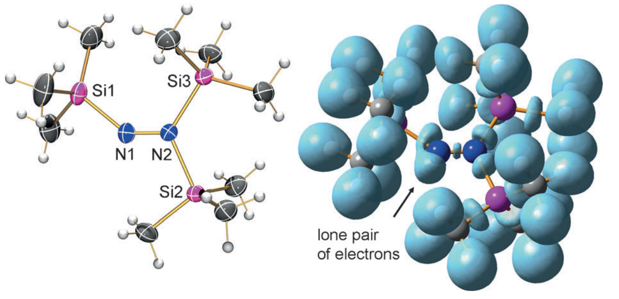

***Figure 2.*** Left: ORTEP representation of the molecular structure of **4**$^+$ in the crystal. Thermal ellipsoids correspond to 50% probability at 173 K. Right: Three-dimensional representation of the ELF at 0.82.

X-ray diffraction analysis (Figure 2) revealed unequivocally the existence of diazenium cation **4**$^+$ with an almost planar N$_2$Si$_3$ skeleton (deviation from planarity less than 5°). There are neither significant cation–anion nor anion–anion contacts. Both N atoms are in a planar environment with two slightly different sets of N−Si bond lengths (N1-Si1 1.829(1), N2-Si2 1.894(1), and N2-Si3 1.899(1); cf. $\Sigma r_{cov}$(Si-N) = 1.87 Å),[6] which can be attributed to hyperconjugation of the lone pair of electrons localized at N1 into the N2-Si and Si1-C σ* orbitals, respectively. The most striking feature is the N−N bond length of 1.254(2) Å, which lies in the typical range of a N=N bond (cf. $\Sigma r_{cov}$(N-N) = 1.42, N=N 1.20, N≡N 1.08 Å; 1.243(3) Å in azobenzene)[6,24] and in accord with those found in tetracyclic and hexacyclic formal bis(trialkyldiazenium) bis(tetrafluoroborate) salts reported by Nelsen et al. (1.244(5)–1.261(5) Å), where the N$_2$ units are, however, part of a six-membered ring.[10b] Comparison of the structural data of **4**$^+$ with those of **2** and **3** reveal only small differences (Table 1). For all species, the N-Si skeleton is planar and two slightly different Si−N bond lengths are observed, except for the $C_2$-symmetric diazene (*trans* configuration). The shortest Si−N bonds are found in **2** because of stronger hyperconjugative effects. The two Me$_3$Si groups in **2** and **3** adopt a *trans* arrangement. The Ga-N donor–acceptor bonds in **3** at 2.036(2) Å[25] are in the expected range (cf. 2.011(4) in NH(SiMe$_3$)$_2$·GaCl$_3$, 1.965(2) Å in Me$_3$Si-N=S=N-SiMe$_3$·GaCl$_3$).[26,27]

Finally, it is interesting to note that the previous structure determination of diazene **2** needs to be revised on the basis of our data.[5] Although the cell data are in agreement (space group $P2_1/c$, $Z = 2$), the previously reported structure of **2** was refined without taking into account that the whole molecule is disordered, which results for example in an unrealistically short N−N bond length of 1.171(7) Å and a large N-N-Si angle of 120.0(4)°. However, if the molecule is refined as disordered over two positions then a significantly longer N-N distance of 1.227(2) Å (cf. $\Sigma r_{cov}$(N=N) = 1.20 Å) and a smaller N-N-Si angle of 117.3(2)° in accordance with the computations are obtained (e.g. 1.247 from B3LYP/6-311+G(d,p),[22] 1.242 Å from M06-2X/aug-cc-pVTZ), which now lie in the expected range for diazenes.[18]

© 2014 Wiley-VCH Verlag GmbH & Co. KGaA, Weinheim

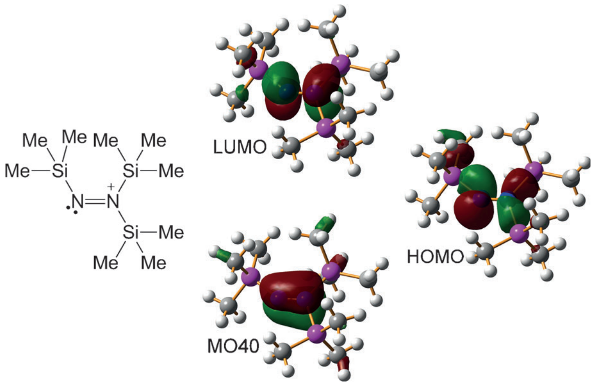

***Figure 3.*** Left: Lewis representations of **4**$^+$ according to NBO/NRT analysis. Right: MO40 (π), HOMO (n/σ), and LUMO (π*).

DFT calculations of the electronic structure as well as ELF, MO, and NBO/NRT analyses (ELF = electron localization function,[28] NBO = natural bond orbital, NRT natural resonance theory)[29] were carried out to gain insight into the structure and bonding of diazenium ion **4**$^+$. MO and NBO calculations show a localized N=N bond and a lone pair of electrons that according to NRT analysis is mainly localized at N1 (Figure 3). This is in accordance with the ELF of 0.82 that exhibits a small dumbbell-shaped region of localized electrons between the two N atoms, which is a good indicator of a classical double bond, along with a monosynaptic valence basin for the lone pair of electrons localized at N1 (Figure 2, right). The calculated natural atomic orbital population (NAO) net charges are $q(\text{N1}) = -0.40$ and $-0.59\,e$ (N2), which means that N1 becomes slightly less negative and N2 even more negative upon formal $[\text{Me}_3\text{Si}]^+$ addition, that is, the overall charge along the N1-N2 unit remains almost constant (cf. **2**: $q(\text{N1}) + q(\text{N2}) = -1.10$, **3**: $-1.02$, **4**$^+$: $-0.99\,e$, Table 1), in accordance with the charge distribution in the adduct **3**. According to TD-DFT calculations,[18] the blue color arises from the weak n/σ→π* HOMO–LUMO electronic transition at $\lambda_{\text{max,calcd}} = 731$ nm in cation **4**$^+$ (Figure 3, right).[17b]

In summary, a highly labile salt bearing the trisilylated homoleptic diazenium ion **4**$^+$ is presented for the first time. Although the direct silylation of **2** failed because of side reactions or low solubility, diazenium ion **4**$^+$ was formed in a straightforward two-electron oxidation process starting from mercury(II) dihydrazide and $\text{Ag}[\text{GaCl}_4]$. Structural and spectroscopic data are in accordance with those of diazene **2** and the hitherto unknown diazene·$\text{GaCl}_3$ adduct **3**. Furthermore, we found that the previous structural data of diazene **2** needed to be revised on the basis of a new single-crystal structure determination, thus solving an old problem in diazene chemistry.

Received: November 23, 2013
Published online: February 14, 2014

**Keywords:** diazenes · diazenium ions · oxidation · silylium ions · structure elucidation

---

[1] P. Griess, *Liebigs Ann. Chem.* **1858**, *106*, 123.

[2] R. Wizinger-Aust, *Angew. Chem.* **1958**, *70*, 199.

[3] A. Bafana, S. Devi, T. Chakrabarti, *Environ. Rev.* **2011**, *19*, 350.

[4] N. Wiberg, W.-C. Joo, W. Uhlenbrock, *Angew. Chem.* **1968**, *80*, 661.

[5] M. Veith, H. Bärnighausen, *Acta Crystallogr.* **1974**, *B30*, 1806.

[6] P. Pyykkö, M. Atsumi, *Chem. Eur. J.* **2009**, *15*, 12770.

[7] A. Modelli, F. Scagnolari, D. Jones, G. Distefano, *J. Phys. Chem. A* **1998**, *102*, 9675.

[8] H. Wieland, E. Wecker, *Chem. Ber.* **1910**, *43*, 3260.

[9] U. Kuhlmann, DE1419789B1, **1969**.

[10] a) S. F. Nelsen, R. T. Landis II, *J. Am. Chem. Soc.* **1974**, *96*, 1788; b) S. F. Nelsen, H. Chang, J. J. Wolff, D. R. Powell, *J. Org. Chem.* **1994**, *59*, 6558.

[11] S. Hünig, H. Balli, E. Breither, F. Brühne, H. Geiger, E. Grigat, F. Müller, H. Quast, *Angew. Chem.* **1962**, *74*, 818; *Angew. Chem. Int. Ed. Engl.* **1962**, *1*, 640.

[12] See, for example: a) G. Cauquis, M. Genies, *Tetrahedron Lett.* **1968**, *32*, 3537; b) G. Cauquis, M. Genies, *Tetrahedron Lett.* **1971**, *48*, 4677.

[13] A. Ferguson, *Tetrahedron Lett.* **1973**, *30*, 2889.

[14] a) W. R. McBride, H. W. Kruse, *J. Am. Chem. Soc.* **1957**, *79*, 572; b) W. R. McBride, E. M. Bens, *J. Am. Chem. Soc.* **1959**, *81*, 5546.

[15] E. Allred, *J. Am. Chem. Soc.* **1982**, *104*, 5422.

[16] a) N. Wiberg, W. Uhlenbrock, W. Baumeister, *J. Organomet. Chem.* **1974**, *70*, 259; b) N. Wiberg, W. Uhlenbrock, *J. Organomet. Chem.* **1974**, *70*, 239; c) N. Wiberg, W.-C. Joo, G. Schwenk, W. Uhlenbrock, M. Veith, *Angew. Chem.* **1971**, *83*, 379; *Angew. Chem. Int. Ed. Engl.* **1971**, *10*, 374.

[17] a) J. Kroner, W. Schneid, N. Wiberg, B. Wrackmeyer, G. Ziegleder, *J. Chem. Soc. Faraday Trans. 2* **1978**, *74*, 1909; b) H. Bock, K. Wittel, M. Veith, N. Wiberg, *J. Am. Chem. Soc.* **1976**, *98*, 109.

[18] Supporting information: a) Synthesis details, b) details of X-ray structure elucidation, c) kinetics of the decomposition of diazene, d) IR, Raman, NMR spectra, e) $^1$H,$^{15}$N HMBC spectra, and f) computational details, g) applied level theory: pbe1pbe/aug-cc-pwCVDZ, h) the precipitate could be identified as a mixture of amalgam $\text{Ag}_{11}\text{Hg}_9$ along with traces of AgCl by a Rietveld refinement of the powder diffraction data, i) diazene **2**: The asymmetric unit was split in two parts and the occupancy of each part was refined freely (0.652(12)/0.348(12)); j) we observed two resonances at $\delta = 310$ ($\text{N}_{\text{Si}}$) and 255 ppm ($\text{N}_{\text{Ph}}$).

[19] a) M. Lehmann, A. Schulz, A. Villinger, *Angew. Chem.* **2009**, *121*, 7580; *Angew. Chem. Int. Ed.* **2009**, *48*, 7444; b) A. Schulz, A. Villinger, *Chem. Eur. J.* **2010**, *16*, 7276; c) M. F. Ibad, P. Langer, F. Reiß, A. Schulz, A. Villinger, *J. Am. Chem. Soc.* **2012**, *134*, 17757.

[20] W. Baumann, A. Schulz, A. Villinger, *Angew. Chem.* **2008**, *120*, 9672; *Angew. Chem. Int. Ed.* **2008**, *47*, 9530.

[21] K. Seppelt, W. Sundermeyer, *Chem. Ber.* **1970**, *103*, 3939.

[22] B. Wrackmeyer, C. Köhler, *Heteroat. Chem.* **2005**, *16*, 84.

[23] H. Seidl, H. Bock, N. Wiberg, M. Veith, *Angew. Chem.* **1970**, *82*, 42; *Angew. Chem. Int. Ed. Engl.* **1970**, *9*, 69.

[24] C. J. Brown, *Acta Crystallogr.* **1966**, *21*, 146.

[25] E. I. Davydova, T. N. Sevastianova, A. V. Suvorov, A. Y. Timoshkin, *Coord. Chem. Rev.* **2010**, *254*, 2031.

[26] C. J. Carmalt, J. D. Mileham, A. J. P. White, D. J. Williams, *Dalton Trans.* **2003**, 4255.

[27] C. Hubrich, A. Schulz, A. Villinger, *Z. Anorg. Allg. Chem.* **2007**, *633*, 2362.

[28] a) B. Silvi, A. Savin, *Nature* **1994**, *371*, 683; b) H. Grützmacher, T. F. Fässler, *Chem. Eur. J.* **2000**, *6*, 2317.

[29] F. Weinhold, C. Landis, *Valency and Bonding, A Natural Bond Orbital Donor-Acceptor Perspective*, Cambridge University Press, Cambridge, **2005** and references therein.

## 5.3 Synthesis, Structure and Reactivity of Diazene Adducts – Isolation of *iso*-Diazene stabilized as Borane Adduct

Fabian Reiß, Axel Schulz, Alexander Villinger.

*Chem. Eur. J.* **2014**, *20,* 11800-11811.

In dieser Publikation wurden sämtliche experimentelle Arbeiten sowie Berechnungen von mir durchgeführt. Ich habe das Manuskript verfasst und das Supportingfile erstellt. Der eigene Beitrag liegt bei ca. 90 %.

Ein ausführliches Supportingfile steht online zur freien Verfügung.

DOI: 10.1002/chem.201402921

ChemPubSoc Europe

DOI: 10.1002/chem.201xxxxxx

CHEMISTRY
A European Journal
Full Paper

**Diazene Chemistry**

# Synthesis, Structure and Reactivity of Diazene Adducts – Isolation of the First *iso*-Diazene Stabilized as Borane Adduct

Fabian Reiß,[a] Axel Schulz,[a],[b],* and Alexander Villinger[a]

**Abstract:** This work describes the synthesis and full characterization of a series of $GaCl_3$ and $B(C_6F_5)_3$ adducts of diazenes $R^1$-N=N-$R^2$ ($R^{1,2}$ = $Me_3Si$, Ph; $R^1$ = $Me_3Si$ and $R^2$ = Ph). While *trans*-Ph-N=N-Ph forms a stable adduct with $GaCl_3$, no adduct but a frustrated Lewis acid base pair is formed with $B(C_6F_5)_3$. The *cis*-Ph-N=N-Ph·$B(C_6F_5)_3$ adduct could only be isolated when UV light was used, which triggers the isomerization from *trans*- to *cis*-Ph-N=N-Ph, which provides more space for the bulky borane. Treatment of *trans*-Ph-N=N-$SiMe_3$ with $GaCl_3$ led to the expected *trans*-Ph-N=N-$SiMe_3$·$GaCl_3$ adduct but the reaction with $B(C_6F_5)_3$ triggered a 1,2-$Me_3Si$ shift resulting in the formation of a highly labile *iso*-diazene $Me_3Si(Ph)N$=N stabilized as $B(C_6F_5)_3$ adduct. *Trans*-$Me_3Si$-N=N-$SiMe_3$ forms a labile *cis*-$Me_3Si$-N=N-$SiMe_3$·$B(C_6F_5)_3$ adduct, that isomerizes to give also the transient *iso*-diazene species $(Me_3Si)_2N$=N·$B(C_6F_5)_3$ upon heating. Both *iso*-diazene species insert easily into one B-C bond of the $B(C_6F_5)_3$ affording hydrazinoboranes. All new compounds were fully characterized by means of X-ray, vibrational spectroscopy, CHN analysis, and NMR experiments. All compounds were further investigated by means of density functional theory and the bonding situation was accessed by natural bond orbital (NBO) analysis.

## Introduction

The rise of the synthetic dyestuffs industry in the middle of nineteenth century began with the discovery of diazonium salts, *e.g.* $[R–N≡N^+]Cl^–$, and diazotation reactions by Peter Griess.[1,2] The development of chemical companies was boosted by textile industry, especially by dyestuffs industry, and vice versa. Azo dyes, compounds that usually contain two aromatic fragments connected by a N-N double bond (diazenes), still play an important role in science and are also of medical, ecological and technical relevance.[3]

Alkyl or aryl substituted 1,2-diazanes are often subject to *trans/cis*-isomerization with the trans-isomer being the thermodynamically favoured species in most cases. For example, for diaryl diazenes it is known, that UV irradiation triggers *trans/cis*-isomerization,[4,5] which can be exploited to develop e.g. photoswitchable drugs. Contrary to the more stable 1,2-diazene isomers, iso-diazene (also known as diimines, 1,1-diazenes, aminonitrenes, *N*-nitrenes, Scheme 1) are usually not isolated or detected by spectroscopic methods, but rather are assumed intermediates.[6] To the best of our knowledge fully characterized iso-diazenes or their adducts are not known yet. Dervan *et al.* reported in a series of papers the in situ synthesis and direct observation of persistent 1,1-diazenes, *N*-(2,2,6,6-tetramethylpiperidyl)nitrene and *N*-(2,2,5,5-tetramethylpyrrolidyl)nitrene, which were characterized on the basis of solution IR and UV spectra and their decomposition kinetics.[7–10] In these compounds the diazene unit is part of a five- and six-membered ring, respectively, which stabilizes these cyclic 1,1-dialkyldiazenes.

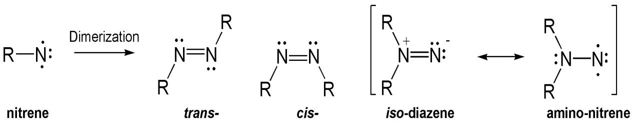

**Scheme 1.** Diazenes derived by formal dimerization of nitrenes.[11]

In 1910 Wieland studied the oxidative coupling of diphenyl hydrazine with NaClO in acidic solution affording an azo dye salt.[12] The *in situ* formation of diazenium ions such as $[Ph_2N=NH]^+$ was discussed.[13] Oxidative coupling of asymmetric

---

[a] F. Reiß, Prof. Dr A. Schulz, Dr. A. Villinger Institut für Chem., Abteilung Anorganische Chem., Universität Rostock, Albert-Einstein-Strasse 3a, 18059 Rostock, Germany
E-mail: axel.schulz@uni-rostock.de
[b] Prof. Dr A. Schulz Leibniz-Institut für Katalyse e.V. an der Universität Rostock, Albert-Einstein-Strasse 29a, 18059 Rostock, Germany
Supporting information for this article is available on the WWW under http://www.chemeurj.org/ or from the author.

diaryl hydrazine with aromatic amines was patented by Ugine-Kuhlmann in 1962 for the synthesis of basic dyes of the type $[R_2N{=}NR]^+Cl^-$ (with R = substituted aryls).

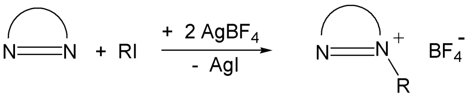

**Scheme 2.** Preparation of bicyclic examples of six-, five-, and four-membered ring diazenium tetrafluoroborate salts (R = alkyl).

McBride found, that 1,1-dialkylhydrazines react with $KEO_3$ (E =Br, I) and halogens ($X_2 = Br_2, I_2$), respectively, in acidic media to form *in situ* $[R_2N{=}NH]^+$ diazenium ions, which in neutral or basic solution (when it is deprotonated) immediately dimerize to form tetraalkyltetrazenes, $R_2N$-N=N-$NR_2$.[14,15] It is assumed, that in basic solution $[R_2N{=}NH]^+$ is deprotonated to give the reactive $R_2N{=}N$ species with nitrene reactivity which then dimerizes (Scheme 1). Considerably more stable are alkyl substituted diazenium salts, in which the N=N moiety is part of a bicyclic ring or cage such as 3-*tert*-butyl-2,3-diazanorborn-2-ene diazenium tetrafluoroborate salts. These salts were prepared from the corresponding diazene and $AgBF_4$ in the presence of R-I (Scheme 2).[16–19] In 1965 Gutmann studied on the basis of IR/UV spectroscopy the formation of different Lewis acid diaryl diazene adducts in solution, however, without any characterization in the solid state.[20,21]

While aryl substituted 1,2-diazenes (azo compounds), which are stabilized by a conjugated π-electron system, have been extensively investigated and represent a class of stable compound, much less is known about alkyl- or silyl substituted diazenes $R^1$-N=N-$R^2$. This can be attributed to the decreasing thermal stability along the series aryl/aryl > aryl/silyl > silyl/silyl (*cf.* $R^1/R^2$ = Ph/Ph: $T_{dec} > 400$ °C, $R^1/R^2$ = Ph/$SiMe_3$: $T_{dec} > 180$ °C, $R^1/R^2$ = $SiMe_3/SiMe_3$: $T_{dec} > -30$ °C) which is accompanied by an increasing reactivity of these diazenes. In a series of papers Wiberg *et al.* reported the synthesis of labile bissilylated diazene $Me_3Si$-N=N-$SiMe_3$ and follow-up chemistry.[22–35] The reaction of tosylazide with lithium tris(trimethylsilyl)hydrazide (**1**) at low temperatures provides readily access to light blue *trans*-diazene $Me_3Si$-N=N-$SiMe_3$ in ca. 65 % yield (**2**, Scheme 3).[22] Since **2** decomposes at ambient temperatures with a half time of 7.6 h it should be stored at temperatures below –50 °C.[36] As shown by Wiberg, a higher silylation at diazenes caused an increase of the HOMO ($n_N$) and lower LUMO ($\pi^*_{NN}$) energies.[37,38] The decrease of the energy gap is also responsible for the bathochromic shift from orange Ph-N=N-Ph ($\lambda_{max}$ = 446 nm) to pale blue $Me_3Si$-N=N-$SiMe_3$ ($\lambda_{max}$ = 784 nm, *cf.* Ph-N=N-$SiMe_3$: $\lambda_{max}$ = 580 nm).

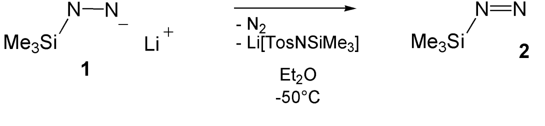

**Scheme 3.** Synthesis of trans-N,N'-bis(trimethylsilyl) diazene (2); Tos = p-$MeC_6H_4SO_2$.

Recently, we reported on the synthesis, structure and bonding of labile bissilylated diazene $Me_3Si$-N=N-$SiMe_3$, its $GaCl_3$ adduct and the intriguing trissilylated diazenium ion, $[(Me_3Si)_2N{=}N{-}SiMe_3]^+$, a dark blue and highly labile ($T_{dec} > -30$ °C) homoleptic cation of the type $[R_3N_2]^+$.[36] While direct silylation of $Me_3Si$-N=N-$SiMe_3$ failed, the $[(Me_3Si)_2N{=}N{-}SiMe_3]^+$ ion was generated in a straightforward two-electron oxidation reaction from mercury(II) bishydrazide and $Ag[GaCl_4]$. Herein, we want to report on the reaction of different diazenes of the type $R^1$-N=N-$R^2$ ($R^{1,2}$ = $Me_3Si$, Ph; $R^1$ = $Me_3Si$ and $R^2$ = Ph) with Lewis acids such as $GaCl_3$ and $B(C_6F_5)_3$.

## Results and Discussion

Starting point of this project was the attempted direct silylation of diazenes $R^1$-N=N-$R^2$ ($R^{1,2}$ = $SiMe_3$,[36] Ph; $R^1$ = $Me_3Si$ and $R^2$ = Ph) with trimethylsilicenium-solvate tetrakis(pentafluorophenyl)borate salts of the type $[Me_3Si{\cdot}X][B(C_6F_5)_4]$ (X = toluene, $Me_3SiH$), which all failed to generate diazenium cations of the type $[R^1\text{-}N{=}N(SiMe_3)R^2]^+$ or $[R^1(Me_3Si)N{=}N\text{-}R^2]^+$. Only decomposition or mixtures of products were observed even at low temperatures. These observations prompted us to utilize less strong, neutral Lewis acids such as $GaCl_3$ and $B(C_6F_5)_3$ in the reaction with diazenes.

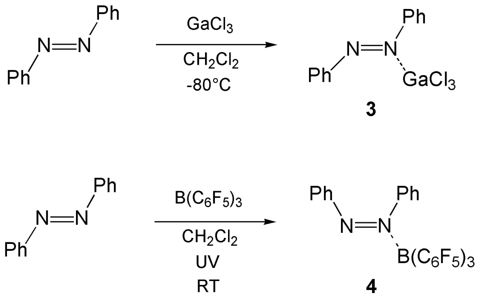

**Scheme 4.** Synthesis of diazene adducts 3 (top) and 4 (bottom).

### *Synthesis*

Ph-N=N-Ph adducts. Treatment of *trans*-N,N'-bisphenyldiazene, *trans*-Ph-N=N-Ph, with $GaCl_3$ in $CH_2Cl_2$ at –80 °C leads after warming to ambient temperatures in a straightforward reaction (Scheme 4) to the expected adduct *trans*-Ph-N=N-Ph·$GaCl_3$ (**3**) in good yields (>50 %, Figure 1). Orange crystals of 3 start to decompose at temperatures above 108 °C. Astonishingly, the same reaction with $B(C_6F_5)_3$ a stronger and bulkier Lewis acid (compared to $GaCl_3$) did not lead to the formation of any adduct. Thus, the mixture of **3** and $B(C_6F_5)_3$ can be referred to as frustrated Lewis acid base pair (FLP).[39] Since a very slow reaction in the presence of daylight was observed and presumably steric hindrance prevented adduct formation (Figure 2), we carried out the same reaction in the presence of UV light to trigger isomerization to cis-Ph-N=N-Ph,[4,5] which should provide more space for the bulky Lewis acid $B(C_6F_5)_3$. Indeed, the yellow reaction mixture of trans-Ph-N=N-Ph and $B(C_6F_5)_3$ in $CH_2Cl_2$ at ambient temperatures turned into deep orange solution under UV irradiation, from which thermally stable (up to 168°), orange crystals of cis-Ph-N=N-Ph·B($C_6F_5$)$_3$ (**4**) could be isolated (yield: 23 %, Figure 1).

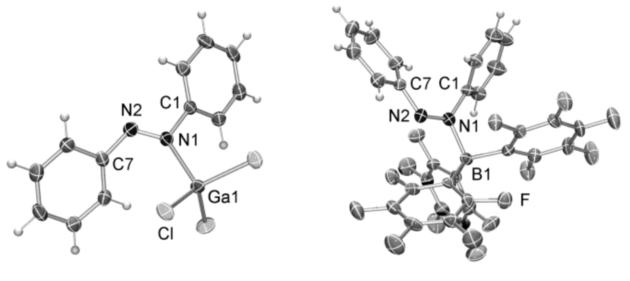

**Figure 1**. ORTEP drawing of the molecular structure of **3** (left) and **4** (right) in the crystal. Thermal ellipsoids with 50 % probability at 173 K. Selected structural data are listed in Table 3.

$^{11}$B and $^{19}$F NMR spectroscopy are particularly well suited to distinguish between three-coordinate boron and the four-coordinate boron found in the Lewis acid-base adducts.[40,41] As depicted in Figure 2, the completeness of the reaction can be monitored by $^{19}$F NMR spectroscopy, which clearly indicates the formation of the adduct. Also $^{11}$B NMR experiments are a suitable tool to detect adduct formation since upon adduct formation the signal of the free borane is shifted by about 59 ppm (cf. B($C_6F_5$)$_3$ in $CD_2Cl_2$: 59.1, **4** in $CD_2Cl_2$: –0.2 ppm).[42,43]

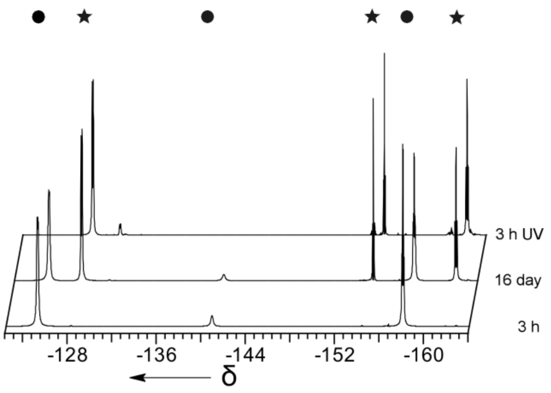

**Figure 2.** $^{19}$F NMR spectra after 3 h reaction time (*bottom*), 16 days reaction time (*middle*) at daylight and 3 h photo activation (*top*) with UV lamb (366 nm/245 nm). Dot marked species: uncoordinated B($C_6F_5$)$_3$, star marked product: *cis*-Ph-N=N-Ph·B($C_6F_5$)$_3$ (**4**).

*Ph-N=N-SiMe$_3$ adducts.* The starting material *N*-phenyl-*N'*-trimethylsilyldiazene (**5**) can be prepared in 90 % yield by oxidation of the *N*-phenyl-*N'*-trimethylsilyl-hydrazine, PhN(H)-N(H)SiMe$_3$, with dimethyl azodicarboxylate in light petroleum.[44] Wiberg *et al.* and Wannagat *et al.* already described the synthesis of **5** by oxidation with molecular oxygen or *p*-benzochinone in the 1964 and 1971, respectively.[45,46] We used a new route starting from a mixture of *N,N*-bis(trimethylsilyl)-*N'*-phenylhydrazine, (Me$_3$Si)$_2$N–N(H)Ph, and *N,N'*-bis(trimethylsilyl)-*N'*-phenylhydrazine, Me$_3$Si(H)N–N(SiMe$_3$)Ph, which was treated with *n*-BuLi and 1.2 equivalents of $CCl_4$ yielding pure *trans*-Ph-N=N-SiMe$_3$ (**5**) after fractional distillation as blue liquid (Figure 3, see supporting information).

As expected treatment of **5** with one equivalent of $GaCl_3$ in $CH_2Cl_2$ at –80 °C (Scheme 5) gives in rather good yields (40 %) the highly labile adduct *trans*-Ph-N=N-SiMe$_3$·GaCl$_3$ (**6**). This adduct is only stable at temperatures below –20 °C and should be stored at temperatures below –50 °C. As unequivocally shown by single crystal X-ray studies, the $GaCl_3$ is attached to the nitrogen atom bearing also the Me$_3$Si group (Figure 3). As indicated by natural bond analysis (NBO) analysis (*vide infra*),[47,48] the larger inductive effect of the Me$_3$Si leads to a larger negative charge at the $N_{SiMe3}$ atom ($q(N_{SiMe3})$ = –0.58*e* vs. $q(N_{Ph})$ = –0.18*e*). Therefore, the coordination of the $N_{SiMe3}$ atom to the $GaCl_3$ is favoured over that of the $N_{Ph}$ atom. Moreover, computation at the B3LYP/6-31G(d,p) level of theory also favours the $N_{SiMe3}$ atom coordination of the $GaCl_3$ over the $N_{Ph}$ atom coordination by 5.4 kcal/mol.

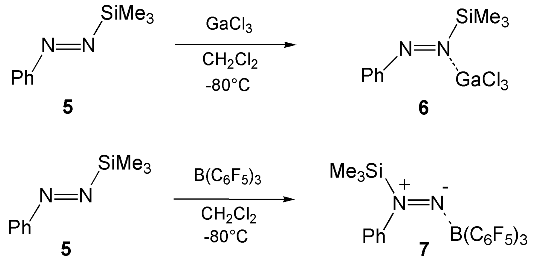

**Scheme 5.** Synthesis of diazene adducts 6 (top) and 7 (bottom).

In the next step we treated **5** with one equivalent of the bulky B($C_6F_5$)$_3$ in $CH_2Cl_2$ at –80 °C (Scheme 5). The resulting golden solution was allowed to warm up to ambient temperature. After concentration and storage at –0 °C over a period of 12 hours orange crystals of a new adduct could be isolated in 30 % yield. X-ray structure elucidation revealed the formation of an intriguing *iso*-diazene adduct (Scheme 1), *iso*-Me$_3$Si(Ph)NN·B($C_6F_5$)$_3$ (**7**), which means, that upon adduct formation the Me$_3$Si group migrates to the N atom bearing already the phenyl substituent (Figure 3). In the solid *iso*-diazene adduct **7** is thermally stable up to 104 °C, while it slowly decomposes in solution even at ambient temperatures (see section nitrene reactivity, *vide infra*), thus not allowing NMR characterization of **7** at ambient temperatures. However, adduct formation was also deduced from low temperature $^{19}$F and $^{11}$B NMR experiments displaying an up-field shift of 63 ppm compared to free B($C_6F_5$)$_3$ ($\delta$[$^{11}$B](**7**) = –4.4 ppm). It should be noted that dimerization of *iso*-diazene forming a tetrazene was not observed (see below).

*Me$_3$Si-N=N-SiMe$_3$ adducts.* Synthesis and structure of bissilylated diazene $GaCl_3$ adduct Me$_3$Si-N=N-SiMe$_3$ · GaCl$_3$ was recently reported (*vide supra*).[36] The reaction of *trans*-Me$_3$Si-N=N-SiMe$_3$ with $GaCl_3$ as Lewis acid or with Ag[GaCl$_4$]/Me$_3$Si–I in $CH_2Cl_2$ at low temperatures resulted in the formation of diazene adduct *trans*-Me$_3$Si-N=N-SiMe$_3$·GaCl$_3$ (**8**) in form of dark blue crystals (yield ca. 95 %), which were thermally stable up to –20 °C. The blue B($C_6F_5$)$_3$ adduct (**9**) is formed, when B($C_6F_5$)$_3$ is added to *trans*-Me$_3$Si-N=N-SiMe$_3$ at –80 °C (yield 30 %)

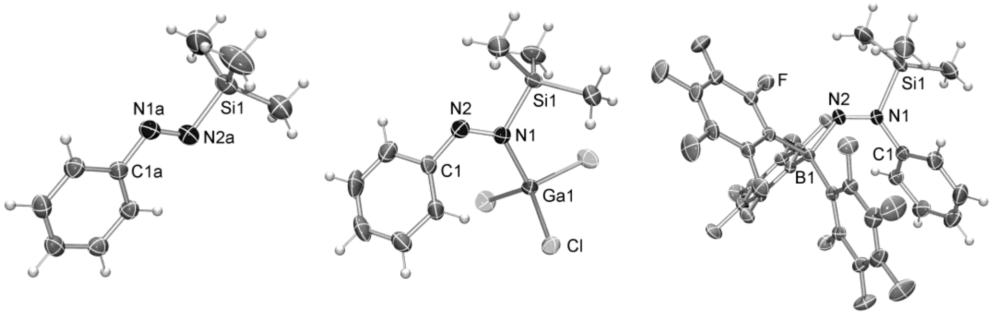

**Figure 3.** ORTEP drawing of the molecular structure of **5** (left), **6** (middle) and **7** (right) in the crystal. Thermal ellipsoids with 50 % probability at 173 K. Selected structural data are listed in Table 3.

A broad singlet could be detected in the up-field region (compared to $B(C_6F_5)_3$, *vide supra*) of the $^{11}B$ NMR spectrum at δ = 0.75 ppm, supportive of an adduct species. However, as depicted in Figure 4, upon addition of $B(C_6F_5)_3$ to *trans*-$Me_3Si$-N=N-$SiMe_3$ the *cis*-adduct is obtained contrary to the reaction with $GaCl_3$. This means *cis*-*trans* isomerization occurred prior to adduct formation thus avoiding frustration between the Lewis acid and base (see above discussion for *trans*-Ph-N=N-Ph). The different products, *cis*- versus *trans*-adduct formation, arises from the significantly larger steric hindrance introduced by $B(C_6F_5)_3$ compared to $GaCl_3$, which triggers the isomerization process. Again, $B(C_6F_5)_3$ adduct **9** is thermally stable to 127 °C as solid but decomposes like **7** slowly in solution even at low temperatures (see section on nitrene reactivity, *vide infra*).

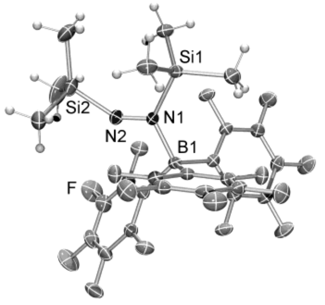

**Figure 4.** ORTEP drawing of the molecular structure of **9** in the crystal. Thermal ellipsoids with 50 % probability at 173 K. Selected structural data are listed in Table 3.

### *Nitrene reactivity of adduct 7 and 9 - Insertion reactions*

The formation of *iso*-diazene species **7** as well as the thermally induced decomposition of **7** and **9** prompted us to have a closer look at the reactivity of both adduct species. For this reason we studied the decomposition reaction at slightly elevated temperature in $CH_2Cl_2$. When **7** is heated up to 75 °C under autogeneous pressure for three hours, a complete conversion of the diazene adduct **7** into a hydrazinoborane species (**10**), which can be regarded as insertion of a nitrene type nitrogen atom into one B-C bond of the Lewis acid $B(C_6F_5)_3$ (Schemes 1 and 6, Figure 5 left), is observed. The activation of the B-C bond might arise from the nitrene character of the *iso*-diazene species **7** (Scheme 6), for which also a nitrene Lewis representation should have a small but significant contribution. Such B-C activation processes are known for transition metal complexes such as zirconocen species as shown by the groups of Rosenthal and Bochmann,[50–52] and in reactions of $B(C_6F_5)_3$ with alkynes as demonstrated by Stephan and Erker *et al.*[53,54] Our group proved, that *in situ* generated, highly labile $(Me_3Si)_2N$-$NP^+$ can activate one B-C bond in $B(C_6F_5)_3$.[55] Colorless crystals of **10** melt at 71 °C and decompose at 102 °C. The $^{11}B$ resonance is found at 40.2 ppm (*cf.* Table 1).

**Table 1. Selected spectroscopic data (Mp. in °C, δ in ppm).**

| | Mp/Tdec | color | δ[$^{19}F$] | δ[$^{11}B$] |
|---|---|---|---|---|
| PhNNPh[a] | 68/>400 | red | - | - |
| $Me_3SiNNSiMe_3$[b,c] | −3/−30- | pale blue | - | - |
| $Me_3SiNNPh$ | 100/>180 | blue | - | - |
| adduct **3** | -/108 | orange | - | - |
| adduct **4** | -/168 | orange | −164.8, −157.3, −131.1 | −0.2 |
| adduct **6**[c] | 40/−20 | orange | - | - |
| adduct **7** | -/104 | orange | −164.7, −158.3, −131.7 | −4.4 |
| adduct **8**[b,c] | 36/−20 | blue | - | - |
| adduct **9** | -/127 | blue | −164.4, −158.1, −129.6 | 0.8 |
| **10** | 71/102 | colourless | −162.0, −161.2, −160.9<br>−154.4, −150.7, −149.9<br>−141.8, −131.6, −127.8 | 40.2 |
| **11** | -/168 | colourless | −162.1, −161.5, −161.4<br>−154.7, −151.0, −150.8<br>−140.3, −131.9, −127.4 | 36.6 |

[a] taken from reference,[49] [b] taken from reference,[36] [c] slow decomposition starts earlier.

In a second experiment *cis*-$Me_3Si$-N=N-$SiMe_3 \cdot B(C_6F_5)_3$ adduct **9** was warmed up to 75 °C for three hours in $CH_2Cl_2$. The reaction was monitored by $^{11}B$ NMR experiments indicating the full conversion of **9** into one new species, which resonated down-field shifted compared to **9** at δ[$^{11}B$] = 36.59 ppm (*cf.* **9**: 0.75 ppm, $B(C_6F_5)_3$: 59.1 ppm).

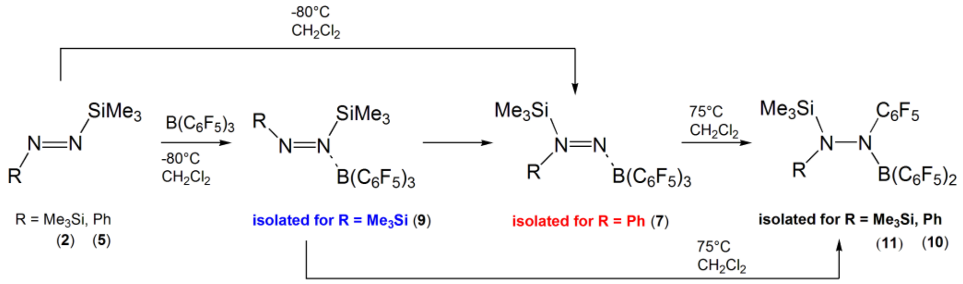

**Scheme 6.** Nitrene like behavior in silylated iso-diazene B(C6F5)3 adducts.[11]

The resulting solution was concentrated and crystallized at 0 °C affording colourless crystals in good yields (40 %). These crystals were shown by X-ray structure elucidation to be hydrazinoborane **11** (Scheme 6, Figure 5 right). Crystals of **11** decompose at the melting point at 163 °C. The formation of hydrazinoborane **11** starting from diazene species **9** led to the assumption, that **11** first isomerizes to give an *iso*-diazene species, which could be isolated in the reaction of Ph-N=N-$SiMe_3$ (**5**) with $B(C_6F_5)_3$ yielding *iso*-diazene **7**. Now the nitrene reactivity of this transient intermediate *iso*-$(Me_3Si)_2N{=}N{\cdot}B(C_6F_5)_3$, which could not be isolated but assumed on the basis of $^{19}F$ NMR spectroscopy (Scheme 6, Figure S22), led to the analogous insertion into one B-C bond finally affording hydrazinoborane **11**. Astonishingly, *iso*-diazene **7** can be isolated in the reaction of Ph-N=N-$SiMe_3$ (**5**) with $B(C_6F_5)_3$ but not the 1,2-substituted diazene adduct (neither *trans* nor *cis*), while in the reaction of $Me_3Si$-N=N-$SiMe_3$ (**2**) with $B(C_6F_5)_3$ the adduct **9** was obtained and the *iso*-diazene species seems to be a transient species generated upon thermal treatment, which leads for both reactions to the formation of the according hydrazinoborane. It should be mentioned, that thermal treatment of the *cis*-Ph-N=N-Ph·$B(C_6F_5)_3$ (**4**) adduct led to the dissociation of the adduct and small amounts of unidentified decomposition products (Figure S20). Moreover, it is interesting to note, that we did not observe dimerization of the *iso*-diazene adduct species as found for *N*-(2,2,6,6-tetramethylpiperidyl)nitrene yielding the tetrazene, $R_2N$-N=N-$NR_2$.[7] Also for $Me_3Si$-N=N-$SiMe_3$ (**2**) it was shown by Wiberg *et al.* that it dimerizes upon thermal treatment forming the tetrakis(trimethylsi1yl)tetrazene $(Me_3Si)_2N$-N=N-$N(SiMe_3)_2$.[23] Later the same group described the almost quantitative dimerization of **2** when equimolar amounts of silicon tetrafluoride are added to **2** at low temperatures.[33] Wiberg *et al.* already speculated on the *in situ* formation of *iso*-diazene, $(Me_3Si)_2N{=}N$, (at larger temperatures or induced by the Lewis acid $SiF_4$), which then dimerizes to give the tetrazene $(Me_3Si)_2N$-N=N-$N(SiMe_3)_2$. Obviously, in the presence of the strong bulky Lewis acid $B(C_6F_5)_3$ the intramolecular insertion reaction into the B-C bond is the preferred reaction channel since we could not observe any experimental hints for tetrazene formation. Furthermore, Wiberg *et al.* reacted $Me_3Si$-N=N-$SiMe_3$ with different metallocene complexes such as $Cp_2M$ (M = V, Cr, Mn) and $Cp_2TiCl_2$, yielding amino-imido complexes of the type $Cp_2MN_2(SiMe_3)_2$ (M = V, Ti) and $[Cp_2MN_2(SiMe_3)_2]_2$ (M = Cr, Mn).[27,56,57] Since all these complexes exhibit rather long N-N bonds (*e.g.* for M = Mn: 1.44(1) *vs.* 1.243(2) Å in *iso*-diazene adduct **7**, see section X-ray crystallography), which are in the range of a N-N single bond, and short M–N bonds featuring partly double bond character, these complexes cannot be regarded as *iso*-diazene complexes but rather as amino-imido complexes depending on the bond situation.[58] Additionally, there are transition metal complexes of the type [M]-N(R)=N-R and [M]-N=N-R bearing aryl-substituted diazene and diazenido ligands, respectively.[59–65]

Finally, hydrazinoboranes (also known as boryl hydrazines) represent a well-established class of compounds,[66–70] however, to the best of our knowledge no pentafluorophenyl substituted hydrazine derivative is known so far. In both hydrazinoboranes **10** and **11** the $^{19}F$ NMR spectra showed nine resonances (*cf.* Table 1, see supporting information), which is in accord with a hindered rotation about the N-B bond. This observation is in agreement with the X-ray and NBO analysis data displaying partially double bond character (*vide infra*).

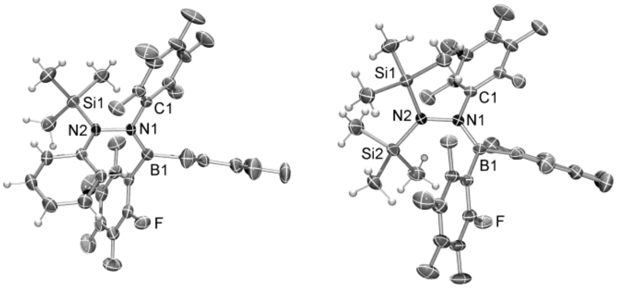

**Figure 5.** ORTEP drawing of the molecular structure of **10** (left) and **11** (right) in the crystal. Thermal ellipsoids with 50 % probability at 173 K. Selected structural data are listed in Table 3.

## *Vibrational spectroscopy*

Both IR and Raman experiments were carried out to study the nitrogen-nitrogen stretching mode and the influence of adduct formation on the position of this mode. Since the intensity of this mode is much stronger in the Raman spectra and Raman experiments could be carried out at low temperatures as well as in a sealed glass container (in contrast to our IR experiments), we want to focus on the Raman data in comparison with theoretically obtained data (Table 2). In addition, the NN stretch of the *trans* species is IR silent. As shown in Table 2, all diazenes and their adducts contain bands, which can be assigned to stretches of the -N=N- unit in the expected range[20,21] between 1463 (*trans*-$Me_3Si$-NN-Ph·$GaCl_3$) and 1593 $cm^{-1}$ (*cis*-$Me_3Si$-NN-$SiMe_3$·$B(C_6F_5)_3$). These results are in reasonable agreement with those obtained by computations (harmonic approximation). Interestingly, for all phenyl substituted compounds the N-N stretching mode strongly couples with the C-C stretching of the phenyl ring. Therefore, for these species two modes are listed in Table 2, whereupon $\nu_{NN}$

describes mainly the -N=N- stretch with a small $C_{phenyl}$-$C_{phenyl}$ contribution and $\nu_{NN+CC}$ is dominated by $C_{phenyl}$-$C_{phenyl}$ motion. There are no obvious trends for the -N=N- stretching mode with respect to adduct formation. For example, while for *trans*-$Me_3Si$-NN-$SiMe_3$·$GaCl_3$ (**8**) the $\nu_{NN}$ vibration is shifted to slightly larger wave numbers (1568 $cm^{-1}$) compared to *trans*-$Me_3Si$-NN-$SiMe_3$ (1555 $cm^{-1}$), the opposite is found for *trans*-Ph-NN-$SiMe_3$ (1510 $cm^{-1}$) and *trans*-$Me_3Si$-NN-Ph·$GaCl_3$ (1479 $cm^{-1}$) indicating that upon adduct formation mainly non-bonding electron density of a lone pair localized at the N atom interacts with the Lewis acid. This in turn is in agreement with the structural data displaying also double bond character along the NN unit for all considered diazene adduct species, which scarcely change upon adduct formation (see Table 3). On the basis of our computed vibrational data it can be concluded, that the *cis/trans/iso*-isomerization process leads to larger shifts in the $\nu_{NN}$ vibration rather than the adduct formation (see supporting information Table S13).

At significant lower wave numbers at 1059 and 1068, respectively, appear the >N–N< stretching frequencies of the hydrazine species **10** and **11** in accord with data for other hydrazines.[71,72]

**Table 2. Experimental (Raman) and theoretical data[a] of the NN stretching mode ($cm^{-1}$).**

| compound | $\nu_{NN, exp}$ | $\nu_{NN, theo}$ | $\nu_{NN+CN,CC, exp}$ | $\nu_{NN+CC, theo}$ |
|---|---|---|---|---|
| *trans*-Ph-NN-Ph | 1491 | 1498 | 1589 | 1593 |
| *trans*-Ph-NN-$SiMe_3$ (**5**) | 1510 | 1523 | 1603 | 1592 |
| *trans*-$Me_3Si$-NN-$SiMe_3$ (**2**) | 1555 | 1528 | - | - |
| *cis*-Ph-NN-Ph | [b] | 1547 | [b] | 1593 |
| *cis*-$Me_3Si$-NN-$SiMe_3$ | [b] | 1603 | [b] | - |
| *iso*-$Me_3Si$(Ph)NN | [b] | 1502 | [b] | 1591 |
| *trans*-Ph-NN-Ph·$GaCl_3$ (**3**) | 1463 | 1480 | 1589 | 1589 |
| *trans*-$Me_3Si$-NN-Ph·$GaCl_3$ (**6**) | 1479 | 1481 | 1591 | 1587 |
| *trans*-$Me_3Si$-NN-$SiMe_3$·$GaCl_3$ (**8**) | 1568 | 1591 | - | - |
| *cis*-Ph-NN-Ph·$B(C_6F_5)_3$ (**4**) | 1516 | 1517 | 1590 | 1598 |
| *cis*-$Me_3Si$-NN-$SiMe_3$·$B(C_6F_5)_3$ (**9**) | 1593 | 1631 | - | - |
| *iso*-$Me_3Si$(Ph)NN·$B(C_6F_5)_3$ (**7**) | 1556 | 1544 | 1603 | 1585 |
| $(Me_3Si)_2NN(C_6F_5)B(C_6F_5)_2$ (**11**) | 1059 | 1034 | - | - |
| $Ph(Me_3Si)NN(C_6F_5)B(C_6F_5)_2$ (**10**) | 1068 | 1047 | - | - |

[a] B3LYP/6-31G(d,p) level, scaled frequencies used with scaling factor = 0.9614,[73] [b] experimentally not known.

### *Computations*

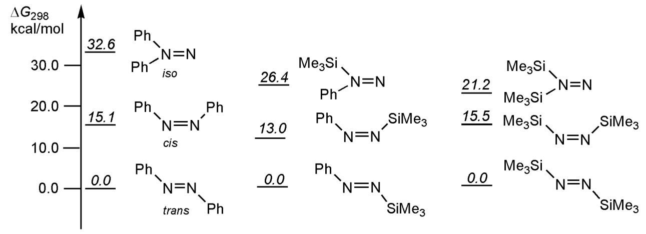

**Scheme 7.** Relative Gibbs energies for the different isomers of diazenes at the B3LYP/6-31G(d,p) level.

The electronic structure of *cis*-, *trans*- and *iso*-diazenes has already been the subject of a number of theoretical investigations,[6,74–79] all indicating that the *iso*-form of the parent species $H_2NN$ has a triplet ground state and is the least stable isomer with the *trans*-isomer being the global minimum species. To get further insight into the structure and bonding of the herein experimentally isolated diazenes and their adducts and especially of the unprecedented formation of the *iso*-form of diazene stabilized as $B(C_6F_5)_3$ adduct, computations utilizing density functional theory at the B3LYP/6-31G(d,p) level of theory were carried out. All structures were characterized as minima by frequency analysis. For each of the three different diazenes ($R^1$-N=N-$R^2$; $R^1$, $R^2$ = Ph and/or $SiMe_3$) all three isomers (*trans*-, *cis*- and *iso*-form, see Scheme 7) were studied. As depicted in Scheme 7, the *trans*-isomer is always energetically preferred over the *cis*-compound by $\Delta_{298}G$ = 15.1 (Ph, Ph), 13.0 (Ph, $SiMe_3$) and 15.5 kcal/mol ($SiMe_3$, $SiMe_3$). As expected the *trans*-isomers are even favoured by 32.6 (Ph, Ph), 26.4 (Ph, $SiMe_3$) and 21.2 kcal/mol ($SiMe_3$, $SiMe_3$) over the *iso* compounds in accord with experimental observations. All three *trans*-diazenes are known and have been isolated and fully characterized (*vide supra*). The same picture is found for the $GaCl_3$ adducts, which is also in agreement with the experimentally observed *trans*-adduct species. The most stabile isomer is always the *trans*-adduct, however, the relative energy gaps between the isomers has considerably decreased (Scheme 8). The *trans*-isomers are only stabilized by 4.9 (Ph, Ph), 7.2 (Ph, $SiMe_3$) and 5.9 kcal/mol ($SiMe_3$, $SiMe_3$).

For the mixed substituted adducts there are six different isomers (*trans*1/2, *cis*1/2 and *iso*1/2) to be considered. In accord with experiment, the *trans*-$GaCl_3$ adduct with the Lewis acid attached to the nitrogen atom bearing also the $SiMe_3$ substituent (*trans*2) is the most stable isomer indicating a larger inductive effect of the $Me_3Si$ group and thus a larger negative charge at this nitrogen atom (*vide supra*, see NBO charges Table S18, see supporting information). This situation dramatically changes when $B(C_6F_5)_3$ is used as Lewis acid. For diphenyldiazene now the *cis*-isomer was found to be the most stable isomer with –7.6 kcal/mol energetically favoured over the *trans*-species. Also the *iso*-diazene·$B(C_6F_5)_3$ adduct is stabilized by 2.2 kcal/mol compared to the *trans*-form, again in accord with our experimental observations. Obviously, the *trans*-isomer is kinetically and thermodynamically disfavoured over the *cis*-isomer. Therefore, the experimental formation of the *cis*-adduct **4** was observed after isomerization of the starting material *trans*-Ph-N=N-Ph, which was triggered by UV irradiation (*vide supra*). Also for the bissilylated diazene **2**, the *cis*-adduct isomer **9** was experimentally observed, although according to our computation **9** is energetically less favoured by 2.8 kcal/mol over the *trans*-species. This energy difference is rather small but presumably, the *trans*-$B(C_6F_5)_3$-adduct formation is slower (due to steric repulsion) than the isomerization process to the *cis*-diazene followed by *cis*-adduct formation. $[Me_3Si]^+$ groups are known to easily migrate along N-N moieties, therefore often referred to as big protons.[72,80–85] It should be noted that $Me_3Si$ group shifts are not triggered by UV-Vis light but by the action of a Lewis acid in contrast to the isomerization process observed in the phenyl substituted diazenes. Interestingly, the stability of the *cis/iso* $B(C_6F_5)_3$ adduct species over the *trans*-form decreases along $R^{1,2}$ = Ph > $R^1$ = Ph, $R^2$ = $SiMe_3$ > $R^{1,2}$ = $SiMe_3$ (Scheme 8). Astonishingly, for the mixed substituted species the lowest lying isomer is the *iso*-adduct (*iso*1 species, $B(C_6F_5)_3$ adduct **7** in Figure 3) which is only stabilized by 1.4 kcal/mol over the *cis1*-isomer and 2.5 kcal/mol over the *trans2*-isomer (Scheme 8 bottom) in accord with our experimental findings.

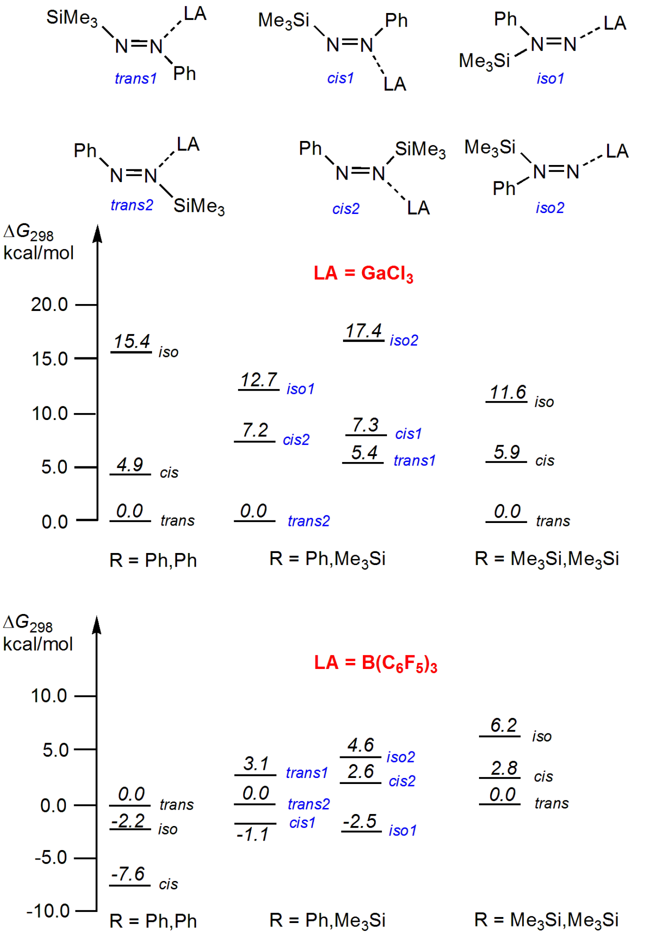

**Scheme 8.** Relative Gibbs energies for the different isomers of diazenes $GaCl_3$ and $B(C_6F_5)_3$ adducts at the B3LYP/6-31G(d,p) level (LA = Lewis acid)

NBO analysis data display for all considered diazenes and their adducts covalently bound nitrogen atoms with double bonds localized between the two nitrogen atoms. The bond between the diazene and the Lewis acids can be referred to as a donor-acceptor bond[86–89] with a total charge transfer between 0.195-0.262*e* for the $GaCl_3$ adduct and between 0.352-0.426*e* for the $B(C_6F_5)_3$ adducts indicating a larger charge transfer when $B(C_6F_5)_3$ is used as Lewis acid. Moreover, as displayed in Table S18 (supporting information), with an increasing degree of $Me_3Si$ substitution increases the partial charges at the nitrogen atom (*cf.* *q*(N1/2, *trans*-PhNNPh) = –0.197 vs. *q*(N1/2, *trans*-$Me_3SiNNSiMe_3$) = –0.553*e*) and thus a larger overall inductive effect occurs (*cf.* *q*(N1+N2): –0.394 in *trans*-PhNNPh *vs.* –1.101*e* in *trans*-$Me_3SiNNSiMe_3$), which is more than twice as large. Therefore, adduct formation always occurs preferably at the nitrogen atoms bearing a trimethylsilyl rather than a phenyl group if the adduct formation is electrostatically driven.

### *X-ray crystallography*

The structures were solved by direct methods (SHELXS-97)[90] and refined by full-matrix least squares procedures (SHELXL-97).[91] Semi-empirical absorption corrections were applied (SADABS).[92] All non-hydrogen atoms were refined anisotropically, hydrogen atoms were included in the refinement at calculated positions using a riding model. Selected structural parameters are summarized in Table 3. Crystallographic Details of all considered species are listed in Tables S1-S3 (supporting information).

*Diazenes.* Since the structures of trans-Ph-N=N-Ph[93,94] and trans-$Me_3Si$-N=N-$SiMe_3$ (**2**)[36] have been reported before, we want to focus in the discussion on trans-Ph-N=N-$SiMe_3$ (**5**). Compound **5** (Figure 3 left) crystallizes in the monoclinic space group $P2_1/c$ with eight formula units per cell. For the two independent molecules the same position disorder was observed as discussed for *trans*-Ph-N=N-Ph[94] and *trans*-$Me_3Si$-N=N-$SiMe_3$.[36] The observed molecular structure exhibits the expected trans configuration (Si-N-N-C 179.7°) with a short N-N distance (1.238(1) Å; cf. *trans*-Ph-N=N-Ph: 1.248(2), *trans*-$Me_3Si$-N=N-$SiMe_3$: 1.227(2), $\Sigma r_{cov}$(N-N) = 1.42 and $\Sigma r_{cov}$(N=N) = 1.20 Å[95]), clearly indicating double bond character along the N-N unit. It can be deduced from these data that with increasing substitution of the phenyl by trimethylsilyl groups the shorter is the N-N distance. The entire phenyl ring lies in the plane spanned by the N-N-Si moiety (dihedral angle C-N-N-Si 179.2°) with a C1a-N1a-N2a angles of 115.3(1)° (cf. *trans*-Ph-N=N-Ph: 114.5(2)°) and a Si1-N2a-N1a angle of 114.7(1)° (cf. 2: 117.3(2)°) indicative for formal $sp^2$ hybridized N atoms.

*Diazene adducts.* X-ray diffraction analysis (Figures 1, 3 and 4) revealed unequivocally the existence of diazene adduct species **3** (*trans*-Ph-N=N-Ph·$GaCl_3$), **4** (*cis*-Ph-N=N-Ph·$B(C_6F_5)_3$), **6** (*trans*-Ph-N=N-$SiMe_3$·$GaCl_3$), **9** (*cis*-$Me_3Si$-N=N-$SiMe_3$·$B(C_6F_5)_3$), and *iso*-diazene adduct **7** $Me_3Si(Ph)N{=}N{\cdot}B(C_6F_5)_3$) exhibiting an almost planar $N_2R^1R^2E$ skeleton ($R^1$, $R^2$ = Ph, Si; E = Ga or B; largest deviation from planarity in **3**: 22.5°, **4**: 13.9°, **6**: 18.4°, **7**: 6.7°, **9**: 13.3°). All tri-coordinated N atoms are in a planar environment ($\Sigma$<N > 358°), which can be attributed to hyperconjugative effects of the lone pair localized at the nitrogen atom into the N2–Si and Si1–C $\sigma^*$ orbitals, respectively, or in case of the phenyl substituted species due to conjugation with the π-electron system of the phenyl group. The most striking structural feature is the short N-N bond length, which only slightly elongates upon adduct formation. For example, the N-N bond lengths increase by 0.016 in $GaCl_3$ adduct **8** and 0.015 Å in $B(C_6F_5)_3$ adduct **9** compared to trans-$Me_3Si$-N=N-$SiMe_3$ or 0.011 in $GaCl_3$ adduct **6** and 0.005 Å in $B(C_6F_5)_3$ adduct **7** compared to trans-Ph-N=N-$SiMe_3$. Similar values (0.006 and 0.015 Å) are observed for **3** (trans-Ph-N=N-Ph·$GaCl_3$) and **4** (cis-Ph-N=N-Ph·$B(C_6F_5)_3$), respectively. The N-N distances of all adducts between 1.242(2) (adduct **9**) and 1.263(4) Å (adduct **4**) are still in the range of a typical N-N double bond ($\Sigma r_{cov}$(N–N) = 1.42 and $\Sigma r_{cov}$(N=N) = 1.20 Å[95]) indicating that the charge transfer from the diazene to the Lewis acid mainly stems from a non-bonding molecular orbital. The bond of the diazenes to the Lewis acids are rather long as well as the E-N-N angles (E = B, Ga), which are observed between 116.3(1) and 130.7(2)° (Table 3). The Ga-N donor acceptor bonds in adducts **3** and **6** with 2.064(3) and 2.042(2), respectively, are in the expected range[87] (cf. **8**: 2.036(2),[36] 1.965(2) Å in $Me_3Si$-N=S=N-$SiMe_3$·$GaCl_3$).[96]

*Table 3.* **Selected structural data from single crystal X-ray experiments (distances in Å, angles in °)**

| | **2**[a] | **3** | **4** | **5**[b] | **6**[b] | **7**[b] | **8**[a,e] | **9**[d] | **10**[b] | **11** |
|---|---|---|---|---|---|---|---|---|---|---|
| N-N | 1.227(2) | 1.254(4) | 1.263(4) | 1.238(2) | 1.249(2) | 1.243(2) | 1.243(2) | 1.242(2) | 1.432(2) | 1.443(2) |
| N-$R^1$ | 1.807(3) | 1.460(4) | 1.465(5) | 1.447(2) | 1.413(3) | 1.461(2) | 1.884(2) | 1.885(1) | 1.421(2) | 1.773(1) |
| N-$R^2$ | 1.807(3) | 1.414(4) | 1.414(4) | 1.804(1) | 1.885(2) | 1.888(1) | 1.826(2) | 1.801(2) | 1.781(2) | 1.778(1) |
| N-E[c] | - | 2.064(3) | 1.657(5) | - | 2.042(2) | 1.591(2) | 2.036(2) | 1.643(2) | 1.394(3) | 1.397(2) |
| $R^1$-N-N | 117.3(2) | 112.1(3) | 123.9(3) | 115.3(1) | 121.0(2) | 125.93(1) | 111.3(1) | 117.2(1) | 115.4(1) | 117.46(9) |
| $R^2$-N-N | 117.3(2) | 118.6(3) | 123.8(4) | 114.7(1) | 108.9(2) | 113.1(1) | 134.6(1) | 144.6(1) | 120.2(1) | 117.79(9) |
| E-N-N | - | 130.7(2) | 116.3(3) | - | 126.52(2) | 128.06(1) | 127.2(1) | 116.3(1) | 121.3(2) | 122.8(1) |

[a] Taken from reference;[36] [b] $R^1$=$C_6H_5$, $R^2$ = $SiMe_3$; [c] E = Ga for species **3**, **6**, **8**; E = B for **4**, **7**, **9**, **10**, **11**; [d] $R^1$ = Si1 is attached to N1 and $R^2$ = Si2 linked to N2, see Figure 4. [e] $R^1$ linked to N which is attached to $GaCl_3$

A close look at the B-N donor acceptor bond lengths reveals a significant different distance for *iso*-diazene adduct **7** with 1.591(2) Å compared to 1.657(5) and 1.643(2) Å determined for diazene adduct **4** and **9**, respectively (cf. 1.616(3) Å in $CH_3CN{\cdot}B(C_6F_5)_3$,[40]$\Sigma r_{cov}$(B–N) = 1.56 Å),[95] which can be attributed to less steric hindrance in **7** and a considerably larger charge transfer from the diazene to the $B(C_6F_5)_3$ Lewis acid (Table S18, see supporting information). The coordination geometry around the boron is tetrahedrally distorted with the smallest angle of around 101° and the largest around 112°.

*Hydrazinoboranes*. Crystals of **11** were grown from $CH_2Cl_2$ at 0 °C, while compound **10** only crystallizes from a saturated benzene solution at 25 °C. **10** crystalizes in the triclinic space group P-1 with two formula units per unit cell as benzene solvate, adduct **11** crystallizes without solvent molecules in the monoclinic space group $P2_1/n$ with four formula units. In both molecules all nitrogen atoms sit in a trigonal planar coordination environment with a dihedral angle of 69.6 and 64.0° between the two planes around N1 and N2. The dihedral angle RNNR strongly depends on the bulkiness of the groups R and delocalization effects. The N-N distances of 1.432(2) and 1.443(2) Å describe a typical single bond (cf. 1.435(3) in $Me(Ph_2B)N\text{-}N(BPh_2)Me$,[67] $\Sigma r_{cov}$(N-N) = 1.42 Å).[95] The B-N bonds are rather short with 1.394(3) and 1.397(2) Å (Table 3), respectively, compared to those of the adducts (cf. 1.59-1.64 Å, vide supra; 1.397(4) Å in $Me(Ph_2B)N\text{-}N(BPh_2)Me$[67]) indicating partial double bond character in accord with NBO analysis. This double bond character arises from delocalization of the lone pair localized at the N atom into the empty p atomic orbital localized at the formally $sp^2$ hybridized B atom describing resonance between Lewis representations $R_2N\text{–}BR_2$ and $R_2N^{(+)}{=}B^{(-)}R_2$.

## Conclusion

Diazenes of the type $R^1\text{-N=N-}R^2$ ($R^{1,2}$ = $SiMe_3$, Ph; $R^1$ = $Me_3Si$ and $R^2$ = Ph) were shown to form stable $GaCl_3$ and $B(C_6F_5)_3$ adducts depending on the reaction conditions temperature and UV light. While *trans*-Ph-N=N-Ph reacts with $GaCl_3$ to give *trans*-Ph-N=N-Ph·$GaCl_3$, due to steric hindrance $B(C_6F_5)_3$ does not react with *trans*-Ph-N=N-Ph. However, when UV light is used *trans*-Ph-N=N-Ph isomerizes yielding *cis*-Ph-N=N-Ph which in the presence of $B(C_6F_5)_3$ forms the stable *cis*-Ph-N=N-Ph·$B(C_6F_5)_3$ adduct. Treatment of *trans*-Ph-N=N-$SiMe_3$ with $GaCl_3$ led to the expected *trans*-Ph-N=N-$SiMe_3$·$GaCl_3$ adduct but the reaction with $B(C_6F_5)_3$ triggered a 1,2 $Me_3Si$ shift leading to the formation of the hitherto unprecedented labile *iso*-diazene $Me_3Si(Ph)N{=}N{\cdot}B(C_6F_5)_3$. In the case of *trans*-$Me_3Si$-N=N-$SiMe_3$ the bulky $B(C_6F_5)$ induces an *trans/cis* isomerization to form a labile *cis*-$Me_3Si$-N=N-$SiMe_3$·$B(C_6F_5)_3$ adduct even at low temperatures without UV activation. The latter was shown to isomerize to give the transient *iso*-diazene species which possesses nitrene type reactivity upon heating. While this *iso*-diazene intermediate could not be isolated in contrast to $Me_3Si(Ph)N{=}N{\cdot}B(C_6F_5)_3$ both species insert easily into one B-C bond of the $B(C_6F_5)_3$ affording hydrazinoboranes. Therefore, nitrene reactive of *iso*-diazene species can be utilized to synthesize (borylated) hydrazines bearing perfluorophenyl groups.

## Experimental

**General information.** All manipulations were carried out under oxygen- and moisture-free conditions under argon using standard Schlenk or drybox techniques. All solvents were dried, freshly distilled and degassed prior to use.

**NMR**: $^1H$ NMR, $^{13}C\{^1H\}$, $^{11}B\{^1H\}$, $^{19}F\{^1H\}$, $^{29}Si$ INEPT, $^1H,^{29}Si$ HMQC, $^1H,^{15}N$ HMBC and spectra were obtained on Bruker AVANCE 300, Bruker AVANCE 400 or AVANCE 500 spectrometers and were referenced internally to the deuterated solvent ($^{13}C$, $CD_2Cl_2$, $\delta_{reference}$ = 53.8 ppm, toluene-$d_8$, $\delta_{reference}$ = 20.4 ppm, benzene-$d_6$, $\delta_{reference}$ = 128.4) or to protic impurities in the deuterated solvent ($^1H$, $CDHCl_2$, $\delta_{reference}$ = 5.32 ppm, $C_7D_7H$, $\delta_{reference}$ = 2.03 ppm, $C_6D_5H$, $\delta_{reference}$ = 7.16). $^1H,^{15}N$ HMBC spectra were obtained on a Bruker AVANCE 500 or AVANCE 400 spectrometer and were referenced externally (33 % (vol.) $MeNO_2$ in the corresponding solvent, $\delta_{reference}$ = 0 ppm).
**IR**: Nicolet 6700 FT-IR spectrometer with a Smart Endurance ATR device or Nicolet 380 FT-IR (HeNe laser, 633nm) with Smart Orbit ATR device.
**Raman**: Horiba LabRAM HR Raman microscope with Olympus optics (10x NA 0.25), 784 nm Laser diode, 800 mm focal length spectrograph. Linkam THMS600 System and PE95/T95 System Controller was used for low temperature Raman measurements. Samples were prepared under $N_2$ atmosphere at an ENRAF NONIUS FR558-S low temperature mounting system.
**MS**: Finnigan MAT 95-XP from Thermo Electron was used ($CI^+$, *isobutene*; $EI^+$, T = 200 °C, 70.0 V).
**CHN analyses**: Analysator Flash EA 1112 from Thermo Quest.
**Melting points** are uncorrected (EZ-Melt, Stanford Research Systems). Heating-rate 20 °C/min. Decomposition point of **6** was estimated with the Raman microscope during slow warming the Linkam THMS600 System. Heating-rate ca. 10 °C/min.
**DSC**: DSC 823e from Mettler-Toledo (Heating-rate 5 °C/min) was used, uncorrected melting points were reported.

**Synthesis of *trans*-$PhNNSiMe_3$ (5):** To a stirred solution of isomer mixture *N,N*-bis(trimethylsilyl)-*N'*-phenylhydrazine and *N,N'*-bis(trimethylsilyl)-*N'*-phenylhydrazine (11.98 g, 47.05 mmol) in $Et_2O$ (100 mL) a solution of *n*-butyl lithium/*n*-hexane (18.8 mL, 47.05 mmol) was added dropwise over a period of 30 minutes at −80 °C and stirred for further two hours. To the resulting pale orange suspension a solution of tetrachloromethane (8.69 g, 56.46 mmol) in $Et_2O$ (20 mL) was added over a period of 30 minutes. The reaction mixture was slowly warmed to ambient temperature. The resulting brownish suspension was concentrated *in vacuo* to an approximate volume of 50 mL and condensed *in* *vacuo* in a smaller flask. This raw product was fractional distilled at $5\cdot10^{-2}$ mbar and separated in two fractions. Yield: 2.71 g, 32 % **Bp.** 110−115 °C ($5\cdot10^{-2}$ mbar).**$^1$H NMR** (25 °C, $CD_2Cl_2$, 300.13 MHz): $\delta$ = 0.40 (s, 9H, $CH_3$, $^1J(^1H-^{13}C)$ = 120 Hz, $^2J(^1H-^{29}Si)$ = 6.8 Hz), 7.62 (m, 5H, $C_6H_5$). **$^{13}$C NMR** (25 °C, $CH_2Cl_2$, 75.48 MHz): $\delta$ = −2.64 (s, $Si(CH_3)_3$, $^1J(^{13}C-^{29}Si)$ = 56.12 Hz), 121.0 (s, 2C, *o*-$C_6H_5$), 129.3 (s, 2C, *m*-$C_6H_5$), 131.3 (s 1C, *p*-$C_6H_5$), 156.7 (s, 1C, *ipso*-$C_6H_5$). **$^1$H,$^{15}$N NMR** (25 °C, $CD_2Cl_2$, 300.13 MHz, 30.43 MHz) : $\delta$ = 255 (d, NPh), 310 (s, $N(Si(CH_3)_3)$. **IR** (ATR, 16 scans): 3062 (w), 2959 (w), 2901 (w), 1599 (w), 1501 (m), 1468 (w), 1450 (w), 1306 (w), 1247 (s), 1177 (w), 1128 (w), 1066 (w), 1020 (w), 961 (w), 923 (w), 867 (s), 835 (s), 760 (s), 686 (s), 630 (m), 566 (w). **Raman** (25 °C, 784 nm, 200 mW, 30 sec, 4 acc. , $cm^{-1}$): 3069 (2), 2969 (1), 2906 (3), 1603 (4), 1510 (5), 1476 (4), 1458 (3), 1314 (1), 1259 (1), 1184 (4), 1163 (1), 1136 (10), 1028 (1), 1006 (8), 877 (1), 847 (1), 775 (1), 756 (1), 705 (1), 687 (1), 640 (3), 622 (2), 577 (3), 314 (1), 248 (1), 190 (2). **UV/VIS** (25 °C, $Et_2O$): 575 nm. Crystals suitable for X-ray crystallographic analysis were obtained, by slow cooling neat **5** to −100 °C using a low temperature mounting device, equipped with an ENRAF NONIUS FR558-S.

**Synthesis of *trans*-PhNNPh $GaCl_3$ (3)**: To a stirred solution of *trans-N,N'*-diphenyldiazene (0.091 g, 0.50 mmol) in $CH_2Cl_2$ (3 mL), $GaCl_3$ (0.088 g, 0.5 mmol) in $CH_2Cl_2$ (1 mL) was added at –80 °C over a period of 10 minutes. The resulting orange solution was allowed to warm to ambient temperatures and stirred for one hour at this temperature. The solution is then concentrated to a volume of 0.5 mL *in vacuo* storage at –25 °C over a period of 12 hours results in the deposition of orange crystals. Removal of supernatant by syringe and short drying *in vacuo* yields (0.094 g, 52 %) **3** as orange crystals. **Mp.** 108 °C (dec.). **Anal. calc.** % (found): C, 40.23 (40.40); H, 2.81 (3.01); N, 7.82 (7.83). **$^1$H NMR** (25 °C, $CD_2Cl_2$, 500.13 MHz): $\delta$ = 7.66 (m, 4H, *m*-$C_6H_5$), 7.73 (m, 2H, *p*-$C_6H_5$), 7.91 (m, 4H, *o*-$C_6H_5$). **$^{13}$C{$^1$H} NMR** (25 °C, $CD_2Cl_2$, 125.77 MHz): $\delta$ = 123.9 (s, 4C, *o*-$C_6H_5$), 130.2 (s, 4C, *m*-$C_6H_5$), 134.6 (s, 2C, *p*-$C_6H_5$), 151.3 (s, 2C, *ipso*-$C_6H_5$). **IR** (ATR, 16 scans): 3170 (w), 3107 (w), 3065 (w), 3036 (w), 2979 (w), 2918 (w), 1583 (s), 1557 (w), 1539 (m), 1504 (w), 1483 (w), 1477 (w), 1452 (m), 1429 (m), 1391 (m), 1332 (w), 1318 (w), 1300 (m), 1241 (m), 1218 (m), 1192 (w), 1171 (m), 1163 (m), 1098 (w), 1071 (w), 998 8m), 973 (m), 947 (m), 926 (m), 882 (m), 842 (w), 826 (w), 768 (s), 683 (s), 673 (s), 665 (s), 617 (m), 595 (w), 569 (m), 549 (m), 523 (s). **Raman** (25 °C, 784 nm, 7 mW, 12 s, 6 acc., $cm^{-1}$): 1589 (2), 1552 (1), 1463 (3), 1432 (10), 1320 (1), 1162 (3), 1144 (1), 1027 (1), 1003 (1), 948 (1), 924 (1), 837 (1), 760 (1), 612 (1), 522 (1), 492 (2), 424 (1), 412 (2), 358 (1), 322 (3), 287 (1), 219 (2), 185 (1), 140 (1), 126 (1), 100 (2). **MS** (CI, m/z,): 239 (2) [PhNNPh + *isobutane*]$^+$, 183 (100) [PhNNHPh]$^+$, 105 (2) [PhNN]$^+$, 94 (8) [$PhNH_3$]$^+$. Crystals suitable for X-ray crystallographic analysis were obtained, by cooling a saturated dichloromethane solution of **3** to –40 °C.

**Synthesis of *cis*-PhNNPh·$B(C_6F_5)_3$ (4):** To a stirred suspension of *N,N'*-diphenyldiazene (0.182 g, 1.00 mmol) in $CH_2Cl_2$ (5 mL), $B(C_6F_5)_3$ (0.512 g, 1.00 mmol) in $CH_2Cl_2$ (5 mL) was added dropwise at –80 °C over a period of ten minutes. The orange reaction solution was allowed to warm to ambient temperatures and stirred in the present of UV light for several days. The completeness of the reaction was monitored by $^{19}F\{^1H\}$ NMR spectroscopy see *Figure S19*. The resulting dark orange solution was concentrated to approximately 2 mL *in vacuo*. Storage at –40 °C over a period of 12 hours results in the deposition of orange crystals. Removal of supernatant by syringe and short drying *in vacuo* at ambient temperatures yields (0.160 g, 23 %) **4** as orange crystals. **Mp.** 168 °C (dec.) **Anal. calc.** % (found): C, 51.90 (51.64); H, 1.45 (1.48); N, 4.04 (4.10). **$^1$H NMR** (25 °C, $CD_2Cl_2$, 300.13 MHz): $\delta$ = 7.05 (m, 2H, *o*-$C_6H_5$), 7.16 (m, 2H, *o*-$C_6H_5$), 7.20 (m, 2H, *m*-$C_6H_5$), 7.30 (m, 1H, *p*-$C_6H_5$), 7.41 (m, 1H, *m*-$C_6H_5$), 7.49 (m, 1H, *p*-$C_6H_5$). **$^{13}$C{$^1$H} NMR** (25 °C, $CD_2Cl_2$, 125.77 MHz): $\delta$ = 117.6 (broad, 3C, *ipso*-$C_6F_5$), 124.1 (s, 2C, *o*-$C_6H_5$), 124.8 (s, 2C, *o*-$C_6H_5$), 130.02 (s, 2C, *m*-$C_6H_5$), 130.08 (s, 2C, *m*-$C_6H_5$), 131.9 (s, 1C, *p*-$C_6H_5$), 134.5 (s, 1C, *p*-$C_6H_5$), 137.5 (m, 6C, *m*-$C_6F_5$, $^1J(^{13}C-^{19}F)$ = 246 Hz), 140.7 (m, 3C, *p*-$C_6F_5$, $^1J(^{13}C-^{19}F)$ = 253 Hz), 147.4 (s, 1C, *ipso*-$C_6H_5$), 148.5 (m, 6C, *o*-$C_6F_5$, $^1J(^{13}C-^{19}F)$ = 242 Hz), 150.1 (s, 1C, *ipso*-$C_6H_5$). **$^{11}$B NMR** (25°C, $CD_2Cl_2$, 96.29 MHz): −0.20 (broad) **$^{19}$F{$^1$H} NMR** (25 °C, $CD_2Cl_2$, 282.38 MHz): $\delta$ = −164.75 (m, *m*-$C_6F_5$), −157.32 (m, *p*-$C_6F_5$), −131.11 (m, o-$C_6F_5$). **IR** (ATR, 16 scans): 3070 (w), 1644 (m), 1579 (m), 1516 (s), 1463 (s), 1451 (s), 1403 (m), 1378 (m), 1337 (w), 1319 (w), 1289 (m), 1282 (m), 1198 (w), 1189 (w), 1169 (w), 1092 (s), 1032 (w), 980 (s), 967 (s), 951 (m), 908 (m), 867 (w), 858 (m), 834 8w), 812 (m), 774 (s), 764 8m), 746 /m), 733 (m), 719 (m), 681 (s), 665 (m), 640 (m), 622 (m), 600 (m), 577 (m), 543 (m), 534 (m). **Raman** (25 °C, 784 nm, 65 mW, 60 s, 6 acc., $cm^{-1}$): 3098 (1), 3072 (1), 1645 (2), 1590 (4), 1579 (2), 1500 (3), 1485 (2), 1455 (2), 1389 (1), 1198 (1), 1191 (1), 1170 (2), 1165 (2), 1141 (5), 1033 (3), 1025 (1), 1005 (5), 835 (2), 814 (1), 765 (2), 602 (1), 584 (3), 579 (2), 535 (1), 493 (2), 449 (2), 409 (4), 401 (2), 294 (1), 241 (1), 212 (2), 146 (2), 140 (2), 96 (6), 84 (10). **MS** (CI, m/z,): 512 (6) [$B(C_6F_5)_3$]$^+$, 183 (100) [PhNNHPh]$^+$, 239 (1) [PhNNPh+*isobutane*]$^+$,105 (1) [PhNN]$^+$. Crystals suitable for X-ray crystallographic analysis were obtained, by cooling a saturated dichloromethane solution of **4** to –40 °C.

**Synthesis of *trans*-$PhNNSiMe_3\cdot GaCl_3$ (6):** To a stirred solution of **5** (0.190 g, 1.170 mmol) in $CH_2Cl_2$ (3 mL), $GaCl_3$ (0.208 g, 1.18 mmol) in $CH_2Cl_2$ (2 mL) was added at –80 °C over a period of 20 minutes. The resulting orange solution was allowed to stir at –80 °C for 80 minutes. The solution is then concentrated to a volume of 1 mL *in vacuo* at −50 °C. Storage at –80 °C over a period of 12 hours results in the deposition of orange crystals. Removal of supernatant by syringe and short drying *in vacuo* at −50 °C yields **6** as orange crystals (40 %). Storage at temperatures below −50 °C. **Mp.** −20 °C (dec.). **$^1$H NMR** (−77 °C, $CD_2Cl_2$, 500.13 MHz): 0.64 (s, 9H, $^1J(^1H-^{13}C)$ = 122.3 Hz, $^2J(^1H-^{29}Si)$ = 6.67 Hz), 7.51 (m, 2H, *o*-$C_6H_5$), 7.61 (m, 2H, *m*-$C_6H_5$), 7.98 (m, 1H, *p*-$C_6H_5$) **$^{13}$C{$^1$H} NMR** (−77 °C, $CD_2Cl_2$, 125.77 MHz): $\delta$ = −0.38 (s, 3C, $CH_3$, $^1J(^{13}C-^{29}Si)$ = 57.74 Hz), 120.8 (s, 2C, *o*-$C_6H_5$), 129.4 (s, 2C, *m*-$C_6H_5$), 134.9 (s, 1C, *p*-$C_6H_5$), 156.6 (s, 1C, *ipso*-$C_6H_5$). **$^{29}$Si NMR** (−77 °C, $CD_2Cl_2$, 99.35 MHz): $\delta$ = 43.1 (1Si). **Raman** (−50 °C, 784 nm, 65 mW, 80 sec., 6 acc., $cm^{-1}$): 3077 (1), 2988 (1), 2909 (1), 1591 (2), 1578 (1), 1479 (1), 1456 (7), 1451 (10), 1400 (1), 1310 (1), 1202 (1), 1165 (3), 1157 (4), 1027 (1), 1001 (2), 996 (1), 930 (1), 887 (1), 831 (1), 774 (2), 746 (1), 705 (1), 633 (1), 616 (1), 512 (1), 490 (2), 416 (2), 399 (1), 358 (2), 338 (2), 305 (1), 242 (1). Crystals suitable for X-ray crystallographic analysis were obtained, by cooling a saturated dichloromethane/trimethylsilyl chloride (1:1) solution of **6** to –80 °C.

**Synthesis of *iso1*-$Me_3Si(Ph)NN\cdot B(C_6F_5)_3$ (7):** To a stirred solution of **5** (0.250 g, 1.54 mmol) in $CH_2Cl_2$ (5 mL), $B(C_6F_5)_3$ (0.789 g, 1.54 mmol) in $CH_2Cl_2$ (6 mL) was added dropwise at –80 °C. The resulting golden solution was allowed to warm to ambient temperature. The solution was then concentrated to an approximate volume of 3 mL. Storage at 0 °C over a period of 12 hours results in the deposition of orange crystals. Removal of supernatant by syringe and short drying *in vacuo* at ambient temperature yields **7** (0.324 g, 30 %) as orange crystals. Storage at temperatures below 0 °C. **Mp.** 104 °C (dec.). **Anal. calc.** % (found): C, 46.98 (46.69); H, 2.08 (2.05); N, 4.06 (4.08).). **$^1$H NMR** (−60 °C, $CD_2Cl_2$, 300.13 MHz): $\delta$ = 0.49 (s, 9H, $Si(CH_3)_3$, $^1J(^1H-^{13}C)$ = 122.8 Hz), 6.73 (m, 2H, *o*-$C_6H_5$), 7.21 (m, 2H, *m*-$C_6H_5$), 7.32 (m, 1H, *p*-$C_6H_5$). **$^{13}$C{$^1$H} NMR** (−60 °C, $CD_2Cl_2$, 75.48MHz): $\delta$ = −1.3 (s, 3C, $Si(CH_3)_3$), 119.3 (s, 2C, *o*-$C_6H_5$), 129.1 (s, 2C, *m*-$C_6H_5$), 130.6 (s, 1C, *p*-$C_6H_5$), 150.2 (s, 1C, *ipso*-$C_6H_5$). **$^{19}$F{$^1$H} NMR** (−60 °C, $CD_2Cl_2$, 282.38 MHz): $\delta$ = −164.68 (m, *m*-$C_6F_5$), −158.34 (m, *p*-$C_6F_5$), −131.74 (m, *o*-$C_6F_5$). **$^{11}$B NMR** (−60 °C, $CD_2Cl_2$, 96.29 MHz): $\delta$ = −4.4 ppm. **$^{29}$Si NMR** (25 °C, $CD_2Cl_2$, 59.62 MHz): $\delta$ = 46.14 (1Si). **IR** (ATR, 16 scans): 2973 (w), 2915 (w), 1645 (m), 1516 (m), 1463 (s), 1455 (s), 1377 (w), 1279 (m), 1263 (m), 1105 (m), 1087 (m), 980 (s), 962 (s), 861 (m), 841 (m), 802 (m), 773 (m), 764 (m), 746 (m), 692 (m), 685 (m), 672 (m), 631 (w), 572 (m). **Raman** (25 °C, 784 nm, 64 mW, 60 sec., 6 acc., $cm^{-1}$): 3108 (1), 3080 (1), 2985 (1), 2929 (2), 1657 (1), 1603 (1), 1556 (5), 1495 (1), 1193 (1), 1162 (2), 1038 (2), 1017 (5), 815 (1), 653 (2), 645 (5), 633 (2), 597 (10), 586 (3), 529 (2), 522 (2), 479 (5), 480 (2), 462 (7), 453 (3), 419 (4), 405 (3), 359 (1), 322 (1), 264 (2), 245 (1), 212 (1). **MS** (CI, m/z,): 179 (100) [$(Me_3Si)PhNNH$]$^+$, 690 (2) [M]$^+$, 746 (66) [M+*isobutane*]$^+$. Crystals suitable for X-ray crystallographic analysis were obtained, by cooling a saturated dichloromethane solution of **7** to –25 °C

**Synthesis of *cis*-$Me_3SiNNSiMe_3\cdot B(C_6F_5)_3$ (9):** To a stirred solution of **2** (0.174 g, 1.0 mmol) in $CH_2Cl_2$ (10 mL), $B(C_6F_5)_3$ (0.563 g, 1.1 mmol) in $CH_2Cl_2$ (5 mL) was added dropwise at –80 °C. The resulting blue solution was stirred at –80 °C for 10 minutes. The solution is then concentrated to an approximate volume of 2 mL *in vacuo* at –50 °C. Storage at –25 °C over a period of 12 hours results in the deposition of blue crystals. Removal of supernatant by syringe and short drying *in vacuo* at ambient temperature yields **9** as blue crystals. Storage at temperatures below 0 °C. **Mp.**: 127 °C (dec.). **Anal. calc.** % (found): C, 42.00 (42.16); H, 2.64 (2.52); N, 4.08 (3.88). **$^1$H NMR** (−16 °C, $CD_2Cl_2$, 400.1 MHz): 0.20 (broad, 9H, $(CH_3)_3Si$, A'), 0.43 (s, 9H, $(CH_3)_3Si$), B') **$^{13}$C{$^1$H} NMR** (−16 °C, $CD_2Cl_2$, 75.5 MHz): $\delta$ = -0.69 (s, $(CH_3)_3Si$), 1.33 (s, $(CH_3)_3Si$). **$^{29}$Si NMR** (−16 °C, $CD_2Cl_2$, 79.5 MHz): $\delta$ = 14.4 (1Si, $(CH_3)_3Si$, B'), 30.9 (1Si, $(CH_3)_3Si$, A'). **$^{19}$F{$^1$H} NMR** (−16 °C, $CD_2Cl_2$, 282.4 MHz): $\delta$ = −164.4 (broad, *m*-$C_6F_5$), −158.1 (broad, *p*-$C_6F_5$), −129.6 (broad, *o*-$C_6F_5$). **$^{11}$B NMR** (−16 °C, $CD_2Cl_2$, 80.3 MHz): $\delta$ = 0.75 (broad). **$^1$H,$^{15}$N HMBC NMR** (−16 °C, $CD_2Cl_2$, 40.6 MHz): 464.50 (s, $NSi(CH_3)_3$,). **IR** (ATR, 32 scans): 2991 (w), 2973 (w), 2913 (w), 1645 (m), 1593 (w), 1518 (s), 1463 (s), 1390 (m), 1379 (m), 1284 (m), 1267 (m), 1256 (m), 1098 (s), 1037 (w), 976 (s), 853 (s), 834 (s), 784 (m), 773 (m), 746 (m), 728 (w), 700 (m), 682 (m), 656 (m), 633 (m), 600 (m), 584 (w), 571 (m), 543 (w). **Raman** (25 °C, 1064 nm, 100 mW, 163 scans, $cm^{-1}$): = 2973 (4), 2911 (10), 1647 (4), 1593 (3), 1421 (2), 1383 (3), 1261 (2), 1116 (1), 1095 (1), 855 (2), 814 (1), 767 (2), 710 (2), 688 (1), 638 (6), 583 (4), 543 (1), 486 (4), 471 (3), 447 (3), 426 (2), 399 (4), 236 (2), 186 (2), 153 (3). **MS** (EI, m/z, >10 %): 73 (73) [$SiMe_3$]$^+$, 168 (23) [$C_6F_5H$]$^+$, 227 (26), 258 (19), 277 (45), 296 (20), 444 (10), 512 (100) [$B(C_6F_5)_3$]$^+$, 614 (1) [M–$SiMe_3$+H]$^+$, 671 (2) [M–Me]$^+$, 686 (3) [M]$^+$. **UV-Vis** (25 °C, $CH_2Cl_2$) : 585 nm. Crystals suitable for X-ray crystallographic analysis were obtained, by cooling a saturated dichloromethane solution of **4** to –25 °C.

**Synthesis of 10:** A solution of **7** (0.324 g, 0.47 mmol) in $CH_2Cl_2$ (5 mL) was heated to 75 °C for 3 hours. The solvent of the resulting colourless solution was removed *in vacuo* and the residue dried for further for 30 minutes. The resulting colourless residue was dissolved in 0.2 mL benzene. Storage at ambient temperature over a period of 12 hours results in the deposition of colourless crystals. The crystals were washed with brenzene (2 x 0.1 mL) and dried *in vacuo* at ambient temperature yields **10** (0.204 g, 63 %) as colourless crystals. **Mp.** 71/102 °C (dec.). **Anal. calc.** % (found): C, 46.98 (46.86); H, 2.04 (2.57); N, 4.06 (4.07). **$^{1}$H NMR** (25 °C, $CD_2Cl_2$, 300.1 MHz): $\delta$ = 0.29 (s, 9H, $(CH_3)_3Si$), $^{1}J(^{1}H-^{13}C)$ = 118.2 Hz, $^{2}J(^{1}H-^{29}Si)$ = 6.65 Hz) 6.87 (m, 1H, *p*-$C_6H_5$) 7.03 (m, 2H, *o*-$C_6H_5$) 7.22 (m, 2H, *m*-$C_6H_5$). **$^{13}$C{$^{1}$H} NMR** (25 °C, $CD_2Cl_2$, 75.5 MHz): $\delta$ = 1.2 (s, 3C, $(CH_3)_3Si$), 110.7 (broad, 2C, *ipso*-$C_6F_5$), 116.2 (s, 2C, *o*-$C_6H_5$), 121.1 (s, 1C, *p*-$C_6H_5$), 121.6 (broad, 1C, *ipso*-$C_6F_5$), 129.2 (s, 2C, *m*-$C_6H_5$), 137.8 (m, 4C, *m*-$C_6F_5$, $^{1}J(^{13}C-^{19}F)$ = 249 Hz), 138.3 (m, 2C, *m*-$C_6F_5$, $^{1}J(^{13}C-^{19}F)$ = 249 Hz), 143.4 (m, 2C, *p*-$C_6F_5$, $^{1}J(^{13}C-^{19}F)$ = 252 Hz), 144.3 (m, 1C, *p*-$C_6F_5$, $^{1}J(^{13}C-^{19}F)$ = 252 Hz), 146.5 (s, 1C, *ipso*-$C_6H_5$), 147.1 (m, 4C, *o*-$C_6F_5$, $^{1}J(^{13}C-^{19}F)$ = 242 Hz), 147.6 (m, 2C, *o*-$C_6F_5$, $^{1}J(^{13}C-^{19}F)$ = 242 Hz). **$^{29}$Si NMR** (25 °C, $CD_2Cl_2$, 59.6 MHz): $\delta$ = 14.87 (m, $(CH_3)_3Si$). **$^{11}$B NMR** (25 °C, $CD_2Cl_2$, 96.3 MHz): $\delta$ = 40.24 (broad). **$^{19}$F{$^{1}$H} NMR** (25 °C, $CD_2Cl_2$, 282.4 MHz): $\delta$ = −161.98 (m, *m*-B($C_6F_5$)), −161.18 (m, *m*-N($C_6F_5$)), −160.91 (m, *m*-B($C_6F_5$)), −154.45 (m, *p*-N($C_6F_5$)), −150.73 (m, *p*-B($C_6F_5$)), −149.85 (m, *p*-B($C_6F_5$)), −141.75 (broad, *o*-N($C_6F_5$)), −131.60 (m, *o*-B($C_6F_5$)), −127.75 (m, *o*-B($C_6F_5$)). **IR** (ATR, 16 scans): 3041 (w), 2975 (w), 2914 (w), 1650 (m), 1597 (w), 1520 (s), 1505 (s), 1476 (s), 1409 (m), 1401 (m), 1310 (m), 1272 (m), 1258 (m), 1231 (m), 1143 (m), 1107 (m), 1068 (w), 1031 (w), 997 (s), 974 (s), 923 (m), 913 (s), 841 (s), 796 (m), 757 (m), 749 (m), 734 (m), 717 (w), 689 (m), 674 (m), 662 (m), 647 (m), 608 (m), 570 (m), 545 (m). **Raman** (25 °C, 784 nm, 16 mW, 12 s, 6 acc., $cm^{-1}$): 3063 (1), 3050 (1), 2948 (1), 2915 (1), 2899 (1), 2861 (1), 1647 (2), 1599 (2), 1586 (2), 1478 (1), 1449 (1), 1404 (1), 1315 (1), 1235 (1), 1173 (1), 1038 (1), 990 (6), 850 (1), 628 (1), 604 (1), 581 (3), 568 (1), 545 (1), 489 (4), 457 (1), 441 (2), 410 (1), 392 (2), 376 (2), 355 (1), 273 (1), 249 (1), 224 (1), 181 (1), 86 (9), 68 (10). **MS** (CI, m/z,): 675 (3) $[M–CH_3]^+$, 691 (100) $[M+H]^+$, 733 (33) [M+*isobutane*–$CH_3$]$^+$, 747 (64) [M+*isobutane*]$^+$. Crystals suitable for X-ray crystallographic analysis were obtained, by storage of a saturated benzene solution of **10** at 25 °C.

**Synthesis of 11:** A blue solution of **9** (0.100 g, 0.15 mmol) in $CH_2Cl_2$ (5 mL) was heated to 75 °C for 3 hours. The resulting colourless solution was concentrated to an approximate volume of 2 mL *in vacuo* at ambient temperatures. Storage at 0 °C over a period of 12 hours results in the deposition of colourless crystals. Removal of supernatant by syringe and drying *in vacuo* at ambient temperature yields **11** (0.040 g, 40 %) as colourless crystals. **Mp.** 163 °C. **Anal. calc.** % (found): C, 42.00 (41.55); H, 2.64 (2.56); N, 4.08 (4.27). **$^{1}$H NMR** (25 °C, $CD_2Cl_2$, 300.13 MHz): $\delta$ = 0.07 (s, 18H, $(CH_3)_3Si$), $^{1}J(^{1}H-^{13}C)$ = 119.2 Hz). **$^{13}$C{$^{1}$H}** (NMR 25 °C, $CD_2Cl_2$, 75.5 MHz): $\delta$ = 1.86 (s, 6C, $Si(CH_3)_3$). **$^{29}$Si NMR** (25 °C, $CD_2Cl_2$, 59.6 MHz): $\delta$ = 13.4 (m, $(CH_3)_3Si$). **$^{11}$B NMR** (25 °C, $CD_2Cl_2$, 96.3 MHz): $\delta$ = 36.59 (broad). **$^{19}$F{$^{1}$H} NMR** (25 °C, $CD_2Cl_2$, 282.4 MHz): $\delta$ = −162.06 (m, *m*-B($C_6F_5$)), −161.53 (m, *m*-N($C_6F_5$)), −161.43 (m, *m*-B($C_6F_5$)), −154.68 (m, *p*-N($C_6F_5$)), −150.96 (m, *p*-B($C_6F_5$)), −150.76 (m, *p*-B($C_6F_5$)), −140.31 (m, *o*-N($C_6F_5$)), −131.87 (m, *o*-B($C_6F_5$)), −127.35 (m, *o*-B($C_6F_5$)). **IR** (ATR, 32 scans): 2977 (w), 2949 (w), 2899 (w), 1650 (m), 1520 (s), 1507 (m), 1476 (s), 1397 (m), 1296 (m), 1261 (m), 1255 (m), 1167 (m), 1143 (m), 1104 (m), 1059 (m), 996 (s), 976 (s), 958 (s), 906 (s), 857 (s), 840 (s), 818 (s), 794 (m), 764 (m), 732 (m), 712 (m), 654 (m), 613 (m), 573 (m), 559 (m). **Raman** (25 °C, 784 nm, 33 mW, 20 s, 5 acc., $cm^{-1}$): 2980 (1), 2967 (1), 2951 (1), 2915 (1), 2900 (1), 1648 (5), 1525 (1), 1510 (1), 1480 (2), 1451 (4), 1404 (4), 1384 (2), 1315 (1), 1272 (1), 1165 (1), 1058 (1), 1011 (1), 980 (1), 960 (1), 861 (1), 840 (2), 764 (1), 751 (1), 682 (1), 654 (3), 613 (1), 586 (6), 572 (1), 560 (1), 491 (4), 467 (2), 458 (2), 446 (3), 433 (1), 429 (2), 391 (3), 379 (2), 355 (1), 334 (1), 283 (1), 237 (1), 186 (1), 149 (2), 124 (1), 68 (10). **MS** (CI, m/z,): 146 (31) $[(Me_3Si)_2NH_2–CH_3]^+$, 162 (100) $[(Me_3Si)_2NH_2]^+$, 671 (61) $[M–CH_3]^+$, 686 (80) $[M]^+$. Crystals suitable for X-ray crystallographic analysis were obtained, by cooling a saturated dichloromethane solution of **11** to 0 °C.

## *Acknowledgements*

Dr. Dirk Michalik and Dr. Wolfgang Baumann are gratefully acknowledged for his help with $^{11}$B and $^{29}$Si NMR experiments. Financial support by the University Rostock and the LIKAT are gratefully acknowledged. We thank Christian Hering for X-ray measurements.

**Keywords**: diazene, nitrene, diazene adducts, hydrazinoboranes, silylium ion, Lewis acids, $GaCl_3$ adducts, $B(C_6F_5)_3$ adducts, structure, bonding, charge transfer, frustrated Lewis acid base pair

## *Referenzes*

[1] P. Griess, *Justus Liebigs Ann. Chem.* **1858**, *106*, 123–125.

[2] R. Wizinger-Aust, *Angew. Chem.* **1958**, *70*, 199–204.

[3] A. Bafana, S. S. Devi, T. Chakrabarti, *Environ. Rev.* **2011**, *19*, 350–371.

[4] M. Stein, A. Breit, T. Fehrentz, T. Gudermann, D. Trauner, *Angew. Chem. Int. Ed.* **2013**, *52*, 9845–8.

[5] F. Cisnetti, R. Ballardini, A. Credi, M. T. Gandolfi, S. Masiero, F. Negri, S. Pieraccini, G. P. Spada, *Chem. Eur. J.* **2004**, *10*, 2011–21.

[6] G. Wagniere, *Theor. Chim. Acta* **1973**, *31*, 269–274.

[7] P. B. Dervan, M. E. Squillacote, P. M. Lahti, A. P. Sylwester, J. D. Roberts, *J. Am. Chem. Soc.* **1981**, *103*, 1120–1122.

[8] W. D. Hinsberg, P. B. Dervan, *J. Am. Chem. Soc.* **1979**, *101*, 6142–6144.

[9] W. D. Hinsberg, P. B. Dervan, *J. Am. Chem. Soc.* **1978**, *100*, 1608–1610.

[10] P. G. Schultz, P. B. Dervan, *J. Am. Chem. Soc.* **1980**, *102*, 878–880.

[11] A. Schulz, A. Villinger, *Angew. Chem.* **2013**, *125*, 3146–3148.

[12] H. Wieland, E. Wecker, *Chem. Ber.* **1910**, *43*, 3260–3271.

[13] S. Hünig, H. Balli, E. Breither, F. Brühne, H. Geiger, E. Grigat, F. Müller, H. Quast, *Angew. Chem.* **1962**, *74*, 818–824.

[14] W. R. McBride, H. W. Kruse, *J. Am. Chem. Soc.* **1957**, *79*, 572–576.

[15] W. R. McBride, E. M. Bens, *J. Am. Chem. Soc.* **1959**, *81*, 5546–5550.

[16] S. F. Nelsen, R. T. Landis, *J. Am. Chem. Soc.* **1974**, *96*, 1788–1793.

[17] S. F. Nelsen, S. C. Blackstock, *J. Org. Chem.* **1984**, *49*, 1134–1135.

[18] E. L. Allred, T. J. Chow, J. E. Oberlander, *J. Am. Chem. Soc.* **1982**, *104*, 5422–5427.

[19] S. F. Nelsen, H. Chang, J. J. Wolff, D. R. Powell, *J. Org. Chem.* **1994**, *59*, 6558–6563.

[20] V. Gutmann, A. Steininger, *Monatshefte für Chemie* **1965**, *96*, 1173–1182.

[21] A. Steininger, V. Gutmann, *Monatshefte für Chemie* **1966**, *97*, 171–177.

[22] N. Wiberg, W.-C. Joo, W. Uhlenbrock, *Angew. Chem.* **1968**, *80*, 661–662.

[23] N. Wiberg, W. Uhlenbrock, *Angew. Chem.* **1970**, *82*, 47–47.

[24] N. Wiberg, H. Bachhuber, G. Fischer, *Angew. Chem.* **1972**, *84*, 889–890.

[25] N. Wiberg, G. Fischer, H. Bachhuber, *Angew. Chem.* **1976**, *88*, 386–387.

[26] N. Wiberg, A. Gieren, *Angew. Chem.* **1962**, *74*, 942–942.

[27] N. Wiberg, H.-W. Häring, G. Huttner, P. Friedrich, *Chem. Ber.* **1978**, *111*, 2708–2715.

[28] N. Wiberg, G. Preiner, O. Schieda, G. Fischer, *Chem. Ber.* **1981**, *114*, 3505–3517.

[29] N. Wiberg, G. Schwenk, *Chem. Ber.* **1971**, *104*, 3986–3988.

[30] N. Wiberg, W. Uhlenbrock, *Chem. Ber.* **1971**, *104*, 3989–3991.

[31] N. Wiberg, W. Uhlenbrock, *J. Organomet. Chem.* **1974**, *70*, 249–257.

[32] N. Wiberg, W. Uhlenbrock, W. Baumeister, *J. Organomet. Chem.* **1974**, *70*, 259–271.

[33] N. Wiberg, S. K. Vasisht, H. Bayer, R. Meyers, *Chem. Ber.* **1979**, *112*, 2718–2729.

[34] N. Wiberg, S. K. Vasisht, G. Fischer, E. Weinberg, *Chem. Ber.* **1976**, *109*, 710–722.

[35] N. Wiberg, E. Weinberg, W.-C. Joo, *Chem. Ber.* **1974**, *107*, 1764–1766.

[36] W. Baumann, D. Michalik, F. Reiß, A. Schulz, A. Villinger, *Angew. Chem. Int. Ed.* **2014**, *53*, 3250–3.

[37] J. Kroner, W. Schneid, N. Wiberg, B. Wrackmeyer, G. Ziegleder, *J. Chem. Soc. Faraday Trans. 2* **1978**, *74*, 1909.

[38] H. Bock, K. Wittel, M. Veith, N. Wiberg, *J. Am. Chem. Soc.* **1976**, *98*, 109–114.

[39] D. W. Stephan, G. Erker, *Angew. Chem. Int. Ed.* **2010**, *49*, 46–76.

[40] A. Bernsdorf, H. Brand, R. Hellmann, M. Köckerling, A. Schulz, A. Villinger, K. Voss, *J. Am. Chem. Soc.* **2009**, *131*, 8958–8970.

[41] M. Becker, A. Schulz, A. Villinger, K. Voss, *RSC Adv.* **2011**, *1*, 128–134.

[42] I. C. Vei, S. I. Pascu, M. L. H. Green, J. C. Green, R. E. Schilling, G. D. W. Anderson, L. H. Rees, *Dalt. Trans.* **2003**, 2550.

[43] A. A. Danopoulos, J. R. Galsworthy, M. L. H. Green, L. H. Doerrer, S. Cafferkey, M. B. Hursthouse, *Chem. Commun.* **1998**, 2529–2560.

[44] J. C. Bottaro, *J. Chem. Soc. Chem. Commun.* **1978**, 990.

[45] U. Wannagat, C. Krüger, *Z. anorg. und allg. Chemie* **1964**, *326*, 288–295.

[46] N. Wiberg, M. Veith, *Chem. Ber.* **1971**, *104*, 3191–3203.

[47] A. E. Reed, L. a. Curtiss, F. Weinhold, *Chem. Rev.* **1988**, *88*, 899–926.

[48] E. D. Glendening, C. R. Landis, F. Weinhold, *J. Comput. Chem.* **2013**, *34*, 1429–1437.

[49] A. Leiba, I. Oref, *J. Chem. Soc. Faraday Trans. 1* **1979**, *75*, 2694.

[50] P. Arndt, U. Jäger-Fiedler, M. Klahn, W. Baumann, A. Spannenberg, V. V Burlakov, U. Rosenthal, *Angew. Chemie, Int. Ed. English* **2006**, *45*, 4195–4198.

[51] P. Arndt, W. Baumann, A. Spannenberg, U. Rosenthal, V. V Burlakov, V. B. Shur, *Angew. Chem. Int. Ed.* **2003**, *42*, 1414–8.

[52] T. J. Woodman, M. Bochmann, M. Thornton-Pett, *Chem. Commun.* **2001**, 329–330.

[53] M. M. Hansmann, R. L. Melen, F. Rominger, a S. K. Hashmi, D. W. Stephan, *J. Am. Chem. Soc.* **2014**, *136*, 777–82.

[54] G. Dierker, J. Ugolotti, G. Kehr, R. Fröhlich, G. Erker, *Adv. Synth. Catal.* **2009**, *351*, 1080–1088.

[55] M. Kowalewski, B. Krumm, P. Mayer, A. Schulz, A. Villinger, *Eur. J. Inorg. Chem.* **2007**, *2007*, 5319–5322.

[56] N. Wiberg, H. W. Häring, O. Schieda, *Angew. Chem. Int. Ed.* **1976**, *15*, 386–387.

[57] M. Veith, *Angew. Chem. Int. Ed.* **1976**, *15*, 387–388.

[58] R. Eikey, *Coord. Chem. Rev.* **2003**, *243*, 83–124.

[59] J. A. Ibers, R. S. Dickson, S. Otsuka, Y. Tatsuno, *J. Am. Chem. Soc.* **1971**, *93*, 4636–4637.

[60] R. Hüttel, A. Konietzny, *Chem. Ber.* **1973**, *106*, 2098–2113.

[61] E. W. Abel, C. A. Burton, M. R. Churchill, K.-K. G. Lin, *J. Chem. Soc. Chem. Commun.* **1974**, 268.

[62] M. A. Aubart, R. G. Bergman, *Organometallics* **1999**, *18*, 811–813.

[63] T. Avilés, A. Dinis, M. G. B. Drew, V. Félix, *Monatshefte fuer Chemie.* **2000**, *131*, 1305–1310.

[64] J. R. Dilworth, H. J. de Liefde Meijer, J. H. Teuben, *J. Organomet. Chem.* **1978**, *159*, 47–52.

[65] R. S. Dickson, J. A. Ibers, *J. Am. Chem. Soc.* **1972**, *94*, 2988–2993.

[66] H. Fuβstetter, H. Nöth, *Liebigs Ann. der Chemie* **1981**, *1981*, 633–641.

[67] H. Hommer, H. Nöth, H. Sachdev, M. Schmidt, H. Schwenk, *Chem. Ber.* **1995**, *128*, 1187–1194.

[68] D. Nölle, H. Nöth, *Chem. Ber.* **1978**, *111*, 469–479.

[69] H. Nöth, W. Regnet, *Chem. Ber.* **1969**, *102*, 2241–2248.

[70] H. Nöth, W. Regnet, H. Rihl, R. Standfest, *Chem. Ber.* **1971**, *104*, 722–733.

[71] N. Götz, S. Herler, P. Mayer, A. Schulz, A. Villinger, J. J. Weigand, *Eur. J. Inorg. Chem.* **2006**, *2006*, 2051–2057.

[72] G. Fischer, S. Herler, P. Mayer, A. Schulz, A. Villinger, J. J. Weigand, *Inorg. Chem.* **2005**, *44*, 1740–51.

[73] A. P. Scott, L. Radom, *J. Phys. Chem.* **1996**, *100*, 16502–16513.

[74] B. J. Smith, *J. Phys. Chem.* **1993**, *97*, 10513–10514.

[75] M. L. McKee, *J. Phys. Chem.* **1993**, *97*, 13608–13614.

[76] J. A. Pople, K. Raghavachari, M. J. Frisch, J. S. Binkley, P. V. R. Schleyer, *J. Am. Chem. Soc.* **1983**, *105*, 6389–6399.

[77] J. Boyd, G. I. Pagola, M. C. Caputo, M. B. Ferraro, P. Lazzeretti, *J. Chem. Theory Comput.* **2009**, *5*, 1343–1349.

[78] B. A. Shainyan, A. V Kuzmin, M. Y. Moskalik, *Comput. Theor. Chem.* **2013**, *1006*, 52–61.

[79] C. J. Casewit, W. A. Goddard, *J. Am. Chem.* **1980**, *102*, 4057–4062.

[80] S. Herler, P. Mayer, J. S. A. der Günne, A. Schulz, A. Villinger, J. J. Weigand, *Angew. Chem. Int. Ed.* **2005**, *44*, 7790–3.

[81] D. Michalik, A. Schulz, A. Villinger, *Inorg. Chem.* **2008**, *47*, 11798–11806.

[82] M. Lehmann, A. Schulz, A. Villinger, *Angew. Chem. Int. Ed.* **2009**, *48*, 7444–7.

[83] A. Schulz, A. Villinger, *Angew. Chem. Int. Ed.* **2012**, *51*, 4526–4528.

[84] M. F. Ibad, P. Langer, F. Reiß, A. Schulz, A. Villinger, *J. Am. Chem. Soc.* **2012**, *134*, 17757–17768.

[85] M. F. Ibad, P. Langer, A. Schulz, A. Villinger, *J. Am. Chem. Soc.* **2011**, *133*, 21016–21027.

[86] A. Haaland, *Angew. Chem.* **2006**, *101*, 1017–1032.

[87] E. I. Davydova, T. N. Sevastianova, A. V. Suvorov, A. Y. Timoshkin, *Coord. Chem. Rev.* **2010**, *254*, 2031–2077.

[88] E. A. Berezovskaya, A. Y. Timoshkin, T. N. Sevastianova, A. D. Misharev, A. V Suvorov, H. F. Schaefer, *J. Phys. Chem. B* **2004**, *108*, 9561–9563.

[89] G. Frenking, S. Fau, C. M. Marchand, H. Grützmacher, *J. Am. Chem. Soc.* **1997**, *119*, 6648–6655.

[90] G. M. Sheldrick, *SHELXS-97 Progr. Solut. Cryst. Struct. Univ. Göttingen, Ger. 1997.*

[91] G. M. Sheldrick, *SHELXL-97 Progr. Refinement Cryst. Struct. Univ. Göttingen, Ger. 1997.*

[92] G. M. Sheldrick, *SADABS. Version 2. Univ. Göttingen, Ger. 2004.*

[93] J. J. de Lange, J. M. Robertson, I. Woodward, *Proc. R. Soc. A Math. Phys. Eng. Sci.* **1939**, *171*, 398–410.

[94] J. A. Bouwstra, A. Schouten, J. Kroon, R. B. Helmholdt, *Acta Crystallogr. Sect. C Cryst. Struct. Commun.* **1985**, *41*, 420–426.

[95] P. Pyykkö, M. Atsumi, *Chem. Eur. J.* **2009**, *15*, 12770–12779.

[96] C. Hubrich, A. Schulz, A. Villinger, *Z. anorg. allg. Chem.* **2007**, *633*, 2362–2366.

## 5.4 Synthesis of the First Persilylated Ammonium Ion $[(Me_3Si)_3NSi(H)Me_2]^+$ By Silylium Catalysed Alkyl/Hydrogen Redistribution

René Labbow, Fabian Reiß, Axel Schulz, Alexander Villinger.

*Organometallics*, **2014**, *33*, 3223-3226.

In dieser Publikation wurde ein groß Teil der experimentellen Arbeiten sowie die gesamten Berechnungen von mir durchgeführt. Ich habe das Manuskript verfasst und das Supportingfile erstellt. Der eigene Beitrag liegt bei ca. 80 %.

Ein ausführliches Supportingfile steht online zur freien Verfügung:

DOI: 10.1021/om500519j

ORGANOMETALLICS
Communication
pubs.acs.org/Organometallics

# Synthesis of the First Persilylated Ammonium Ion, $[(Me_3Si)_3NSi(H)Me_2]^+$, by Silylium-Catalyzed Methyl/Hydrogen Exchange Reactions

René Labbow,[†] Fabian Reiß,[†] Axel Schulz,*[,†,‡] and Alexander Villinger[†]

[†]Institut für Chemie, Abteilung Anorganische Chemie, Universität Rostock, Albert-Einstein-Strasse 3a, 18059 Rostock, Germany
[‡]Leibniz-Institut für Katalyse e.V. an der Universität Rostock, Albert-Einstein-Strasse 29a, 18059 Rostock, Germany

*Supporting Information*

**ABSTRACT:** This work describes the unexpected synthesis and characterization of the first persilylated ammonium ion, $[(Me_3Si)_3NSi(H)Me_2]^+$, in the reaction of $(Me_3Si)_3N$ with $[Me_3Si{-}H{-}SiMe_3][B(C_6F_5)_4]$. NMR and Raman studies revealed a transition-metal-free silylium ion catalyzed substituent redistribution process when $[Me_3Si{-}H{-}SiMe_3]^+$ was used as the silylating reagent. These observations were affirmed in the reaction with $[Et_3Si{-}H{-}SiEt_3][B(C_6F_5)_4]$. A Lewis acid catalyzed scrambling process always occurs if an excess of silanes is present in the formation of silylium cations while employing the standard Bartlett−Schneider−Condon type reaction. Additionally, the thermodynamics of this process was accessed by DFT computations at the pbe1pbe/aug-cc-pVDZ level, indicating alkyl substituent exchange equilibria at the silane and preference of the formation of $[(Me_3Si)_3NSi(H)Me_2]^+$ over $[(Me_3Si)_4N]^+$.

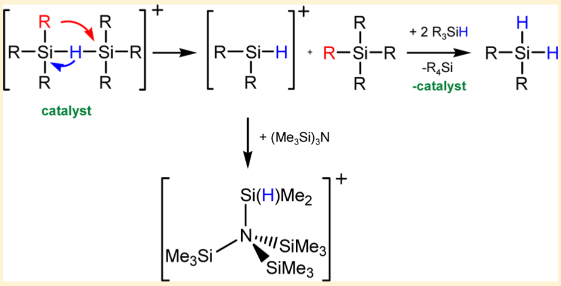

The rise of silylium cation chemistry was motivated by the search for a three-coordinate silicon cation $[R_3Si]^+$ (where R is an alkyl or aryl group) in analogy to the well-studied lighter group 14 carbenium ions $[R_3C]^+$.[1−3] In 2002 Reed and Lambert solved the silylium ion problem by the synthesis and full characterization of the salt $[(Mes)_3Si][CHB_{11}Me_5Br_6]\cdot C_6H_6$ (Mes = 2,4,6-trimethylphenyl) with a sterically encumbered silylium cation.[4] The major problem in the synthesis of "naked" $[R_3Si]^+$ cations arises from their electron sextet and an empty 3p valence orbital on the silicon, resulting in super Lewis acidic character. This leads to the formation of Lewis acid−base adducts even with weak Lewis bases (e.g., toluene,[5−7] $Me_3Si{-}H$[8,9]) or close cation−anion contacts with weakly coordinating anions (wca; e.g., $[CHB_{11}H_5Br_6]$,[10] $[CHB_{11}F_{11}]$[11]), respectively.

In 1963 Corey and West[12] used the Lewis acid assisted hydrogen/halogen exchange Bartlett−Schneider−Condon[13] reaction for the first time in silicon chemistry. Thirty years later Lambert used a borate ($[B(C_6F_5)_4]^-$) as a wca in this reaction type and published a general synthetic approach to trialkylsilylium cations $[R_3Si]^+$ for the first time.[6] However, Nava and Reed[9] showed that the commonly used triethylsilyl perfluorotetraphenylborate salt, $[Et_3Si][B(C_6F_5)_4]$, was misidentified. As prepared, the cation is the hydride-bridged silane adduct $[R_3Si{-}H{-}SiR_3]^+$. The effective combination of a H-silane ($R_3Si{-}H$) and a triphenylmethylium (tritylium) salt with a wca (e.g., $[Ph_3C][B(C_6F_5)_4]$ (**1**)) has been shown to be a well-established method, which was used to synthesize a variety of silylium cations on numerous occasions. This reaction is tolerant toward different solvents (benzene, toluene, 1,2-dichlorobenzene) or can be even carried out in neat silanes $R_3Si{-}H$ as solvent, yielding $[R_3Si{-}H{-}SiR_3][B(C_6F_5)_4]$ (**2** for R = Me) (Scheme 1).

**Scheme 1. General Synthesis of Silylium Ions**

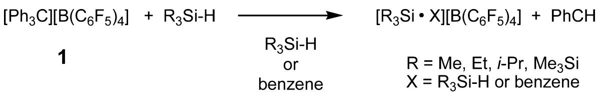

$$\underset{\mathbf{1}}{[Ph_3C][B(C_6F_5)_4]} + R_3Si\text{-}H \xrightarrow[\text{or benzene}]{R_3Si\text{-}H} [R_3Si\cdot X][B(C_6F_5)_4] + PhCH$$

R = Me, Et, *i*-Pr, $Me_3Si$
X = $R_3Si$-H or benzene

Furthermore, especially $[Me_3Si{\cdot}X][wca]$ salts (X = $Me_3SiH$, arene; wca = $[B(C_6F_5)_4]^-$, $[CHB_{11}H_5Y_6]^-$ (Y = Br, Cl)) allowed access to homoleptic onium ions, for example bissilylated halonium and pseudohalonium cations of the type $[Me_3Si{-}X{-}SiMe_3]^+$ (X = F, Cl, Br, I;[14] X = CN, OCN, SCN, NNN),[15] which could be isolated and fully characterized as their $[B(C_6F_5)_4]^-$ salts. The persilylated chalcogonium ions $[(Me_3Si)_3O]^+$ and $[(Me_3Si)_3S]^+$ were prepared and investigated by Olah et al.[16,17] Recently, we reported the fully characterized pseudochalcogonium salts $[(Me_3Si)_2NCN(SiMe_3)][B(C_6F_5)_4]$ and $[(Me_3Si)_2NNC(SiMe_3)][B(C_6F_5)_4]$.[18] In 2001 Driess et al. presented the first structurally characterized persilylated phosphonium $[(Me_3Si)_4P]^+$ and arsonium $[(Me_3Si)_4As]^+$ ions (pnictonium).[19] All of these examples of onium ions can be obtained in a general silylation reaction combining the super Lewis acidic[20] media of $[Me_3Si\cdot$

**Received:** May 16, 2014

ACS Publications © XXXX American Chemical Society

(solvent)][$B(C_6F_5)_4$] and the neutral silylated group 15−17 compound in suitable solvents, as depicted in Scheme 2.

**Scheme 2. Synthesis of Homoleptic Onium Cations**[a]

$$[Me_3Si\cdot X][B(C_6F_5)_4] + (Me_3Si)_nE \longrightarrow [(Me_3Si)_{n+1}E][B(C_6F_5)_4] + X$$

[a] $n$ = 1: E = F, Cl, Br, I, CN, OCN, SCN, NNN with X = $Me_3SiH$. $n$ = 2: E = O, S, NCN, NNC with X = $Me_3SiH$. $n$ = 3: E = P, As with X = benzene.

We have long been interested in the preparation of the missing homoleptic tetrakis(trimethylsilyl)ammonium cation, $[(Me_3Si)_4N]^+$. Herein we describe the attempted synthesis of the $[(Me_3Si)_4N]^+$ cation and show that a $[(Me_3Si)_3NSi(H)Me_2]^+$ cation is formed instead. In addition, while studying the problem with the synthesis of $[(Me_3Si)_4N]^+$ we discovered a hidden silylium-catalyzed methyl/hydrogen exchange at the silane $Me_3SiH$, which finally explained the loss of one methyl group.

The starting point of this project was the attempted direct silylation of $(Me_3Si)_3N$, as depicted in Scheme 2. Although Driess and Wiberg[21] failed in similar experiments, we decided to reinvestigate the preparation of the missing persilylated ammonium ion. The gas-phase reaction (1) of $(Me_3Si)_3N$ with

$$(Me_3Si)_3N(g) + [Me_3Si]^+(g) \rightarrow [(Me_3Si)_4N]^+(g) \qquad (1)$$

$[Me_3Si]^+$ calculated at the pbe1pbe/aug-cc-pVDZ level of theory ($\Delta H_{298} = -427.1$ kJ mol$^{-1}$) also strongly supported the idea of direct silylation (cf. −127.2 kJ mol$^{-1}$ for toluene, −131.0 kJ mol$^{-1}$ for $Me_3Si{-}H$ and −227.6 kJ mol$^{-1}$ for $Me_3Si{-}CN$).[14,15]

We repeated the reactions reported by Driess[19] and coworkers, who attempted to use [$Me_3Si\cdot$(toluene)][$B(C_6F_5)_4$] (**3**) as the silylation agent with no success. However, in an earlier work we noticed that the salt **3** slowly decomposes during drying in vacuo and isolation, which was indicated by a gradual color switch from colorless to yellow.[7] Therefore, we decided to prepare **3** in situ. [$Me_3Si{-}H{-}SiMe_3$][$B(C_6F_5)_4$] (**2**) was treated with an excess of toluene. Then trimethylsilane (bp 6.7 °C) was removed with a freeze−pump−thaw procedure, affording colorless crystals of [$Me_3Si\cdot$(toluene)][$B(C_6F_5)_4$] (**3**). The resulting suspension was reacted with 1 equiv of $(Me_3Si)_3N$ (**4**) and heated to 70 °C, where a characteristic biphasic system was observed. Slow cooling of this solution to −40 °C resulted in the deposition of colorless crystals of the unexpected salt [$(Me_3Si)_3NSi(H)Me_2$][$B(C_6F_5)_4$] (**5**) in a moderate isolated yield of 46% (Figure 1).

As an isolated solid, **5** is thermally surprisingly stable up to 152 °C, while it immediately decomposes in $CH_2Cl_2$ solution at ambient temperature, which is indicated by a switch from colorless to deep orange. This prompted us to carry out NMR experiments at −80 °C in $CD_2Cl_2$. However, only decomposition products of the cation could be detected. Remarkably, the borate anion is not involved in the decomposition, as visualized by its characteristic $^{19}F\{^1H\}$ NMR resonance pattern and $^{11}B$ NMR shift of −17 ppm. Actually, the use of *o*-dichlorobenzene as the solvent in NMR experiments failed to identify the cation. This observation is in contrast to the case for the analogous phosphonium and arsonium cations, which remain unchanged in $CH_2Cl_2$ solution. These results gave evidence for the dissociation of **5** even in weak Lewis basic solvents followed by uncontrolled decomposition. The IR spectrum of **5** showed a weak mode at 2192 cm$^{-1}$, which could be assigned to stretches of the Si−H unit. This is in reasonable agreement with the calculated value for $\nu_{SiH}$(calcd) 2232 cm$^{-1}$ (pbe1pbe/aug-cc-pVDZ level; see the Supporting Information). The existence of ammonium salt **5** was unequivocally proven by X-ray diffraction analysis (Figure 1). **5** crystallizes in the monoclinic space group $P2_1/c$ with four formula units per cell. It is interesting to note that crystallization at higher temperatures (3 °C) resulted in the crystallization of another modification of **5** (triclinic space group $P\overline{1}$; see the Supporting Information), which, however, showed a highly disordered cation. Therefore, only the ordered structure is discussed. There are neither significant cation−anion nor anion−anion contacts. The observed molecular structure exhibits the expected nearly tetrahedral coordination environment around the nitrogen atom with Si−N−Si angles between 106.32(2) and 112.27(2)° (cf. $[(Me_3Si)_4P]^+$, Si−P−Si 107.30(7)−111.06(7)°; $[(Me_3Si)_4As]^+$, Si−As−Si 108.8(1)−110.0(1)°). The N−Si bonds of **5** (N−Si1 1.889(2) Å, N−Si2 1.899(2) Å, N−Si3 1.891(2) Å, N−Si4 1.870(2) Å) are in good agreement with those observed in the persilylated diazonium cation $[(Me_3Si)_2NN(SiMe_3)]^+$ (cf. 1.829(1), 1.894(1), 1.899(1) Å,[22] $\sum r_{cov}$(Si−N) = 1.87 Å).[23] It should be mentioned that the silicon−nitrogen bond of the dimethylsilyl group (N−Si4) is significantly shortened in comparison to those of the three trimethylsilyl groups (N−Si1, N−Si2, N−Si3) as a consequence of less steric hindrance (cf. N−Si1 1.889(2) Å, N−Si2 1.899(2) Å, N−Si3 1.891(2) Å, N−Si4 1.870(2) Å).

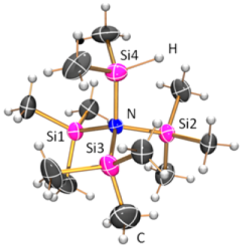

**Figure 1.** ORTEP drawing of the molecular structure of the cation $[(Me_3Si)_3NSi(H)Me_2]^+$ in the crystal. Thermal ellipsoids are drawn with 50% probability at 153 K, and the $[B(C_6F_5)_4]^-$ anion is omitted for clarity. Selected distances (Å) and angles (deg): N−Si1 1.889(2), N−Si2 1.899(2), N−Si3 1.891(2), N−Si4 1.870(2); Si1−N−Si2 112.27(2), Si1−N−Si3 110.27(2), Si3−N−Si2 107.92(2) Si4−N−Si1 111.24(2) Si4−N−Si2 106.32(2) Si4−N−Si3 108.69(2).

All of these results highlighted the difficulties in the synthesis of the intended homoleptic $[(Me_3Si)_4N]^+$ ion but gave no satisfactory explanation for the loss of a methyl group at one silyl group. For this reason, we took a closer look at our starting materials and their preparation. The analytical data of **1**, **2**, and **4** showed no appreciable impurities. Therefore, we decided to examine the stability of **2** in solution. After the treatment of [$Ph_3C$][$B(C_6F_5)_4$] (3 mol %) with an excess of $Me_3SiH$ and storage over a period of 12 h (Scheme 1), we recondensed the excess silane into a sealed NMR tube. The $^1H$ NMR data revealed, in addition to the expected signals for $Me_3SiH$ ($\delta(^1H)$ 0.92 (d), 4.87 (dec)), additional signals which could be assigned to $Me_4Si$ ($\delta(^1H)$ 0.86 (s)), $Me_2SiH_2$ ($\delta(^1H)$ 0.97 (t), 4.67 (sep)), and $MeSiH_3$ ($\delta(^1H)$ 4.41 (q)).[24] The composition of the mixture (0.14 ($MeSiH_3$):0.88 ($Me_2SiH_2$):1 ($Me_3SiH$):0.70 ($Me_4Si$)) was rather unexpected to us (Figure

2), but the formation of this methylsilane mixture now explained the presence of one $Me_2SiH$ group in **5**.

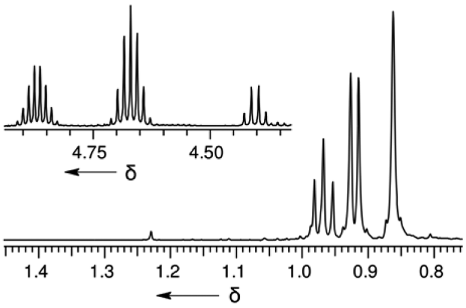

**Figure 2.** $^1H$ NMR spectrum of the recovered silane mixture (25 °C, $C_6D_6$ (external), 300.13 MHz): $\delta$ 0.86 (s, $(CH_3)_4Si$, $^2J(^1H-^{29}Si) = 6.4$ Hz), 0.92 (d, $(CH_3)_3SiH$, $^3J(^1H-^1H) = 3.59$ Hz), 0.97 (t, $(CH_3)_2SiH_2$, $^3J(^1H-^1H) = 4.15$ Hz). 4.41 (quart, $(CH_3)SiH_3$, $^3J(^1H-^1H) = 4.72$ Hz), 4.67 (sep, $(CH_3)_2SiH_2$), 4.87 (dec, $(CH_3)_3SiH$).

To gain more insight into the formation of these mixed methylsilanes, we treated 0.26 mol % of **1** with $Me_3SiH$ as reactant and solvent at ambient temperature, resulting in the precipitation of $[Me_3Si-H-SiMe_3][B(C_6F_5)_4]$ (**2**), which represented the catalytically active species in this reaction. The upper silane phase was investigated in a series of $^1H$ NMR and Raman experiments. This long-term analysis showed an unambiguous catalytic reaction, as depicted in Scheme 3 and Figure 3 (see also the Supporting Information).

**Scheme 3. Catalytic Exchange Reaction of $Me_3SiH$[a]**

$$n\ Me_3SiH \xrightarrow[rt]{PC} r\ MeSiH_3 + s\ Me_2SiH_2 + t\ Me_3SiH + u\ Me_4Si$$

[a] PC = precatalyst = $[Ph_3C][B(C_6F_5)_4]$.

Since the increase of $Me_2SiH_2$ and $Me_4Si$ was accompanied by the decrease of $Me_3SiH$ (Figure 3, left), the reaction might be regarded as a methyl/hydrogen redistribution reaction (Scheme 4, reaction A with R = Me). Moreover, a second much slower equilibrium reaction interfered with the aforementioned exchange reaction. This equilibrium could be attributed to the substituent redistribution of $Me_2SiH_2$ into the methylsilane $MeSiH_3$ and the starting material $Me_3SiH$, as depicted in Scheme 4 (reaction B with R = Me) and Figure 3 (right). The small enthalpy changes along reactions A ($-0.6$ kJ $mol^{-1}$) and B ($-1.9$ kJ $mol^{-1}$) support this assumption.

**Scheme 4. Alkyl Exchange Reactions (R = Me, Et)**

$$\mathbf{A}\quad R_3SiH + R_3SiH \rightleftharpoons R_4Si + R_2SiH_2$$

$$\mathbf{B}\quad R_2SiH_2 + R_2SiH_2 \rightleftharpoons R_3SiH + RSiH_3$$

In further experiments we studied the influence of the wca. For this reason we added catalytic amounts of $[Ph_3C][CHB_{11}H_5Cl_6]$ to neat $Me_3SiH$, leading also to the formation of a silane mixture, as depicted in Schemes 3 and 4. Additionally, the reaction of **1** as precatalyst (0.34 mol %) and $Et_3SiH$ was examined by a $^{29}Si$-INEPT NMR study, which showed signals for $Et_4Si$ ($\delta(^{29}Si)$ 8.33), $Et_3SiH$ ($\delta(^{29}Si)$ 0.52) and $Et_2SiH_2$ ($\delta(^{29}Si)$ $-22.56$) after an equilibration time of 70 days (see Supporting Information, Figure S18). Again the in situ formed silylium ion (here $[Et_3Si-H-SiEt_3][B(C_6F_5)_4]$ (**6**)) catalyzes the ethyl/hydrogen exchange reactions, for which also very small enthalpies were computed (equilibrium A, 0.3 kJ $mol^{-1}$; equilibrium B, $-0.1$ kJ $mol^{-1}$; see Scheme 4 with R = Et). Interestingly, no signal for the $EtSiH_3$ species was observed, which might be due to the less sensitive $^{29}Si$-INEPT NMR method. The estimated turnover numbers (TON) and turnover frequencies (TOF) were calculated at the 50% state of equilibration and are depicted in Table 1. The higher activity of the smaller "$[Me_3Si]^+$" silylium ion is impressively demonstrated by a 3 times larger TOF and should be taken into account when preparing **2** or homoleptic species bearing $Me_3Si$ groups.

**Table 1. Estimated Parameters for the Catalyzed Alkyl/Hydrogen Exchange Reaction**

| silane | amt of PC, mol %[a] | $TON_{50}$[b] | $TOF_{50}$[c] |
|---|---|---|---|
| $Me_3SiH$ | 0.26 | 63 | 1.28 |
| $Et_3SiH$ | 0.34 | 39 | 0.41 |

[a] PC = precatalyst = $[Ph_3C][B(C_6F_5)_4]$. [b] Referenced to $R_4Si$ species at 50% of equilibration state. [c] $TOF_{50}$ = TON/time (h).

These results can be compared to earlier observations by Müller and co-workers[25,26] and Oestreich et al.,[27] who described substituent scrambling in the formation of the arene silylium cation $[(Mes)_3Si]^+$ and the ferrocene-substituted species $[iPrSi(Fc)_2]^+$, respectively. As these reports focused on the substituent scrambling at the silylium cation center, there was no report of catalytic substituent redistribution at the silane compounds. Brookhart et al. reported on a reaction of $Me_2EtSiH$ with the transition-metal complex $Et_3Si(H)_2Ir(\mu\text{-}SiEt_2)_2Ir(H)_2SiEt_3$ as catalyst in the presence of hydrogen and observed a substituent redistribution, affording $Et_2MeSiH$,

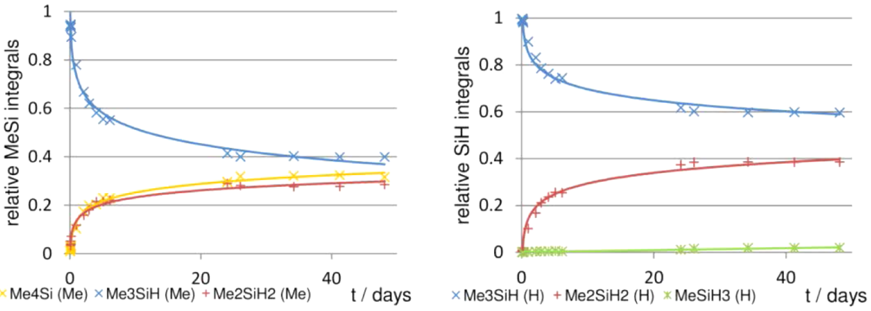

**Figure 3.** Time-dependent relative integrals taken from $^1H$ NMR spectra: (left) high-field region $Me_xSi$; (right) low-field region $SiH_x$.

$Me_2EtSiH$, $Me_3SiH$, and $Et_3SiH$.[28] Astonishingly, the transient metal complex seemed to be restricted in the catalysis of redistribution on the substitution pattern $R_3SiH$ without forming $R_4Si$ and $R_2SiH_2$ species. Nonetheless, this work represented the first catalytic alkyl redistribution reaction via an assumed silyl−silylene intermediate. Just recently, Heinekey and co-workers described the structural characterization of $[Et_3Si{-}H{-}SiEt_3][B(C_6F_5)_4]$ (**6**).[29] When **6** was dissolved in benzene or toluene, the evolution of hydrogen gas and the formation of tetraethylsilane was observed. The latter observation clearly indicated a substituent redistribution. Thus, Heinekey proposed "This suggests that the highly reactive, Lewis acidic silylium species are promoting redistribution of the ethyl groups. Further, the reaction appears to be catalytic."[29]

With these results in mind, we can now explain the formation of $[(Me_3Si)_3NSi(H)Me_2]^+$ instead of $[(Me_3Si)_4N]^+$ in the reaction of $(Me_3Si)_3N$ with in situ generated $[Me_3Si{\cdot}(toluene)][B(C_6F_5)_4]$ (**3**) (vide supra). In situ generated **3** (precipitation in toluene) always contains $Me_3SiH$ (Figure S3, Supporting Information). In combination with Lewis acidic $[Me_3Si]^+$ a methyl/hydrogen redistribution process at $Me_3SiH$ can be considered as discussed above, leading to $Me_2SiH_2$ and $Me_4Si$ dissolved in toluene. Now $Me_2SiH_2$ is easily activated by formation of a $[Me_3Si{-}H{-}Si(H)Me_2]^+$ cation ($7^+$), as depicted in Scheme 5.

**Scheme 5. Activation of Dimethylsilane by Formation of Dimethylsilylium Ion $7^+$**

$$[Me_3Si\text{-}H\text{-}SiMe_3]^+ + Me_2SiH_2 \longrightarrow \underset{\mathbf{7^+}}{[Me_3Si\text{-}H\text{-}Si(H)Me_2]^+} + Me_3SiH$$

Dimethylsilylium ion $7^+$ is kinetically and thermodynamically favored to bind to $(Me_3Si)_3N$ by about −60.6 kJ $mol^{-1}$ (cf. $[(Me_3Si)_3NSi(H)Me_2]^+$, $\Delta H_{298} = -487.7$; $[(Me_3Si)_4N]^+$, −427.1 kJ $mol^{-1}$), affording the acid−base adduct $[(Me_3Si)_3NSi(H)Me_2]^+$ and $Me_3SiH$ rather than the intended homoleptic cation $[(Me_3Si)_4N]^+$ and $Me_2SiH_2$. Hence, the formation of $[(Me_3Si)_3NSi(H)Me_2]^+$ and its precipitation as a $[B(C_6F_5)_4]^-$ salt superimposes the described exchange equilibria (Scheme 4, reactions A and B), leading to a new equilibrium adjustment. By this equilibrium adjustment consumed $Me_2SiH_2$ is reproduced. Furthermore, it can be assumed that $(Me_3Si)_3N$ as base itself may accelerate the Me/H exchange.

The foregoing describes the synthesis and characterization of the first persilylated ammonium cation in the salt $[(Me_3Si)_3NSi(H)Me_2][B(C_6F_5)_4]$. The unexpected loss of one methyl group during direct silylation of $(Me_3Si)_3N$ led to the discovery of a transition-metal-free silylium-catalyzed alkyl scrambling process starting from $Me_3SiH$ and $Et_3SiH$, respectively. This scrambling process occurs if an excess of silanes is present in the formation of silylium cations while employing the standard Bartlett−Schneider−Condon type reaction.[6]

## ■ ASSOCIATED CONTENT

### Ⓢ Supporting Information

Text, tables, figures, and CIF and xyz files giving detailed information about experiments and computations. This material is available free of charge via the Internet at http://pubs.acs.org.

## ■ AUTHOR INFORMATION

### Corresponding Author

*E-mail for A.S.: axel.schulz@uni-rostock.de.

### Notes

The authors declare no competing financial interest.

## ■ ACKNOWLEDGMENTS

Dr. Dirk Michalik is gratefully acknowledged for the attempted low-temperature NMR experiments. Financial support by the Universität Rostock and the LIKAT is gratefully acknowledged.

## ■ REFERENCES

(1) Reed, C. A. *Acc. Chem. Res.* **1998**, *31*, 325−332.

(2) Lambert, J. B.; Kania, L.; Zhang, S. *Chem. Rev.* **1995**, *95*, 1191−1201.

(3) Lambert, J. B.; Zhao, Y.; Zhang, S. M. *J. Phys. Org. Chem.* **2001**, *14*, 370−379.

(4) Kim, K.-C.; Reed, C. A.; Elliott, D. W.; Mueller, L. J.; Tham, F.; Lin, L.; Lambert, J. B. *Science* **2002**, *297*, 825−827.

(5) Lambert, J. B.; Zhang, S.; Ciro, S. M. *Organometallics* **1994**, *13*, 2430−2443.

(6) Lambert, J. B.; Zhang, S. *J. Chem. Soc., Chem. Commun.* **1993**, 383.

(7) Ibad, M. F.; Langer, P.; Schulz, A.; Villinger, A. *J. Am. Chem. Soc.* **2011**, *133*, 21016−21027.

(8) Hoffmann, S. P.; Kato, T.; Tham, F. S.; Reed, C. A. *Chem. Commun.* **2006**, 767−769.

(9) Nava, M.; Reed, C. A. *Organometallics* **2011**, *30*, 4798−4800.

(10) Xie, Z.; Bau, R.; Benesi, A.; Reed, C. A. *Organometallics* **1995**, *14*, 3933−3941.

(11) Küppers, T.; Bernhardt, E.; Eujen, R.; Willner, H.; Lehmann, C. W. *Angew. Chem., Int. Ed.* **2007**, *46*, 6346−6349.

(12) Corey, J. Y.; West, R. *J. Am. Chem. Soc.* **1963**, *85*, 2430−2433.

(13) Bartlett, P. D.; Condon, F. E.; Schneider, A. *J. Am. Chem. Soc.* **1944**, *66*, 1531−1539.

(14) Lehmann, M.; Schulz, A.; Villinger, A. *Angew. Chem., Int. Ed.* **2009**, *48*, 7444−7447.

(15) Schulz, A.; Villinger, A. *Chem. Eur. J.* **2010**, *16*, 7276−7281.

(16) Olah, G. A.; Li, X.-Y.; Wang, Q.; Rasul, G.; Prakash, G. K. S. *J. Am. Chem. Soc.* **1995**, *117*, 8962−8966.

(17) Prakash, G.; Bae, C.; Wang, Q.; Rasul, G.; Olah, G. A. *J. Org. Chem.* **2000**, *65*, 7646−7649.

(18) Ibad, M. F.; Langer, P.; Reiß, F.; Schulz, A.; Villinger, A. *J. Am. Chem. Soc.* **2012**, *134*, 17757−17768.

(19) Driess, M.; Barmeyer, R.; Monse, C.; Merz, K. *Angew. Chem., Int. Ed.* **2001**, *40*, 2308−2310.

(20) Müller, L. O.; Himmel, D.; Stauffer, J.; Steinfeld, G.; Slattery, J.; Santiso-Quiñones, G.; Brecht, V.; Krossing, I. *Angew. Chem., Int. Ed.* **2008**, *47*, 7659−7663.

(21) Wiberg, N.; Schmid, K. H. *Z. Anorg. Allg. Chem.* **1966**, *345*, 93−105.

(22) Baumann, W.; Michalik, D.; Reiß, F.; Schulz, A.; Villinger, A. *Angew. Chem., Int. Ed.* **2014**, *53*, 3250−3253.

(23) Pyykkö, P.; Atsumi, M. *Chem. Eur. J.* **2009**, *15*, 12770−12779.

(24) Schmidbaur, H. *Chem. Ber.* **1964**, *97*, 1639−1648.

(25) Schäfer, A.; Reißmann, M.; Jung, S.; Schäfer, A.; Saak, W.; Brendler, E.; Müller, T. *Organometallics* **2013**, *32*, 4713−4722.

(26) Schäfer, A.; Reißmann, M.; Schäfer, A.; Saak, W.; Haase, D.; Müller, T. *Angew. Chem., Int. Ed.* **2011**, *50*, 12636−12638.

(27) Müther, K.; Hrobárik, P.; Hrobáriková, V.; Kaupp, M.; Oestreich, M. *Chem. Eur. J.* **2013**, *19*, 16579−16594.

(28) Park, S.; Kim, B. G.; Göttker-Schnetmann, I.; Brookhart, M. *ACS Catal.* **2012**, *2*, 307−316.

(29) Connelly, S. J.; Kaminsky, W.; Heinekey, D. M. *Organometallics* **2013**, *32*, 7478−7481.

# 6 Anhang

## 6.1 Abbildungsverzeichnis

Abbildung 1. Allgemeines Konzept der Säure-Base-Theorie nach Lewis. ............................... 2

Abbildung 2. Vereinfachtes Energiediagramm einer Addukt-Bindung. .................................. 3

Abbildung 3. Stabilisierung klassischer Lewis-Säuren über Halogenbrücken.......................... 3

Abbildung 4. Synthese von 25; $^{19}F\{^1H\}$-NMR Spektren nach 3 h Reaktionszeit (unten), 16 Tagen (mitte) und 3 h Photoaktivierung (oben) mit einer UV-Lampe (366 nm/ 245 nm). Mit Punkt markierte Spezies ist das Edukt ($B(C_6F_5)_3$), der Stern markiert das Produkt 25............ 15

Abbildung 5. Verknüpfungsschemata der Aminoisonitril- und Diazen-Addukte ($R^1$, $R^2$ = $Me_3Si$ in Aminoisonitrilen, 4, 20, 23 19; $R^1$ = $Me_3Si$, $R^2$ = Ph in 5, 21, 24; $R^1$, $R^2$ = Ph in 6, 22, 25). ......................................................................................................... 17

Abbildung 6. Darstellung der Positionsfehlordnung in den Silyl-substituierten-Diazenen. .... 19

Abbildung 7. ORTEP Darstellung der Pseudochalkogonium-Kationenstrukturen von 15 (links) und 14 (rechts). Die thermischen Ellipsoide entsprechen 50% Aufenthaltswahrscheinlichkeit bei 173 K. ................................................................... 20

Abbildung 8. ORTEP-Darstellung von 19 (links) und 24 (rechts). Die thermischen Ellipsoide entsprechen 50% Aufenthaltswahrscheinlichkeit bei 173 K. ................................................ 22

Abbildung 9. ORTEP-Darstellung der Kationenstruktur von 26. Die thermischen Ellipsoide entsprechen 50% Aufenthaltswahrscheinlichkeit bei 173 K. ................................................ 23

Abbildung 10. Retrosynthetische Betrachtung der möglichen Cycloadditionen zur Bildung des Trimers. ......................................................................................................... 28

Abbildung 11. Isomerisierung an silylierten Diazen $B(C_6F_5)_3$-Addukten (R = $SiMe_3$ oder Ph). ......................................................................................................... 29

Abbildung 12. ORTEP-Darstellung der Molekülstrukturen von 28 (links) und 27 (rechts) im Kristall. Die thermischen Ellipsoide entsprechen 50% Aufenthaltswahrscheinlichkeit bei 173 K. ......................................................................................................... 29

Abbildung 13. $^1$H-NMR-Spektrum (links), Raman-Spektum (rechts) der Silanmischung aus $Me_4Si$, $Me_3SiH$ und $Me_2SiH_2$ (rot gemessenes Spektrum, blau berechnetes Spektum). ......... 31

Abbildung 14. Allgemeine Darstellung des katalytischen Alkylgruppenaustausches (R = Me,Et). ........ 32

## 6.2 Tabellenverzeichnis

Tabelle 1. Zusammenfassung der isolierten Diazen-Addukte. ........ 15

Tabelle 2. Summe der NX-Kovalenzradien nach P. Pyykkö.[79] ........ 17

Tabelle 3. Ausgewählte Strukturparameter der Lewis-Basen und ihrer isolierten Addukt-Spezies. Bindungslängen in Å, Bindungswinkel in ° ........ 18

Tabelle 4. Zusammenfassung ausgewählter Eigenschaften der isolierten Addukte. ........ 24

Tabelle 5. Als Pre-Katalysatoren der Trimerisation identifizierte Lewis-Säuren. ........ 27

## 6.3 Schemataverzeichnis

Schema 1. Modifizierte Wasserstoff/Halogen Austauschreaktion nach Corey und West. ........ 4

Schema 2. Allgemeine Synthese von Silylium-Supersäuren nach Lambert et al. (R = Me,Et, i-Pr, $Me_3Si$; X = Solvens = $R_3SiH$ oder Benzol). ........ 4

Schema 3. Neuartige Synthese von sterisch überfrachteten Silylium-Salzen nach Müller et al.[23] ........ 5

Schema 4. Lewis-Säure-assistierte [3+2]-Cycloadditionen unter Verwendung versteckter Dipolarophile und 1,3-Dipole bilden Addukt stabilisierte Azapniktole. (LS = $GaCl_3$; E =P, As; R = Mes*, Ter, $N(SiMe_3)_2$). ........ 6

Schema 5. Synthese eines cyclo-Diphosphadiazans über die formale Insertion eines NNP-Fragmentes in die BC-Bindung des $B(C_6F_5)_3$. ........ 6

Schema 6. Chlor/Methyl Austausch am $Me_3SiNSNSiMe_3 \cdot GaCl_3$ gefolgt von Bildung des isolierten Oxadisilathiadiazin-Ring nach Schulz et. al.[42] ........ 7

Schema 7. Definition der Trimethylsilyl-Affinität. ........ 8

Schema 8. Allgemeine Synthese von homoleptischen Onium-Kationen (n = 1: E = F, Cl, Br, I, CN, OCN, SCN, NNN, wobei X = $Me_3SiH$; n = 2: E = O, S, mit X = $Me_3SiH$; n = 3: E = P, As mit X = Benzol). .......... 8

Schema 9. Aufklärung des Zerfalls von labilen Trimethylsilylium-Verbindungen über die Abfangreaktion mit $CS_2$ nach Schulz et al.[17] .......... 9

Schema 10. Silylium katalysierte CC-Kupplung (links) und Hydrodefluorierung (rechts). .......... 10

Schema 11. Silylium katalysierte Diels-Alder Cyclisierung. .......... 10

Schema 12. Synthese von $[(Me_3Si)_2NNCSiMe_3][WCA]$ Salzen in stöchiometrisch geführten Reaktionen ($[WCA]^- = [B(C_6F_5)_4]^-$, $[CHB_{11}H_5Br_6]^-$). .......... 12

Schema 13. Fehlgeschlagene direkte Silylierungen des Bis(trimethylsilyl)diazens (A: [WCA] = $[GaCl_4]$, $[SbF_6]$; B: [WCA] = $[GaCl_4]$, $[SbF_6]$, $[B(C_6F_5)_4]$, $[AsF_6]$; C: $[B(C_6F_5)_4]$, $[CHB_{11}H_5X_6]$, X = Br, Cl). .......... 13

Schema 14. Synthesen des homoleptischen Diazenium-Salzes über Oxidation von Hydrazinoverbindungen. .......... 14

Schema 15. Trimerization von 1 zum Pytrazolderivat (16). .......... 26

Schema 16. Ein möglicher bimolekularer Isomerisierungsweg. .......... 27

# Lebenslauf

## Persönliche Daten

| | |
|---|---|
| Name | Fabian Reiß |
| Geburtsdatum | 17. Juni 1983 |
| Geburtsort | Goslar |
| Familienstand | ledig, ein Kind |

## Schulbildung

| | |
|---|---|
| 1989 - 2000 | RS Goldene Aue Goslar, Realschulabschluß. |
| 2000 - 2004 | Berufsbildende Schulen I Braunschweig. |
| 2004 - 2005 | Fachoberschule Technik BBS – Goslar Fachabitur Technik. |
| 2005 - 2006 | Berufsoberschule Technik BBS- Goslar Fachgebundene Hochschulreife. |

## Berufsausbildung

| | |
|---|---|
| 2000 - 2004 | Ausbildung zum Chemielaboranten am Institut für Aufbereitung und Deponietechnik an der Technischen Universität Clausthal. |

## Studium

| | |
|---|---|
| 10/2006 – 09/2008 | Chemie - Studium an der Universität Rostock. Abschluss Vordiplom. |
| 09/2008 – 07/2011 | Chemie - Studium an der Universität Rostock. Abschluss Diplom. |

| | |
|---|---|
| 11/2010 – 07/2011 | Diplomarbeit: „Darstellung und Charakterisierung von niedrigkoordinierten Pniktogen-Stickstoffverbindungen“ Abschluss: Diplom-Chemiker (univ.). |
| 07/2011 – 06/2014 | Anfertigung der Dissertation im Arbeitskreis Prof. Dr. Axel Schulz an der Universität Rostock. |

## Berufstätigkeit

| | |
|---|---|
| 02/2004 – 04/2004 | Chemielaborant am Institut für Aufbereitung und Deponietechnik an der Technischen Universität Clausthal, Arbeitskreis Prof. Dr. – Ing. Eberhard Gock. |
| 12/2004 – 07/2006 | Teamleiter der Lerngruppen im Rahmen des Förderprogramms „Schüler helfen Schülern im Fach Mathematik“, auf Honorar. |
| 10/2008 – 09/2011 | Hilfswissenschaftlicher Mitarbeiter am Institut für Chemie der Universität Rostock, Lehrstuhl für Anorganische und Elementorganische Chemie, Arbeitskreis Prof. Dr. Axel Schulz. |
| Seit 10/2011 | Wissenschaftlicher Mitarbeiter Mitarbeiter am Institut für Chemie der Universität Rostock, Lehrstuhl für Anorganische und Elementorganische Chemie, Arbeitskreis Prof. Dr. Axel Schulz. |

## Auszeichnung

| | |
|---|---|
| 02/2004 | Auszeichnung durch die IHK Braunschweig der sehr guten Gesamtprüfungsleistung in der Abschlussprüfung zum Chemielaborannten. |

## Wissenschaftliche Arbeiten

### Publikationen

1. „Synthesis of Sterically Encumbered 2,4-bis-*m*-terphenyl-1,3-dichloro-2,4-*cyclo*-dipnictadiazanes $[\text{m-TerNPnCl}]_2$, (Pn = P, As)“, F. Reiß, A. Schulz, A. Villinge, N. Weding, *Dalton Trans.* **2010**, *39*, 9962 – 9972.

2. „The *N,N*-Bis(terphenyl)aminophosphenium Cation – A Sensetive Probe for Interactions with Different Anions“, F. Reiß, A. Schulz, A. Villinger, *Eur. J. Inorg. Chem.* **2012**, *2012*, 261–271.

3. “Catalytic Trimerization of Bis-silylated Diazomethane”, M. F. Ibad, P. Langer, F. Reiß, A. Schulz, A. Villinger, *J. Am. Chem. Soc.* **2012**, *134*, 17757 – 17768.

4a. “Isolation of a Labile Homoleptic Diazenium Cation”, W. Baumann, D. Michalik, F. Reiß, A. Schulz, A. Villinger, *Angew. Chem. Int. Ed. Engl.* **2014**, *53*, 3250 – 3253.

4b. “Die Isolierung eines labilen homoleptischen Diazeniumkations“, W. Baumann, D. Michalik, F. Reiß, A. Schulz, A. Villinger, *Angew. Chem.* **2014**, *126*, 3314 – 3318.

5. “Synthesis, Structure and Reactivity of Diazene Adducts – Isolation of the First *iso*-Diazene stabilized as Borane Adduct”, F. Reiß, A. Schulz, A. Villinger, *Chem. Eur. J.* **2014**, *im Druck.*

6. “Synthesis of the First Persilylated Ammonium Ion $[(Me_3Si)_3NSi(H)Me_2]^+$ By Silylium Catalyzed Methyl/Hydrogen Exchange Reactions“, R. Labbow, F. Reiß, A. Schulz, A. Villinger, *Organometallics* **2014**, *im Druck*.

## Posterbeiträge

1. “The *N,N*-Bis(terphenyl)aminophosphenium Cation – A Sensetive Probe for Interactions with Different Anions”, 14th. Frühjahressymposium 2012, Young Scientists Conference On Chemistry, Rostock, 18.03. – 21.03.2012, Fabian Reiß, Axel Schulz, Alexander Villinger.

2. “Catalytic Trimerisation of Bissilylated Diazomethane and Aminoisonitrile“, 15th Northern-German Doctoral Student Colloquim of Inorganic Chemistry, Walsrode, 24.09. – 21.03.2012, Muhammad Farooq Ibad, Peter Langer, Fabian Reiß, Axel Schulz, Alexander Villinger.

## Vortrag

1. “Activation of Diazenes with Lewis Acids“,16th Northern-German Doctoral Student Colloquim of Inorganic Chemistry, Bremen, 19.09. – 20.03.2012, Fabian Reiß, Axel Schulz, Alexander Villinger.